Faculty of Science and Engineering
Department of Chemical Engineering

Simulation of LNG rollover in storage tanks

Pooya Arjomandnia

This thesis is presented for the degree of

Doctor of Philosophy

of

Curtin University

July 2015

Declaration

To the best of my knowledge and belief this thesis contains no material previously published by any other person except where due acknowledgment has been made.

This thesis contains no material, which has been accepted for the award of any other degree or diploma in any university.

Signature: *P.Arjomandnia*

July 2015

Biography of the Author

Pooya Arjomandnia was born on 15th March 1975 in Tehran, Iran. He completed his BEng. degree (Chemical Engineering) from the Iran University of Science and Technology (IUST) in 1997 as a top student.

In 1997, Pooya started working as a chemical and process engineer in the oil and gas industry for operation and consultant companies. From 2004 onward he was promoted to senior process engineer and later to lead process engineer. In 2007, he continued working in oil and gas industry and enrolled part-time at the University of Western Australia (UWA), for Master degree. In 2008, he became a full-time student and was awarded Sir Julian Hunka scholarship by UWA and completed his MSc. (Chemical Engineering) degree at UWA in 2010.

Later in 2010, Pooya returned back to full-time work in the oil and gas industry. In 2011, he enrolled part-time for Ph.D. at Curtin University, while working full-time as a senior process engineer. As the Ph.D. research became more intense, he switched to full-time student, in the second half of 2013and was awarded the Australian Postgraduate Award (APA) scholarship by Curtin University.

Pooya is a Chartered Professional Engineer (CEng) member of Engineers Australia (EA) and also national registered engineer (NPER). He is also a trained HAZOP leader, certified by Orica Australia and he has been lecturing process safety and risk management course at Curtin University, department of chemical engineering from 2014. He has worked in LNG industry from 2007 for companies such as Technip and Fluor Australia for clients such as Woodside, Chevron and Origin Energy. During his career, he worked in projects using different LNG technologies such as PPMR process and Shell DMR and used internationally known design standards such as American Petroleum institute standards (API), Shell design and engineering practice (SHELL DEP),

British Standard (BS) and local standards such as Australia/New Zealand Standards (AS/NZs).

Publications in support of the thesis

Arjomandnia P., M. O. Tade, V. Pareek, E. F. May; Analysis of available data from liquefied natural gas rollover incidents to determine critical stability ratios, AIChE Journal, Jan 2014 Vol. 60 P 362–374, No. 1

Summary

Liquefied Natural Gas (LNG) rollover refers to the sudden mixing of stratified LNG layers, which can cause the generation of significant amounts of boil-off gas. Such events are significant safety concerns in LNG storage but there are no reliable models for its description at industrial scales available in the open literature. In this research, the data and models for LNG rollover existing in the open literature are reviewed and a new framework for quantitatively analyzing the limited available data is presented. We extended the definition of the hydrostatic stability ratio for binary mixtures to allow its estimation for multi-component mixtures, either from the reported LNG layer compositions or measurements of the LNG layer densities.

In this Thesis, the fundamental issues associated with rollover are reviewed, a summary of past simulations plus their limitations is given and a new program for simulating rollover is presented. The new simulation links the software packages REFPROP[1] (MATLAB version, which is called REFPROPM) and MATLAB[2]; the former is used to calculate the physical properties of LNG as a function of temperature, pressure and composition and the latter is used to solve the coupled differential equations describing the material and energy balance relations for each layer. Importantly the software REFPROP[1] uses the most accurate available model, the GERG-2004 Equation of State[3], to calculate the thermodynamic properties of the LNG within a reasonable period of time. The model also allows different correlations and analogies to be used to calculate the coefficients of heat and mass transfer between the layers.

By analyzing the graphical data of Bates and Morrison[4], who suggested 2 phases in LNG rollover, the value of the critical stability ratio R_c, separating the first phase of LNG rollover from the second phase, was estimated to be around 3.8. This is significantly larger than the critical ratio of 2 reported by Tuner[5] for saline solutions and is also larger than the initial stability ratio of 1.7 estimated from the best documented LNG rollover incident at La Spezia in 1971[6].

Models for LNG rollover previously reported in the literature have only described the La Spezia incident successfully, by using the Reynolds analogy to estimate mass transfer rates from heat transfer correlations. However, these same models are unsuccessful when applied to other reported LNG rollover incidents with the predicted rollover time being too short because the mass transfer coefficient is over-estimated. This thesis investigated the following hypothesis, which builds on the concept proposed by Bates and Morrison of LNG rollover occurring in two phases: that both the interlayer heat and mass transfer rates differ during the two phases, and not just the mass transfer rate. Specifically, in Phase 1 smaller heat and mass transfer coefficients are relevant, with the latter estimated from the former using the Chilton-Colburn analogy. In Phase 2, once the multi-component system's stability ratio reaches the critical value, both the heat transfer coefficient and the mass transfer coefficient increase with the latter estimated from the former using Reynold's analogy.

First, computational fluid dynamics (CFD) models of idealized rollover scenarios were developed and used to simulate the early stages of rollover. The objective of these CFD studies was to assess qualitatively whether a transition in the heat transfer coefficient was consistent with the process. These CFD results indicated such an approach was plausible and should be incorporated into the lumped parameter model to enable quantitative predictions.

The new lumped parameter model was calibrated by comparison with the data of Bates and Morrison, which allowed the magnitude of the heat transfer coefficient to be estimated in the two phases. The model was then used to simulate the Partington LNG rollover incident reported by Baker and Creed[18]. A sensitivity analysis was also done on the fraction of heat absorbed by the vapour phase and the initial temperature difference between the vapour and upper liquid layer. The simulation was found to be very sensitive to these parameters and varying each of these parameters caused the predicted time to rollover to vary from 20 hours to 8.6 days.

Several simulations were done on auto-stratification rollover to investigate the impact of nitrogen content on the time to rollover and the boil-off gas (BOG) generation. The results obtained suggested that, although 1% or higher amount of nitrogen in LNG, does not directly increase the potential of rollover, it makes the LNG mixture less stable, which requires a lower (more expensive) storing temperature to avoid excessive boil off.

In future work the new model should be extended to allow it to use either the Reynolds analogy or a penetrative convection type model in the second phase of LNG rollover. However, the current version of this model improved the previous lumped parameter models and could be used to investigate further the issue of auto-stratification in LNG storage and, in particular, the impact of N_2 content on the likelihood of an auto-induced rollover event.

"For me, there is only the traveling on the paths that have a HEART. On any path that may have a heart, there I travel and the only worthwhile challenge is to traverse its full length. And, there I travel, looking; looking, breathlessly."

From: "The teachings of Don Juan, A Yaqui Way of Knowledge", by Carlos Castaneda, 1968, UC Press, Oakland, California, ISBN 0-520-21757-8

Acknowledgments

I am deeply indebted to my supervisors Professor Moses O. Tade, Professor Vishnu Pareek from the Curtin University and Professor Eric F. May from the University of Western Australia for their patience, guidance, encouragement and excellent advice throughout this research. I would like to thank them for trusting me and always supporting and encouraging me. Without their help, this work would not be possible.

I would like to extend my sincere gratitude to Professor Eric F. May, which guided me through this research as a supervisor, a true scientist and as an academic role model. I'm also grateful of Professor Jeremy Leggoe from UWA, for reviewing and commenting on the CFD simulations results.

I would also like to especially thank my family; my grandmother Tahereh, my sister Sara and particularly my mother, for their love and support and I take this opportunity to dedicate this Ph.D. thesis to my dearest mother Mrs. Mahsima Nouban.

Pooya Arjomandnia
July 2015

To my mother:
> **Who gave me life, to start**
> **Who gave me love, to continue**
> **Who gave me courage, to fulfil**
>
> **The journey…**

Pooya Arjomandnia

تقدیم به مادر عزیزم سرکار خانم مه سیما نوبان.

Table of Contents

Nomenclature and Abbreviations

A	Tank cross section
Adiab.	Adiabatic
a_z	Acceleration of the liquid parcel (Z axis)
Bcf/d	Billion cubic feet per day
BOG	Boil-off Gas
C_P	Molar heat capacity
c_P	Specific heat capacity
C, C'	Constant values
CFD	Computational Fluid Dynamics
D	Tank diameter
D_{AB}	Molecular diffusion coefficient
DEs	Differential equations
E	Stability parameter (Hydrostatic)
EOS	Equation of State
F	Rayleigh flow
f	Boil-off flow rate
F_B	Buoyancy force
Fs	molar flux through layers' interface
F_W	Weight force
g	Acceleration of gravity
Gr	Grashof Number
H	Heat flux
h	Heat transfer coefficient
H_j	Molar enthalpy of layer
hr	Hours (Time)
i	Refers to the component
IPL	Independent Protection Layer
j	Refers to the layer
K	K value, ratio of vapour mole fraction to liquid mole fraction
k	Mass transfer coefficient
L	Bottom liquid layer (Lower layer)
L_j	Height of each layer

Le	Lewis Number
LNG	Liquefied natural gas
LP	Lumped Parameter
LPA	Layer of protection analysis
LTD	Level temperature density
M	Prefix for thousand
Max/Min	Maximum/Minimum
min	Minutes (Time)
MSDS	Material Safety Data Sheet
MM	Prefix for million
$Mole_j$	Number of moles in layer "j"
mtpa	Million tonnes per annum
MW	Molar mass (molecular weight)
NA	Not Applicable
n_{Total}	Total number of moles
Nu	Nusselt Number
Pr	Prandtl Number
Q	Latent heat
q_L	Heat flux to the bottom liquid from outside
q_U	Heat flux to the top liquid from outside
q_{UV}	Heat flux to the top liquid from vapour
q_v	Heat flux to the vapour from outside
Ra	Rayleigh Number
R_s	Stability ratio
R_c	Critical stability ratio
S, (S_i)	Molal concentration (of component i)
Sc	Schmidt Number
T_j	Layer "j" temperature
t	Time
U	Top liquid layer (Upper layer)
V	Vapour
X_i	Liquid phase mole fraction of component "i" in Bottom Layer
Y_i	Liquid phase mole fraction of component "i" in Top Layer
Z	Vertical axis

Greek Letters

α	coefficient of volume expansion, due to temperature change
$\hat{\alpha}_i$	Liquid phase mole fraction of component "i" in film layer
β, (β_i)	The coefficient of volume expansion due to concentration change, (for component i)
$\hat{\beta}_i$	Vapour phase mole fraction of component "i" in vapour
Δ	Difference of a quantity
κ	Thermal diffusivity
κ_{Adiab}	Adiabatic compressibility
κ_T	Isothermal compressibility
λ	Liquid Thermal conductivity
Φ	Potential energy ratio
μ	Absolute viscosity
ν	kinematics' viscosity
ρ	Density
$\bar{\rho}$	Average Density

Chapter 1
Introduction

In this Thesis, the fundamental issues associated with liquefied natural gas rollover are reviewed, a summary of past simulations plus their limitations is given and a new program for simulating rollover is presented. The model allows different correlations and analogies to be used to calculate the coefficients of heat and mass transfer between the layers. Several rollover cases are tested to verify the accuracy and sensitivity of the proposed model to simulate the thermodynamic and transport properties as well as time to rollover. Furthermore, the key parameters used to determine the hydrostatic stability and the ratio of heat to mass transfer from binary mixtures have been extended to multicomponent mixtures to obtain a more accurate rollover criterion. Considering the importance and criticality of liquefied natural gas rollover in oil and gas industry, a safety case and risk assessment of a hypothetical rollover incident has been done to highlight the hazards, rank the risks, review the available safeguarding and finally give some recommendations for the future research.

Liquefied natural gas (LNG) is one of the world's major hydrocarbon exports. LNG is become increasingly important for the world fuel market because natural gas combustion creates less carbon dioxide relative to heavier fuels such as petroleum and coal. As LNG is non-corrosive and non-toxic, it does not pollute water or land resources. These characteristics make it a safer choice for the environment as well as allow it to be shipped and stored more safely and economically for delivery to international markets[7].

Australia is a major exporter of LNG in the global energy market, with potential for further development based on its abundant natural gas resources. Australia is the third largest LNG exporter in the Asia-Pacific region and the fourth largest LNG exporter in the world, exporting 18.9 million tonnes in 2011 with a value of around $11.1 billion. The LNG industry is attracting significant new project

investments providing major long-term employment, economic benefits and government revenue[8].

Figure 1.1 shows the global LNG production capacity (supply) from the year 2000 to 2014 and the forecast to 2025 presented by BG Group in 2015[9]. It shows Australia, Qatar and the USA will be the largest producers of the LNG in the world by 2025.
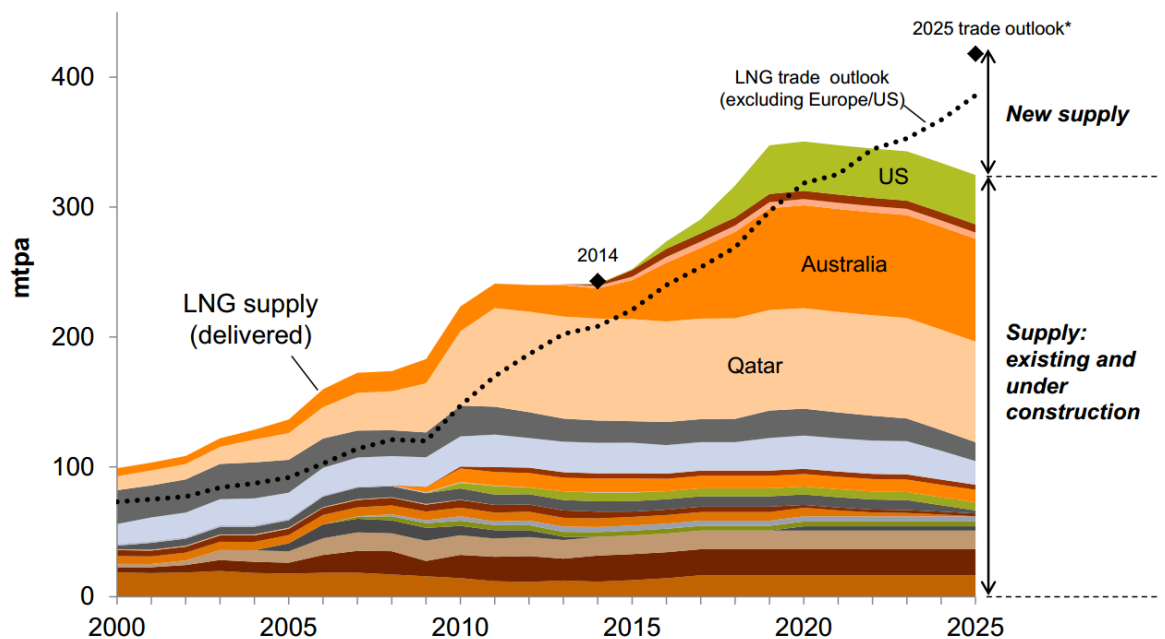
Figure 1.1: Global LNG supply from 2000 to 2025[9] (major suppliers)[i].

1.1. What is LNG?

LNG is purified natural gas that is stored and transported in liquid form at the cryogenic condition with atmospheric pressure and temperature near -160 to -165 °C. This liquid is a mixture of predominately methane, with lower levels of other components such as ethane, propane, butane and nitrogen. The composition of LNG changes slightly from region to region and plant to plant, based on the source raw gas composition, the technology used for liquefaction

---

i) Permissions have been granted from the publishers for all the copyrighted materials, photos and pictures (refer to appendix 5 of this thesis)

process and the level of purification. Various LNGs compositions from different sources are given in Table 1.1[10].

Component	Australia	Abu Dhabi	Malaysia	Indonesia		Brunei	Qatar
(mole %)	Karratha	Das Island	Bintulu	Arun	Bontang	Lumut	Ras Laffan
Methane	87.8	87.1	91.2	89.2	90.6	89.4	89.6
Ethane	8.30	11.40	4.30	8.60	6.0	6.35	6.30
Propane	2.98	1.27	2.87	1.67	2.48	2.8	2.19
Butanes	0.875	0.141	1.360	0.51	0.82	1.3	1.07
Pentanes	0.000	0.001	0.010	0.02	0.01	0.00	0.04
Other (Heavier)	-	-	0.18	-	-	0.11	0.77

Table 1.1: Typical LNG compositions from various sources[10].

Figure 1.2 shows a simplified block flow diagram of the process of LNG production. The raw gas extracted from wells is separated from water, solid particles, sulphur components and other impurities based on the end user requirements and the final product specifications. For LNG production, natural gas must be highly purified mainly for preventing blockage and solidification of the associated water (ice) and CO_2 during the liquefaction process. Corrosion prevention in equipment is another reason for this high level of purification.
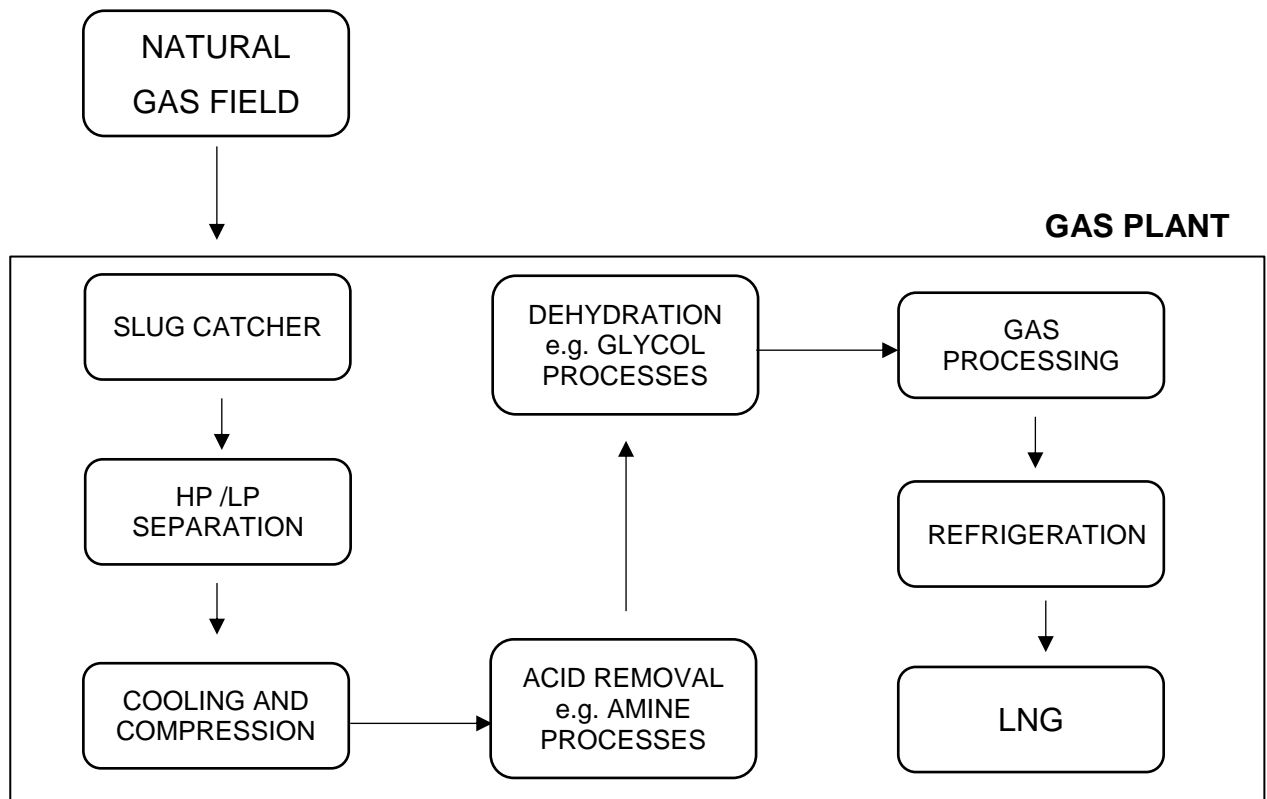
Figure 1.2: Simplified LNG production flow diagram.

In LNG plants, natural gas is converted into a liquid phase, using one of the several refrigeration processes in a liquefaction unit. Some of the most famous liquefaction processes are as follows[11]:

- Cascade process (ConocoPhillips Petroleum)
- Prico process (Pritchard - Kobe steel)
- MRC process: (Technip - Snamprogetti)
- PPMR process (C3MR sometimes referred to as APCI, Air Products - Chemicals International)
- Shell DMR process (Shell)

In general, production of LNG including processing and liquefaction consumes about 8 ~ 15% of the whole energy stream. Liquefying the natural gas reduces its volume by a factor of about 600. The reduction in volume increases the volumetric energy density of the fuel and makes it more practical to transport

and store. The liquefaction process provides an easier and safer means of transporting it long distances when pipeline transport is not feasible or the transportation distance is $\geq$ 4000 km[12].

At LNG plants and receiving terminals, LNG is usually stored in atmospheric cryogenic full containment tanks[13], such as the one shown in Figure 1.3. In international trade, LNG is transported in specially built tanks in double- hulled ships as shown in Figure 1.4 (a and b)[14], to a receiving terminal where it is stored in heavily insulated tanks. The LNG is then sent to regasifiers, which turn the liquid back into gas that then enters the receiving pipeline system for distribution to the customers as part of the natural gas supply network.
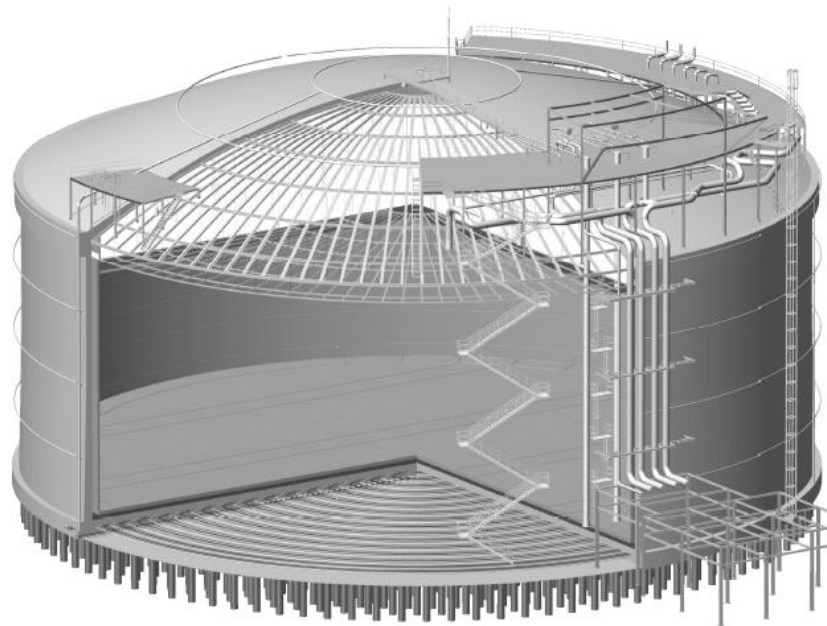
Figure 1.3: Full containment above-ground LNG storage tank[13].
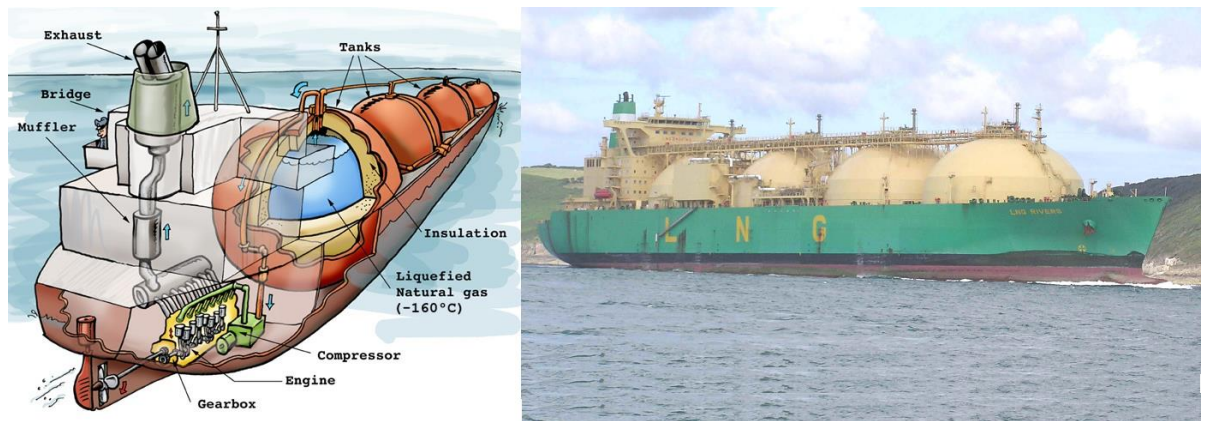
Figure 1.4 a and b: Typical LNG ship carriers[14].

A conventional chain of LNG supply begins with production in the field, purification, liquefaction, storage, transport, receiving and regasification and finally delivery to the end users. LNG could be used by consumers in various forms such as power generation, industrial and chemical uses, or distribution to domestic customers. On a smaller scale, LNG may also be produced by liquefying gas directly taken from a pipeline, storing and then regasifying it for the pipeline distribution to customers when demand is high, such as on cold winter days. These small regasification plants are usually called "peak shaving plants". Another storage method used during high demand periods is to transport LNG in special tanker trucks to smaller facilities called "satellite plants" where it is stored and regasified as needed.

1.2. What is rollover?

Rollover is a phenomenon that can occur in systems containing stratified liquids. Some examples of these systems are salt water layers in the ocean, fresh water layers in the volcanic lakes, LPG or LNG layers in storage tanks when loaded with different products from different sources as it is shown in Figure 1.5(B). Rollover is a sudden mixing of existing layers of liquid. The stratified layers are characterised by different values of temperature and composition. Originally the layers were in mechanical equilibrium ($\rho_L > \rho_U$, where ρ_L is the mass density of the lower layer and ρ_U is the mass density of the upper

layer), but over time these densities can alter through changes in temperature and composition, driven by heat and mass exchanges between the layers. If the layer densities evolve in such a way that the density difference ($\rho_L - \rho_U$) $\rightarrow 0$ but the temperature difference remains finite, the system can reach a point of hydrostatic instability, causing the liquid layers to mix rapidly.

The rollover phenomenon was first studied by physical oceanographers. They tried to explain the reason water layers of different temperatures and salinities in deep oceans and volcanic lakes suddenly invert their positions[15]. As discussed in Chapter 2, they found that changes in the salinity and temperature of the water layers are the driving forces for rollover and defined a criterion for the hydrostatic stability of the layers[5].

For LNG, rollover is most likely to occur following the loading of two or more LNGs from different sources into a single storage tank, each with a different temperature and composition, as shown in Figure 1.5 stage "A". The potential for rollover occurs if the richer composition layer (with higher mass density but lower temperature) is on the bottom and the lighter layer on top[16,17].

1.3. Effect of temperature change on layer densities:

With time, the LNG layers absorb heat from the surrounding tank walls and the tank's bottom base plate as shown in Figure 1.5, Stage "B". The amount of heat entering through the tank bottom is greater than through the tank wall and so the temperature of the lower layer increases faster than the upper layer. As a result of thermal expansion, the mass density of the lower layer decreases at a faster rate than the density of the upper layer. As the lower layer's temperature rises so does its vapour pressure; however, it does not boil, because of the additional static pressure head from the upper layer. Although the temperature of the upper layer is increasing, its mass density can increase or decrease depending upon the effects of mass transfer. If the mass density of the upper layer increases in spite of its temperature increase, then the system's stability decreases and there is a potential for rollover.

1.4. Effect of compositional change on layer densities:

Mass is exchanged across two interfaces: the boundary between the upper and lower liquid layers and the boundary between the top liquid layer and the vapour. The liquid layers exchange components initially through diffusion in a direction governed by the difference in molar concentration of each component. Mass transfer between the upper liquid layer and the vapour is driven by the boil-off of the more volatile components in the liquid. If the effect of temperature on the upper layer is not too large, the combination of these two mass transfer mechanisms can cause the density of the upper layer to increase. The effect of mass transfer on the density of the lower layer is usually smaller than the effect of temperature but it can help to increase the rate at which the lower layer density decreases. After some time, there may be no significant density difference between the top and bottom layers and the layers then mix rapidly. It is this rapid mixing that is generally referred to as rollover.

When a rollover occurs, the hotter, more volatile liquid is brought rapidly to the upper surface. The removal of the previously existing hydrostatic head (≈ 30 kPa) results in a "flash" and a large amount of boil-off, as shown in the Figure 1.5 Stage "C". This boil-off may be too large for the storage tank's pressure relief valves to handle, regardless of whether the vented material is released catastrophically to the atmosphere or properly flared. If the vapour is not properly released, pressure can build up in the tank and wall cracks or other structural failure modes may occur.
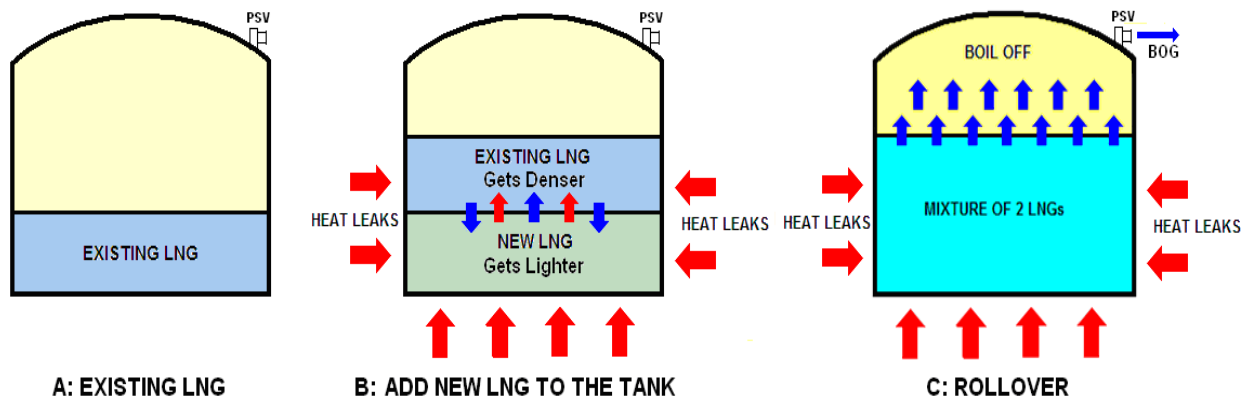
Figure 1.5: Stages of LNG rollover[7].

In addition to over-pressurization of atmospheric tanks, rollover can cause other hazards, such as losing valuable product through venting and environmental pollution.

1.5. Engineering issues related to the rollover

Rollover is one of the major engineering and safety issues concerning LNG storage before, during and after shipping. To ensure safe operation during long-term storage of LNG, rollover must be avoided. In modern engineering practice, the approach to rollover is similar to the approach taken to prevent a potential explosion, which is theoretically possible wherever LNG storage and loading occurs. In chapter 6 of this thesis, a safety and risk assessment case study of a hypothetical rollover incident has been conducted to identify the likelihood and consequence severity of rollover. In general conservative tank design and LNG loading and unloading procedures are employed to ensure rollover cannot occur; however, these precautions are expensive and sometimes technically difficult.

The amount of nitrogen in the LNG cargo is a crucial parameter and it is greatly related to the phenomenon of rollover. This type of rollover is called nitrogen-induced stratification (also known as auto-stratification). Nitrogen is the most volatile component of LNG, which boils off preferentially leading to an increase

in the remaining liquid's bubble point temperature but also a reduction in its mass density, (the molar masses of N_2 and CH_4 are 28 and 16, respectively). These density variations due to auto-stratification can also lead to rollover[18]. Several hypothetical cases of auto-stratification rollover simulations are also presented in Chapter 5 of this thesis.

Generally, the engineering specifications of allowed N_2 content in LNG are very low (about 1%[16, 17, 19]) primarily because the exact details about nitrogen-induced rollover phenomenon are not well known. In general, the removal of N_2 from LNG feed streams is a difficult and expensive process, so a better understanding of exactly how N_2 content in the LNG leads to auto-stratification would be very valuable[20, 21, 22].

In Australia, the UK, Europe, East Asia and the United States, the Wobbe Index[23] specifications for natural gas used in domestic burners (stovetops, water heaters, etc.) are quite variable. To meet specifications, the heating value of the LNG arriving in a given country must be adjusted before distribution to domestic users. For example, in the UK, a lower heating value is specified and LNG is ballasted with nitrogen at regasification terminals. In contrast, natural gas sold in Japan and South Korea requires a heating value greater than that of most LNG imported; therefore, rich components like propane are blended with the LNG during regasification. This means that sometimes N_2 must be removed from the LNG cargo for safe transportation and must then be replaced to adjust the heating value.

1.6. Modelling LNG rollover

In general, there are two main approaches to simulate LNG rollover. The first is lumped parameter modelling, which has been used by Heestand et *al.*[24] and more recently by Deshpande et *al.*[25]. In this approach, two layers of LNG divided by a sharp interface is considered. The second approach is the distributed parameter modelling method such as using Computational Fluid Dynamic (CFD) tools to simulate the rollover phenomenon. This method

predicts fluid flow, heat transfer, mass transfer and related transport phenomena by solving the mathematical equations such as Navier–Stokes equations[26], which govern the conservation of momentum, mass, energy, species and the effects of body forces, using a numerical process (called discretization) to develop approximations of the governing equations of fluid mechanics in the fluid region of interest[27].

There are benefits and limitations of using each of these methods. In Chapters 2 and 4, both approaches will be reviewed and compared and the best one will be selected and used to model the LNG rollover phenomenon effectively.

In 1983, Heestand *et al.*[24] developed a LNG rollover model using the lumped parameter method, which described the data from the first recorded LNG rollover incident in La Spezia, Italy, as reported by Sarsten[6]. All rollover models require the solution of a set of differential equations describing the heat and material balances in the liquid layers over time. Heat and mass are transferred between the liquid layers as well as the vapour and heat also leaks into the layers from the outside world. The model for two liquid layers is shown in Figure 1.6 and the key differential equations of material and energy balance for the liquid layers are below:

$$\frac{d(n_{tot}X_i)}{dt} = k_i.A\Delta A_i - F_R \times X_i \qquad\qquad \text{material balance} \qquad (1\text{-}1)$$

$$n_{tot}C_P \frac{dT}{dt} = hA\Delta A + q_{out}. \qquad\qquad \text{energy balance} \qquad (1\text{-}2)$$

Here, "n_{tot}" is the total number of moles in the layer, "C_P" is the molar heat capacity of the liquid layer, "h" and "k_i" are heat and component mass transfer coefficients, "q_{out}" is the total heat transferred from the vapour or from outside the tank, "T" is the layer's temperature, "ΔT" is the temperature difference between the layers, "X_i" are the component mole fractions in the layer, "ΔX_i" are the differences in component mole fractions between the layers, "F_R" is any

31

molar flow between the upper layer and an assumed film in equilibrium with vapour on top of the upper LNG layer , "A" is the tank cross section and "t" is the time. The detailed forms of the basic differential equations (material and energy balance) used in the present simulation are described in Chapter 4.
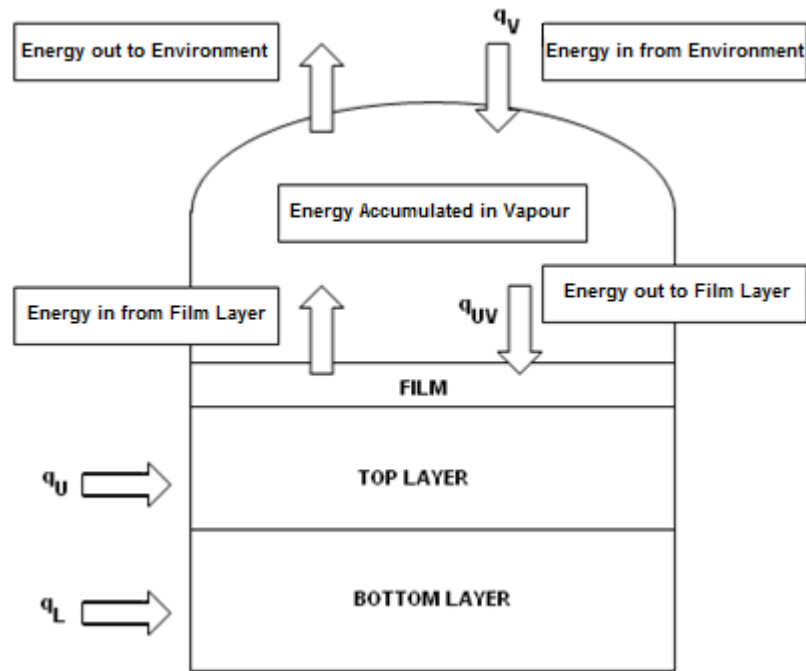
Figure 1.6: Schematic of LNG tank with stratified layers[7].

The key quantities needed for the model and for solving these differential equations are:

- **Initial values** for the temperatures, compositions and total number of moles in each layer. These values were described by Heestand *et al.*[24] for the particular case of the La Spezia rollover incident.
- **Values for the physical properties of the LNG layers.** These are calculated using thermodynamic and transport property models from the (calculated) temperatures and compositions and the reported pressures.
- **External heat fluxes,** which were given by Heestand *et al.*[24] for the La Spezia condition or, in general, could be measured or derived from tank's design datasheet.

- **Heat transfer coefficient,** which can be calculated from well-established correlations such as those of McAdams[28] or Globe and Dropkin[29].

- **Mass transfer coefficient(s),** which can be calculated from analogies between heat and mass transfer, such as the Reynolds analogy [48] or the Chilton-Colburn analogy[48], or alternatively from the empirical data for salt solutions measured by Turner[5].

- **A criterion for the initiation of rollover,** such as equalization of densities or hydrostatic stability parameter.

Heestand *et al.*[24] used the Soave-Redlich-Kwong (SRK)[30] equation of state (EOS) for the calculation of the LNG's thermodynamic properties. Since 1983, the EOS's used for LNG and natural gas have improved and therefore, these EOS's might be able to improve the accuracy of rollover models.

Central to the study of rollover is the quantification of heat and mass transfer coefficients, "h" and "k_i", between the layers, which appear directly in the mass and energy differential equations and unfortunately, there has not yet been a dedicated model developed in the open literature describing mass transfer between LNG layers, partly because of the cryogenic temperatures required. The mass transfer between the layers of LNG is normally assumed to be by equimolar counter diffusion and double diffusion convection[24, 16]. This means that a two-way mass flux occurs with an equal number of moles entering and exiting the interface film between the two layers in a given time. The double-diffusive equimolar mass transfer has been studied experimentally most extensively in the context of physical oceanography. Water layers in the ocean are often found to have potentially unstable temperature and salinity gradients, which are established by a process known as thermohaline circulation (THC)[5, 35]. Once these layers are established, double diffusive heat and mass transfer can lead to a rollover event in the ocean; further discussion of this process is given in Chapter 2.

Heestand *et al.*[24] used the equalisation of the layer densities as the criterion for rollover. This criterion ignores the small effect of compressibility in determining the hydrostatic stability of the layers. Furthermore, most previous stability analyses only consider the liquid to be a binary solute-solvent system. In Chapter 3, we present a full hydrostatic stability analysis for two multi-component liquid layers to address previous deficiencies.

1.7. Objectives of this study

The model of Heestand *et al.*[24] explained the La Spezia incident very closely to what was reported by Sarsten[6] and became a standard industry tool for describing LNG rollover; however, their model cannot simulate the Partington rollover incident correctly as described by Deshpande et *al.*[25]. Since 1983, the improvement of equations of state for LNG and natural gas has been significant, offering an opportunity to improve upon the model of Heestand *et al.*[24]. Moreover, since that time, great improvements in software science have occurred, giving us the ability to rapidly test the sensitivity and accuracy of the new model to its various parameters.

A new hypothesis has been proposed in this thesis, to verify and apply the Bates and Morrison[4]'s suggestion of the existence of two stages (phases) in LNG rollover, with different governing heat and mass transport regimes in each phase. This objective has been achieved by applying lower heat transfer coefficient and the Chilton-Colburn analogy for the mass transfer in Phase 1 and a higher heat transfer coefficient and the Reynolds analogy for the mass transfer in Phase 2. Therefore, a new model has been constructed for simulating rollover in LNG storage tanks that uses the modern equation of state (GERG-2004[3]) for the thermodynamic and transport properties of the LNG. Later, we have used this model to perform sensitivity analysis over the critical parameters of rollover, such as time to rollover and amount of boil off gas (BOG) generated to verify the new hypothesis.

The initial objectives of this research were as follows:

1. Review the fundamental issues associated with rollover through studying past simulations and identify their limitations.
2. Investigate the effects and divergence of hydrostatic stability of stratified LNG systems as the system evolves towards a rollover event.
3. Extend the definitions of key parameters used to determine hydrostatic stability and the ratio of heat to mass transfer from ones applicable to binary mixtures to definitions valid for multi-component mixtures.
4. Construct a new LNG rollover model, which predicts the LNG thermodynamic properties with the GERG-2004 equation of state[3], as a modern and successful EOS for natural gas and LNG[3].

This model uses three major software programs, REFPROPM 2009A[1], which is a version of REFPROP software developed to use in MATLAB[2], to calculate the LNG physical properties, MATLAB[2] software to solve the ordinary differential equations describing the system and Microsoft Excel to save and represent the simulation data in the form of graphs. REFPROP has been chosen due to its proven accuracy (developed by the American National Institute of Standards and Technology NIST[31]), MATLAB[2] has been chosen as a powerful mathematical software to solve the differential equations fast and accurate. Moreover, a program code written in MATLAB has the capability of converting into a standalone executable file. Finally, Microsoft Excel has been chosen to store the simulation data for further processing, better graphical presentation and statistical analysis if required.

Once the model was constructed and the investigation into the hydrostatic stability of stratified LNG systems was underway, additional research objectives were identified. These were:
5. Validate the newly developed LNG rollover model and test the new hypothesis of improvement of simulation by utilizing two heat and mass transfer regimes (Chilton-Colburn and Reynolds analogies[48]) for the following LNG rollover incidents:
    - La Spezia rollover incident

- Nantes' rollover experiment
- Partington rollover incident

6. Investigate several hypothetical (but close to real) auto-stratification rollover incidents (self-induced rollover) to derive insight about effects of nitrogen content in LNG on rollover.

1.8. Contributions of this research

After addressing the above objectives, significant contributions have been made in this study by conducting several simulations of LNG rollover in storage tanks. Specific contributions are:

1. Established a qualitative CFD model for two LNG layers in a storage tank and detect the existence of rollover Phase 1 (natural convection stage).
2. Introduced new software, developed specifically for this research, by the author in the MATLAB[2] environment and linked it to a sophisticated and accurate Thermodynamic software, REFPROP[1], using Lumped Parameter (LP) method. This code can be linked to "Tank Farm Management" software systems (TFM) to predict LNG rollover and its critical parameters such as boil-off gas (BOG) in an operating LNG tank farm or terminal.
3. The use of data from the Nantes rollover experiment, described graphically by Bates and Morrison[4], to estimate the change in heat transfer coefficient between Phase 1 and Phase 2.
4. The use of a combination of both the Chilton-Colburn and Reynolds analogies to model the mass transfer between LNG layers and improved the previous simulation done by Deshpande *et al.*[25] on the Partington rollover incident.
5. Successful simulations of several cases of Auto-stratified LNG rollover and the results of sensitivity analysis for the nitrogen content in LNG and its relationship to safe storage and rollover.

6. A safety and risk assessment review for LNG rollover, which highlighted that LNG rollover can be categorised as "extreme" and must be treated with a corresponding degree of caution by industry.

1.9. Organization of this thesis

This thesis starts with an introduction and background of the LNG process and LNG rollover in Chapter 1. In Chapter 2, the literature regarding rollover and the modelling of LNG rollover is reviewed, as is the literature on methods of calculating the parameters and physical properties required for the model. Later in Chapter 3, the hydrostatic stability analysis is extended to multi-component LNG mixtures and the results of this analysis are applied to the available LNG rollover data in the literature. The methodology of the simulation is presented in Chapter 4 and the results of the modelling and sensitivity studies are given and discuss in Chapter 5. A qualitative risk assessment on a hypothetical rollover incident in onshore LNG storage tanks is conducted in Chapter 6 and finally, conclusions from this work and recommendations for future research are given in Chapter 7. Figure 1.7, represents a schematic structure of the chapters of this thesis.
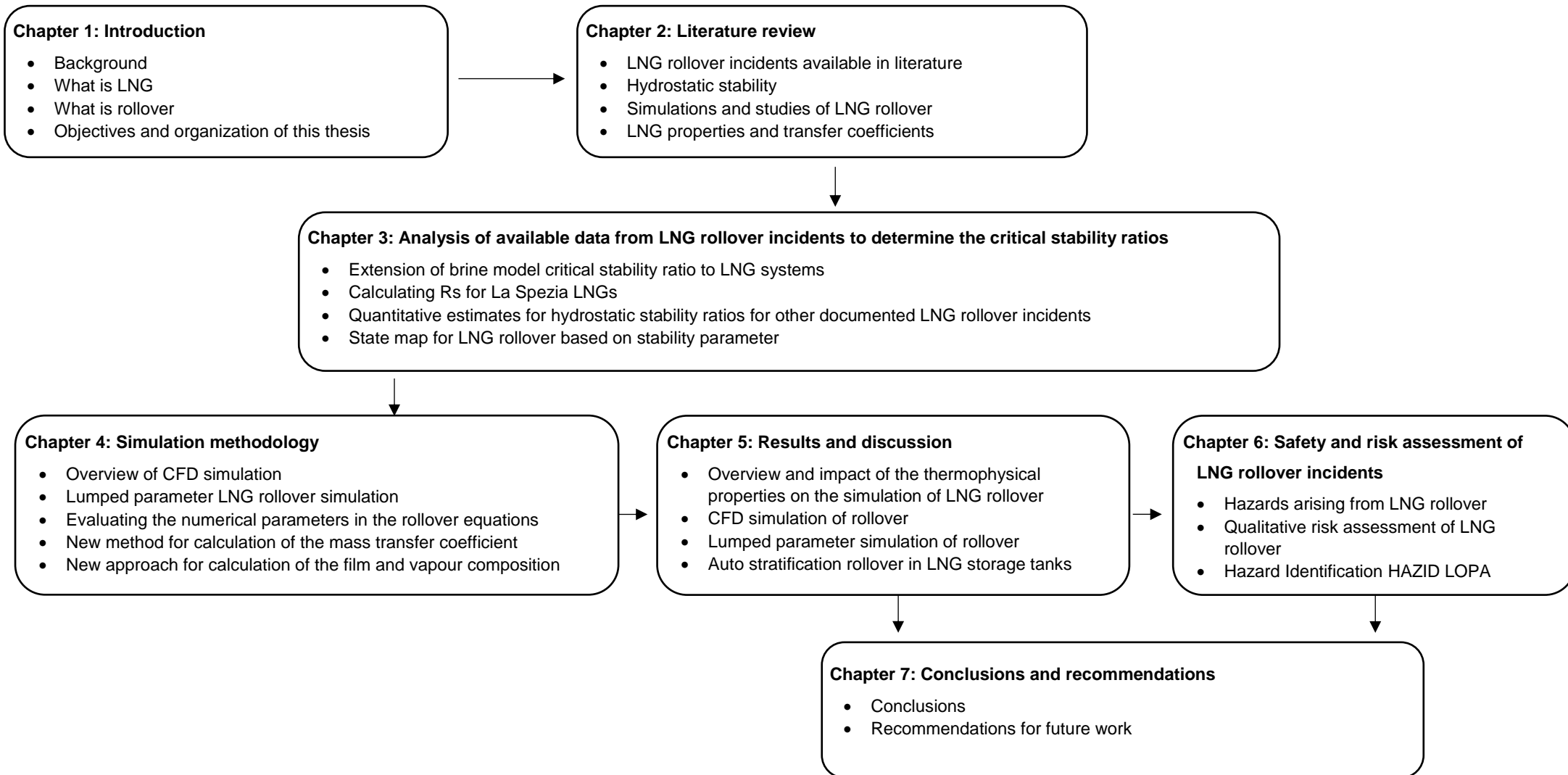
Figure 1.7: The thesis structure.

This thesis is presented in a hybrid format. Some contents of Chapters 1, 2, 3 and 4 have been already published in the AIChE journal[7] as a refereed publication, so the content has been partially re-formatted here to be consistent with the style of the thesis. Work is in progress to publish the results of Chapters 5 and 6 in a peer-reviewed journal in the near future.

Chapter 2
Literature review

2.1. LNG rollover incidents reported in the open literature:

Industrial incidents of rollover, whether caused by LNG weathering or loading LNGs from different sources, are rarely documented in the open literature. The reason is mainly for confidentiality reasons and inability to access the internal operational and commercial data of LNG companies. However, there are few companies, who have sponsored some research in conjunction with universities or independent researchers, who have published their findings, although these data are limited.

Acton and van Meerbeke[32] reviewed several incidences of LNG rollover in the LNG industry and found that over a period of 13 years from 1970 to 1982, 41 incidents occurred in 22 plants. They did not, however, discuss any technical data about rollover cases but mentioned that over half of the incidents reviewed were attributed to loading new LNG to a storage tank with an existing inventory and four were attributed to N_2-induced auto-stratification.

The most thoroughly documented occurrences of LNG rollover in the open literature are the La Spezia (Italy) incident, as reported by Sarsten[6] and the Partington incident (UK) reported by Baker and Creed[18]. In comparison, the data recorded by Sarsten[6] for the La Spezia incident contains more technical details rather than the Partington incident. The reason that the Partington rollover incident does not have enough technical details could be due to the confidentiality issues and limitations on sharing the British Gas commercial and technical data.

Other reports that discuss LNG rollover related issues, did not provide enough technical input data to simulate a rollover incident as well. Bates and Morrison[4]

also presented limited data from measurements conducted at a facility in Nantes, France. In 2013, Lukaszewski *et al.*[33] presented some information from instrumented LNG storage tanks about a rollover incident that occurred in the USA during 2007. However, none of these reports could be used for simulation of the rollover incident. A summary of attempts to simulate LNG rollover is presented in Table 2.1 below:

Note: to be loyal to the original works reviewed here, the same symbology that had been chosen by the original authors of the literature, have been used in this chapter.

Year	Reference	Model Type	Source of heat trans. coefficient	Source of mass trans. coefficient	Comparison case	$\dfrac{t_{\text{rollover}}^{(\text{predicted})}}{t_{\text{rollover}}^{(\text{observed})}}$	Comment
1971	Chatterjee and Geist	LP-Pred	Correlation (flat-plate)	Saline analogy	La Spezia (1971)	1.35	(T, x) equalization as rollover criterion
1975	Germeles	LP-Pred	Correlation (flat-plate)	Adapted saline analogy	La Spezia (1971)	1.10	Density equalization as rollover criterion
1983	Heestand et al.	LP-Pred	Correlations	Reynolds	La Spezia (1971)	0.98	Abandoned Turner's method for Reynolds analogy to match La Spezia data
1993	Shi et al.	CFD	Not used. Replaced by thermal diffusivity + convection	Not used. Replaced by mass diffusivity + convection	Freon experiments	N.A	Predicted circulation and entrainment confirmed by visualization experiments
1997	Bates and Morrison	LP (diffusive Phase 1) Parametric (convective Phase 2)	Assumed constant (diffusive phase)	Saline analogy (diffusive phase)	Nantes (1987-89)	N.A	Identified diffusive and convective phases in LNG rollover
2007	Zimmerman et al.	CFD	Not used. Replaced by thermal diffusivity + convection	Not used. Replaced by mass Diffusivity + convection	-	N.A	Transition of corner eddy mode drives interface instability
2011	Deshpande et al.	LP-Pred	Correlation	Reynolds	La Spezia (1971)	1.01	Improved description of vaporization
		LP-Pred	Correlation	Reynolds	Partington (1993)	0.01	Demonstrates Reynolds analogy not generally appropriate
		LP-Inv	Calculated from tank data	Calculated from tank data	USA (2007)	1.12	Optimization method (regression)
2013	Lukaszewski et al.	LP-Inv	Calculated from tank data	Calculated from tank data	USA (2007)	0.90	Normal equations method

Table 2.1: Summary of the lumped parameter (LP) and CFD models for LNG rollover described in the open literature. The LP models are classed as predictive (Pred) or inverse method (Inv) depending on whether the heat and mass transfer coefficients were predicted or derived from tank data. For models that were compared with rollover incidents the ratio of the predicted to observed rollover time is listed.

As mentioned above, the majority of efforts to simulate industrial incidents of LNG rollover have benchmarked their simulations against the data reported by Sarsten[6] for the La Spezia incident. Heestand et al.[24] were the first to develop a model that adequately matched the observations of the La Spezia incident.

On August 21, 1971, a LNG carrier named "Esso Brega" transferred new LNG cargo into one of the SNAM's LNG storage tanks which was already half filled with an existing LNG[6]. The new LNG cargo was loaded into the bottom of the tank, beneath the existing LNG in their storage terminal, which had a lower temperature than the new cargo. The different LNG liquids did not mix initially and formed two separate layers with different densities as a result of their different temperatures and compositions. The details of the layers' conditions and compositions are summarized in Tables 2.2 and 2.3. Approximately one and half days, after the LNG cargo transfer, a rollover incident occurred with the layers mixing suddenly, the tank pressure increased rapidly and a large amount of boil-off gas was generated. About 2,000 tonnes of LNG vapour was discharged from the tank's safety valves over a period of a few hours, which damaged the roof of the tank and consequently made the authorities evacuate the city.

Sarsten[6] reported this incident and gave operational data based on the available measurements of the tank process variables such as layer densities, temperatures and the pressure. The data showed that the LNG densities approached each other over the time prior to the rollover. He reported that the time from the start of the cargo transfer up to the start of the rollover incident was approximately 111600 seconds (31 Hours). Sarsten's report is still the most sufficiently detailed source of data for an actual LNG rollover event that is available in the open literature. It is the basis of comparison for most LNG rollover simulations. The number of studies about the LNG rollover phenomenon in the open literature is limited and thus, very little quantitative data about such events is available.

COMPONENTS	BOTTOM (CARGO) MOLE %	TOP (INITIAL HEEL) MOLE %
Methane	62.26	63.62
Ethane	21.85	24.16
Propane	12.66	9.36
i-Butane	1.20	0.90
n-Butane	1.94	1.45
i-Pentane	0.06	0.11
n-Pentane	0.01	0.05
Nitrogen	0.02	0.35
Total	100	100

Table 2.2: Initial compositions of the LNG layers in the La Spezia rollover incident[6, 24].

CONDITION	BOTTOM (CARGO)	TOP (INITIAL HEEL)
Temperature (K)	118.994	114.356
Density (kg/m^3)	545.486	541.742
Liquid depth (m)	17.831	5.029
TANK DATA		
Tank diameter (m)	49.08	

Table 2.3: Initial conditions and tank dimensions of the LNG layers in the La Spezia LNG rollover incident assumed by Heestand *et al.*[24].

In October 1993, a LNG rollover incident occurred in one of the British Gas LNG storage tanks, in Partington, UK. Baker and Creed[18] published some limited information about this incident; however, there are many inaccuracies and missing data in their report, making the simulation of the incident very hard. The most important deficiency in that report, is that they did not identify the temperature of each LNG layer, or provide any information about vapour conditions. They also stated that the tank pressure was 1.08 bar (gauge) by

mistake instead of 1.08 bar (absolute), which is the normal storage pressure in most LNG plants.

Furthermore, the composition of the LNGs and the heat leaks into the tank were not sufficiently detailed in their report, especially as there was no information about C_3^+ in the upper layer, or the heat leaks into the vapour part. They reported that 68 days after starting to add a new LNG to the existing LNG in the tank, the pressure rose rapidly until the emergency relief valves lifted and vented approximately 150 tonnes of gas into the atmosphere over the period of two hours[18]. The composition of LNGs and the tank construction data are presented in Table 2.4:

	Lower layer	Upper layer	Total
Quantity (tonnes)	18650	1900	20550
Level (m)	31.44	3.30	34.74
Tank diameter (m)	-	-	41.15
Comp (mole %)			
N_2	0.47	0.50	-
C_1	92.60	97.50	-
C_2	6.47	2.00	-
C_3^+	0.46	-	-
Molecular weight	17.14	16.30	-
Density (kg/m3)	446	433	-
Heat leak (kW)	21.505	15.495	37.0

Table 2.4: Initial conditions of the LNG layers and tank dimensions in Partington LNG rollover incident[18].

They also reported adding the new LNG over a period of 24 days, which is a very long filling procedure and unusual practice in LNG operation. It also means that although the initial filling started 68 days before the rollover, the presence of two distinguishable stratified LNG layers occurred at day 24 after completion of filling. Therefore, the actual rollover time to be considered in the simulation

should be 44 days after completion of filling, NOT 68 days from the commencement of loading.

Furthermore, they mentioned that during the first 58 days (which had 24 days overlap with the initial filling); there were 160 tonnes of LNG vented. This means that the compositions reported by them as the initial composition of LNGs are not accurate at all. The composition of both layers after 24 days of continuous filling and continuous venting cannot be what has been reported. In addition, they have 11 tonnes (18799 − 18650 = 11) discrepancy in their liquid material balance as per Table 1 and 2 on page 28 of their paper[18] as follows:

Lower layer mass = Heel mass + Phase 1 mass
                  = 17266 + 1533 = 18799 tonnes

while the reported lower layer mass is 18650 tonnes. This discrepancy could be caused by either an error in the measurement or just an inaccurate round up of the figures; however, it has a negative effect on the accuracy of the total mass and heat balance. They did not also mention anything about any existing boil-off vapour recovery system (compressors) as it is common to use vapour recovery system in long-term LNG storage.

2.2. Rollover in saline solutions

Most of what is known about rollover comes from the study of the phenomenon in saline solutions. Rollover happens naturally in the deep ocean and in volcanic lakes[15] and has been studied for about 50 years by physical oceanographers.

Thermohaline circulation, which causes temperature and salinity gradients in seawater, is one process that establishes the conditions necessary for a rollover event in the ocean. Thermohaline circulation refers to the global density and temperature driven circulation of the water in the oceans. This circulation can cause a region of the ocean or a volcanic lake to consist of warmer, higher

salinity layers below cooler, lower-salinity layers. Initially, the densities of the warmer deeper layers are larger than those of the cooler upper layers. However, the layers exchange heat and mass through double diffusive convection at their interface and, given sufficient time, their densities change until the system is no longer hydrostatically stable, which initiates the rollover.

The heat and mass transfer between the saltwater layers occur through a process known as double-diffusive convection. Normally, heat transfer by convection in fluids is driven by thermally induced density variations within the layers. However, these density variations may also be caused by gradients in the composition of the fluid.

Double-diffusive convection is a form of two-way convection, driven by two different density gradients in adjacent layers; different rates of diffusion occur within each layer because of their different physical properties[34]. Double-diffusive convection occurs in a number of systems that have multiple causes for density variations. These include convection in the oceans (as mentioned above), in magma chambers and in the sun, where temperature and helium diffuse at differing rates[35].

A particular case of double diffusive convection relevant to oceans and volcanic lakes is the formation of "salt fingers" between the water layers. A photograph of such "salt fingers" is shown in Figure 2.1. As the layers start to transfer heat and mass, a part of the liquid in the lower, more saline layer referred to as a salt finger, enters the upper layer by convection. When the salt finger enters the colder water above, it loses its heat more rapidly than it does salinity because the diffusion of heat is faster than the mass diffusion of the salt. Therefore, the salt finger becomes cooler but still rich in salt. This makes it denser than the fluid around it and causes the salt finger to sink back to the lower layer. This process continues until the bulk liquids reach the same density and mix completely[36].

Figure 2.1: Vertical cross section of salt fingers (diffusion fingers)[36].

2.3. Hydrostatic stability

The hydrostatic stability of two liquid layers is crucial to the rollover phenomenon. When modelling rollover it is necessary to understand whether the system is initially hydrostatically stable and if so, how stable are they.

In general, when there is a lower mass density fluid on the top of a higher mass density fluid, the system is hydrostatically stable. This means that if the positions of the layers are perturbed the layers will return to the original position. Conversely, if the denser liquid is on top, the system is hydrostatically unstable and the layers will move from their initial positions towards a more stable configuration[37]. Clearly, then the vertical mass density gradient has a key role in determining the stability of stratified liquids.

A mathematical relation for establishing hydrostatic stability can be derived by considering the force balance on a parcel of liquid as a function of depth. Hesselberg[37] defined the stability parameter "E", as the ratio of the vertical

acceleration "a_z" of a displaced liquid parcel to the acceleration due to gravity "g", or equivalently the ratio of the buoyancy force to the gravity force[ii].

$$E \equiv \frac{-a_z}{g}$$

(2-1)

By this definition, if E>0 then the liquid parcel will return to its original position and the system is stable. If E<0 the parcel will accelerate away from its original position and the system is unstable. Figure 2.2 shows a schematic of a liquid parcel displaced upwards rapidly by a distance δz. In its original position the density ρ, temperature T and pressure P of the parcel was the same as that of the surrounding liquid. The density, temperature and pressure of the surrounding liquid at position 2 are in general, different from those at position 1. The rapid displacement of the parcel means that there is no time for heat (or mass) transfer with the surrounding liquid. It therefore, undergoes an adiabatic expansion, causing its density and temperature to decrease because the surrounding liquid pressure is lower at position 2 by an amount $|\delta P|$.
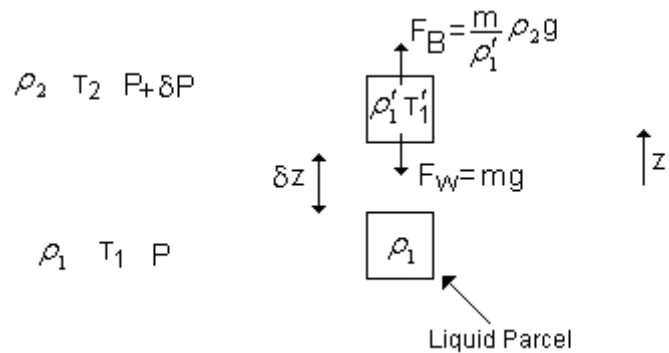
Figure 2.2: Adiabatic movement of the liquid parcel between two layers.

---

ii) **Note:** To be loyal to the original article, the same symbology has been used in this literature review chapter.

The net vertical acceleration "a_z" is given by the difference between the buoyancy force F_B and the parcel's weight F_W. In terms of E, this force balance leads to:

$$E = \frac{-a_z}{g} = -\left(\frac{\rho_2}{\rho_1'} - 1\right) = \frac{\rho_1' - \rho_2}{\rho_1'}$$

(2-2)

If the displacement is small, the densities ρ_1' and ρ_2 can be written in terms of ρ_1 with

$$\rho_2 = \rho_1 + \left(\frac{d\rho}{dz}\right)\delta z$$

(2-3)

and

$$\rho_1' = \rho_1 + \left(\frac{\partial\rho}{\partial z}\right)_{Adiab}\delta z$$

(2-4)

where the subscript "Adiab" indicates an adiabatic pathway. The full density derivative $d\rho/dz$ can be expanded in terms of the partial density derivatives with respect to pressure, temperature and solute concentration, Sand the vertical gradients of these quantities. Combined with the hydrostatic relation $dP/dz = -\rho g$, the numerator of Eq. (2-2) can then be expressed as

$$\rho_1' - \rho_2 = \left(\frac{1}{\rho_1}\left(\frac{\partial\rho}{\partial P}\right)_{T,S} - \frac{1}{\rho_1}\left(\frac{\partial\rho}{\partial P}\right)_{AdiabS}\right)\rho_1 g - \frac{1}{\rho_1}\left(\frac{\partial\rho}{\partial T}\right)_{S,P}\left(\frac{dT}{dz}\right) - \frac{1}{\rho_1}\left(\frac{\partial\rho}{\partial S}\right)_{T,P}\left(\frac{dS}{dz}\right)$$

(2-5)

Utilising the thermal and concentration expansion coefficients, α and β, together with the isothermal compressibility κ_T and adiabatic compressibility κ_{Adiab} of the liquid defined as follows

$$\alpha = \frac{1}{\rho}\left(\frac{\partial \rho}{\partial T}\right) \tag{2-6}$$

$$\beta = \frac{1}{\rho}\left(\frac{\partial \rho}{\partial S}\right) \tag{2-7}$$

$$\kappa_T = \frac{1}{\rho}\left(\frac{\partial \rho}{\partial P}\right)_T \tag{2-8}$$

$$\kappa_{Adiab} = \frac{1}{\rho}\left(\frac{\partial \rho}{\partial P}\right)_{Adiab} \tag{2-9}$$

and setting $\Delta\kappa = \kappa_T - \kappa_{Adiab}$, the stability criterion can be written as

$$E = \frac{\left(\Delta\kappa\rho g - \alpha\dfrac{dT}{dz} - \beta\dfrac{dS}{dz}\right)\delta z}{1 - \kappa_{Adiab}\rho g\delta z} \tag{2-10}$$

The term in brackets in Eq. (2-10) determines whether the system is hydrostatically stable. For LNG liquids, the key properties $\Delta\kappa$, α and β have values of about $4 \times 10^{-9}\,Pa^{-1}$, $-2 \times 10^{-3}\,K^{-1}$ and $3 \times 10^{-3}\,kgmol^{-1}$, where the concentration effect is averaged over all solute components in a methane solvent using the molal scale. (A detailed calculation of β for LNG is given in Section 3.1). The compressibility term $\Delta\kappa\rho g$ means that a liquid can support a small negative temperature gradient and/or a small concentration gradient and still remain stable. For LNG liquids, the rough magnitudes of these maximum gradients are $-1 \times 10^{-3}\,K\,m^{-1}$ and $1 \times 10^{-3}\,mol\,kg^{-1}m^{-1}$. The effect of

compressibility is so small that it can be ignored. The criterion for stability then becomes

$$-\alpha\frac{dT}{dz} - \beta\frac{dS}{dz} = 0 \Rightarrow -\alpha\frac{\Delta T}{\Delta z} - \beta\frac{\Delta S}{\Delta z} \cong 0 \qquad (2\text{-}11)$$

Multiplying through by Δz leads to:

$$-\alpha\Delta T - \beta\Delta S \cong 0 \qquad (2\text{-}12)$$

which leads to the definition of the stability ratio, R_s and the requirement for stability[7].

$$R_s \equiv \frac{\beta\Delta S}{\alpha\Delta T} \geq 1 \qquad (2\text{-}13)$$

A layered liquid system with R_s less than 1 will be hydrostatically unstable and therefore. will undergo rollover (α has a negative value in above equation).

2.4. Double-diffusive heat and mass transfer coefficients in saline solutions

Turner[5] investigated and quantified the relationship between the heat and the mass transfer for brine layers with differences in salt concentration and temperature. In several experiments with salt-water solutions, he measured the change in salinity, temperature and density of the liquids over time. He also measured the heat and mass fluxes, "H" and "F_s" between layers as a function of time. To do this he used two 12 cm thick layers of common salt solutions, in a 30 cm diameter cylindrical tank with an electrical heater under the tank's bottom. He calculated the heat transfer coefficient "h" directly based on the rate of the measured temperature change in the layers and the inlet heat flux supplied by the electrical heater using the equation:

$$H = hA\Delta T \tag{2-14}$$

The salinity of each layer was measured using a conductivity meter. The measured mass transfer of salt over time could therefore, be used to determine the mass transfer coefficient k using the equation:

$$F_s = kA\Delta S \tag{2-15}$$

where ΔS is defined by Turner[5] as change in salinity (concentration).

The reader should note that in the literature describing double diffusive mass transfer and rollover several different versions and definitions of mass transfer coefficient, k, are used. In Eq. (1-1) of this work, the species specific, mole-fraction based mass transfer coefficient, k_i, was defined. Most other workers, including Turner, have referred only to an average or overall mass transfer coefficient, based on either mass fraction (salinity)[5, 38] or mole fraction. Given the definition of concentration, S, defined in Eq. (2-5) of this work, the quantity k in Eq. (2-15) corresponds to an overall mass transfer coefficient with a concentration basis. The relationships between the different types and definitions of mass transfer coefficients are given explicitly in Appendix 1). It should also be noted that the particular type of mass transfer coefficients, heat capacities and mass flux rates used in some formulae can vary (e.g. from a molar to a mass basis) as long as the dimensions of their combination have the appropriate dimension.

Turner[5] defined the quantity $\dfrac{\beta F_s c_p}{\alpha H}$ as the ratio of the potential energy change of the upper layer due to the lifting of salt as a result of the transfer of heat over the same interval of time. Here c_p is the specific heat capacity of the solution. (Note that as Turner used a system of units with $c_p = 1$ cal/K/kg for water and thus the symbol c_p does not appear explicitly in Turner's definition of the potential energy change ratio. Furthermore, because c_p here is the specific heat capacity, F_s must be the mass flux rate. It is possible, however, to replace c_p

with the molar heat capacity, C_p forcing F_s to be the molar flux. Such a change also implicitly requires that "k" changes from a mass fraction basis to a mole fraction basis.)

In Figure 2.3, the observations of $\dfrac{\beta F_s c_p}{\alpha H}$ and $\dfrac{k c_p}{h}$ versus R_s made by Turner (Figure 5 and 7 in Turner's paper) are reproduced. (Note again the inclusion here of the specific heat capacity in the ratio of the mass to heat transfer coefficients, which was omitted by Turner because of the unit system he employed.) Turner observed that for values of R_s greater than a critical value R_c, the potential energy change ratio had a constant, stable value. For his experiments with salt solutions, the ratio value was about 0.15 for $R_c \approx 2$. Below this critical value of R_s, the potential energy change ratio increased up to a value of 1 at the limit of hydrostatic stability, $R_s = 1$. Note that Turner stated that $\dfrac{\beta F_s c_p}{\alpha H} = R_s \dfrac{k c_p}{h}$, so Figure 10(b) is the slope (derivative with respect to R_s) of Figure 2.3(b).

As a consequence of the relationship between the potential energy change ratio and R_s, Turner observed that if the value of R_s is known then the ratio of the mass transfer coefficient to the heat transfer coefficient could be calculated. Therefore, if the heat transfer coefficient can be calculated via an independent means, Turner's data could be used to determine the mass transfer coefficient.
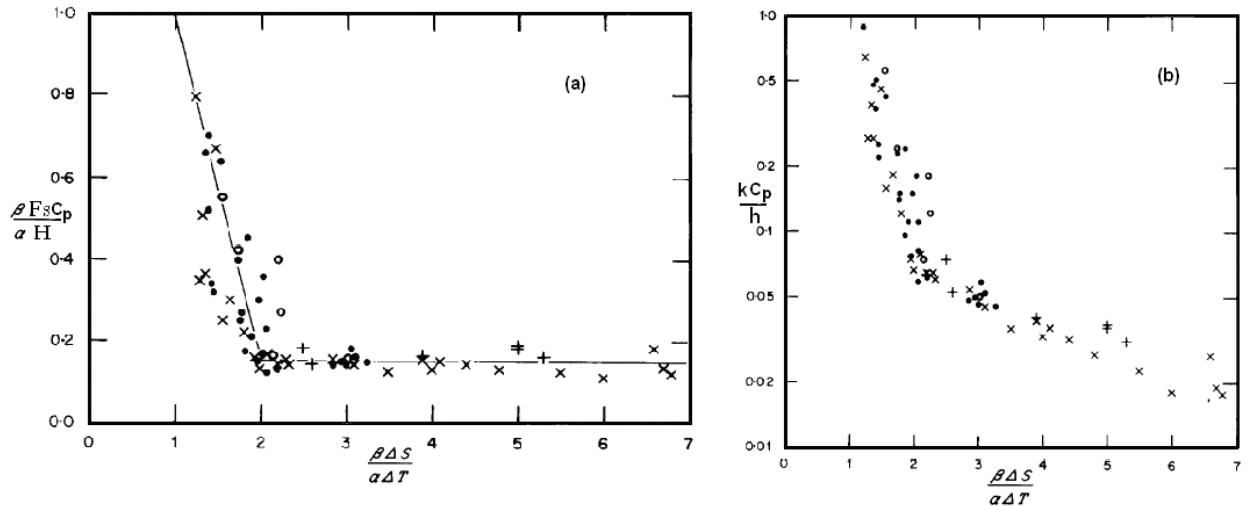
Figure 2.3: Turner's experimental results for equimolar double diffusion in salt solutions[5], (a) R_s versus potential energy ratio and (b) R_s versus the ratio of the mass and heat transfer coefficient.

Turner's observations indicate that as the hydrostatic stability of the system decreases, as quantified by R_s, the ratio of mass to heat transfer increases, reaching a maximum value of one at the point of rollover. In addition, Turner's results indicate two different regimes for the ratio k/h, with the transition occurring at $R_s = R_c$.

In 2002, Cho *et al.*[39] conducted some experiments on saline solutions for $Ra>10^7$, which differed from those of Turner by eliminating the external stirring of the mixer in the upper layer. Their results, although noisier, were consistent with Turner's observations shown in Figure 2.3. They commented that, as is apparent from Figure 2.3(b), the heat transfer rate for $R_s>3$ is about 30 times larger than the mass transfer rate.

2.5. Simulations and studies of LNG rollover

Among all simulations done so far on LNG rollover, there are two distinguishable eras. The first one is from 1972, which is when the La Spezia rollover incident happened until the successful simulation of it, presented by Heestand *et al.*[24] in 1983. The second time period starts from 1983 onwards, with the introduction of distributed parameter modelling such as CFD methods and especially with the report from Bates and Morrison[4] dividing the rollover occurrence into two phase, Phase 1 and Phase 2.

2.5.1. Simulations of the La Spezia Incident (1972-1983)

The industry standard LNG rollover model of Heestand *et al.*[24] was preceded by several models developed by other researchers. Chatterjee *et al.*[16] were amongst the first to develop a LNG rollover model in 1972 and use it to simulate the La Spezia incident. They assumed that double diffusive mass transfer had occurred between the LNG layers using an analogy with Turner's salt solution observations with minor modifications to account for the different physical properties of LNG. Their model treated LNG as a binary mixture of methane as the solvent and C_2^+ as the solute. Furthermore, Chatterjee *et al.*[16] used the equalisation of layer temperatures as the criterion for rollover. Their model predicted a much longer time to rollover than given in the Sarsten's report[6] of the La Spezia incident 151,200 seconds (42 hrs) vs. 111,600 seconds (31 hrs). This indicated that either their model's mass transfer rates were too low and/or their model's rollover criterion was inaccurate[16].

In 1975, Germeles[17] improved the model of Chatterjee *et al.*[16] by assuming density equalization as the criterion for rollover. He also used empirical equations adapted from Turners' thermohaline observations to calculate the heat and mass transfer coefficients for LNG. Germeles also treated the LNG as a two-component system and used the Clausius Clapeyron equation and the ideal solution model to describe the equilibrium of the upper liquid layer with the tank vapour. Germeles suggested an extension to Turner's observations

[Figure 10(a)] by noting that the plateau region for the potential energy ratio was believed to be related to the Lewis number, $\mathrm{Le} = \dfrac{Sc}{Pr} = \dfrac{\lambda}{\rho C_p D_{AB}}$, where λ is the thermal conductivity and D_{AB} is the molecular diffusion coefficient. Germeles stated that "*Some argue that the value of the plateau* [in Figure 10(a)] *should be equal to 1/Le; others maintain that it should be equal to* $1/\sqrt{Le}$". He assumed that the former was true and estimated Le for LNG to be one-half that of salt solutions. Thus, for $R_s > 2$, Germeles took the potential energy ratio $\dfrac{\beta F_s c_P}{\alpha H}$ for LNG to be about 0.3, twice that implied by Turner's observations.

The agreement between Germeles model and the data from Sarsten's report was better than that of Chatterjee *et al.*, but was still poor. The time to rollover in his model was 122400 seconds, which implied that the mass transfer rates being used were still too small[17].

Heestand *et al.*[24] rejected the use of Turner's observations and instead used the Reynolds analogy to calculate the mass transfer coefficient directly from the heat transfer coefficient. With "k" defined on a mole fraction basis, the Reynolds analogy is: (see Section 2.7)

$$\frac{kC_P}{h} = 1 \tag{2-16}$$

This rejection of Turner's method was on the basis that the thermohaline model did not allow enough rapid mass transfer between the layers to reconcile the observations from the La Spezia incident. Their results for the simulated temperatures and the densities of the LNG layers in the La Spezia storage tank are shown in Figure 2.4.

The general model of Heestand *et al.*[24] allowed for "N" stratified layers in a storage tank and, as shown in Figure 1.6, included a vaporizing film on the top of the upper liquid layer, which was assumed to be in thermodynamic

equilibrium with the vapour phase. They considered the LNG liquids to be multi-component rather than binary mixtures. Heestand *et al.*[24] used the SRK[30] EOS for their thermodynamic model and the equalization of layer densities as the criterion for rollover.

Heestand *et al.*[24] assumed the system to be fully turbulent (a prerequisite for using the Reynolds analogy), which meant that the Rayleigh number[48] for the liquid layers and film were greater than 10^{10}. The Rayleigh number is a dimensionless group that is a product of the Grashof number "Gr" and the Prandtl number "Pr"[48].

Ra = Pr x Gr   (2-17)

where the Prandtl number, which characterises the ratio of momentum diffusivity to thermal diffusivity, is given by

$$\mathbf{Pr} = \frac{\mathbf{C_p \mu}}{\mathbf{MW\lambda}} = \frac{c_p \mu}{\lambda}$$ (2-18)

where MW is the molar mass of the fluid. The Grashof number, which characterises the ratio of buoyancy force to viscous force, is given by

$$Gr \equiv \frac{L^3 \rho^2 g\alpha\alpha\Delta}{\mu^2} = \frac{gL^3 \Delta\rho}{\nu^2 \bar{\rho}} \quad .$$ (2-19)

Here "L" is the length scale of the layers, μ is the viscosity, ν is the Kinematic viscosity, $\Delta\rho$ is the difference between two layers' density and $\bar{\rho}$ is the average density of two layers. The second equality in Eq. (2-19), which was used extensively by Heestand *et al.*[24] is obtained by substituting Eq. (2-6) into Eq. (2-19). These and other dimensionless groups were important to and used extensively in, the rollover model of Heestand *et al.*[24]. For example, the heat transfer coefficient was estimated using correlations for the dimensionless Nusselt number defined as:

$$Nu \equiv h\, L/\lambda \qquad\qquad\qquad\qquad\qquad\qquad (2\text{-}20)$$

The Nusselt number is correlated with the Rayleigh number through the general relation

$$Nu = C\,(Ra)^{1/3} = C\,(Gr \times Pr)^{1/3} \qquad . \qquad\qquad\qquad (2\text{-}21)$$

Combining and re-arranging Eqs. (2-20) and (2-21) gives

$$h = C\frac{\lambda}{L}(PrGr)^{1/3} \qquad\qquad\qquad\qquad\qquad (2\text{-}22)$$

Heestand *et al.*[24] investigated the effects of using different literature correlations for Nu in their simulation. A summary of these correlations is given in Table 2.5. Often the correlations assumed the value of the Prandtl number was fixed at that of air, Pr = 0.7and absorbed its effect into the numerical value of the constant "C". In doing so, they simplified Eq. (2-22) further and used the following general relation to calculate the inter-layer heat transfer coefficient.

$$h = C'\lambda \left[\frac{g(\rho_U - \rho_L)}{v^2(\dfrac{\rho_U + \rho_L}{2})} \right]^{1/3} \qquad\qquad\qquad (2\text{-}23)$$

	Equation for Intercellular Nusselt number		Year	Rollover Time Secs (Hr)	Prandtl number Effect
1	$Nu= 0.0731(Ra)^{1/3}$	Globe and Dropkin[29]	1959	73400 (20.4)	Assumed
2	$Nu= 0.0556(Ra)^{1/3}$	McAdams[28]	1954	89200 (24.8)	Assumed
3	$Nu= 0.0597(Gr)^{1/3}$	Globe and Dropkin[29]	1959	102200 (28.4)	Not Assumed
4	$Nu= 0.0493(Gr)^{1/3}$	McAdams[28]	1954	119200 (33.1)	Not Assumed
5	$Nu= 0.0425(Ra)^{1/3}$	Modified by Heestand *et al.*	1983	109800 (30.5)	Assumed
6	$Nu= 0.0553(Gr)^{1/3}$	Modified by Heestand *et al.*	1983	108700 (30.2)	Not Assumed

Table 2.5: Different correlations used by Heestand *et al.*[24] for calculating the Nusselt number[48] and, thus, the heat transfer coefficient between the two liquid layers.

The variation with time of the heat transfer coefficient used in their simulation is shown in Figure 2.4. With the heat transfer coefficient determined, the simulation could proceed once the mass transfer coefficient was calculated using Eq. (2-16). Heestand *et al.*[24] noted the sensitivity of the time to rollover determined by their simulation to the method used to determine the heat transfer coefficient. Using the Globe and Dropkin[29] correlation with no value of "Pr" assumed, the predicted rollover time was 40% shorter than observed, while using the McAdams correlation[28] with Pr = 0.7 the predicted rollover time was 20 % longer than observed. Their best result (prediction of 109,800 seconds vs. observed 111,600 seconds) was obtained using a value of C = 0.0425 in Eq (2-22). The Figures showing their simulation results in their paper and reproduced here in Figure 2.4, were generated using this value of "C".

To determine the boil-off (vaporisation) rate in the assumed vaporizing film on the top of the upper liquid layer, Heestand et al.[24] assumed the presence of a Rayleigh circulation flow "F", between the upper layer and the film. This flow is also related to the Nusselt number and was previously defined by Hashemi and Wesson[40] in 1971 for LNG who used Eq. (2-21) with C = 0.3276. Heestand et al. modified the original Hashemi-Wesson correlation by expressing the Grashof number in terms of $\Delta\rho$ rather than ΔT.

$$F = 0.3276 \frac{\lambda A}{C_{PU}} \left(\frac{g(\rho_U - \rho_F)}{v^2 \kappa (\frac{\rho_U + \rho_F}{2})} \right)^{1/3} \tag{2-24}$$

From this Rayleigh flow the boil-off molar flow rate, f, was calculated from an energy balance on the film layer with no accumulation allowed.

$$f = \frac{(H_U - H_F)F + q_v}{Q} \tag{2-25}$$

Here, C_{PU} is the upper layer's molar heat capacity; ρ_F and ρ_U are the film and the upper layers' densities, respectively, λ is the upper layer's thermal conductivity, $\kappa = \frac{\lambda}{\rho c_p}$ is the thermal diffusivity, H_U and H_F are the upper layer and film enthalpies, respectively and Q is the heat of vaporization.

Heestand et al.[24] modelled the vapour in the La Spezia storage tank as being in thermodynamic equilibrium with the film. However, they stated the initial vapour composition to be simply 0.95 CH_4 + 0.05 N_2, which is inconsistent with a flash calculation of the upper liquid layer using the SRK[30] EOS. Furthermore, they stated that the initial temperature of the vapour was 122 K, which was 8 K above the stated initial upper liquid layer temperature. This is a significant inconsistency with their statement that the film and vapour were always in thermodynamic equilibrium unless initially the film had a very different

composition and temperature to the upper liquid layer. (Note the new LNG cargo was added below the upper layer, which had been in the tank for several days). In addition, they have considered a tailor-made vapour phase height of 20.42 meters in their simulation, instead of 3.96 meters mentioned as vapour height in Sarsten report[6], without any justification.
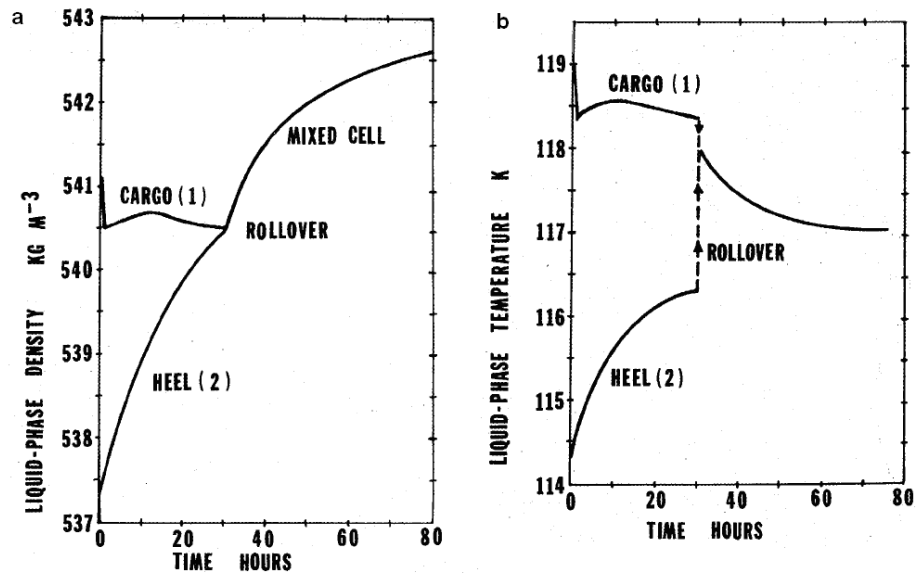
Figure 2.4(a): Heestand *et al.*[24] simulation results for density change in liquid layers and **2.4(b):** temperature change in liquid layers**.**
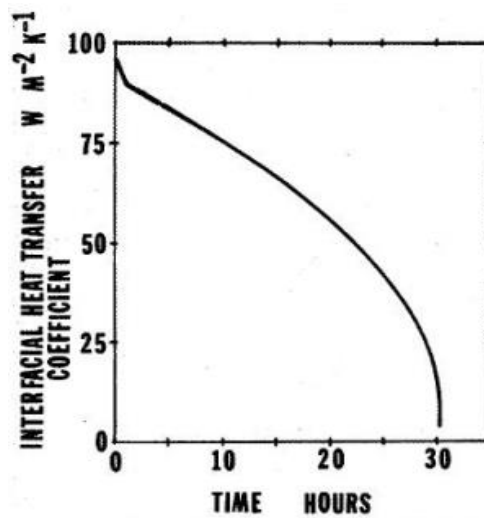
Figure 2.4(c): Heestand *et al.*[24] heat transfer coefficient change over time.

In Figure 2.5, the progress of the "traditional" rollover simulation models between 1972 and 1983 is shown in terms of their predicted time to rollover for the La Spezia incident. This progress was achieved primarily by increasing the effective mass transfer coefficient by use of the Reynolds analogy and by using the more realistic density equalisation as the criterion for rollover.
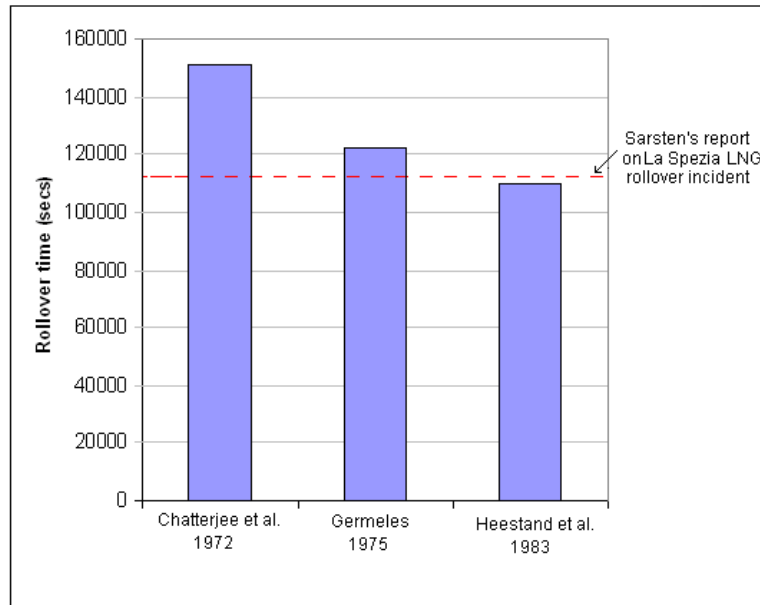
Figure 2.5: Comparison of simulations for La Spezia rollover incident time between different works until 1983[11].

2.5.2.   Further Investigations of LNG Rollover: 1993 onwards

In 1993, Shi *et al.*[41] were one of the first groups to apply distributed parameter approach such as CFD modeling of fluid dynamics to the study of mixing between stratified liquid layers of liquid nitrogen and liquid oxygen mixtures as shown in Figure 2.6. They also conducted ambient temperature experiments with liquid Freon mixtures, applying flow visualization techniques. The use of Freon meant that boil-off rates could not be measured reliably during their experiments and thus, the experiments focused only on the liquid phase motions. Their results showed that the mixing of the two stratified layers involves two stages in sequence: migration of the interface followed by rapid mixing between the remaining liquids. These observations were consistent with

63

the numerical simulations which used a free convective flow regime to model the mixing in rectangular tanks. A key conclusion of their work was that the ratio of the base to side heat flux into the tank is a major factor in determining the mode and intensity of the subsequent rollover event. This heat flux ratio determines the entrainment rates on the two sides of the (initial) interface and helps determine when it starts to migrate. The longer the period prior to migration, the greater the rollover severity in terms of layer mixing and boil-off generation. Shi *et al.*[41] pointed out that that of the incidents reviewed by Acton and Van Meerbeke[32], the amount of boil-off gas produced was quite variable and that their model was only applicable to the most dramatic (end) stages of the rollover. The ability to describe the comparatively long periods of time prior to interface migration is an essential feature of a comprehensive model for LNG rollover in industrial scenarios.
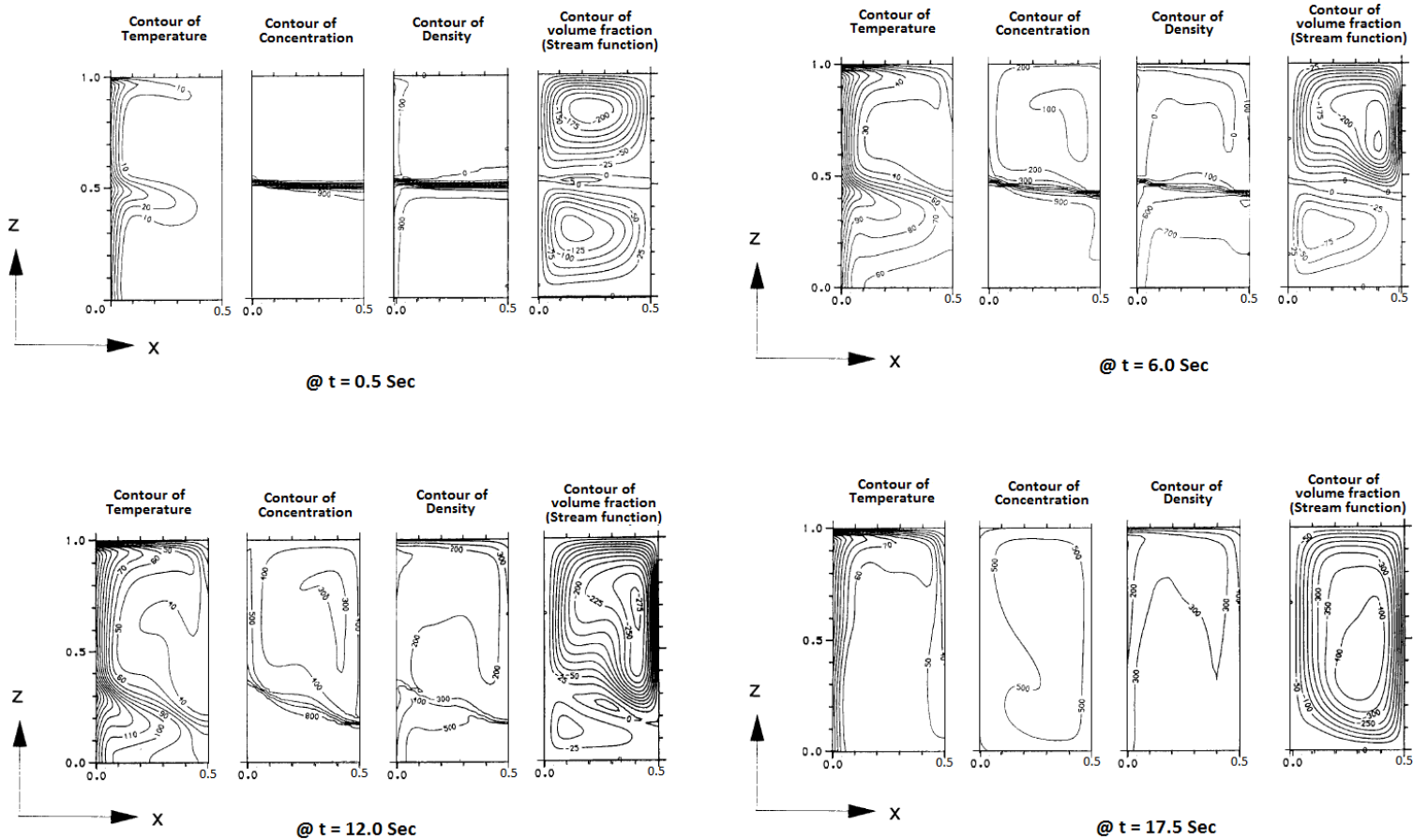
Figure 2.6: Simulation results for mixing of two initially stratified liquid layers subjected to uniform heating reported by Shi *et al.*[41].

In 1997, Bates and Morrison[4] suggested that LNG rollover in fact, occurs in two phases (Phase 1 and 2), in which the mass transfer regimes are significantly different. This suggestion was based on some graphical data included in their publication and reproduced here in Figure 2.7, which is a subset of some confidential, inaccessible data attributed to Gaz de France and "British Gas Research and Technology". Bates and Morrison[4] stated that the British Gas Research and Technology results obtained in the mid-1980s from a series of experiments with liquefied petroleum gas (LPG) were consistent with the later Gaz de France studies with LNG in large-scale tanks.

When discussing the data presented in Figure 2.7, Bates and Morrison[4] stated that in Phase 1, double diffusive convection occurred. Heat transfer from outside the tank caused the temperature of the lower layer (top line in Figure 2.7(a)) to increase steadily. There was only modest heat transfer between the layers, which resulted in a reduced rate of temperature increase for the upper layer (bottom line in Figure 2.7(a)). The density of the lower layer decreased with time, as its temperature increased. Most of the mass transfer occurred subsequently during what they called Phase 2 of the rollover process as shown in Figure 2.7(b).

In contrast with the double-diffusive convection, Bates and Morrison[4] characterized the mass transfer in Phase 2 as being driven by penetrative convection. Penetrative convection can be described as plumes from one layer entering and entraining fluid from another before returning under its own weight. The time and length scales of this convection are significantly faster and longer respectively, than in double-diffusive convection and result in the appearance of a migrating interface. As the scale of the plumes increases, the interface between the two layers moves perceptibly and the density difference between them decreases until the rollover begins[4]. The onset of this new mass transfer mechanism coincides with a significant increase in the boil-off rate, as shown in Figure 2.7(c).
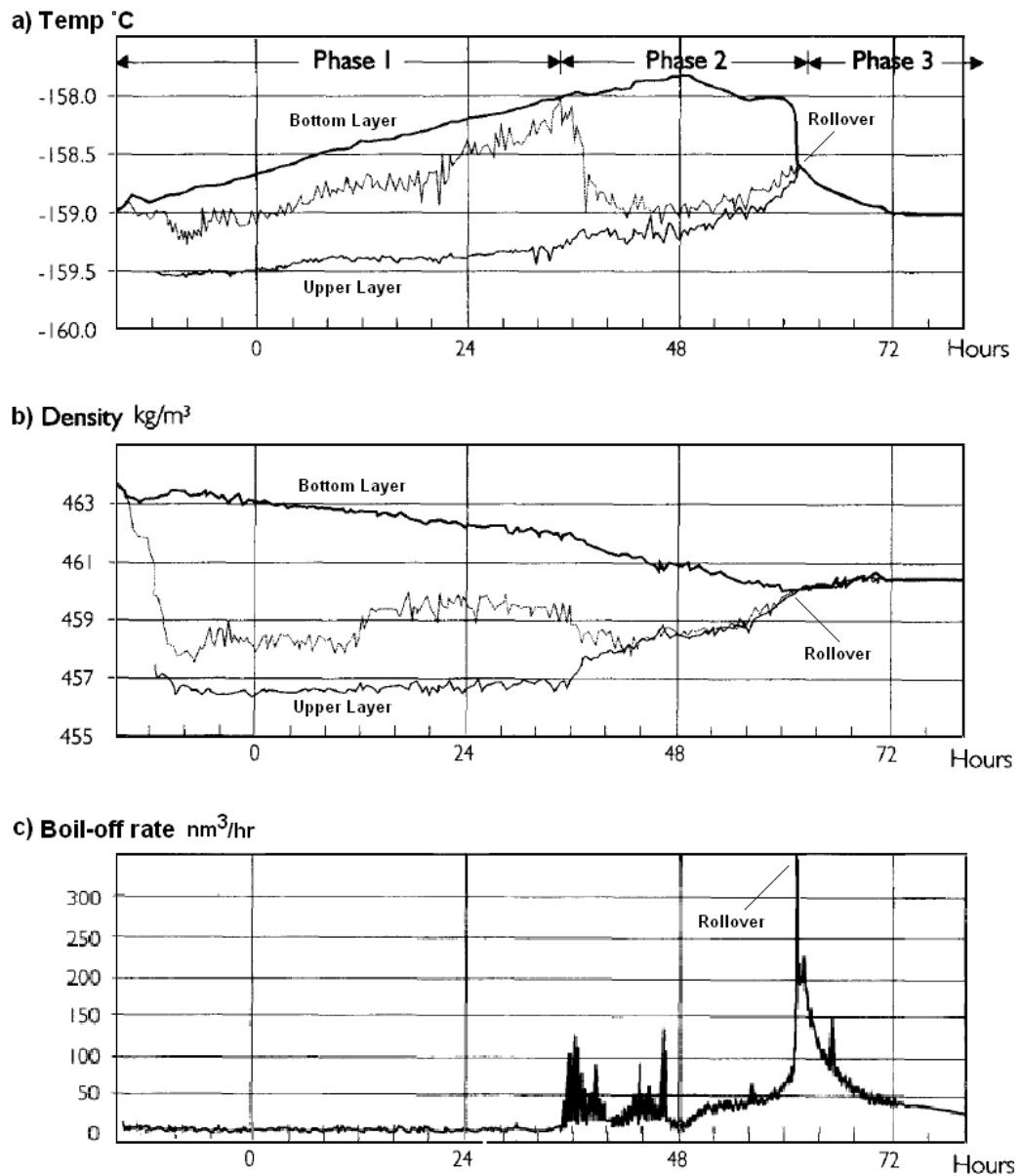
Figure 2.7: Bates and Morrison experimental results[4]. (a) Measured LNG temperatures at three levels in the tank. (b) Measured LNG densities at three levels in the tank. (c) Measured boil-off rate.

Bates and Morrison[4] also reported the development of a new model for LNG rollover, which following their experimental results was separated into the description of the two Phases. Unfortunately, many of the specific details of about this model were not reported. However, for the simulation of Phase 1, Bates and Morrison[4] used a similar model to previous researchers, presenting a series solution to the set of differential equations describing energy and

material balances in the liquid layers. Bates and Morrison[4] used a lumped parameter model to describe the data from Phase 1 when the liquid layer interface was stationary, which they then extended on a parametric basis to describe Phase 2 when the liquid layer interface was moving. Unfortunately, many of the specific details about their model were not reported. Importantly, though, as a result of the existence of Phase 2, large mass transfer coefficients were not required in the lumped parameter model of Phase 1, so it was unnecessary to utilise the Reynolds analogy.

Bates and Morrison stated that they varied h and k according to Turner's observations for the salt solutions and, during Phase 1, they conducted a sensitivity study, holding the potential energy ratio used to calculate the mass transfer flux from the heat transfer flux at 0.15, while varying the interfacial heat flux from 0.1 to 2.0 W m^{-2}. They stated that such a change in the interfacial heat flux only caused the duration of Phase 1 to vary by 16%; they defined Phase 1's duration to be such that the stability ratio R_s be greater than some critical value R_c. Unfortunately, Bates and Morrison[4] did not specify what the value of R_c for LNG systems was, although they did state that the predicted rollover times were very sensitive to the value it was assigned in the model. In contrast to the results obtained by Heestand et $al.$[24] and Deshpande et $al.$[25] for models utilising the Reynolds analogy, Bates and Morrison stated that the results of their simulation for Phase 1 were $insensitive$ to the specific values of the heat transfer coefficient used in the model.

For the Phase 2, they proposed a simple linear model linking the density difference between the two layers to their temperature difference. Apart from the data in the graphs shown in Figure 2.7, Bates and Morrison[4] did not provide any information on the initial properties of the LNG in their experiments or how the key physical properties were measured. They also did not describe how they calculated physical properties of the LNG for the models. Their model ignored the vapour phase entirely and several typographical errors appear in the manuscript. Most significantly, the recursive relation they give for computing the series coefficients used to calculate the total mass (mole) in the upper liquid

layer (Eq. (22) in the original paper[4]) does not appear to depend on any mass transfer coefficients. In addition, their series solution for energy balance refers only to the temperature difference between the two layers; knowledge of the absolute layer temperatures is required for reliable calculation of the LNG's physical properties.

The work of Bates and Morrison on LNG rollover is seminal in its identification of the two different phases and the transition from one to the other at a critical value of the stability ratio, in a fashion similar to that observed by Turner[5] for salt solutions. However, to utilise these observations in an improved lumped-parameter model of LNG rollover, it is necessary to have a numerical value for the critical stability ratio R_C, which was not provided by Bates and Morrison. Turner's data suggest that for saline solutions $R_C = 2$, but it would be surprising if the critical stability ratio for LNG systems was the same given the very different nature of the solvent and solutes. Furthermore, LNG is a multi-component mixture whereas the salt solutions contained only a single solute.

In 2006, Bashiri *et al.*[42] presented a conference paper about LNG rollover. They claimed to re-developed the model of Heestand *et al.*[24] using the Peng-Robinson[43] equation of state instead of the SRK[30] EOS used by Heestand *et al.*[24]. However, they did not give any details about their results or any improvement over the original Heestand *et al.*[24] model to Sarsten's[6] data.

In 2008, Kim *et al.*[44] presented a conference paper based on the model of Heestand *et al.*, which they used in the optimization of vent gas recovery compressors. They did not give any further details on how they calculated the LNG physical properties or the interfacial heat and the mass transfer coefficients. Their main focus was to model the operation of the boil-off gas handling systems and they used the modified Hashemi and Wesson[40] correlation to calculate the boil-off rate in a stratified LNG tank. Although their paper was not directly related to any LNG rollover, they confirmed that using the modified Hashemi and Wesson[40] correlation, gave good results for boil off gas (BOG) prediction in LNG tanks.

In 2007, Koyama *et al.*[45] conducted a computational fluid dynamics (CFD) simulation of the loading and unloading of LNG tanks to improve safety and reduce costs. They studied the process of filling the tank with different-density LNGs with numerical models and compared the model predictions with some limited operational measurements of temperature, density, volume fraction and pressure in a small tank. To develop a numerical model for tank filling in CFD environment, they used a liquid-liquid, Eulerian-Eulerian homogeneous multiphase model in ANSYS FLUENT software[46]. They monitored the volume fractions of the fluid changing over time in a turbulent environment. They used Tetra, Wedge, Pyramid type 3D meshes. The system was consisted of 62,286 nodes and 152,795 elements. They also considered standard k - ε turbulent model for their simulation.

The main selected LNG tank capacity was 200,000 m^3 with a diameter of 72 meters. The tank was modelled as bottom filled with lighter LNG using B1L type nozzle[45] based on the type of the LNG tank used in Tokyo Gas Co. They also assumed no pumping out during the filling process. Figure 2.8 shows their simulation results for change in LNG density after 30 minutes and volume fraction after 10 minutes.
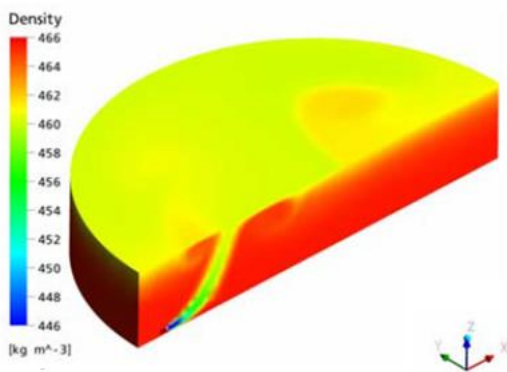
Density contour (30 min) Volume fraction contour of lighter LNG (10 min)
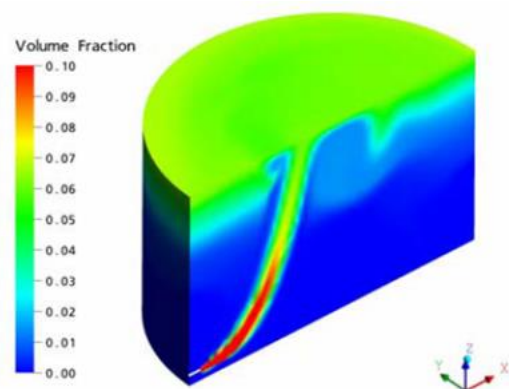
Figure 2.8: Koyama *et al.*[45] CFD simulation results for LNG tank bottom filling.

They concluded that the initial density difference, the initial LNG depth and the filling rate were directly related to any resulting stratification. However, they did not use their simulation to model any subsequent approach to LNG rollover event. Furthermore, their proposed equations for simulating LNG densities are not accurate and have large discrepancies with the mentioned densities. They did not identify how they simulate the vapour and BOG in CFD environment.

Later that same year (2007), Zimmerman et al.[47] further extended the numerical modelling approach by using the distributed parameter techniques for investigating the rollover hydrodynamic instability and its dependence on diffusion. They used hydrodynamic and heat and mass transport equations to study the stability characteristics of rollover. They conducted a linear stability analysis of the system in a transient hydrodynamic state and concluded that the transition from a "corner eddy" mode spinning down to spinning up is the driver for the rollover instability.

In building the numerical model, Zimmerman et al.[47] identified and used time and length scales to convert the equations into relations between dimensionless quantities and groups. They identified that the indicative timescale for describing the rollover in the systems they simulated was the conductive time scale. However, if this time scale were to be applied to LNG storage tanks of industrial dimensions, the characteristic rollover times would be of order 100 years.

A likely reason for the inapplicability of the results obtained by Zimmerman et al.[47] to industrial-sized tanks was the choice of the model boundary conditions selected for the nominal vapour-liquid interface in their CFD model. Zimmerman et al.[47] investigated four different boundary conditions but all of them related to variations in the heat transfer at the interface with no mass transfer permitted at the vapour-liquid boundary: The absence of a significant vaporization rate in the CFD model means that the dominant boundary effects were not included. The effect on the CFD simulation of using any of the four thermal boundary conditions was found to be small, which further suggests that

the heat loss due to vaporization and the change in composition of the upper liquid layer due to the preferential boil-off of more volatile components are the more important phenomena that need to be captured in any model of LNG rollover.

To simulate rollover in LNG storage tanks, it is clear that CFD models need to account properly for boil-off at the vapour-liquid interface and the convective Rayleigh flow that drives this boil-off. However, as Zimmerman and co-workers point out in a subsequent paper[47], extending CFD simulations to realistic LNG storage scenarios is problematic because of the need to develop the appropriate Reynolds-averaged Navier-Stokes[26] equations. Incorporating such a realistic boundary condition remains a significant challenge for future, improved CFD models of LNG rollover.

Zimmerman *et al.*[47] also identified that the hydrodynamicly interesting features of the rollover process were proceeded by a long-period dominated by diffusive mass transfer between the liquid layers, which is consistent with observations and industrial records of LNG rollover incidents. It is apparent that while CFD models offer insight into rollover, they are not yet able to fully describe events that occur in industrial LNG storage and that significant advances in multi-phase CFD modelling will be required to achieve this. Thus, lumped parameter models offer the only current prospect of analysing and/or predicting LNG rollover incidents and, in particular, the conditions and slow evolution of the system towards the brief period of hydrodynamic activity that can be described by CFD models.

Later in 2011, Deshpande et *al.*[25] described a rollover model similar to that of Heestand *et al.*[24], implemented in modern software and tested its predictions against the data reported for both La Spezia[6] and Partington[18] rollover incidents. However, they did not mention what software package they used for the simulation.

Deshpande et *al.*[25] demonstrated the sensitivities of time to rollover predictions on the various parameters used in such models. Furthermore, while they could replicate the results reported from the La Spezia incident; however, they found a large discrepancy between the predicted and observed rollover times in the case of the Partington incident (18 hours versus 68 days).

They also added some extra information to Baker and Creed's data[18] for the Partington rollover incident, such as vapour height, and deleted the components heavier than propane. They assumed the layers' temperatures to be 114 K for the lower layer and 112 K for the upper layer; however, using the SRK[30] or the GERG-2004[3] EOS, they showed that LNG with mentioned composition at 108 kPa, will become 2 phase at these temperatures. Furthermore, their referenced value for the total heat leak is much larger than what mentioned in the previous rollover incidents (~10 times more), which could be a recording or measurement error. Table 2.6 below shows their assumptions for the Partington rollover incident simulation:

Comp (mole %)	Lower layer	Upper layer
N_2	0.47	0.5
C_1	92.6	97.5
C_2	6.47	2.0
C_3	0.46	0
Density (kg/m³)	435.9	423.36
Temperature (K)	114	112
LNG level (m)	31.4	3.3
Total heat leak (kW)	21.505	15.495
Heat leakage rate (W/m²)		
Bottom	7.5	0
Sidewalls	3	3
Top	0	10

Table 2.6: Deshpande *et al.*[25] input data for Partington rollover simulation.

Using the above-mentioned data, Deshpande et al.'s [25] model reached rollover after 18 hours, much faster than the 68 days reported by Baker and Creed[18].

Figures 2.9 shows their simulation results for density and BOG evolution over time for the Partington rollover simulation. Unfortunately, they did not publish any data on the evolution of the temperature of the LNG layers and vapour phase.
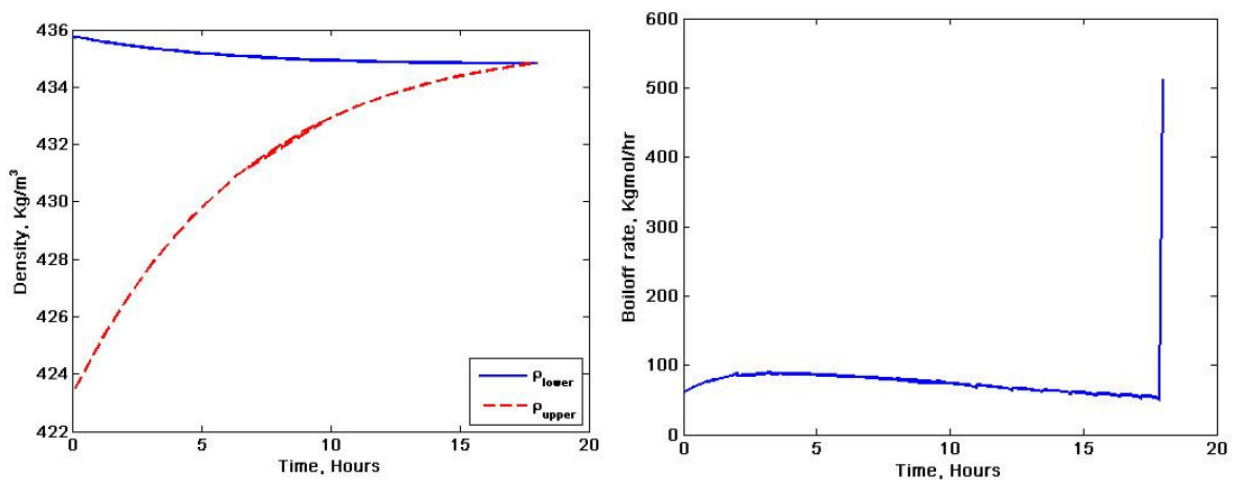
Figure 2.9: Deshpande et al.[25] results for density and BOG evolution over time for the Partington rollover simulation.

Deshpande et al.[25] identified that accurate defining of heat and mass transfers between the layers were crucial to the prediction of any rollover models. Accordingly, they extracted values of effective heat and mass-transfer coefficients by monitoring level-temperature-density data from instrumented LNG storage tanks and then regressing the model parameters to force agreement between the predicted and observed data. However, the results of Deshpande et al.[25] indicate that the generality of current rollover models appears to be effectively limited to the description of the La Spezia incident. Although their simulation for the Partington rollover incident was not successful, they revealed more data than previously reported by Baker and Creed's on British Gas rollover incident and showed that the current the data and their

assumptions such as using the Reynolds analogy for mass transfer are not sufficient to accurately model the Partington rollover.

2.6. LNG properties and transfer coefficients

As identified in Chapter 1, the calculation of the physical properties of the LNG is critical to the simulation of rollover, as is the calculation of the heat and mass transfer coefficients. In the previous section, the correlations used to estimate the heat and mass transfer coefficients were discussed in the context of previous rollover simulations. In this section, we discuss methods of physical property and mass transfer coefficient prediction not previously used in rollover simulations.

2.6.1. The Reynolds and Chilton-Colburn Analogies between heat and mass transfer

Similarities between the diffusive transport of momentum, energy and mass were first noted by Reynolds in 1874[48.] He noticed that all the fluxes in transport of momentum, heat and mass followed the general rule:

(Flux of transport property) = (diffusivity of transport property) X (gradient of transport property)

He concluded that the nature of convective heat and mass transfer was essentially the same. Reynolds assumed that the effective film thicknesses governing the transfer of momentum, energy and mass were equal. In this situation, the difference between the heat diffusivity and mass diffusivity can be neglected, which is equivalent to stating that the fluid's Prandtl number is equal to its Schmidt number. Such an assumption leads to Eq. (2-16), which was used by Heestand *et al.*[24] in their rollover simulation.

Subsequently in 1929, Chilton and Colburn[48] suggested that the thickness of the films governing heat and mass transfer were functions of the fluid's local

Reynolds number and either its Prandtl number or Schmidt number, respectively, as shown for a common case in Eqs. (2-26) and (2-27).

$$\frac{hz}{\lambda} = 0.323 Pr^{1/3} Re^{1/2} \qquad (2\text{-}26)$$

$$\frac{kz}{D_{AB}} = 0.323 Sc^{1/3} Re^{1/2} \qquad (2\text{-}27)$$

Here "$Re = \frac{z\rho\rho}{\mu}$" is the local Reynolds number, z is the film length, D_{AB} is the molecular diffusivity and v is the local fluid velocity. By assuming that the effective film thickness for the transfer of energy and mass were equal but allowing for differences in the Pr and Sc numbers, Chilton and Colburn extended the Reynolds analogy.

$$\frac{h}{vC_P} Pr^{2/3} = \frac{k}{v} Sc^{2/3} \qquad (2\text{-}28)$$

$$\frac{h}{C_P k} \left(\frac{Pr}{Sc}\right)^{2/3} = 1 \qquad (2\text{-}29)$$

The Reynolds analogy is a limiting form of the Chilton-Colburn analogy in the case of a fully turbulent system[48]. To determine the Schmidt number needed for the Chilton-Colburn analogy, it is necessary to calculate the molecular diffusion coefficient D_{AB}. In this research the Wilke–Chang equation[49], was used for this purpose so that we could implement the Chilton-Colburn analogy in the rollover simulation.

$$Sc = \frac{v}{D_{AB}} \qquad (2\text{-}30)$$

$$D_{AB} = \frac{7.4 \times 10^{-8} T \sqrt{MW_B f_B}}{\eta_B V_{bA}^{0.6}} \qquad (2\text{-}31)$$

75

Here, MW_B is the solvent molecular weight, (16.04 g/mol for methane[49]), V_{bA} is the molar volume of the solute at its normal boiling point, η_B is the solvent viscosity and f_B is an empirical association factor, which takes the values of 2.6 for water, 1.9 for methanol, 1.5 for ethanol and 1.0 for non-associated solvents.

The Chilton-Colburn analogy gives mass transfer coefficients that differ from the Reynolds analogy in two respects. First for LNG the use of D_{AB} to calculate the Schmidt number leads to component specific mass transfer coefficients, with one for each species in the LNG, whereas the Reynolds analogy (and Turner's method[5]) only give a single, overall mass transfer coefficient. Second, for LNG the term $(Pr/Sc)^{2/3}$ are approximately 10, which means that the mass transfer coefficients are an order of magnitude smaller than those obtained with the Reynolds analogy.

2.6.2.   Physical and thermophysical properties

For calculating the thermodynamic properties of the LNG an equation of state or equivalent thermodynamic model is needed. For computational reasons, most simulations use cubic equations of state, such as SRK[30] or Peng-Robinson[43] even though these equations of states are known to predict liquid densities poorly. In this work the GERG-2004 equation of state[3] was used to calculate all thermodynamic properties. This equation of state is an example of a new multi-parameter (~40) equation that has been regressed to all of the available high-quality thermodynamic data for natural gas and LNG and claims to represent that data within its experimental uncertainty.

The GERG-2004 equation of state[3] is a formulation based on the multi-fluid approximation and provides a functional form for the reduced Helmholtz energy explicit in the fluid's density, temperature and composition for a mixture. All thermodynamic properties can be calculated from appropriate derivatives of the Helmholtz energy function. The GERG-2004 equation of state has been adopted recently as the reference equation of state for natural gas and LNG by

the Groupe Europeen de Recherché Gazieres (GERG) who commissioned its development[3]. As the review of the modern multi-parameter GERG-2004 equation of state is not the objective and the main focus of this thesis, the reader is referred to Span *et al.*[50] for further information than above.

This equation of state has been implemented both as an add-in function for Microsoft Excel and also in the software REFPROP[1] and its link to MATLAB, which is called REFPROPM[1]. A slight difference was found in the values of the properties calculated using the two implementations and ultimately utilized the REFPROPM[1] version for all the results presented in this work.

The REFPROPM[1] software allows the computation of transport properties natural gas mixtures and pure components. For the mixtures, the model used by REFPROPM[1] to calculate the thermal conductivity and viscosity is based upon the modified Ely-Hanley method[51], which is an extended corresponding states model. It should be noted that the methods used to calculate the LNG's viscosity and thermal conductivities in previous simulations were not described. For example, Heestand *et al.*[24] used a constant value for these transport properties but did not state where they came from.

After defining the physical properties of LNG and transport coefficients, we need a criterion for the occurrence of rollover. Most of the previous attempts to simulate LNG rollover, used equalization of densities as rollover criteria; however, in this study, the more accurate stability ratio R_s has been used in the simulation of rollover. This approach will be discussed in Chapter 3.

This Chapter reviewed the accessible data and efforts done so far to describe and simulate the LNG rollover event. Lack of agreement between the recorded data and the majority of proposed models, especially the latest simulation of Deshpande *et al.*[25] with the recorded data of Baker and Creed[18], showed the importance of having a rigorous and better approach to model and simulate the LNG rollover. Furthermore, although in some works, there is a limited reference to the auto stratification rollover, no operational data and model is available in the open literature for any auto stratification rollover event.

Most importantly, the significance of accurate modelling of the physical and thermophysical properties, as well as the approach taken towards modelling of the heat and mass transfer regime, have been highlighted. In general, lack of reliable recorded data on actual LNG rollover incidents in the open literature is another major deficiency towards an accurate modelling, as there are not many references available for comparison and validation of the proposed models.

Chapter 3

Analysis of available data from Liquefied Natural Gas rollover incidents to determine the critical stability ratios

This chapter is an adapted version of the journal article by P. Arjomandnia *et al.* published in the AIChE journal[7] in 2013. While some headings from the journal article have been retained, the figures, equations, tables and references have been renumbered to be in line with the thesis format.

As described in Chapter 2, Turner's observations[5] quantifying the relationship between diffusive heat and mass transfer were obtained for binary mixtures of salt and water. One of the questions addressed in this research was whether the binary mixture stability criteria is applicable to multi-component systems. Answering this question leads to the identification of the research objective 3 given in Section 1.7. In this chapter, a rollover criterion consistent with the observations of Turner but tailored for multicomponent mixtures is developed, the result of which is shown in a State map, Figure 3.1 at the end of the chapter.

To develop Figure 3.1, it was first necessary to generalize some of the concepts and definitions previously given for binary mixtures and extend them to cover multi-component mixtures as discussed below:

3.1. Extension of Turner's model to LNG systems

3.1.1. Calculating R_s for the La Spezia LNGs as pseudo binary mixtures

There are two contributions to the stability ratio: the effect of the temperature gradient on the density gradient (the denominator in Eq. (2-13)) and the effect of the concentration gradients on the density gradient (the numerator in Eq. (2-

13)). The former can be calculated directly using the known mixture composition and an equation of state for the LNG to determine the volume expansivity -α (see Eq. (2-6)). The latter requires a more involved investigation of the effect of changes in composition on the mixture's density. This is most easily done by treating the mixture as a pseudo-binary solvent-solute system. The question is whether this simplistic treatment gives an adequate result.

The volume expansivity, -α (see Eq. (2-6)) for the upper and lower LNG layers were calculated directly from the initial compositions, temperatures and pressure using the GERG-2004 EOS in REFPROPM to be 2.34×10^{-3} K^{-1} and 2.31×10^{-3} K^{-1}, respectively. (For comparison, the value -α for pure liquid methane at approximately the La Spezia temperature and pressure is 3.5×10^{-3} K^{-1}).

For the purpose of calculating R$_s$, the average value $\alpha = -2.3 \times 10^{-3}$ K^{-1} was used both for the initial and subsequent hydrostatic stability analyses because its variation with temperature and composition over the 30 hours prior to rollover was negligible. The initial product of $\alpha \Delta T$ for the La Spezia system was 0.0108.

To establish whether treating LNG as a pseudo-binary mixture is a satisfactory approximation, the effect of composition gradients on the stability ratio was evaluated by considering the La Spezia LNGs as mixtures of methane plus a pseudo-component given the name C$_2{}^+$. The LNG compositions were converted from a mole fraction basis into molal concentrations, with methane as the solvent. The molal scale was selected in preference to the molar scale of concentration for its ease of use in performing the necessary calculations; molal concentrations are temperature independent and the difficulties in converting the reported mole fractions into a volume of solution are significant in comparison with the effort required to calculate just the mass of solvent.

It is convenient to establish some standard relations between the molal concentration and the mole fraction composition of a mixture. To do this we first consider an LNG sample containing 1 kg of methane (MW_{CH4} = 16.043 g/mol).

The number of moles of methane and the total number of moles in this sample are

$$n_{CH_4} = \frac{1000}{16.043} = 62.33 \text{ moles} \tag{3-1}$$

$$n_{total} = \frac{n_{CH_4}}{X_{CH_4}} \tag{3-2}$$

The number of moles, n_i of the "i^{th}" solute component is given by

$$n_i = X_i n_{total} = X_i \frac{n_{CH_4}}{X_{CH_4}} \tag{3-3}$$

where X_i is the mole fraction of component "i". The molality of component "i" will thus be:

$$S_i = \frac{n_i}{m_{CH4}} = (\frac{X_i}{X_{CH_4}})(\frac{n_{CH_4}}{MW_{CH_4} n_{CH_4}}) = (\frac{X_i}{X_{CH_4}})(\frac{1}{MW_{CH_4}}) \tag{3-4}$$

Here m_{CH4} is the mass of methane, which for these calculations is 1 kg. The difference in molal concentrations for a solute species between two different LNG samples, each with the same mass of methane, is therefore:

$$\Delta S_i = S_i^{(2)} - S_i^{(1)} = (\frac{X_i^{(2)}}{X_{CH_4}^{(2)}} - \frac{X_i^{(1)}}{X_{CH_4}^{(1)}})(\frac{1}{MW_{CH_4}}) \tag{3-5}$$

where the superscripts (1) and (2) identify the two LNG samples.

To calculate the value of the concentration expansion coefficient(s) it is necessary to vary the concentration of (one of) the solute(s) and then evaluate the change in the mixture's mass density. This is achieved by varying the

number of moles of component "i" by a small amount, δn_i, while keeping the amount of methane solvent constant. It is convenient to establish the relationships between δn_i and the new mole fraction compositions before and after this hypothetical addition is done. The change in the solute concentration is simply:

$$\delta S_i = \frac{\delta n_i}{m_{CH4}} \tag{3-6}$$

Once δn_i is added to the solution, the new mole fractions are given by

$$X_{CH_4}^{(2)} = \frac{n_{CH_4}^{(1)}}{n_{total}^{(2)}} = \frac{n_{CH_4}^{(1)}}{n_{total}^{(1)} + \delta n_i} \tag{3-7}$$

$$X_i^{(2)} = \frac{n_i^{(1)} + \delta n_i}{n_{total}^{(1)} + \delta n_i} \tag{3-8}$$

$$X_j^{(2)} = \frac{n_j^{(1)}}{n_{total}^{(1)} + \delta n_i} \tag{3-9}$$

For example, adding 0.1 mol of ethane to 1 kg of methane at 114 K and 0.13 MPa, changes X_{CH4} from 1 to 0.9984 CH_4 and X_{C2H6} from 0 to 0.0016. The mass density of the pure methane changes from 418.4103 to 418.8902 kg/m^3 for the mixture. Using Eq. (2-7), we can calculate β for this case as:

$$\beta = \frac{1}{\rho}\left(\frac{\Delta\rho}{\Delta S}\right) = (\frac{1}{418.4103})(\frac{418.8902 - 418.4103}{0.1}) = 0.0114 \text{ kg/mol}$$

To calculate β for a multi-component LNG mixture by treating it as a binary mixture, the concentration of a heavier single pseudo-component called C_2^+ must be evaluated from the specified LNG component mole fractions. Changes in the concentration of this pseudo-component must then be converted back

into new mole fractions for all the real components. This requires an additional constraint; specifically, it is assumed that the Δn_{C2+} is the equivalent of varying all the (actual) solute species in a ratio equivalent to their initial mole fractions.

For the case of the La Spezia LNGs, addition of 0.1 mol/kg of C_{2+} changes the composition of the upper layer from 0.6362 CH_4 + 0.3638 C_{2+} to 0.6356 CH_4 + 0.3644 C_{2+} and causes the density to change from 536.9516 to 537.1266 kg/m^3. For the lower layer the composition changes from 0.6226 CH_4 + 0.3774 C_2^+ to 0.6219 CH_4 + 0.3781 C_2^+ and the density changes from 541.0316 to 541.2038 kg/m^3. Thus, if the La Spezia LNGs are treated as binary mixtures, β has the value of 3.25×10^{-3} kg/mol for the upper layer and 3.18×10^{-3} kg/mol for the lower layer, which gives the average value of 3.22×10^{-3} kg/mol. The results are shown in Table 3.1 and Table 3.2.

Component	Initial Mole Fractions		Component	New mole fraction due to addition of 0.1 mol/kg C_2^+	
	Bottom	Top		Bottom	Top
methane	0.6226	0.6362	methane	0.6219	0.6356
nitrogen	0.0002	0.0035	C₂+	0.3781	0.3644
ethane	0.2185	0.2416			
propane	0.1266	0.0936			
butane	0.0314	0.0235			
isobutane	0	0			
pentane	0.0007	0.0016			
isopentane	0	0			

Table 3.1: Initial and new composition of La Spezia LNGs due to addition of 0.1 mol/kg of C_2^+ solute.

	Initial Condition		New Condition	
T (K)	118.997	114.355	118.997	114.355
P (MPa)	0.15	0.131	0.15	0.131
ρ (kg/m^3)	541.0316	536.9516	541.2038	537.1266
$\Delta\rho$ (kg/m^3)			0.1722	0.1750
$\Delta\rho/\rho$			0.00031	0.00032
β (kg/mol)			0.00318	0.00325
Average β (kg/mol)			0.0032	
S_{top} - S_{bot}			-2.14018	
$\beta(S_{top}$ - $S_{bot})$			-0.00689	
$\alpha(T_{top}$ - $T_{bot})$			0.01077	

Table 3.2: Calculation of β due to 0.1 mol/kg change in the initial concentration of each solute for La Spezia incident initial condition.

With these values of α, β, ΔS and ΔT, the system's value of R_S can be calculated and is equal to 0.63. This means that the system is hydrostatically unstable at the initial condition, which is inconsistent with the observations reported by Sarsten[6]. Clearly the assumption that LNG can be treated as a binary mixture for the purpose of rollover simulation is a very poor one.

3.1.2. Quantitative estimates of the hydrostatic stability ratios for other documented LNG rollover incidents

Clearly, to reliably evaluate the hydrostatic stability of a multi-component mixture like LNG, the individual effect of each solute component must be considered. Such an extension begins by defining a concentration expansion coefficient for each solute:

$$\beta_i \equiv \frac{1}{\rho}\left(\frac{\partial\rho}{\partial S_i}\right) \to \beta_i \cong \frac{1}{\rho}\left(\frac{\Delta\rho}{\Delta S_i}\right) \tag{3-10}$$

The solute specific β_i quantify the fractional change in the mixture's mass density caused by a small change in that solute's concentration. The total effect

of solute concentration on the mixture density is then the sum of the contributions of each species. The implication of this extension on the requirement for hydrostatic stability is given by the following modification to Eq. (2-10):

$$E = \Delta\kappa\rho g - \alpha\frac{\Delta T}{\Delta Z} - \sum_i \beta_i \frac{\Delta S_i}{\Delta Z} = 0 \qquad (3\text{-}11)$$

Since $\Delta\kappa \approx 0$, the effects of compressibility can be ignored and thus for an arbitrary length scale, the stability ratio becomes

$$R_S = \frac{\sum_i \beta_i \Delta S_i}{\alpha\Delta T} = \sum_i R_{S,i} \qquad (3\text{-}12)$$

In Eqs. (3-10) to (3-12) the index refers only to solute species and in Eq. (3-12) we introduce the component specific stability ratio, $R_{s,i}$. It should be noted that while R_s is defined to be positive, the $R_{s,i}$ are not necessarily; the contribution of one component's concentration distribution can in principle be offset by that of another component. To calculate the initial hydrostatic stability of the La Spezia LNGs using this multi-component model, the calculation done above is repeated but instead of a single value of β, five component specific values of β_i must be evaluated. This is achieved by varying the number of moles of each solute component by $\delta n_i = 0.01$ mol in a hypothetical sample of the LNG containing 100 kg of methane, while holding the number of moles of each other solute component constant. The resulting mole-fraction composition of the modified LNG is calculated and then the mass density of (each) new LNG is calculated at the same temperature and pressure, using the GERG-2004[3] EOS. The results of these calculations are shown in Table 3.3.

This analysis shows that the contribution over changes in concentration to changes in mixture density is not equal for all components as assumed in the pseudo-component binary model. The values of the β_i vary from 2×10^{-3}

kg/mol for C_2H_6 to 8×10^{-3} kg/mol for C_5H_{12}. There is also some dependence on mixture composition and temperature apparent as the values of the β_i are slightly different for the upper and lower layers. The differences range from 3×10^{-4} kg/mol for C_2H_6 to 6×10^{-4} kg/mol for C_5H_{12}. For the purpose of calculating R_s, the average value of β_i for the two layers was used for each solute.

To calculate the hydrostatic stability ratio, the differences in solute concentration between the two layers, ΔS_i, must be evaluated, which can be determined from the differences in layer mole fraction compositions using Eq. (3-5). The results are shown in Table 3.3. Combining each of the ΔS_i with the β_i and then with $\alpha \Delta T$ for the two layers gives the initial hydrostatic stability ratio for the La Spezia LNGs.

Component being varied:	Nitrogen New Mole Fractions		Ethane New Mole Fractions		Propane New Mole Fractions		Butane New Mole Fractions		Pentane New Mole Fractions	
	Bottom	Top	Bottom	Top	Bottom	Top	Bottom	Top	Bottom	Top
methane	0.62254	0.63614	0.62254	0.63614	0.62254	0.63614	0.62254	0.63614	0.62254	0.63614
nitrogen	**0.00030**	**0.00360**	0.00020	0.00350	0.00020	0.00350	0.00020	0.00350	0.00020	0.00350
ethane	0.21848	0.24158	**0.21858**	**0.24168**	0.21848	0.24158	0.21848	0.24158	0.21848	0.24158
propane	0.12659	0.09359	0.12659	0.09359	**0.12669**	**0.09369**	0.12659	0.09359	0.12659	0.09359
butane	0.03140	0.02350	0.03140	0.02350	0.03140	0.02350	**0.03150**	**0.02360**	0.03140	0.02350
isobutane	0	0	0	0	0	0	0	0	0	0
pentane	0.00069	0.00159	0.00069	0.00159	0.00069	0.00159	0.00069	0.00159	**0.00079**	**0.00170**
isopentane	0	0	0	0	0	0	0	0	0	0

	Bottom	Top	Bottom	Top	Bottom	Top	Bottom	Top	Bottom	Top
Number of moles total (2)	100.126	97.986	100.126	97.986	100.126	97.986	100.126	97.986	100.126	97.986
T (K)	118.997	114.355	118.997	114.355	118.997	114.355	118.997	114.355	118.997	114.355
P (MPa)	0.15	0.131	0.15	0.131	0.15	0.131	0.15	0.131	0.15	0.131
ρ (kg/m^3)	**541.046**	**536.968**	**541.041**	**536.963**	**541.057**	**536.979**	**541.071**	**536.994**	**541.074**	**536.997**
$\Delta\rho$ (kg/m3)	0.0144	0.0164	0.0096	0.0111	0.0249	0.0274	0.0393	0.0425	0.0421	0.0453
$\Delta\rho/\rho$	0.00003	0.00003	0.00002	0.00002	0.00005	0.00005	0.00007	0.00008	0.00008	0.00008
β_i (kg/mol)	0.0026	0.0030	0.0017	0.0020	0.0046	0.0050	0.0072	0.0078	0.0077	0.0083
Average β_i (kg/mol)	0.0028		0.0019		0.0048		0.0075		0.0080	
ΔS_i (mol/kg)	0.3228		1.7956		-3.5041		-0.8412		0.0866	
$\beta_i\Delta S_i$	0.0009		0.0034		-0.0169		-0.0063		0.0007	

Table 3.3: New mole fractions due to 0.01 mol/kg change in the initial concentration of each solute in the La Spezia LNGs. The original compositions are listed in Table 2.2[7].

$$R_S = \frac{\sum\limits_i \beta_i \Delta S_i}{\alpha \Delta T} = \frac{0.0009 + 0.0034 - 0.0169 - 0.0063 + 0.0007}{-0.0023 \times 4.642} = 1.70$$

An initial R_s of 1.7 for the La Spezia fluid is consistent with Sarsten's observations[6]. However, it is notably less than the critical value of $R_s = 2$ observed for saline systems by Turner[5]. If Turner's value of R_c were assumed to apply to LNG, then in terms of Bates and Morrison[4] model of LNG rollover, the initial La Spezia system was already in "Phase 2" with migrating interfaces rather than the double-diffusive mass convection.

However, Turner's observations and the results of Bates and Morrison[4] indicate that for $R_s > R_c$ (Phase 1), the ratio of heat to mass transfer is essentially independent of R_s. Therefore, to define the situation, which Phase 1 turns into Phase 2, a critical first step is to establish R_c.

Unfortunately, Bates and Morrison[4] only published graphical data illustrating their Phase 1 and Phase 2 concepts for LNG rollover. The graphs showed time series data for the densities and temperatures of two LNG layers as they approach hydrostatic instability with rollover occurring at about 60 hours after the measurements started. On these graphs they indicated that Phase 1 lasted from t = 0 to 36 hours and Phase 2 lasted from t = 36 to 60 hours. However, although they made reference to Turner's concept of a critical stability ratio governing the transition from Phase 1 to 2, Bates and Morrison[4] did not give numerical values of R_s or even the LNG compositions for the data they show. However, at constant pressure any difference in density between two LNG samples must be due to differences in their temperature and/or solute concentrations. The effect of small changes ΔT and ΔS_i can be related to the fractional density difference through the equation:

$$\frac{\Delta \rho}{\rho} = \alpha \Delta T + \sum_i \beta_i \Delta S_i \tag{3-17}$$

Since the thermal expansion coefficient α is approximately constant for all LNG mixtures, it is therefore, possible to estimate the magnitude of $\sum_i \beta_i \Delta S_i$ and thus the value of R_s from the graphical density and temperature data provided by Bates and Morrison[4].

For example, the lower LNG layer in Figure 2.7 has at t = 0 a density of 463 kg/m^3 and a temperature of -159 C while the upper LNG layer has a density of 456.75 kg/m^3 and a temperature of -159.5 °C. The fractional density difference between the upper and lower layers is -0.0135 and the temperature difference is -0.5 K. Assuming that α = -0.0023 K^{-1}, Eq. (3-17) can be re-arranged to give $\sum_i \beta_i \Delta S_i$ = -0.0147. Thus, the initial hydrostatic stability ratio for the Bates and Morrison LNGs can be calculated as $R_s \approx 12.6$.

In Table 3.4, the calculation is repeated for t = 36 hours (the end of Phase 1) and t = 56 hours, which is approximately three-quarters of the way through Phase 2. The transition from Phase 1 to 2 can be inferred to occur at a critical value of approximately $R_s \approx 5$, which is significantly higher than the critical value of 2 observed by Turner in saline solutions. In fact, the calculation at t = 56 hours gives $R_s \approx 2.4$, which is still significantly larger than Turner's critical value, even though Phase 2 is nearing completion.

	t=0 Hours		t=36 Hours		t=56 Hours	
	Bottom	**Top**	**Bottom**	**Top**	**Bottom**	**Top**
T (K)	114.15	113.65	115.15	113.9	115.15	114.15
ρ (kg/m^3)	462.97	456.82	461.52	456.54	459.64	458.09
$\rho_{top} - \rho_{bot}$	-6.15		-4.98		-1.55	
$(\rho_{top} - \rho_{bot})/\rho$	-0.0133		-0.0108		-0.0034	
$T_{top} - T_{bot}$	-0.50		-1.25		-1.00	
$\alpha(T_{top} - T_{bot})$ (1/K)	0.00116		0.00290		0.00232	
Estimated $\Sigma\beta i\Delta S_i$	-0.01466		-0.01372		-0.00558	
Estimated R_S	12.64		4.73		2.40	

Table 3.4: Calculation of assumed LNG physical properties corresponding to Bates and Morrison's data[4].

Turner's observations also coupled the ratios of heat and mass transfer to the stability ratio, which Bates and Morrison[4] related to the different mass transfer regimes in the two Phases. It is possible to estimate the relative magnitude of heat and mass transfer from the data of Bates and Morrison[4] but only if one assumes a composition for each of the initial LNG layers. The assumed compositions are constrained; however, by the reported densities and temperatures. For each layer, the GERG-2004 EOS was used with an assumed composition, an assumed pressure of 0.15 MPa and the reported temperature to calculate the LNG density.

This was compared with the reported density and the composition was adjusted manually. This process was guided by some simple principles: the components in the LNG were limited to methane, ethane, propane, butane and nitrogen; and given the mole fraction of methane was chosen to be quite high because the reported mass density of 460 kg/m^3 suggested a lean LNG. The assumed compositions chosen are listed in Table 3.5 and in comparison with the LNG, compositions listed in Table 1.1 are quite representative of a modern LNG.

	t =0 Hours		t=36 Hours		t=56 Hours	
	Bottom	**Top**	**Bottom**	**Top**	**Bottom**	**Top**
	Mole Frac.	**Mole Frac.**	**Mole Frac.**	**Mole Frac.**	**Mole Frac.**	**Mole Frac.**
Methane	0.8630	0.8970	0.86334	0.89666	0.87269	0.88731
Nitrogen	0.0050	0.0050	0.0050	0.0050	0.0050	0.0050
Ethane	0.1090	0.0690	0.1086	0.0694	0.0976	0.0804
Propane	0.0200	0.0210	0.02000	0.02099	0.020285	0.020715
Butane	0.0030	0.0080	0.00305	0.00795	0.004425	0.006575
isobutane	0	0	0	0	0	0
Pentane	0	0	0	0	0	0
Isopentane	0	0	0	0	0	0
Sum	1.0000	1.0000	1.0000	1.0000	1.0000	1.0000
P (MPa)	0.15	0.15	0.15	0.15	0.15	0.15
T (K)	114.15	113.65	115.15	113.9	115.15	114.15
EOS α [per K]	0.00230	0.00233	0.00231	0.00231	0.00231	0.00231
EOS C_p (J/molK)	57.38	57.33	57.47	57.35	57.40	57.31
EOS ρ (kg/m³)	462.97	456.82	461.51	456.54	459.64	458.01
Measured ρ (kg/m³)	463	456.75	462	457	460.5	459
Fractional density difference	-0.0135		-0.01082		-0.00326	

Table 3.5: Assumed LNG compositions chosen to represent the Bates and Morrison LNGs by matching the reported densities.

At t = 0, the densities obtained from GERG-2004 EOS for upper and lower layers are 462.97 and 456.68 kg/m³, which are very close to the measured values of 463 and 456.75 kg/m³. It shows that the assumed LNG compositions are reasonable. (The calculated volume expansivities for these assumed compositions are also consistent with the value of -0.0023 K⁻¹ assumed above.)

Once the initial LNG compositions were assumed, the relative effects of heat and mass transfer on the LNG mass density were assessed. At t = 36 hours, the temperatures for the two LNG layers were used with the original compositions and the GERG-2004 EOS to calculate a density. Then the compositions were modified to force the EOS density to match the reported

density at t = 36 hours. The composition changes were constrained to be representative of double diffusive convection in that each layer's mole fraction for a given species changed by an amount with the same magnitude but opposite sign, towards the average value for that component for the two layers. The results of these calculations at t = 36 and 56 hours are also shown in Table 3.5.

For the period of t = 0 to t = 36 hours (Phase 1), the compositions remained fairly constant and the temperature change was enough to account for almost all of the density change. This suggests that virtually no mass transfer occurred in Phase 1, with only about 2% of the total possible mass transfer required to equalize the layers' compositions. For the period of 36 hours to 56 hours (three-quarters of Phase 2), the temperature change is small and in isolation would leave the density virtually unchanged. It is necessary to have significant mass transfer during this time to achieve the observed change in density. The calculated change in composition is over 50% of the total change required to equalize the layers' compositions.

Unfortunately, without knowing further details (such as total mass or tank size) about the two LNGs reported by Bates and Morrison, this is as far as the re-analysis of their data can extend in terms of estimating the mass and heat transfer coefficients between the layers. However, the re-analysis that can be performed confirms that in Phase 1 mass transfer is negligible and heat transfer dominates the change in LNG density, while in Phase 2 the situation is reversed. Thus, Turner's observations of saline solutions are likely to be relevant to LNG mixtures, even if only in terms of the shape of the relationship between Φ and R_s.

The initial stability ratio for the stratified LNGs reported by Baker and Creed for the Partington rollover incident can also be estimated from Table 2.6. The LNG compositions reported were even leaner than those assumed for the LNGs in Table 3.5 for Bates and Morrison's data, with methane mole fractions of 0.926 and 0.975 for the lower and upper layers, respectively and only N_2, C_2H_6 and

C_3H_8 being present in the mixtures. The initial temperatures were assumed to be 114 and 112 K for the lower and upper layers by Deshpande et al.[25].

Baker and Creed report that the LNG densities were calculated to be 446 kg/m^3 and 433 kg/m^3, although they did not specify the method used for this calculation. Using the GERG-2004 EOS with the reported compositions and temperatures leads to predicted densities of 441 and 429 kg/m^3 and an average volume expansivity for the two LNGs of 20.0033 K^{-1}. These values correspond to an initial R_s = 5.4 for the Partington LNGs.

A similar calculation for the LNGs involved in the 2007 USA rollover incident described by Lukaszewksi et al.[33] gives an initial R_s = 4.6. Table 3.6 contains a summary of the R_s values calculated from the initial layer densities and temperatures reported for four LNG rollover incidents: La Spezia (1971), Nantes (1987–89), Partington (1993) and USA-Chattanooga (2007)[33]. Also shown is the time to rollover from the stated initial condition and, for three cases, the value of R_S at an intermediate time.

For the La Spezia incident, the intermediate values of R_S were estimated from the layer densities and temperatures predicted from the model of Heestand et al.[24]. The system started in the convective Phase 2 of the rollover process and remains there, which is consistent with (and reflects) the successful use of the Reynolds analogy when modelling the La Spezia incident. For the 2007 USA incident reported by Lukaszewski et al.[33], the intermediate R_S correspond to the times at which the level, temperature and density (LTD) profiles used for their normal-equations inverse model were measured. Interestingly, while the initial R_s indicate the system started in the diffusive Phase 1, at the three times used by Lukaszewski et al.[33] to determine the ki and h values used in their lumped parameter (LP) model, the system was in the convective Phase 2. This might partly explain why the rollover time predicted by their model was 10% too short: the values of ki derived from the LTD data were representative of a convective mass transfer regime, whereas the system in fact, started in a diffusive mass transfer regime.

93

LNG Rollover Incident	Initial R_s	Rollover time (hours)	t_{int} (hours)	R_s (t = t_{int})
La Spezia (1971)	1.7	31	20	1.3
			28	1.06
Nantes (1987-89)	9.9	60	18	4.9
			36	**3.8 ± 0.5**
			52	2.1
Partington (1993)	5.4	1632	-	-
USA (2007)	4.6	69	18	3.1
			30	2.9
			32	2.8

Table 3.6: Time to rollover for documented LNG rollover incidents, where possible, R_s values at some intermediate times, tint, during the system's evolution to rollover are also given. For the Nantes rollover, when t_{int} = 36 hours the system transitioned from the diffusive Phase 1 to the convective Phase 2and thus the corresponding value of R_s is the critical stability ratio for LNG, R_c.

Note: The temperature data used for calculating the initial R_s in Table 3.6, were obtained from the data provided by the related papers' authors. Our analysis in Chapter 5 of this thesis showed that some of those data are slightly different.

3.2. State map for LNG rollover based on stability parameter

A state map for the stability parameter of a multicomponent mixture defined in (Eq. 3-12) is shown in Figure 3.1 and is broken into five regions of interest corresponding to various combinations of the values of $-\alpha\Delta T$ and $\Sigma\beta_i\Delta S_i$.

In Region 1, where $R_s<0$, the system is stable with no potential for rollover. In Region 2, the system is unstable because the upper layer is denser than the lower layer. The unstable region is wherever $\Sigma\beta_i\Delta S_i$ is more positive than $-\alpha\Delta T$; the numerical values of R_s have no physical meaning beyond the boundary

between these two regions where $R_s = 1$. In Region 3, where $R_s > 0$ and $R_s > 1$, the system is stable but has the potential for rollover, which would result in the production of a boil-off vapour because the lower layer is at a higher temperature than the upper layer. In Region 4, where $0 < R_s < 1$, the system is stable and has also the potential for rollover, which would result in condensation because the temperature of the lower layer is below that of the upper layer. Such a rollover would be the opposite of that normally considered in LNG scenarios; however, it could in principle arise if the lower LNG were very lean but sufficiently cool so that its initial density was greater than the warmer, richer LNG above it. The effects of such an inverse rollover could potentially generate a partial vacuum in the storage tank that could cause problems with the containment and/or BOG handling systems.
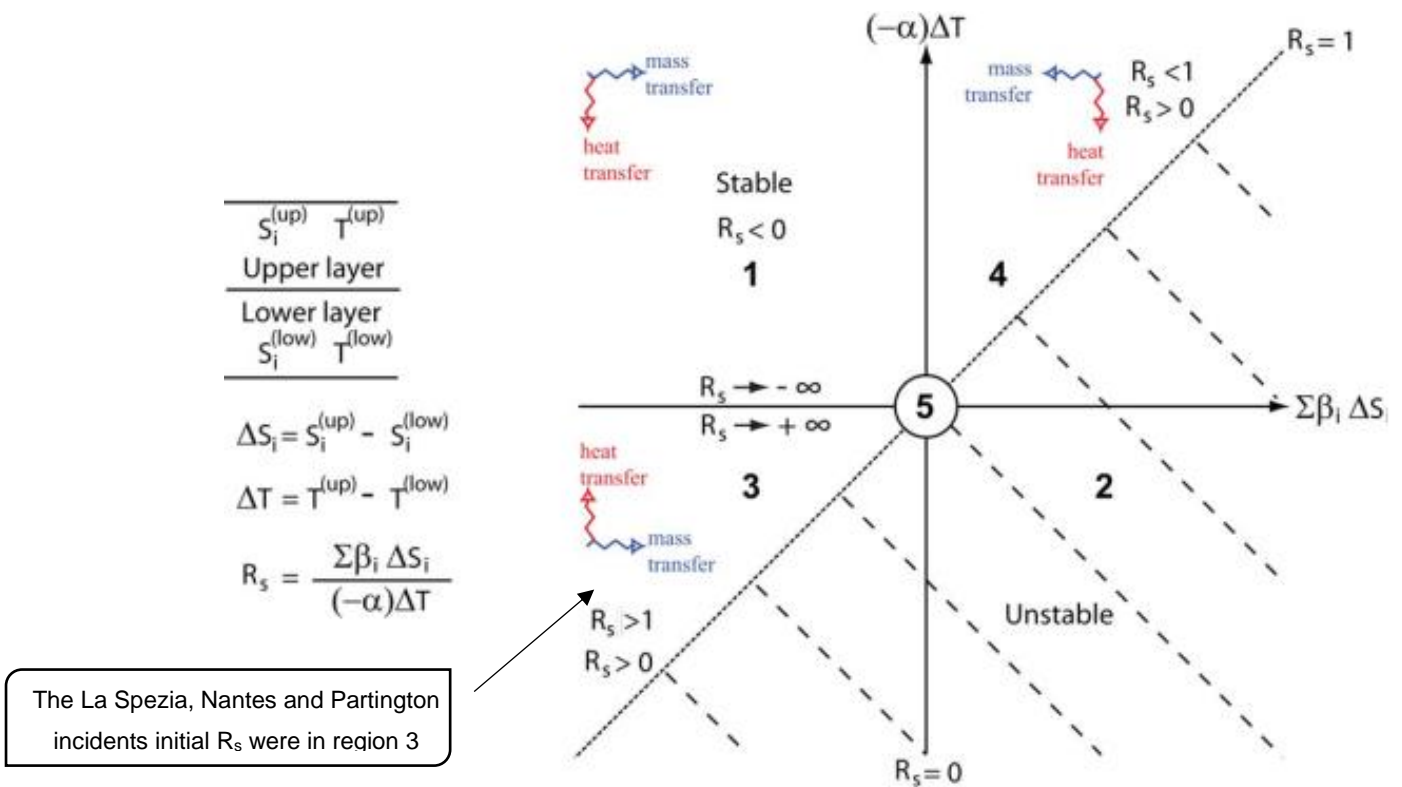
Figure 3.1: State map for the generalized stability ratio, "R_s" in a multicomponent system[7].

In Region 5 in the centre of the map, the system is nearly homogeneous with any gradients being too small for significant global effects. Similarly, the

mathematical divergence of R_s to infinity along the abscissa between Regions 1 and 3 simply reflects a thermally uniform system with $\Delta T = 0$. Arrows indicating the effects of heat and mass transfer on an isolated system are shown in each of the stable regions.

For Regions 3 and 4, it is the relative magnitudes of interlayer heat and mass transfer, combined with any heat leak into the system from the external environment, that governs whether the system evolves toward stability in Region 1 or a rollover event at $R_s = 1$. All the recorded rollover incidents such as the La Spezia, Nantes and the Partington have initially their R_s in region 3.

In this Chapter, the data and models for the LNG rollover existing in the open literature have been reviewed and a new framework for quantitatively analysing the limited available data is presented. We have extended the definition of the hydrostatic stability ratio for binary mixtures to allow its estimation for multi-component mixtures, either from the reported LNG layer compositions or measurements of the LNG layer densities. By analysing the graphical data of Bates and Morrison[4] the critical value of the stability ratio, R_c, separating the diffusive phase of LNG rollover from the penetrative convection phase was estimated to be 3.8 ± 0.5. This is significantly larger than the critical ratio of 2 reported for saline solutions and is also larger than the initial stability ratio of 1.7 estimated from the best documented LNG rollover incident at La Spezia in 1971. Finally, a state map for the stability parameter of a multicomponent mixture has been presented for a graphical description of stability parameter and potential of rollover. The map showed that the La Spezia, Nantes and the Partington rollover incidents' R_s were initially in region 3.

Chapter 4
Simulation methodology

The primary function of any LNG rollover simulation model is to predict the occurrence and the time to rollover as well as the amount of BOG generated by this phenomenon. To achieve this, the model must have the capability to accurately calculate the physical and thermodynamic properties of LNGs as time goes by toward rollover and finally correctly predict the time rollover in an acceptable period of time.

As described in previous chapters, there are two approaches to simulate the LNG rollover, lumped parameter and distributed parameter methods such as using Computational Fluid Dynamics (CFD) techniques. In this research, both mentioned approaches were tested to simulate a case similar to the La Spezia rollover incident (as the incident data are fully recorded by Sarsten), to investigate and highlight pros and cons of both methods, in order to choose the best approach for simulation of LNG rollover.

4.1. Overview of CFD simulation

Computational Fluid Dynamics (CFD) is a distributed parameter tool for predicting fluid flow, heat and mass transfer, chemical reactions and related phenomena by solving the set of governing mathematical equations numerically[27]. These equations are:

- Conservation of momentum
- Conservation of mass
- Conservation of energy
- Conservation of species
- Effects of body forces

In general, a CFD simulation has two major parts[27]:

1. Geometric model definition or the simulation domain, which can be done using a Computer Aided Design tool (CAD). The domain will be meshed into computational cells and numerical calculation will be performed in within these cells. The simulated domain can be modelled in 2D or 3D, a domain is defined with its boundary conditions.

2. Mathematical solver based on Navier-Stokes equations[26], which has been presented below. The equations can be solved in steady or unsteady state. The results can be presented in a graphic form allowing immediate visualisation and interpretation of hydraulic and thermal profiles.

Inertia (per volume)   Divergence of stress

$$\rho \left(\partial v / \partial t + v \nabla v \right) = -\nabla p + \mu \nabla^2 v + f \tag{4-1}$$

unsteady acceleration   Convective acceleration   Pressure gradient   Viscosity   Other body forces

In this study, ANSYS FLUENT[27] software has been chosen to simulate the LNG rollover, due to its capability of simulating industrial applications with high speed, and its accuracy to model heat transfer, especially natural convection.

ANSYS FLUENT solvers are based on the finite volume method. In this software, the domain is discretised into a finite set of control volume and then general conservation (transport) equations for momentum, mass, energy, species, etc. are solved on this set of control volumes using partial differential equations that are discretised into a system of algebraic equations.

Finally, all algebraic equations are then solved numerically to obtain the solution field. A simple flowchart that shows how the ANSYS FLUENT[27] software model the simulation is presented in Figure 4.1:
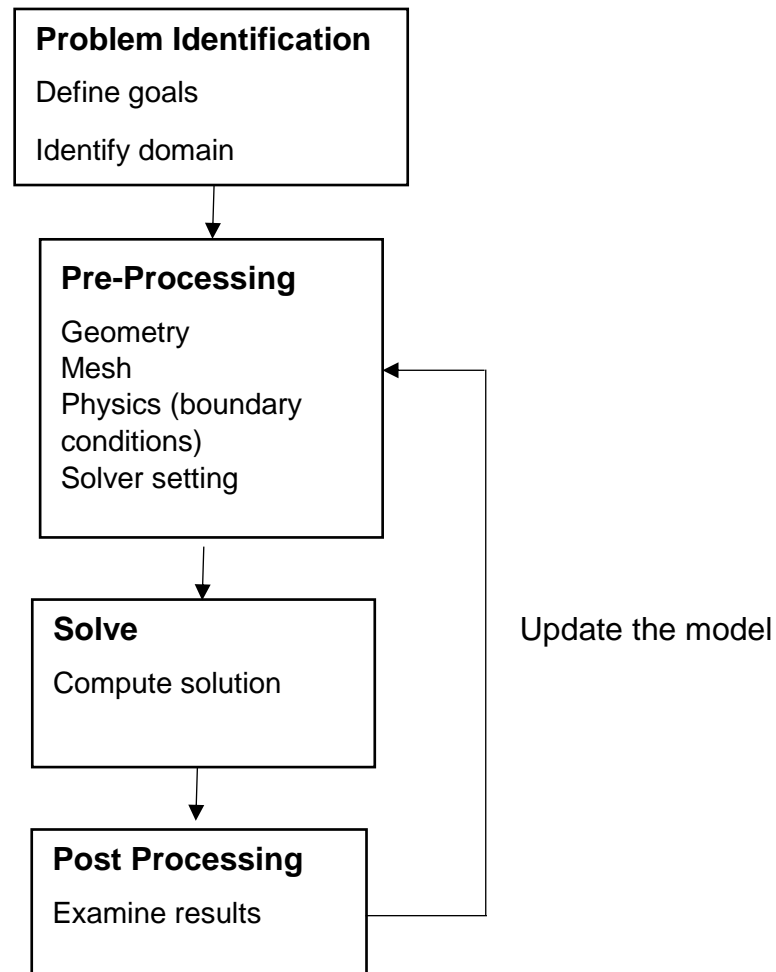
Figure 4.1: Simplified ANSYS FLUENT modelling flowchart.

Although the CFD approach has some major limitations, such as a very limited capability to handle thermodynamics, it is a useful tool to study the hydrodynamic and hydrostatic behaviour of the liquids before the rollover, to verify the mechanism of heat and mass diffusion at the liquids' interface. Furthermore, one of our main objectives in this thesis is to verify the Bates and Morrison's claim of having 2 phases in the rollover, by detecting the existence of the natural convection cells in the LNG tank after loading the LNGs.

This method of considering only two liquid layers has also been used by the previous researchers, who used CFD techniques in modelling LNG, such as Koyama *et al.*[45] and Zimmerman *et al.*[47]. They also considered only two liquid

LNG layers and their interactions were simulated as the primary and secondary phase, due to limitations of setting up the boundary conditions for the third phase (vapour). A closer look at Figure 2.7 also shows that in Phase 1 of the LNG rollover, the evolution of the vapour phase shown as BOG generation rate is very smooth, linear and minimum. This means that considering only two liquid layers for studying the Phase 1 of the rollover, is not a vague assumption.

Our first step to model the LNG rollover using CFD technique was to select a suitable geometry and use an appropriate mesh to render it, which would represent the LNG storage tank correctly; while not being too complicated, that makes the simulation complex and the running time longer than necessary. It was assumed that the LNG tank is a cylindrical above-ground tank and two layers of LNG with different density and temperature has been loaded into the tank. To simplify the problem, it was also assumed that a 2D domain could represent an accurate profile of the LNGs' volume fractions (density and temperature) change in the tank since there is no velocity and LNG flow in the tank as shown in Figure 4.2:
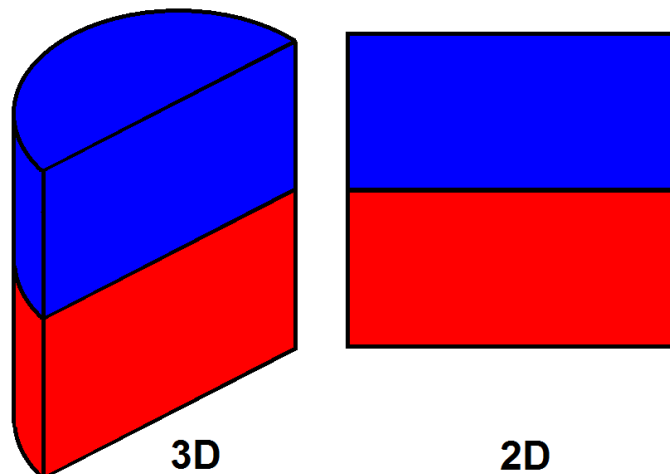
Figure 4.2: Schematic geometry selection for CFD rollover simulation. Red (bottom layer) and blue (top layer) colours represent different liquid layers.

Then the mentioned geometry was meshed into 100,000 rectangular cells assuming the tank dimension was 1 x 1 meters by using ANSYS FLUENT Work

Bench toolbox. The reason for scaling down the tank to 2D and 1 x 1 meters was to speed up the simulation process, as the CFD simulations normally take long time to converge. As the objective of the CFD modelling was only to simulate Phase 1 of rollover, this scaling down did not affect the accuracy of the simulation and the results.

The above-mentioned mesh was then loaded into FLUENT environment for the next step of the simulation. The system "solution set up" was set to the following:

- General:
    - For better accuracy, Double precision, 2D launcher was selected.
    - Solver: Pressure based solver (PBS) was selected, over the density base, since the LNGs in the tank are considered to be low-speed incompressible flows.
    - Time: set as transient[52]

- Euler-Euler multiphase models:
    - Multiphase: both volume of fluid (VoF) and Eulerian (as Koyama *et al.*[45] suggested) methods were tested. VoF method considers both layers being immiscible and not interpenetrating, while the Eulerian method is the most complex of the multiphase models and allows the layers to be mixed. The Eulerian method solves a set of "n" momentum and continuity equations for each phase. Testing both methods was to study the effect of minimum mass transfer in Phase 1.
    - Energy tab was "on" to enable heat transfer to model the natural convection.
    - Viscous model: both laminar and standard k-epsilon as Koyama *et al.*[45] suggested were tested, to see the effect of different turbulence models on the predicted results.
    - Species transport was enabled to consider mass diffusion. However, this mass diffusion was set to minimum (close to zero) to model Phase 1.

- Material: Wall, base and roof material were selected to be steel (mild steel) as per FLUENT database for the tank and a mixture of methane, ethane, propane, butane and nitrogen was used for LNGs.

After setting up the remaining parameters and inputting the initial data such as temperature, pressure, composition, layers' heights and external heat leaks to the program, the simulation was started. The objective of the CFD simulation was to detect that the system evolves to a natural convection circulation (Phase 1)

It is important to know how ANSYS Fluent software simulates the natural convection. FLUENT uses the Boussinesq approximation[53] model as follows:

$$(\rho - \rho_0)\, g = -\rho_0\, \beta\, (T - T_0)\, g \tag{4-2}$$

Boussinesq approximation is used when temperature / composition dependent density is simulated. Boussinesq approximation is very accurate when simulating inside a closed domain while the density variations are small, such as our model in Phase 1, which the density changes only due to temperature change (heat diffusion) rather than mass diffusion[46].

As described above, different models of viscosity and multiphase were tested; however, the results were not majorly different. The details of these CFD case studies are described in Chapter 5 of this thesis.

4.2. Lumped parameter LNG rollover simulation

The new advanced model for LNG rollover proposed in this thesis, consists of two multi-component liquid layers, a liquid vaporising film over the top of the upper liquid layer and a vapour phase, which is in equilibrium with the mentioned film. It was assumed that a pressure relief valve kept the tank pressure constant by allowing vapour to be vented as boil-off occurs.

This configuration is intended to represent the La Spezia conditions described by Sarsten[6] and then Heestand *et al.*[24]. The schematic diagram, which the mathematical model is based on, is shown in Figure 4.3.
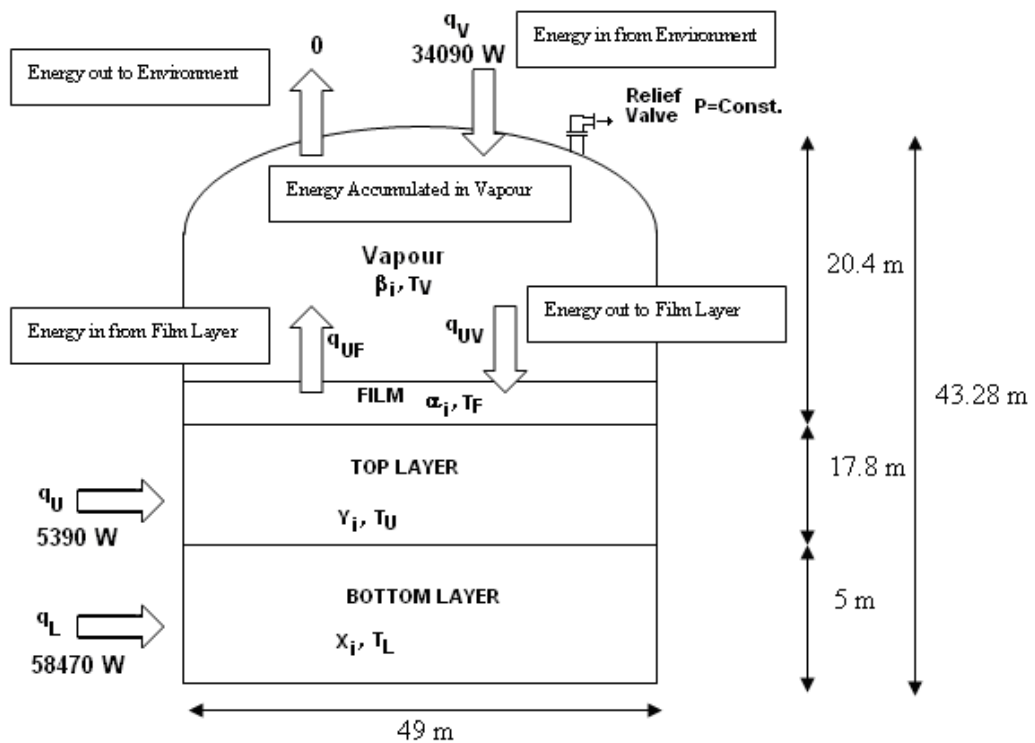
Figure 4.3: Schematic diagram of the LNG storage tank considered in the new simulation.

The core of LNG rollover simulation is the solution of the coupled differential equations (DEs) governing the energy and material balance in each layer over

time. The solution of these DEs gives the mole fractions of each of the components as well as the temperatures in the lower layer, upper layer and vapour regions of the storage tank. The DEs contain parameters, such as heat capacity, heat and mass transfer coefficients, which depend on the compositions and temperatures of the layers and which must be evaluated numerically before the DEs can be solved.

To achieve this, the simulation utilised two component software tools linked together as shown in Figure 4.4.

$$X_i \quad Y_i \quad B_i \quad T_i$$

| REFPROP SOFTWARE MATLAB INTERFACE USING GERG-2004 EOS | MATLAB DIFFERENTIAL EQUATION SOLVER |

$$X_{i+1} \quad Y_{i+1} \quad B_{i+1} \quad T_{i+1}$$
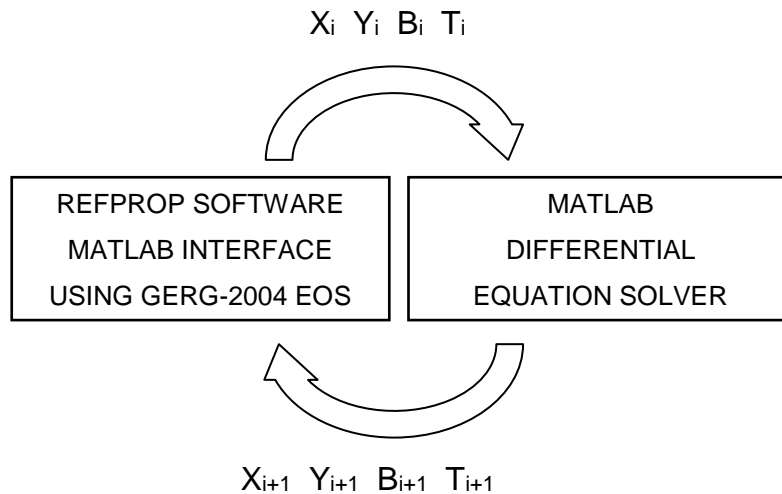
Figure 4.4: New simulation loop used in this research.

Commercial process simulators such as PRO/II[54] and HYSYS[55] have been tested, to see if they were suitable to do the rollover simulation with; however, as they all considered the liquid stored in a tank/vessel as a homogenous inventory with a single layer, it was decided not to proceed and write an individual program specific to LNG rollover. Furthermore, none of those mentioned commercial process simulator, had the GERG-2004 EOS implemented or link to them.

MATLAB software has been selected and a code has been written and linked to the REFPROPM[1] software was used to calculate numerical values of the parameters in the DEs, starting from the initial compositions and temperatures.

The MATLAB[2] code was then used to define symbolically the system of DEs, substitute the parameter values calculated with MS Excel into the DEs and then solve them simultaneously for a user-specified sub-interval (1000 seconds) of the total simulation time. 1000 seconds has been selected over 100, 500 and 5,000 seconds, as an optimised time step that predicts the changes in thermodynamic properties accurately, without slowing down the simulation process speed drastically.

Over these sub-intervals, the parameters in the DEs were assumed to be constant. At the end of each sub-interval, the new compositions and temperatures used as new (updated) values of the parameters in the MATLAB code. Iterations of this loop continued until the rollover criterion ($R_s = 1$) was met. Another feature of the program, which is new in the simulation of LNG rollover, is the ability to choose the mass transfer regime based on critical stability ratio (R_c), in Phase 1 (using the Chilton-Colburn analogy) or Phase 2 (using the Reynolds analogy). After the numerical simulations have finished, all data was transferred to a Ms Excel file to also have a graphical data representation or statistical analysis for further studies.

4.3. Evaluating the numerical parameters in the rollover equations

The critical numerical parameters required for the solution of the rollover model's equations were the external heat leaks into the storage tank, the amounts of thermophysical properties of the LNG and vapour layers and the heat and mass transfer coefficients between the layers. In this work, the values for the external heat leaks and the tank volumes (used in calculating the initial amounts of LNG in each layer) were taken from the values reported for the La Spezia incident by Heestand *et al.[24]* and Baker and Creed[18].

The required thermodynamic properties of the LNG liquid layers, the film and the vapour were: the heat capacities and enthalpies for the energy balance equations, the equilibrium ratios, K_i, for the film and vapour material balance equations, the densities for calculating the Rayleigh flow (Eq. (2-24)) and the values of α and β_i used in the calculation of R_s. Each of these was calculated using the GERG-2004 equation of state[3], as implemented in the software REFPROPM[1]. Calculation of the β_i required an additional perturbation of the mole fraction compositions as indicated in Section 3.1 with an example shown in Table 3.1.

The transport properties required were the thermal conductivities, viscosities and the molecular and thermal diffusivities. These were used in the calculation of dimensionless groups required for evaluation of the Rayleigh flow as well as for the heat and mass transfer coefficients. Most of these transport properties were calculated using the correlation of Ely and Hanley[51] as implemented in the software REFPROPM[1]. As an accurate and fast method of prediction of the molecular diffusivities, the correlation of Wilke-Chang[49], were implemented directly into the MATLAB code.

The heat and the mass transfer coefficients were calculated in the MATLAB code from the calculated thermophysical properties and a user-specified

correlation for the particular transfer coefficient. For example, one of the heat transfer coefficient correlations from Table 2.5 could be chosen to calculate h. Mass transfer coefficients were calculated from h using either the Reynolds analogy or the Chilton-Colburn analogy.

The overall process for evaluating the numerical parameters required in the rollover equations (4-3) to (4-16) is shown as a flow chart in Figure 4.5. Once evaluated, the numerical values of the parameters were substituted into the equations and assumed to be constant for a user-defined sub-interval of the total simulation time. The values of the sub-intervals ranged from 100 to 5000 seconds was tested, and 1000 seconds has been selected as the optimum time step. After each sub-interval, the new values of the compositions and temperatures determined from the solution of equations (4-3) to (4-16) were used to calculate updated values of the parameters described in this section using the MATLAB code.
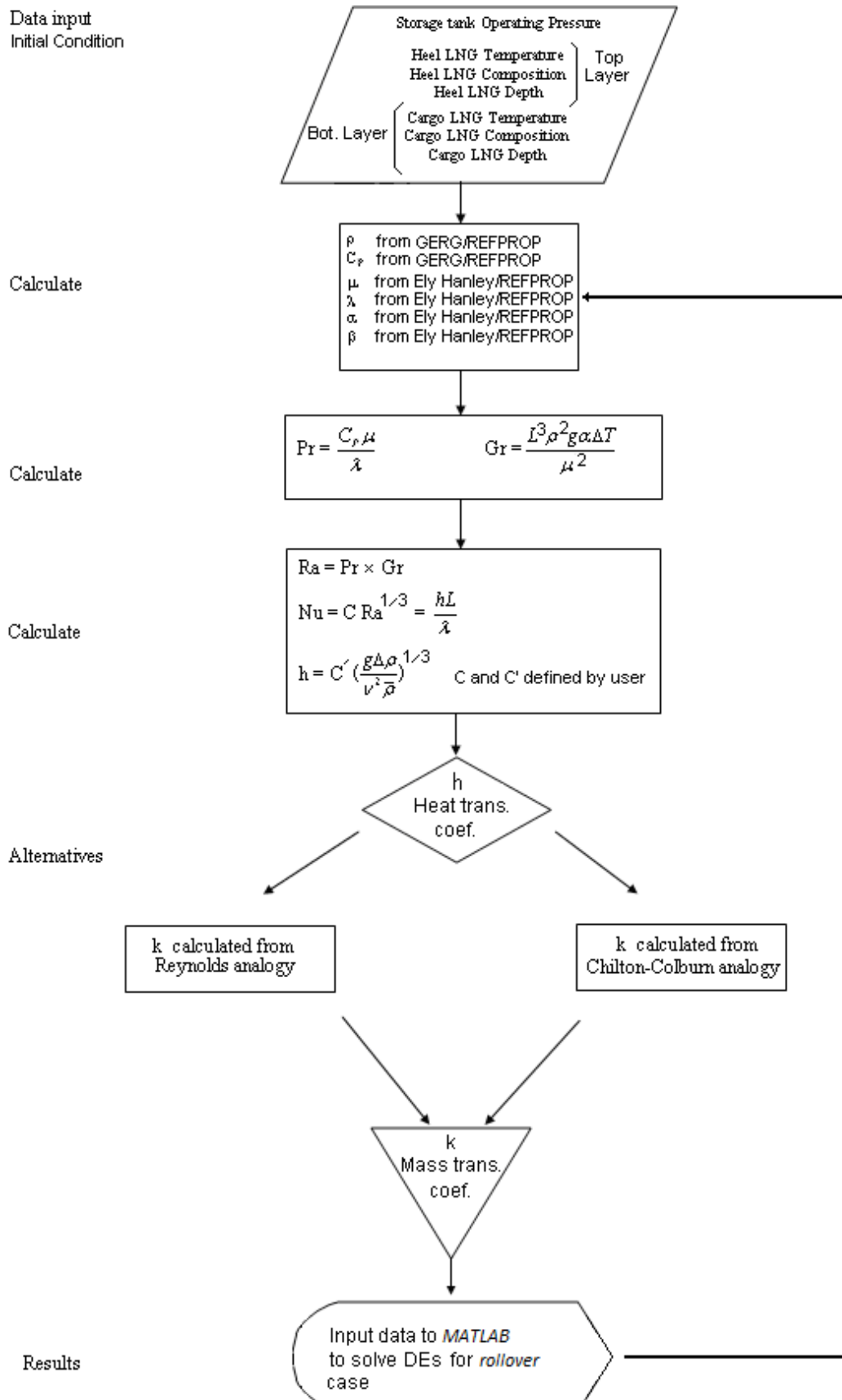
Figure 4.5: Simulation flowchart of rollover model used in this work.

4.4. The rollover equations from energy and material balance considerations

In this section, the specific mathematical form of the differential and ancillary equations used in the simulation of LNG rollover in a six-component system is described. The six components included in this simulation were methane, ethane, propane, n-butane, n-pentane and nitrogen as the most common compositions of commercial LNGs as describe in Chapter 1; however, the model is capable of incorporating additional components if required.

Material balance in the lower layer

In the lower layer, mass diffusion is equimolar, so the total number of moles remains constant for this layer over time. Thus, the material balance relations are:

$$\frac{d(Mole_L)}{dt} = 0 \qquad\qquad\qquad (4\text{-}3)$$

$$\frac{d(Mole_L \times X_i)}{dt} = k_i.A(Y_i - X_i) \qquad \text{for } i = 1 \text{ to } 6 \qquad (4\text{-}4)$$

$$\sum_{i=1}^{i=6} X_i = 1. \qquad\qquad\qquad (4\text{-}5)$$

Here, the subscript "i" refers to the component, the subscript "L" denotes the lower layer, X_i is the mole fraction of component i in the lower liquid layer, Y_i is the mole fraction of component i in the upper liquid layer, $Mole_L$ is the total number of moles in the lower liquid layer, A is the tank cross-sectional area, k_i is the component mass transfer coefficient and t is time. k_i is calculated by using analogies between the heat and mass transfer. Of the eight equations represented by Eqs. (4-3) to (4-5), only seven are independent since the sum of the component material balance equations is equivalent to the overall

material balance equation. Accordingly, in the MATLAB code, Eq. (4-5) was not explicitly included as an independent equation and the seven equations in Eq. (4-3) and (4-4) were solved for the seven time-dependent functions {$Mole_L(t)$, $X_i(t)$}. However, as a check that round-off or other numerical-type errors were not accumulating, Eq. (4-5) was evaluated at the end of each sub-interval simulated with the MATLAB code. No such round-off or numerical errors were ever detected.

Energy balance in the lower layer

The energy balance in the lower layer is affected by heat transferred from the upper layer and heat transferred from outside the tank into the lower layer. Thus, the energy balance equation is:

$$\text{Mole}_L C_{PL} \frac{dT_L}{dt} = hA(T_U - T_L) + q_L \tag{4-6}$$

Here, the subscript U denotes the upper liquid layer, C_{PL} is the molar constant pressure heat capacity of the lower layer, T_L is the temperature of the lower liquid layer and q_L is the heat absorbed by the lower liquid layer through the tank walls and base plate. "h" is calculated from Eq (2-23).

Material balance in the upper layer

The material balance in the upper layer is affected by equimolar diffusion with the lower layer and the Rayleigh flow between the film and the upper layer. Thus, the total number of moles in the upper layer is not conserved and the material balance equations are:

$$\frac{d(\text{Mole}_U)}{dt} = (-f) - [\sum_{i=1}^{i=6} k_i.A(Y_i - X_i)] \tag{4-7}$$

$$\frac{d(\text{Mole}_U \times Y_i)}{dt} = (-Y_i(f + F) + \hat{\alpha}_i) - k_i.A(Y_i - X_i) \text{ for } i = 1 \text{ to } 6 \tag{4-8}$$

$$\sum_{i=1}^{i=6} Y_i = 1. \tag{4-9}$$

Here, f is the molar vapour boil-off flow rate and F is the Rayleigh flow, which are defined by Eqs. (2-24) and (2-25) and $\hat{\alpha}_i$ is the mole fraction of component "i" in the film between the vapour and upper liquid layer. Similar to Eq. (4-5), Eq. (4-9) was not included in the solution of the equations, but rather it was used as a consistency check at the end of the sub-interval calculations.

Energy balance in the upper layer

The energy balance in the upper liquid layer is affected by heat transferred from the lower layer, heat transferred from outside the tank into the upper layer, heat transferred from the vapour phase to the upper liquid layer and the heat lost from the upper layer through the boil-off process. Thus, the energy balance equation is:

$$C_{PU}\frac{d(\text{Mole}_U \times T_U)}{dt} = hA(T_L - T_U) + q_U + q_{UV} - Qf \tag{4-10}$$

Here Q is the enthalpy of vaporization, C_{PU} is the molar constant pressure heat capacity of the upper layer, q_U is the heat absorbed by the upper layer from outside through the tank walls and q_{UV} is the heat absorbed by the upper layer from the vapour. Heestand et $al.$[24] commented that the specification of q_{UV} was somewhat arbitrary and that if it was set to about 5% of the heat transferred to the vapour from outside the tank reasonable values of T_U were maintained. Thus in this work, q_{UV} was also defined as:

$$q_{UV} = 0.05q_V = 0.05(q_{wall} + q_{Dome}) \tag{4-11}$$

where $q_V = q_{wall} + q_{dome}$ is the total heat transferred to the vapour from the outside through the tank walls and dome. In the next Chapter, a sensitivity analysis has been done to investigate the sensitivity of the simulation to this value.

Material and energy balances in the film and vapour

Following Heestand *et al.*[24] the film was assumed to be liquid in thermodynamic equilibrium with the vapour phase, with no accumulation of energy or material permitted in the film. Equation (2-25) which gives the boil-off rate, f, in terms of the Rayleigh flow, F, between the film and upper layer was derived by considering a non-accumulative energy balance on the film. The material balance and energy balance equations for the film were combined with the thermodynamic vapour-liquid equilibria equations for the film – vapour system to derive the material and energy balance equations for the vapour. Accordingly, the material balance equations for the vapour are:

$$\frac{d(Mole_V)}{dt} = 0 \qquad (4\text{-}12)$$

$$\frac{d(Mole_V \times \hat{\beta}_i)}{dt} = (K_i\hat{\alpha}_i - \hat{\beta}_i)f \qquad \text{for } i = 1 \text{ to } 6 \qquad (4\text{-}13)$$

$$\sum_{i=1}^{i=6} \hat{\beta}_i = 1. \qquad (4\text{-}14)$$

Here the subscript "V" denotes the vapour phase, $\hat{\beta}_i$ is the mole fraction of the component "i" in the vapour phase and $K_i \equiv \hat{\beta}_i / \hat{\alpha}_i$ is the equilibrium ratio of the mole fractions of component "i" in the vapour and film. In the program, the value of K_i obtained from the last sub-interval will be based to calculate the vapour phase new composition. In this model, a constant tank pressure was assumed (maintained by a relief valve), requiring that the total number of moles of vapour was constant and thus, that the liquid boil-off rate *f*, vapour was equal to the

vapour vent rate. The vapour phase was assumed to be well mixed and thus, the vented gas had the same composition as the rest of the vapour in the tank. As for Eqs (4-5) and (4-9), Eq (4-14) was not included in the solution of the equations, but rather it was used as a consistency check at the end of the sub-interval calculations.

The $K_i \hat{\alpha}_i$ term in Eq. (4-13) indicates that the composition of the boil-off gas corresponded to the composition of a vapour in equilibrium with the film. (Note the composition of the boil-off gas was <u>not</u> the same as that of the film, which had a mole fraction composition $\hat{\alpha}_i$). Although Heestand et al.[24] introduced the film concept into the modelling of LNG rollover they did not give adequate detail about the compositions of the film or vapour phase or the material balance relations governing their evolution. Such details are however, crucial, to the reliability of the rollover simulation and the approach taken in this work is described in Section 4.4 below. The energy balance equation for the vapour is:

$$C_{PV} \frac{d(Mole_V \times T_V)}{dt} = q_V + (Q - C_{PV}(T_V - T_{ref}) - h_{Vref})f \cdot \qquad (4-15)$$

Here "T_{ref}" and "h_{Vref}" are the temperature and enthalpy of vaporization ($h_{vapour} - h_{film}$) at a reference condition and C_{PV} is the constant pressure molar heat capacity of the vapour. The reference condition in this work was chosen to be the initial condition for the film, which was assumed to initially be identical in composition, temperature, pressure and hence enthalpy to the upper liquid layer. Strictly, when converting a balance on enthalpies to an ordinary differential equation for temperature, a constant of integration is required corresponding to the enthalpy of the system at the initial temperature. However, when considering the energy balance on the lower liquid layer, the conservation of its total mass means that this constant of integration drops out of the final equation, Eq. (4-6). This constant does not drop out of the final energy balance equation for the upper liquid layer; however, because only changes in enthalpy are physically important, the enthalpy datum in Eq. (4-10) was chosen to be the initial condition of the upper layer. However, once this datum is chosen,

changes in the vapour's enthalpy must be calculated relative to it. Thus, the difference between the vapour's initial enthalpy and the film's initial enthalpy must be included when calculating the evolution of the vapour's temperature. The fact that in this simulation the total vapour mass was also held constant does not remove the requirement of including h_{vref} in Eq. (4-15) because of the enthalpy introduced to the vapour from the boil-off flow. It should be noted that the enthalpy of vaporization "Q" in Eq. (4-15) varies with time, whereas h_{vref} is a constant.

4.5. New method for calculating the heat and mass transfer coefficient in this work

Previous attempts to simulate the LNG rollover have used either the Reynolds analogy (Heestand *et al.*[24] and Deshpande *et al.*[25]) or Turner's method[5] (Germeles[17] and Bates and Morrison[4] in Phase 1) to calculate mass transfer coefficient. However, using only Reynolds analogy for this purpose may lead to an overestimated and large mass transfer coefficient that shortens the time to rollover and gives inaccurate simulation results especially if the system is in Phase 2 of rollover such as Deshpande *et al.'s*[25] results for the predicted time to rollover in the Partington incident, which is largely shorter than time reported by Baker and Creed[18]. On the other hand, Turner's method, which is mainly applicable for salt water gives very slow mass transfer rates and much unrealistic, longer times to rollover.

Heestand *et al.*[24] also showed that the predicted rollover time was very sensitive to the choice of the heat transfer coefficient correlation. Only by using a correlation for "h" with a value of "C" in Eq. (2-21) that was 40% and 25% smaller than the empirical values reported by Globe and Dropkin[29] and McAdams[28], respectively; Heestand *et al.*[24] were able to achieve results consistent with the report of Sarsten[6], by using the Reynolds analogy; however, their simulation was successful because the La Spezia LNGs were initially in Phase 2. Therefore, it is possible that a different heat-to-mass transfer relation could result in a better prediction of the rollover time for a different value of "C"

in Eq. (2-21), particularly if the system is in Phase 1 and LNG physical properties are calculated using more accurate thermodynamic and transport property models.

As described in the research hypothesis, to get more accurate results in the simulation, and overcome above mentioned limitations, a smaller heat and mass transfer coefficients (estimated from the Chilton-Colburn analogy) should be applied to Phase 1 and the system should be monitored by tracking the multi-component system's stability ratio until the critical value is reached whereupon the heat and mass transfer regimes change (Phase2).

To apply the above-mentioned features and the new heat and mass transfer regime hypothesis in this research and incorporate it into the program, first we need to understand and quantify the mass transfer analogies. The Chilton-Colburn analogy $[(k_i\, c_p\, /\, h) = (Pr\, /\, Sc_i)^{2/3}]$ provides lower mass transfer rates (~1/10) than Reynolds analogy $[(k_i\, c_p\, /\, h) = 1]$. As well as it can calculate component specific mass transfer coefficients. For example, to calculate the Prandtl and Schmidt number for the La Spezia LNGs, we used the average properties for both layers at the interface calculated using REFPROP. This gave $c_p = 2.59$ J/kg/K, $\mu = 270.6$ mPas and $\kappa = 203.79$ mW/m/K. Using Eq. (2-18) the Prandtl number is:

$$Pr = \frac{c_p \mu}{k} = \frac{2.59 \times 270.60}{203.79} = 3.42$$

The Schmidt number Eq. (2-30) depends on the molecular diffusion coefficient, which is species dependent and which was calculated using the Wilke-Chang correlation, Eq. (2-31). The results for each of the different components are summarized in Table 4.1:

	D_{AB}	$\langle Sc_i \rangle$	(kc_p/h)
	m^2/s		
Methane-Methane	5.67 e -9	88.6	0.11
Methane-Ethane	4.53 e -9	111	0.10
Methane-Propane	3.75 e -9	134	0.09
Methane-Butane	3.24 e -9	155	0.08
Methane-Pentane	2.87 e -9	175	0.07
Methane-Nitrogen	5.98 e -9	83.8	0.12
Mole fraction weighted average	5.13 e -9	101	0.11

Table 4.1: Values of the molecular diffusion coefficient, the corresponding Schmidt numbers for each component averaged over the two La Spezia LNG layers and the ratio ki cp/ h = $(Pr/Sci)^{2/3}$ for the Chilton-Colburn analogy. The mole fraction weighted average is also shown for the average initial La Spezia LNG compositions.

As shown in Table 4.1, at the initial La Spezia conditions the value of $(Pr/Sc_i)^{2/3}$ for each of the LNG components is approximately 0.1, with a mole fraction average of 0.11. Repeating the calculation for the La Spezia LNGs at the moment before rollover, the mole fraction average of $(Pr/Sc_i)^{2/3}$ is 0.10. A more stringent test is to evaluate the $(Pr/Sc_i)^{2/3}$ for the LNGs studied by Bates and Morrison[4] using the assumed compositions in Table 3.4. The value of the sum $\sum_i x_i \left(Pr/Sc_i \right)^{2/3}$ averaged over both layers and all three times listed in Table 3.4 is 0.123 with a standard deviation of 0.003. This indicates that to within about 10 %, the value of $(Pr/Sc_i)^{2/3}$ for LNG components can be taken as about 0.11, independent of the component or the overall mixture composition. The implication of the result $(k_i C_p / h) \cong 0.11$ is that, for the same heat transfer coefficient, the Chilton-Colburn analogy gives mass transfer coefficients about ten times smaller than the Reynolds analogy, as required.

The MATLAB program developed for this research is capable of using the lower heat transfer coefficient and the Chilton-Colburn analogy to calculate mass transfer when $R_s > R_c$ (~3.8) and higher heat transfer coefficient such as the Globe and Dropkin[29] and the Reynolds analogy[48] when $R_c > R_s > 1$. This approach

improved the previous rollover simulation results, especially for the Partington incident, compared with Deshpande et al.'s[25] simulation result of 18 hours.

4.6. New approach for calculation of the film and the vapour composition in this work

Heestand et al.[24] modelled the vapour in the La Spezia storage tank as being in thermodynamic equilibrium with the film. However, they also stated the initial vapour composition to be simply 0.95 CH_4 + 0.05 N_2 and they did not discuss the details of the initial film composition. Given that the La Spezia upper layer was in equilibrium with the vapour for weeks prior to the loading of the second, lower layer LNG, it is unrealistic to assume such a vapour composition. It is also inconsistent with their statement that the film was in thermodynamic equilibrium with the vapour, unless the film had a very (impossibly) different composition to that of the upper layer. Furthermore, Heestand et al.[24] stated that the initial temperature of the vapour was 122K, 8K above the stated initial upper liquid layer temperature and they gave no details of the evolution of the vapour phase composition or temperature over the duration of the rollover simulation. Thus, it is impossible to establish and verify quantitatively how their model treated the interactions between the upper LNG layer, the film and the vapour.

In this work, these interactions were treated quantitatively by first assuming that the initial temperature and composition of the film was equal to that of the upper liquid layer. The second assumption was that the vapour was always in thermodynamic equilibrium with the film, with the implication that the temperature and composition of the film could differ from that of the upper layer, which would give rise to a Rayleigh flow. Accordingly, the initial vapour temperature was set equal to the film and upper liquid layer and the initial vapour composition was determined by calculating the equilibrium mole fraction ratios K_i for the film at its initial conditions using the GERG-2004 EOS. This resulted in the more realistic initial vapour composition of

0.8179 CH_4 + 0.1816 C_2H_6 + 0.0004 N_2 for the La Spezia incident and 0.8833 CH_4 + 0.0034 C_2H_6 + 0.1133 N_2 for the Partington incident.

In contrast with the calculation of the initial vapour condition, for the rest of the simulation, the vapour composition $\hat{\beta}_i$ was calculated from material balance considerations using Eqs. (4-12) and (4-13), with the values of K_i and $\hat{\alpha}_i$ held constant for the duration of the sub-interval. At the end of the sub-interval, the values of K_i and $\hat{\alpha}_i$ were updated. The K_i were re-calculated by using the GERG-2004 EOS[1] to calculate the dew point composition of a liquid in equilibrium with a vapour at the new temperature and composition determined by the solution of the material and energy balance equations. The film composition was then calculated simply as $\hat{\alpha}_i = \hat{\beta}_i / K_i$. With the composition and temperature (and pressure) of the film specified, the GERG-2004 EOS could then be used to calculate film mass density, which in turn allowed the Rayleigh flow between the film and upper liquid layer to be determined using Eqs. (2-24) and (2-25). The updated Rayleigh flow, F, was used to determine the updated flow rate of the boil-off using Eq (2-24), f, which was in turn used with the updated values of $\hat{\alpha}_i$ and K_i in the material balance calculation for the vapour during the next sub-interval.

In an attempt to compare our model results with those of Heestand *et al.*[24], we attempted an alternative method of determining the initial conditions of the vapour and film. The initial vapour composition was specified by Heestand *et al.*[24] as 0.95 CH_4 + 0.05 N_2 and the initial film composition was calculated as described in the preceding paragraph. With this method, we tested two initial vapour temperatures: 114.355K and 122.039K, the latter matching the specification in Heestand *et al.*[24]. The initial film temperature was set to be equal to that of the vapour. In both cases, the Rayleigh flow calculated for the initial condition was extremely large because of the very large difference between the film and upper layer densities. The flow was so large that the simulation could not proceed beyond the third sub-interval (about 3000 seconds)[11].

4.7. Criterion for LNG rollover and R_s calculation

Apart from Chatterjee *et al.*[16], all the past LNG rollover simulations used the equalization of layer densities as the criterion for rollover. A more rigorous analysis of hydrostatic stability, as given in Section 2, shows that strictly the criterion should be E = 0 with E given by Eq. (2-10); this criterion accounts for the effect of fluid compressibility. Accordingly, this criterion was adopted for the simulations done in this work, rather than the simple equalisation of densities. However, the difference between these two criteria for the La Spezia case is very small, because the term $\Delta\kappa\rho g$ is only 2.4×10^{-6} per meter; such a contribution is negligible in comparison with the uncertainties inherent in the model and the available data. Furthermore, at LNG tanks atmospheric operating pressure, liquids are incompressible. Fundamentally this "compressibility term" will always be small in most conceivable practical situations and would only be significant in liquids approaching their critical point. Hence, it will generally be adequate to consider $R_s = 1$ or, equivalently, the equalization of densities as the criterion for rollover.

Depending on the heat and the mass transfer analogy used, it is necessary to calculate R_s as the simulation proceeds. If Turner's observations for saline solutions (Figure 10) or heat to mass transfer analogies are being used to calculate k from h, then R_s must be evaluated after each sub-interval. To do this efficiently Eq. (3-17) was re-arranged to give:

$$R_S = \frac{\Delta\rho}{(-\alpha\Delta T)\bar{\rho}} + 1 \qquad\qquad (4\text{-}16)$$

Here $\Delta\rho \equiv \rho_U - \rho_B$ and $\bar{\rho}$ is the average mass density of the layers. It would also be possible to evaluate R_s by determining the all of βi and ΔSi at each point in the simulation. However, particularly for the multi-component systems this is more numerically intensive and is unnecessary since each term in Eq. (4-16) is already determined by the new simulation.

In this Chapter, a brief overview of the two approaches to simulate LNG rollover has been given. Distributed parameter approach such as CFD modelling and lumped parameter methods. Both approaches have their own merits such as simulation speed and result accuracy and their limitations such as handling of the thermodynamics of complicated mixtures due to assumptions needed to be made to set up the initial model or the inherited limitations resulted by the software capabilities.

Furthermore, a new approach for calculating the mass transfer coefficient from the heat transfer coefficient has been developed based on a new hypothesis has been described in this Chapter. The new hypothesis suggested that the use of lower heat transfer rate and lower mass transfer rate such as resulted by the Chilton-Colburn analogy for phase 1 and use of higher heat transfer regime and higher mass transfer rate such as the Reynolds analogy for phase 2, will improve the transport properties and hence the rollover simulation.

A rigorous criterion for multi-component LNG mixture has been also defined for the transition of the system from Phase 1 to 2, as well as the rollover occurrence, based on the hydrostatic stability of the LNG liquid layers.

The above-mentioned hypothesis along with this criterion will be tested through several simulations in Chapter 5.

Chapter 5

Results and discussion

5.1. Overview and the impact of the thermophysical properties on the simulation of LNG rollover

In this Chapter, the results obtained using the new LNG rollover model are presented and discussed. The objectives of the tests done with the new model were:

1. Use the distributed parameter technique and CFD model to determine if it can successfully simulate Phase 1 of the LNG rollover incident and address its deficiencies and limitations toward Phase 2 rollover modelling.

2. Build an advanced lumped parameter (LP) model, using the improved GERG-2004 EOS[3] and new mass transfer hypothesis and verify that the new model is working correctly by comparing the results with Heestand *et al.*[24] model.

3. While the new rollover model has been verified, simulate the Partington rollover incident with data reported by Baker and Creed[18] to compare our results from simulations with Deshpande *et al.'s*[25] results to improve previous LNG rollover simulations by better defining the thermodynamic and transport properties and the rollover criteria.

4. For the first time (available in the open literature), used an advanced developed lumped parameter model to simulate several hypothetical case studies of auto-stratification rollover incidents.

5. Study the effect of thermophysical property selection, using different heat and mass transfer analogies on the predicted path and time to rollover.

6. Conduct a sensitivity analysis on the critical parameters of rollover such as the amount of heat absorbed by vapour, heat and mass transfer regimes, external heat leaks and their effects on the time to rollover.

7. Discuss the new model advantages and limitations for simulation of rollover.

Attaining objective (1) was very complicated, due to the limited capabilities of CFD software to handle the thermodynamics, especially flash calculations in each iteration, closer to Phase 2 of rollover, as well as being time-consuming. Hence, CFD modelling was only used to verify the diffusion mechanism and provide qualitative evidence for a transition from Phase 1 to Phase 2. The lumped parameter modelling approach has been chosen as the simulation method for both phases, which could be also linked to a thermodynamic software such as REFPROP and was much faster to run. For example, in one case, LP simulation of Phase 1 converged 10 times faster than CFD simulation (~5 min. versus 55 min.).

Achieving objectives (2 and 3) were also problematic in particular because of the sensitivity of the rollover simulation to the calculation of the heat transfer coefficient between the LNG layers. Heestand *et al.*[24] illustrated this sensitivity by showing that the different correlations for "h" listed in Table 2.5 resulted in a 40% variation in the predicted rollover time. Their best result was obtained using the correlation Nu= $0.0425(Ra)^{1/3}$ (Row 5 of Table 2.5) and accordingly this correlation was chosen for use in this work to verify the reliability of the new simulation. However, when this correlation was implemented in the new code, significant discrepancies were found between the predictions of Heestand *et al.*[24] and those with the new model.

These discrepancies were studied and found to be the result of both differences in the predicted LNG transport properties, such as the thermal conductivity and the calculated Prandtl number and in the boil-off rate resulting from the temperature difference between the film and the upper layer.

In Table 5.1, values of the key thermophysical properties reported by Heestand *et al.*[24] for the initial La Spezia LNGs and those calculated in this work are compared[11].

	Heestand et al.[24]	REFPROP		% Difference
		(GERG-2004)[3]	Ely-Hanley[51]	
ρ_L (kg/m³)	541.118	541.032	-	0.02
ρ_U (kg/m³)	537.316	536.952	-	0.07
C_{PL} (J/mol/K)	61.62 *	60.78	-	1.36
C_{PU} (J/mol/K)	62.39 *	61.80	-	0.96
ν_L (m²/s)	2.787 x 10⁻⁷	-	4.959 x 10⁻⁷	43.80
ν_U (m²/s)		-	5.083 x 10⁻⁷	45.17
λ_L (W/mK)	0.185	-	0.202	8.42
λ_U (W/mK)		-	0.206	10.19
Pr	2.1	3.4		67

Table 5.1: Comparison between the initial physical properties calculated by Heestand *et al.*[24] and with the new simulation for the La Spezia LNGs[11]. The heat capacities listed for Heestand *et al.*[24] were calculated using the SRK equation of state[30] as implemented in the software Aspen HYSYS[55] as they were not explicitly given in reference 24.

It is apparent that the difference between the predicted thermodynamic properties is about 1% or smaller; the use of a significantly improved thermodynamic model had little impact on the quality of the simulation. The discrepancies between the predicted transport properties range from 8.5% to 45%. Unlike thermodynamic equations of state, transport property models for LNG have not improved significantly since the publication of Ely and Hanley's 1981 correlation[51], in part because few improved measurements of such properties have been conducted at LNG conditions. Thus, it cannot be stated that the transport property model used in this work is any better than the values used by Heestand *et al.*[24] at the initial condition (unfortunately, they did not provide any reference to their method of calculating the values). However, in our model these properties are not considered to remain constant throughout the simulation (as in Heestand *et al.*[24] model) and are recalculated at each time step based on the new condition (new temperature and composition). Furthermore, the results of the simulation are more sensitive to the values

estimated for the transport properties. Future progress in modelling the heat and mass transfer and rollover in LNG systems will, therefore, require improved measurements of transport properties at cryogenic conditions.

5.2. CFD simulation of LNG rollover

As described in Chapter 4, a CFD model has been created using ANSYS FLUENT 14.0 software, based on the compositions and heat fluxes of the La Spezia rollover incident (as the incident data are fully recorded by Sarsten[6] and could be used as an accurate base for comparison), using different viscosity and multiphase models (VoF/ Eulerian) to investigate the mechanism of the interactions between the LNG layers before and during the rollover and validate which model's results have the best agreement with reported data of Sarsten[6]. The La Spezia rollover incident was selected because all the required technical data was available in Sarsten[6] and Heestand *et al.*[24] papers.

The first few models were very basic, comprising of a single component (methane), with only heat diffusion between the layers, gradually added more complexity to the models such as having multi-component LNG mixtures and considering heat and mass diffusion between layers.

The convergence of each simulation was verified by the observation of three generalised areas:

    a) The target residual values have been met.
    b) The overall domain imbalances are less than 1% (as recommended in ANSYS user manual).
    c) Quantitative monitors (such as temperature and density differences) that have been placed, were no longer changing significantly (i.e. they have reached and maintained a static value).

After several simulations and setting up different CFD models, the results were satisfactory for detection of the Phase 1 in a stratified LNG tank, which was the

main objective of CFD simulation; however, have not been extend to Phase 2 due to limitations of CFD modelling software on simulating of multi-component mixtures, especially near their saturation points just before the rollover. Hence, after verifying the existence of Phase 1, lumped parameter modelling has been chosen to do the rollover modelling.

For referencing purposes, one of the CFD simulation cases with 2D domain, Eulerian multiphase model, Pressure based Navier–Stokes type solver, heat and species transport (minimum species transport) enabled and transient time set up (see Section 4.1) is presented here, in order to show the stages and the mechanism of the rollover in Phase 1 as suggested by Bates and Morrison[4].

Figure 5.1 shows the initial condition of the simulation. The model simulates the changes in the contour of the density of LNGs over time. There are two discreet layers of LNGs, red colour as the lower LNG layer (in FLUENT known as the primary phase) and blue colour as the upper layer LNG (known as the secondary phase), divided by a sharp interface, due to density difference (caused by composition and temperature difference) as shown in Figure 5.1 at t = 0. The different values of density are shown in the legend section, initially started from 432 kg/m^3 for the upper LNG and 439 kg/m^3 for the bottom LNG.

As time goes by, layers start to diffuse into each other, because of the temperature and compositional difference as well as the heat leaks from the outside (Figure 5.2), set in the boundary condition of the model.
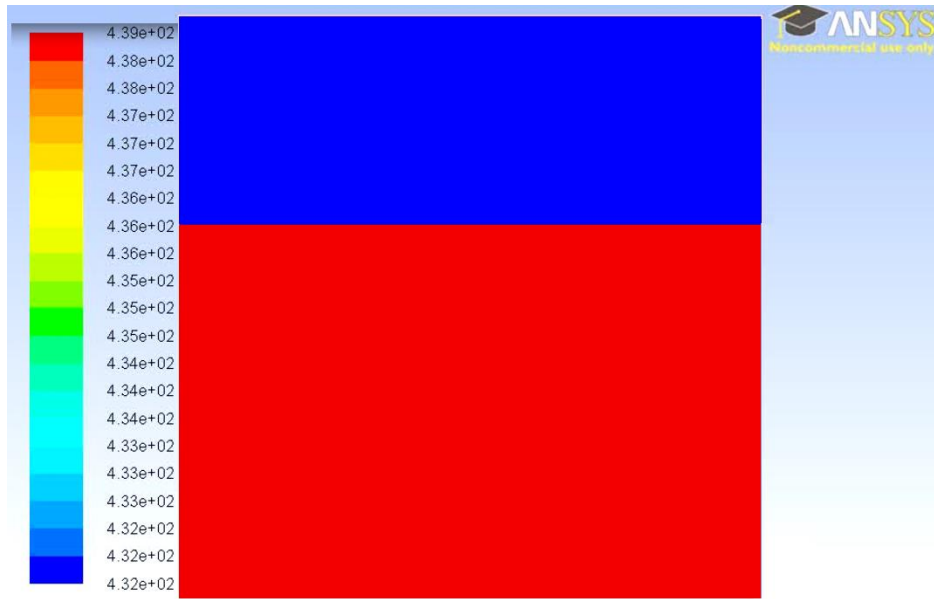
Contours of Density (phase-1) (kg/m3) (Time=0.0000e-01)   Mar 17, 2016
ANSYS FLUENT 14.0 (2d, dp, pbns, eulerian, spe, lam, transient)

Figure 5.1: At t = 0, start of the CFD simulation, LNG layers are placed on top
of each other.
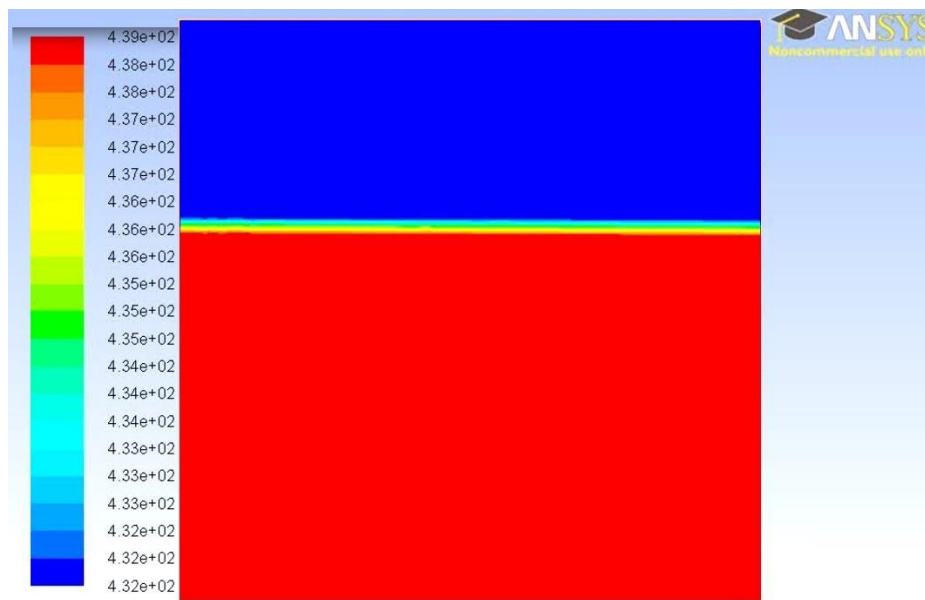
Contours of Density (phase-1) (kg/m3) (Time= 7.5000e+01)   Mar 17, 2016
ANSYS FLUENT 14.0 (2d, dp, pbns, eulerian, spe, lam, transient)

Figure 5.2: At t = 7.5 min, the heat transfer (diffusive heat transfer,
characteristic of Phase 1, while the mass transfer is set to minimum) started,
the interface starts to change colour, which shows density gradients.

126

Continuation of the heat (dominant) and mass (minimal) transfer between layers gradually formed some finger shaped columns of one liquid diffused into the other liquid shown with green/yellowish colours in Figure 5.3. These different colours showed the contour of the density of the diffused liquid into the other layer. (Refer to the legend on the left-hand side of each figure). This was in line with Turner's observation on the salt-water mixtures[5] diffusion and the formation of what he called "salt fingers" at the early stage of LNG layers interaction as well.

Contours of Density (phase-1) (kg/m3) (Time=2.7000e+01)   Mar 17, 2016
                              ANSYS FLUENT 14.0 (2d, dp, pbns, eulerian, spe, lam, transient)
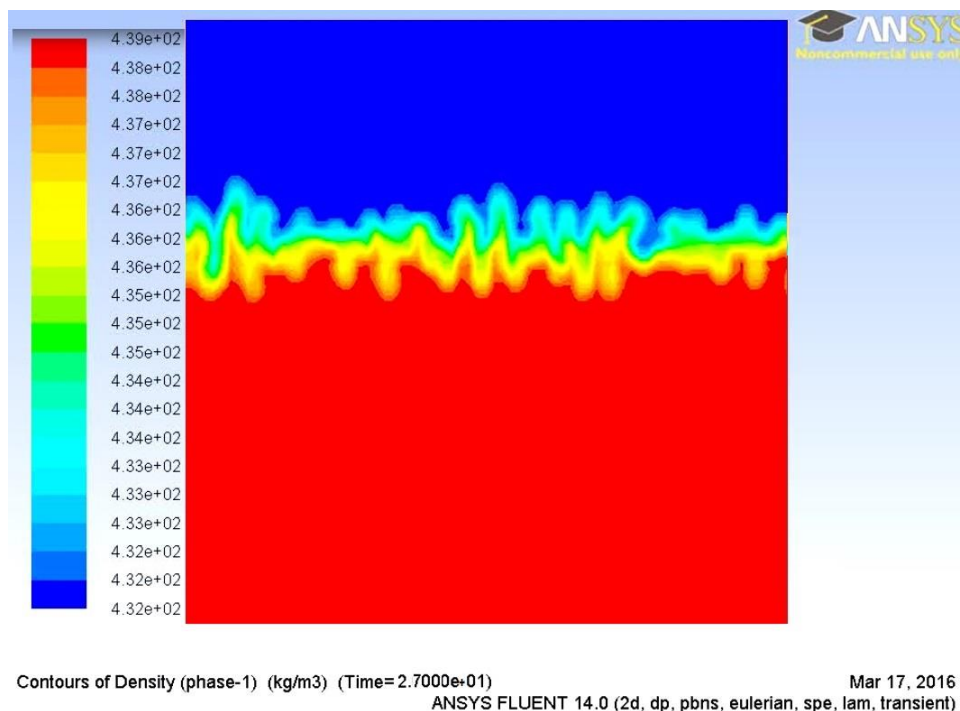
Figure 5.3: Formation of diffusion fingers[5] at the interface at t = 27 min. Diffusive heat transfer is dominant although the system is clearly evolving towards a transition.

In Figure 5.4, the diffusion fingers are developing more and getting bigger through combining with each other and the Rayleigh flow is increasing especially near the tank walls due to higher heat transfer on the wall surface. This shows diffusive heat transfer is still dominant although the system is clearly evolving towards a transition.

The temperature difference between the layers also start to affect the density and creates a natural convection circulation flow, known as Rayleigh Bernard flow[56].
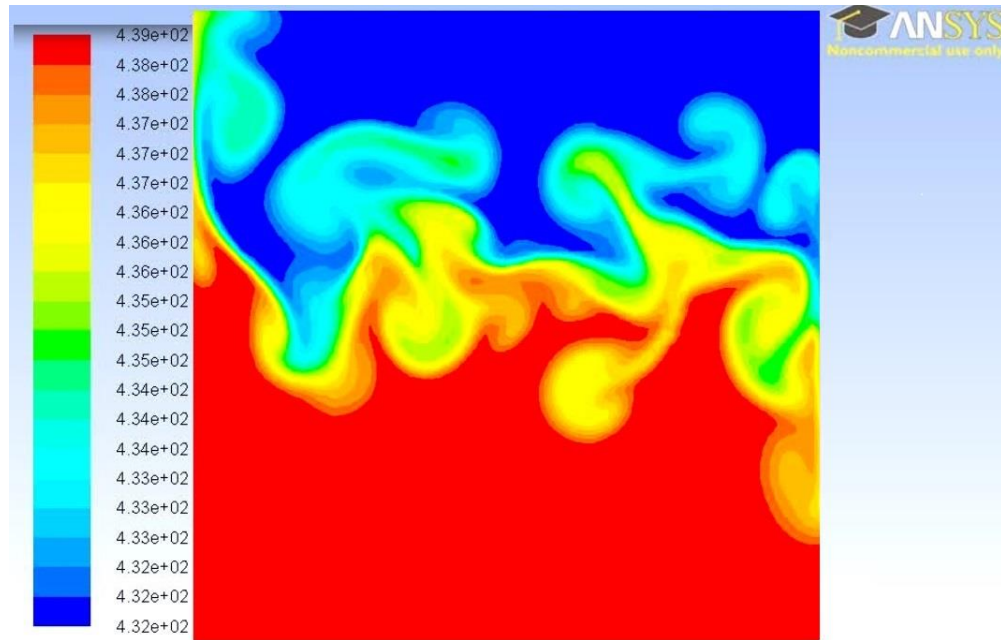
Contours of Density (phase-1) (kg/m3) (Time= 4.7000e+01) Mar 17, 2016
ANSYS FLUENT 14.0 (2d, dp, pbns, eulerian, spe, lam, transient)

Figure 5.4: At t = 47 min., diffusion fingers become larger, which was also observed by Turner[5] in the salt water solutions. This is the transition from the diffusive heat transfer to convective heat transfer.

Figure 5.5 shows how the Rayleigh-Benard flow increases over time and the natural convection speeds up as more heat leaks into the tank from outside, until the columns of liquid join and form two big circulation regions of liquid in each layer after a while due to natural convection as shown below. The dark blue and red colours are the original bulk LNGs in each layer with the densities closer to the initial values, and the lighter colours show the LNGs with different values of densities, varies between the two initial densities as they slowly mix.

This figure also shows that the layers still cannot fully mix, due to the density difference; however, interlayer natural convection circulation gradually mixes them. This is the transition stage from the diffusive heat transfer to convective.

128

The variation of light blue and yellow colours show different densities. Figure 5.6 is a schematic of Figure 5.5 with flow direction arrows show the direction of the natural convection circulation in the tank. Figure 5.7 is velocity vector output of FLUENT confirming the existence of two natural convection circulation cells and their directions.

Contours of Density (phase-1) (kg/m3) (Time=2.0700e+02)   Mar 17, 2016
ANSYS FLUENT 14.0 (2d, dp, pbns, eulerian, spe, lam, transient)
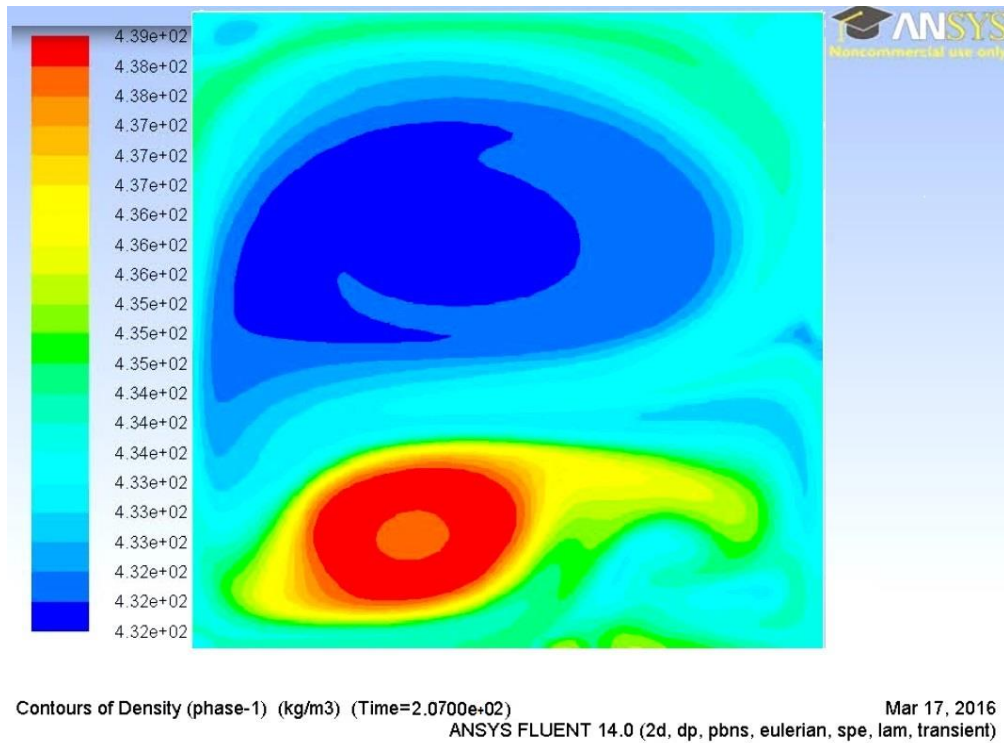
Figure 5.5: Natural convection flow becomes fully developed at t = 207 min. Diffusive heat transfer changed to convective heat transfer, which represents early Phase 2.
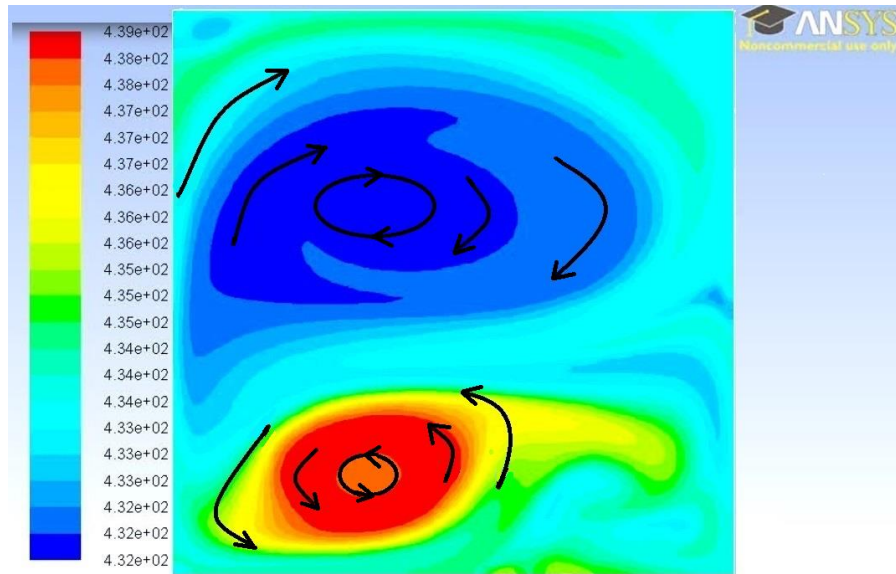
Contours of Density (phase-1) (kg/m3) (Time=2.0700e+02)   Mar 17, 2016
ANSYS FLUENT 14.0 (2d, dp, pbns, eulerian, spe, lam, transient)

Figure 5.6: Arrows show fully developed natural convection circulation direction in each layer known as Rayleigh Bernard flow.

phase-2-velocity Colored By Velocity Magnitude (phase-2) (m/s) (Time= 2.0700e+02)   Jun 18, 2016
ANSYS FLUENT 14.0 (2d, dp, pbns, eulerian, spe, lam, transient)

Figure 5.7: Velocity vector output results for Figures 5.5 and 5.6. Velocity vectors show natural convection circulation direction in each layer known as Rayleigh Bernard flow.

130

Figures 5.5, 5.6 and 5.7, clearly show the formation of the natural convection circulation flows and the existence of the Rayleigh-Benard cells in the simulated tank containing two LNGs after some time. This is consistent with Bates and Morrison's proposal for the occurrence of rollover in two phases, and it also suggests that at least two different interfacial heat transfer regimes should be used to accurately describe it.

As time goes by, Phase 1 starts to transit into Phase 2. The Rayleigh Bernard circulation flow continued to mix the LNGs and more LNG with density closer to the bottom layer were created until a bigger bulk of denser LNG generated in the bottom/middle of the tank as shown in Figure 5.8 in green/yellowish colour. From this stage forward, as the bulk LNG in the bottom of the tank got hotter due to the heat leaks from the outside, it started to form plumes of liquid going upwards, getting mixed with the colder top liquid and came back down due to the buoyancy force. However, each time this plume of liquid entered the top portion, it mixed with more liquid from the top (shown in blue, which was less dense/cooler) and created more mixing. This is in line with the description of penetrative convection[4] and start of Phase 2. Figure 5.9 shows the direction of the plumes going up and coming back. The simulation was terminated at this point because the model was not capable of simulating the BOG generation, which is essential to realistic descriptions of rollover. This simulation took about 15 hours to reach this point, with Intel i7 CPU and 16 GB of RAM hardware.
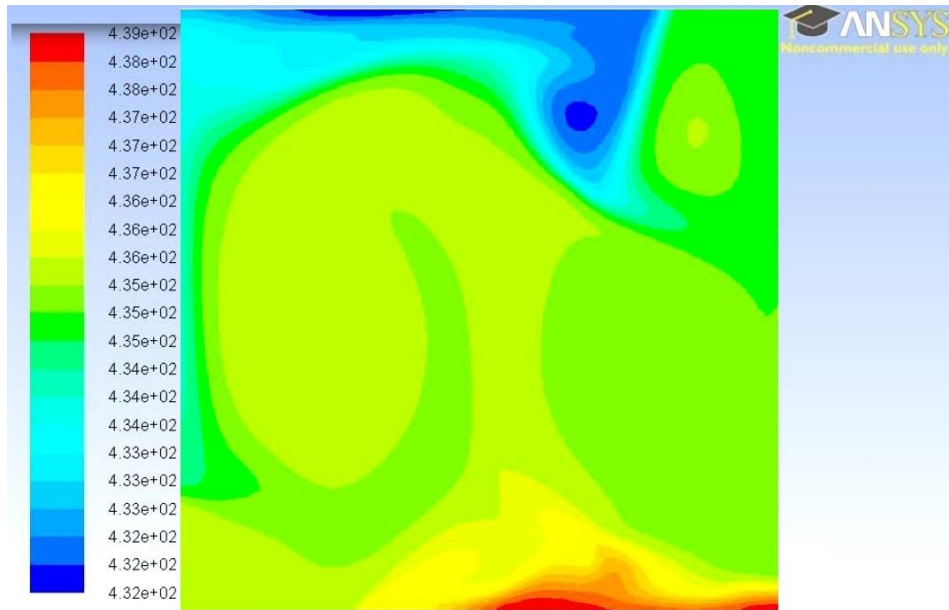
Contours of Density (phase-2) (kg/m3) (Time=3.0150e+02)   Mar 17, 2016
ANSYS FLUENT 14.0 (2d, dp, pbns, eulerian, spe, lam, transient)

Figure 5.8: Simulation result after Phase 1, formation of plumes of liquid (penetrative convection) at t = 301.5 min (5 hrs).
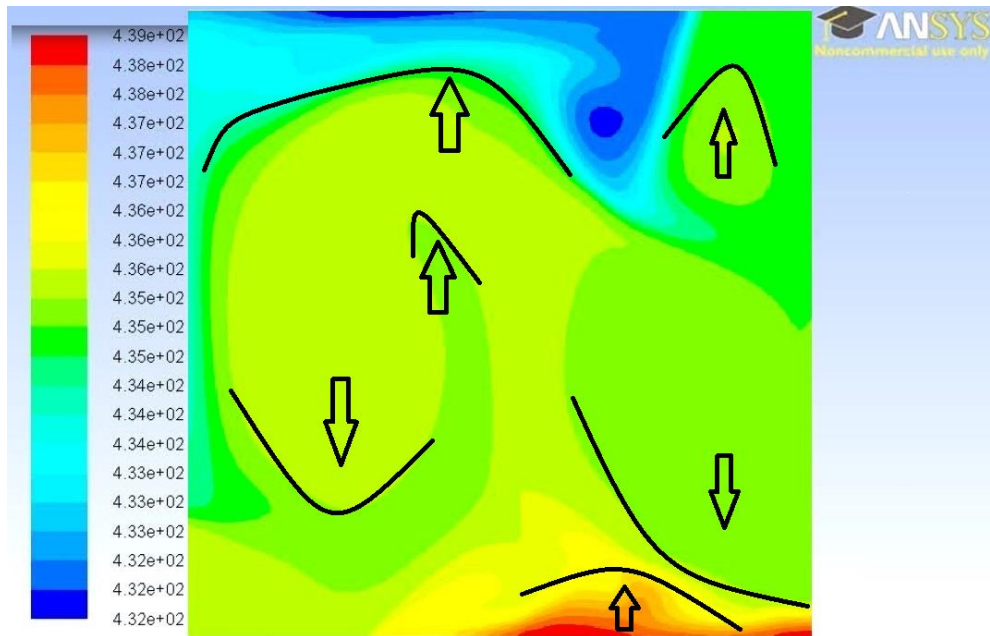
Contours of Density (phase-2) (kg/m3) (Time=3.0150e+02)   Mar 17, 2016
ANSYS FLUENT 14.0 (2d, dp, pbns, eulerian, spe, lam, transient)

Figure 5.9: Arrows show the direction of plumes of liquid movements (start of penetrative convection) at t = 301.5 min (5 hrs).

In general, to simulate the whole rollover process with CFD tools, CFD models need to account properly for boil-off at the vapour-liquid interface and the convective Rayleigh flow that drives this boil-off. This was also pointed out by Zimmerman and co-workers in a subsequent paper[47]. The major limitations of above-mentioned method are summarized as follows:

1. ANSYS FLUENT software database is very limited for physical properties (it mainly used for some general systems such as steam, water and pure fluid), especially calculating the complex hydrocarbon mixtures' properties such as LNG. All the required mixture data must be fed into the software in case of multicomponent simulation. This problem was solved by using a "User Defined Function" (UDF) in C++ programming language for La Spezia LNGs to define density changes as the function of temperature over time. However, this model was very specific to the La Spezia incident results obtained from the lumped parameter simulation data, using Reynolds analogy for mass transfer. Moreover, for engineering purposes or safety and risk assessment of LNG unloading, a faster and easier method is needed to simulate the rollover. The knowledge of processing the data and the availability of above-mentioned software in any LNG plants are very improbable. However, a lumped parameter program code written in widely available programming software (capable of turning into an executable file), such as MATLAB codes can solve this problem.

2. ANSYS FLUENT software is not capable of handling the thermodynamics for complex mixtures, as it is primarily a hydrodynamic program and normally used to simulate the fluid flows with turbulence. Phase changes and flash calculations that are central to multi-phase hydrocarbon simulations such as LNG rollover, cannot be simulated in FLUENT environment. Coupling of any external thermodynamic software such as HYSYS or REFPROP with the FLUENT is also problematic. Due to the nature of CFD simulation, which divides the system into millions of subsystems (cells) and extends any changes in the property of one cell to the adjacent cells over several small fractions

133

of time, transferring data between two software is both complicated and slows down the simulation speed tremendously (using subroutines of HYSYS/ REFPROP several times per second for each cell and refresh data over a period of for example 30.5 hours).

3. As mentioned in item 2 above, due to nature of CFD simulation methods, each simulation takes a long time to converge to its goals. For slow phenomena such as LNG rollover, which takes days and weeks to occur, CFD simulation methods are extremely time-consuming and slow. Considering the aim of LNG rollover simulation, which is to predict the time from unloading of the LNG cargos to storage tank, to the occurrence of rollover, CFD simulation may take even longer time than the real rollover.

Extending the CFD simulations to realistic LNG storage scenarios up to the actual rollover event were found to be very problematic because of the need to develop appropriate Reynolds-averaged Navier-Stokes[26] equations for fluid phases. Incorporating such a realistic boundary condition remains a significant challenge for future, improved CFD models of LNG rollover. Therefore, after achieving our goal of simulating the Phase 1 and detection of natural convection cells, we decided not to proceed any further with CFD models and develop a lumped parameter model capable of incorporation the thermodynamics and BOG of the LNGs.

5.3. Lumped parameter rollover model results:

As previously mentioned, there are relatively few studies of rollover simulation in LNG systems in the open literature and the ones that are accessible do not provide much useful additional information. Among those, the lumped parameter simulations for rollover done by Heestand *et al.*[24] for the La Spezia incident and Deshpande *et al.*[25] for the Partington incident are significantly important. However, the simulation of the Partington rollover incident by Deshpande *et al.*[25] was not successful (18 hours vs 68 days) due to the unavailability of some part of the initial condition data for the tank and LNGs as well as a questionable simulation method, which is previously described in Chapter 2 of this thesis.

In order to improve on previous simulations; in this research, we have incorporated the feature of using either lower or higher heat retransfer regimes along with the Chilton-Colburn or the Reynolds analogy for mass transfer regime based on the stability ratio of the system, in our lumped parameter model as our suggested hypothesis. Later the model has been linked to the REFPROP software to calculate physical properties and solve the differential equations at each time step using the results as the starting conditions of the next step until the rollover occurs. We have tested this model with the La Spezia incident to verify the accuracy of the model and after getting satisfactory results, it was used it to simulate the Nantes and the Partington rollover incidents. Furthermore, several sensitivity analyses were conducted over the critical values of the heat transfer coefficient and the heat absorbed by the vapour in rollover incidents to evaluate the criticality of these parameters on the rollover time and BOG.

The following cases have been selected among several simulations done for LNG rollover for comparison and discussion:

5.3.1. La Spezia rollover incident (30.5 hours)

The first lumped parameter simulation was that of the La Spezia system using the Reynolds analogy to calculate the mass diffusion regime from the heat transfer correlation, which Heestand *et al.*[24] reported giving the best fidelity to the observations of Sarsten[6] (Row 5 of Table 2.5 in Chapter 2). The Reynolds analogy was automatically chosen by our simulation program as the initial La Spezia LNGs' R_s = 1.7 was lower than the critical ratio of R_c = 3.8.

The thermophysical properties needed for the simulation were calculated using the GERG-2004 implemented in REFPROPM software while the vapour temperature (which is equal to the film temperature) was calculated by setting the initial value equal to that of the upper layer. Finally, following Heestand *et al.*[24] it was initially assumed that the vapour absorbed only 5% of the heat transferred to it through the tank walls and the roof (Eq. (4-11)) for comparison of the results, then a sensitivity analysis was done to investigate this assumption of Heestand *et al.*[24] in the next section.

It should be noted that although Sarsten[6] gave a very accurate description of the density evolution and the initial physical properties for the heel and cargo LNGs in the La Spezia rollover incident including the tank data; however, he did not specify the initial temperatures of each layer. He only mentioned the localized temperature of the LNG inventory based on the tank's level after the filling as demonstrated in Figure 5.10. He also did not specify the evolution of temperatures over time from the initial loading up to the rollover. Heestand *et al.* assumed 114.3 K and 118.9 K as the initial heel and cargo's temperatures, and modelled their simulation based on this assumption.
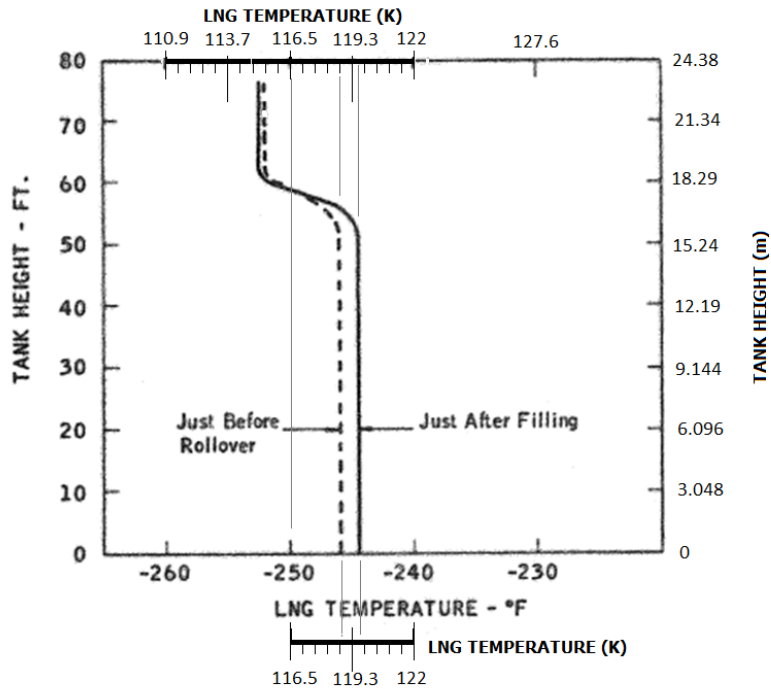
Figure 5.10: Sarsten temperature data for the La Spezia rollover event, which have been modified in this thesis to represent SI unit on the right-hand side.

In this study, we extracted the initial temperature data from the Sarsten paper[6], and converted them to SI unit, assuming that "*Just after filling*" temperature is the initial LNGs' temperature, and "*Just before rollover*" are the final temperatures. Furthermore, in lack of any specific data, highest liquid level in the tank was assumed to represent the top layer and lowest liquid level as the bottom layer. The extracted temperature data from the above graph shows the initial LNG temperatures to be equal to 119.3 K for the bottom layer and 114.9 K for the upper layer. However, as there is not data available on how the temperatures evolved between "*Just after filling*" and "*just before rollover*" in the above graph, to verify the accuracy of our model, we compared our density and temperature data with the Heestand *et al.* results not the Sarsten's, and the BOG with both Sarsten's and Heestand *et al.*'s.

The results obtained for Case 1 were highly in accordance with those reported by Heestand *et al.*[24]. The results for Case 1 are shown in Figures 5.10, 5.11, 5.12 and 5.13. Most of the plots in Heestand *et al.*[24] work have time scales of 80 hours and show modelled results after the rollover event but in this work,

the simulation was terminated once rollover had occurred (around 30.5 hours = 1.24 days); however, the time scale is equal to 80 hours for ease of comparison. The original Heestand *et al.*[24]s' Figures for density and temperature are presented on top and our results on the bottom for comparison, except the BOG figure, which Sarsten's Figure was also used as Heestand *et al.*[24]'s result was incomplete and inaccurate.
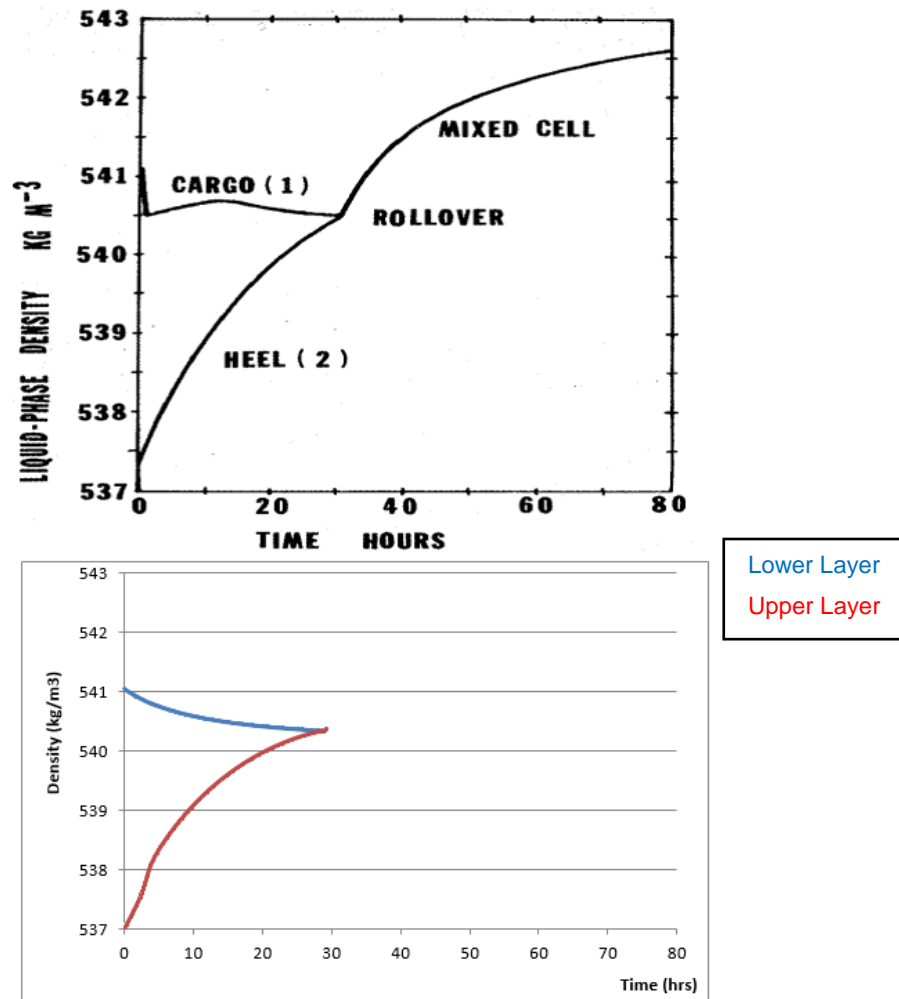
Figure 5.11: Simulation results for the evolution of mass densities of the lower and upper liquid layers in the La Spezia rollover incident. The top Figure is Heestand *et al.*[24]'s results and the bottom Figure is this research results.

The results shown in Figure 5.11 can be summarized as follows:

The simulation demonstrates an internal consistency with the equalisation of the densities of the lower and upper liquid layers in that time. The evolution of

the upper layer's density over time is very similar to the results of Heestand *et al.*[24], increasing from the initial value of 537.1 kg/m^3 and reaching a final value of 540.4 kg/m^3, similar to what is shown in the top Figure. The lower layer density simulated in this case, decreases smoothly with time, from the initial value of 541.1 kg/m^3 to the final value of 540.4 kg/m^3 after 30.5 hours. A small difference in the initial densities between our results and Heestand *et al.*[24] is due to using different EOS in simulation programs as described in Chapter 2. Furthermore, a sudden drop in Heestand *et al.*[24] lower layer's density in first few hours (wasn't justified by Heestand) was not observed in our results.
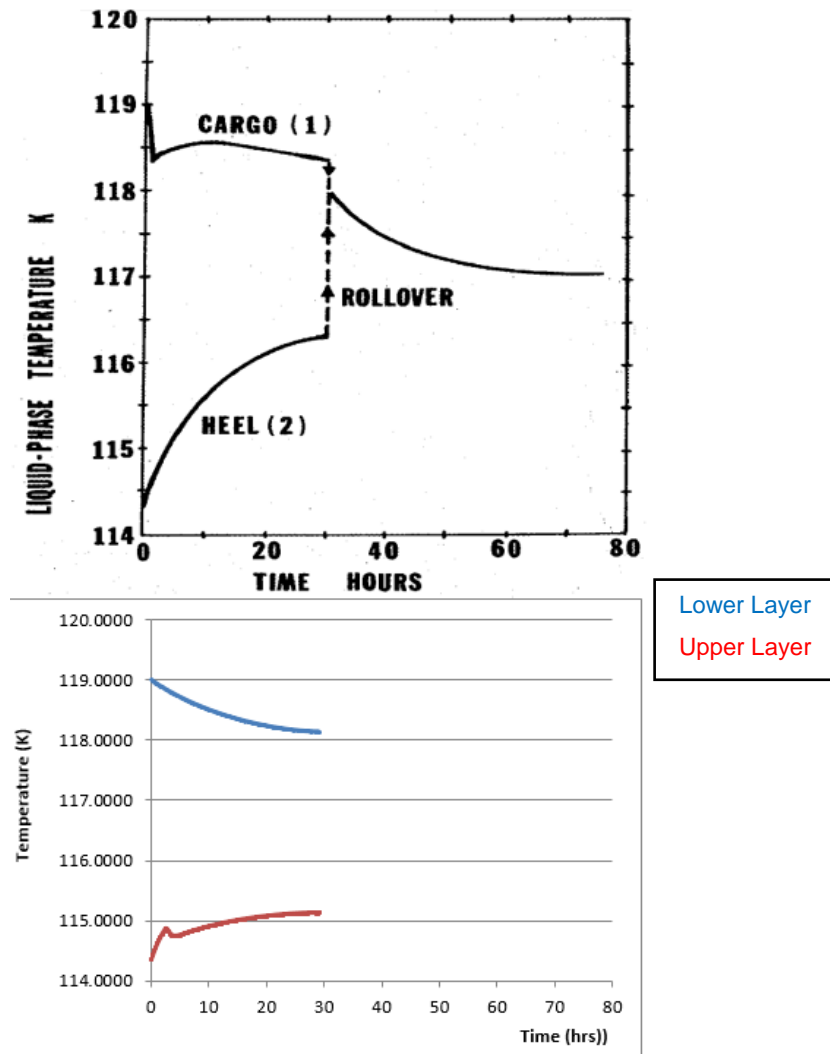
Figure 5.12: Simulation results for temperatures of the lower and upper liquid layers. The top Figure is Heestand *et al.*[24] result and the bottom Figure is this research result.

139

The results shown in Figure 5.12 for the La Spezia rollover incident, demonstrates the evolution of the lower and upper layers' temperatures versus the time. The change of the upper layer's temperature has a similar shape (with less curvature) to the top layer's temperature reported by Heestand, started from 114.3 K and ended at 115.1 K. After about 2 hours, our results for the upper layer's temperature suddenly decreased (the small peak at the beginning) at a time around 2-6 hours, which is corresponding to the peak in the BOG generation shown in Figure 5.13 that resulted in temperature drop due to the vaporization. After that, the upper layer's temperature smoothly increased with time due to the interlayers' convection heat transfer until the rollover occurrence at 30.5 hours. Our simulated temperature result for the upper layer, at the time of rollover is lower than predicted by Heestand *et al.*[24] (116.4 K vs 115.2 K), due to the different heat transfer coefficient selected by us and more accurate vapour phase composition, calculated by our program at each time step versus what was considered by Heestand *et al.*[24], which was constant values of 0.95% methane and 5% nitrogen, which had direct effect on the BOG rate and hence the upper layer's temperature.

Although the initial and the final values for the lower layer temperature of our simulation results were very similar to the Heestand *et al.*'s (118.9 K initial and 118.2 K final); however, the sudden decrease in the lower layer's temperature in the first few hours reported by Heestand *et al.*[24] was not observed in our simulation, while as mentioned before, Heestand *et al.*[24] did not provide any reason for why this temperature drop occurred in their simulation.
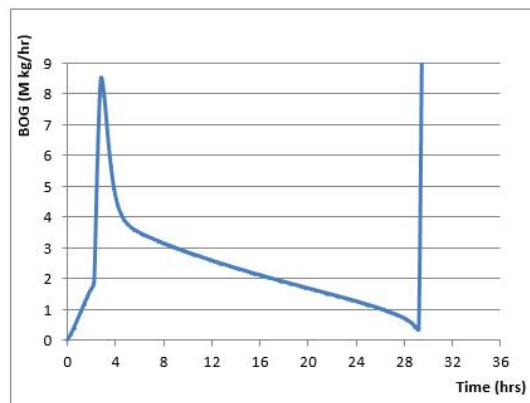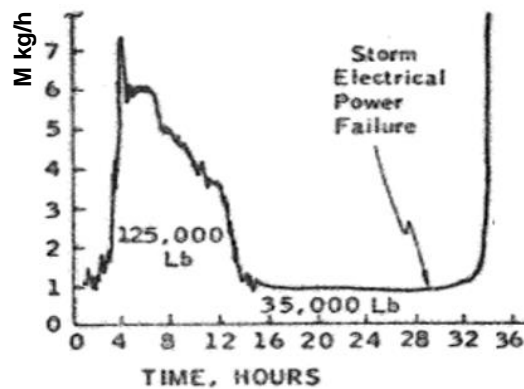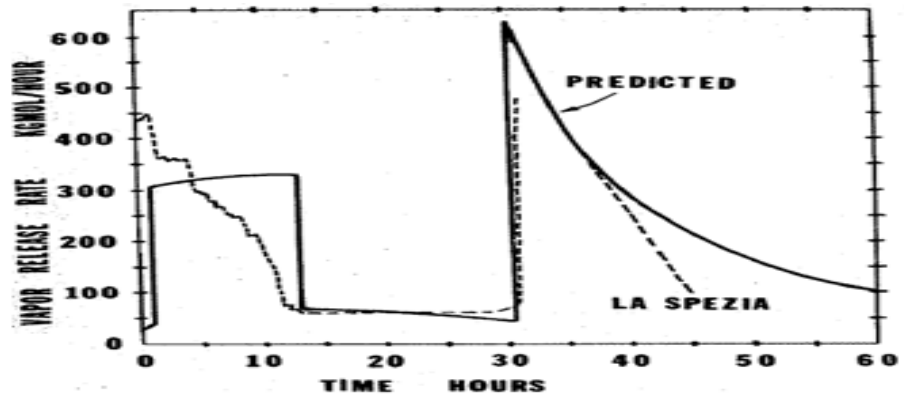
Figure 5.13: Simulation results for the boil-off flow rate. The top Figure is the Heestand *et al.*'s result, the middle Figure is the Sarsten's report and the bottom Figure is this research result.

Figure 5.13 shows the evolution of the generated BOG over time in the La Spezia rollover incident. As the graph reported by Heestand *et al.*[24] did not completely match with the Sarsten data[6] (for example time to rollover is reported 32 hours by Sarsten, while 30.5 hours reported by Heestand *et al.*, and the first peak of BOG occurred at time equal to 2 to 6 hours in Sarsten

report, but initially in Heestand's, etc.), we used the original Sarsten figure (middle graph above) as the main basis for the comparison; however, Heestand's result (top graph) has been brought as well. Our simulation results have a similar shape to Sarsten BOG report, with first BOG peak at time about 2 to 6 hours, caused by a high Rayleigh flow (Eq. 4-13) due to large initial density difference, generated 8.4 M kg/hr BOG versus 7.5 M kg/hr BOG reported by Sarsten[6], decreasing as the layers' density and temperature difference became less. At the rollover point, as the bulk liquid temperature (mixture of both LNGs) had a higher temperature than the previous upper layer in contact with the vapour, it started to boil off to reach to a new thermodynamic equilibrium and created the final peak of BOG (8.9 M kg/hr versus 8.1 M kg/hr reported by Sarsten[6]). However, there is about 9% difference between our predicted BOG and Sarsten's, because of the errors in the Heestand *et al.* selection of the initial temperature as described in the beginning of this section, which has been inherited to our simulation results as well.
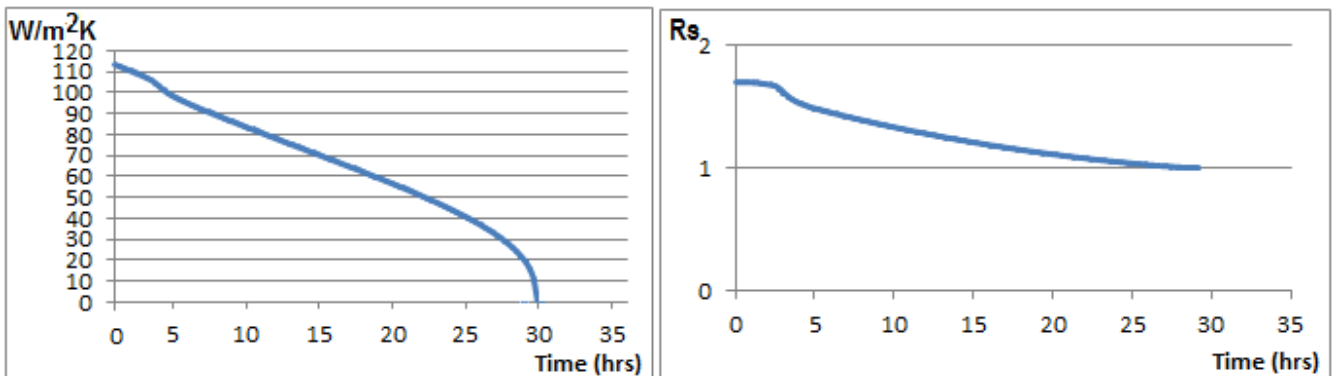
Figure 5.14: Simulation results for the heat transfer coefficient, h (left) and stability parameter R_s (right) versus time.

Figure 5.14 above (left graph) shows our results for the heat transfer coefficient "h" started from 112 W/m²K versus 85 W/m²K predicted by Heestand *et al.*[24] (Figure 2.4c). The difference between our value of "h" and Heestand's is because of Heestand's selection of a smaller coefficient in the Globe and Dropkin equation (see Table 2.5) while we used the original Globe and Dropkin equation. However, the shape of our predicted heat transfer coefficient graph

is very similar to the Heestand $et\ al.$'s, starting from the initial value of 112 W/m^{2}K and constantly decreased by time as the density and temperature differences between the layers became smaller, until rollover time which $\Delta\rho$ = 0, hence h = 0.

Figure 5.14 (right graph) presents the evolution of R_s versus time. Same as above, for the stability ratio R_s, started from the initial value of 1.7 and as the density and temperature differences between the layers got smaller, R_s decreased too, until rollover time that R_s =1 as $\Delta\rho$ = 0. R_s being less than R_c implies that only Reynolds analogy should be used as the governing mass transfer regime.

5.3.2. Sensitivity analysis on the La Spezia rollover incident simulation parameters

As previously mentioned, Heestand $et\ al.$ tailored their heat transfer equation to get the closest results to Sarsten's report. They also considered that 5% of the external heat leaks to the vapour space, will be transferred to the top layer and 95% of this energy remains in the vapour. However, they did not explain the basis and the reason for this assumption. For this research, we believed that there is no energy transfer from the vapour to the upper layer (film), as the vapour and the film are in thermodynamic equilibrium and have the same temperature. Hence, we performed a sensitivity analysis on the effect of assuming 95% or 100% of the energy stays in the vapour and compared the results as shown tin Table 5.2. Furthermore, we checked the effect of choosing the heat transfer coefficient constant on the time to rollover as well as the effect of the total external heat leaks into the tank (effect of insulation) in the La Spezia rollover simulation. The reason that we chose the La Spezia rollover incident to perform these sensitivity analyses, were that among all other available incidents in the open literature, this one had the most detailed recorded information, and the results could be used for our further case investigations and incident simulations.

Test no.	Coefficient of Globe and Dropkin's equation	h (W/m²)	%q Heat flux from the outside stays in the vapour phase	Total external heat flux Coefficient	Time to rollover (Hrs)
1	0.77 (Heestand's)	85.5	95% (Heestand's)	1	30.5
2	0.77 (Heestand's)	85.5	100% (This Study)	1	31.9
3	1 (This Study)	112.5	95% (Heestand's)	1	30.5
4	1 (This Study)	112.5	100% (This Study)	1	29.16
5	1 (This Study)	112.5	100% (This Study)	1.1	29.16
6	1 (This Study)	112.5	100% (This Study)	1.2	29.16
7	1 (This Study)	112.5	100% (This Study)	1.4	28.88

Table 5.2: Comparison between different selected simulation parameters in the La Spezia rollover models

The sensitivity analysis has been summarized in Table 5.2; the first row is the original Heestand et al.[24] selected parameters for the heat transfer coefficient, portion of external heat leak stays in the vapour and the total external heat leak into the system, as they used in their simulation to get 30.5 hours to rollover. In the second row, we used the same heat transfer coefficient as Heestand's, but considered no external heat transfer from the vapour to upper liquid. This increased the time to rollover by ~4%, as it took more time for the upper layer to reach to the temperature and density required for the rollover. In our La Spezia rollover simulation base case, which has been presented in the third row, we used the original Globe and Dropkin's[29] heat transfer equation without modification, which gave a bigger initial heat transfer coefficient than Heestand's and set our model to have 95% external heat transferred from the outside stayed in the vapour. This gave the same time to rollover as Heestand et. al.'s model. In row 4, q has been set to 100% with the original Globe and

Dropkin's[29], which reduced the time to rollover about 4.5%. In rows 5 to 7, all parameters are equal to row 4, except the total external heat leak, which has been increased from 10% to 40%. This increase in the external heat leaks showed that up to 40%, it did not affect the time to rollover, while changing 5% in the q value, affect the rollover time immediately. It means that rollover simulation is more sensitive to the value of the q rather the external heat leaks or the selected heat transfer coefficient.

Last but not the least, simulation results shown in rows 4 to 7, indicated that increasing the external heat leaks (or error in the measurement/reporting) can shorten the rollover time. As mentioned in Chapter 2, this could be the case in the Baker and Creed[18] report of the Partington rollover incident, and the cause of getting very short time to rollover in the Deshpande *et al.*'s[25] simulation (18 hours vs 68 days). We will address this issue later in Section 5.4.4.

5.3.3. Nantes rollover incident, (56 hours)

It was shown in Chapter 3 that although the data of Bates and Morrison[4] were only presented graphically, it was possible to extract additional information from their results with only a few reasonable assumptions about the compositions of the LNG mixtures they studied such as mentioned in Table 3.5. Hence, we developed an extended rollover simulation using the entire graphical data presented by Bates and Morrison[4] that incorporated both Phase 1 and 2 for the first time available in the open literature.

This required additional assumptions being primarily the size of the LNG tank and the heat flux into the tank from the environment. Some information regarding these assumptions was extractable from the free videos available from Gaz de France describing their commercial "LNG Master" software[57]. These videos purport to show some experimental facilities used for their proprietary experimental investigations into LNG rollover, which may be similar to the ones that generated the data reported by Bates and Morrison[4]. Furthermore, a reverse calculation has been done to calculate the heat leaks

into the tank from the outside that changed the lower layer's temperature from the initial temperature to the final Phase 1's temperature (extracted from the Figure 2.7), and assumed this heat leak will be constant during the rollover process and also assumed that the upper portion of the tank received almost the same amount of heat leak, and used this value in our simulations. These information are presented in Table 5.3.

Nantes rollover data used in our model	
Lower layer Level (m)	5.5
Upper layer Level (m)	1.6
Lower layer initial T (°C)	-158.8
Lower layer initial ρ (kg/m^3)	462.8
Upper layer initial T (°C)	-159.5
Upper layer initial ρ (kg/m^3)	456.9
Tank height (m)	8.5
Tank diameter (m)	8.5
Heat leak (kW)	16 (calculated)

Table 5.3: Nantes rollover incident's tank data extracted from Bates and Morrison[4]'s paper.

We used our hypothesis of having two stages (phases) in LNG rollover, with different governing heat and mass transport regimes in simulating the Nantes rollover incident. As mentioned in previous chapters, as the initial stability ratio of the Nantes LNGs (Table 3.4) was higher than the critical ratio of $R_c = 3.8$, we used a lower heat and mass transfer coefficients for the Phase 1, with the heat transfer coefficient being smaller than the heat transfer coefficient in Phase 2 with the same ratio of the mass transfer coefficient in Phase 1 (obtaining from the Chilton-Colburn analogy), being smaller than the mass transfer coefficient obtaining from the Reynolds analogy (in Phase 2). A sensitivity analysis has been done through several simulations to fine-tune this ratio of the heat transfer coefficients in different phases as well as the calculated external heat leak to

the tank. The best result has been presented in this section while the sensitivity analyses have been described in Section 5.4.4.

In general, the results for this simulation were in good accordance with those reported by Bates and Morrison[4] especially for the time to rollover (56 hours). The results are shown in Figures 5.14, 5.15, 5.16 and 5.17. As the plots in Bates and Morrison[4] work have time scales of 72 hours, our results have the same time scale. Original Bates and Morrison[4] graphs are also presented on the top of our results for easier comparison.
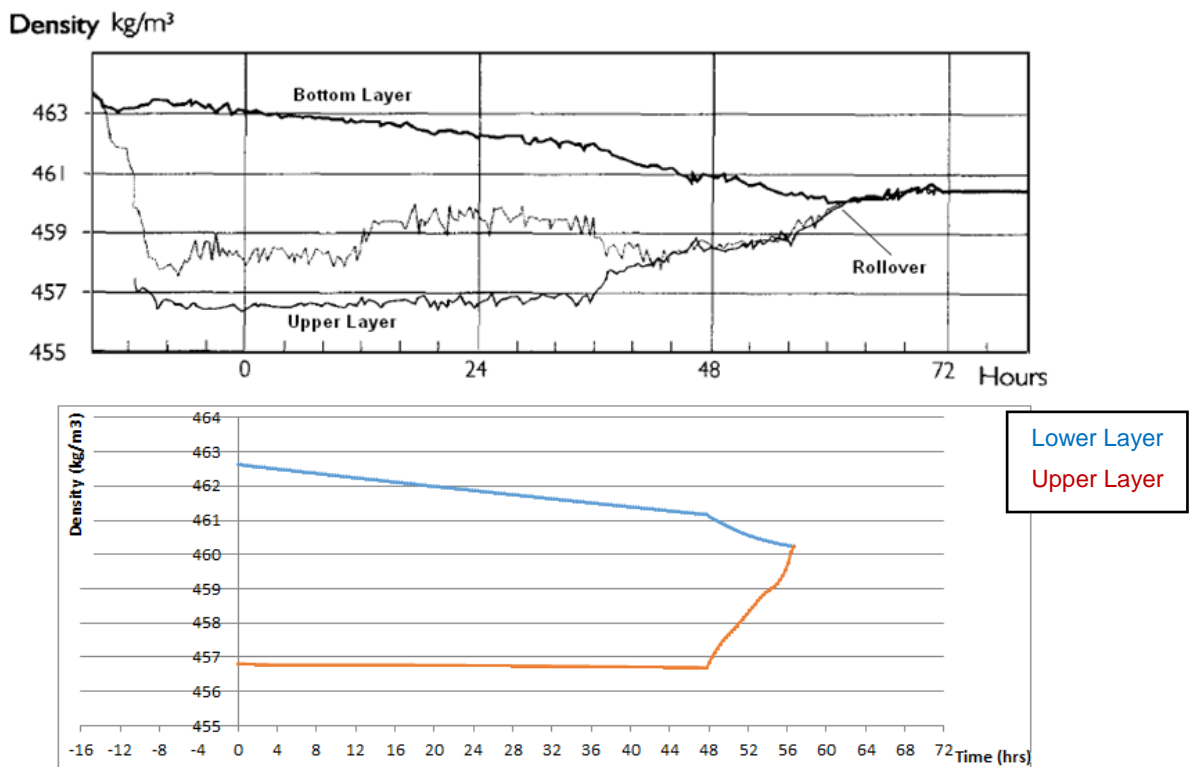
Figure 5.15: Simulation results for the evolution of mass densities of the lower and upper liquid layers in the Nantes rollover incident. The top Figure is Bates and Morrison[4]'s results and the bottom Figure is this research results.

Figure 5.15, shows the evolution of densities of LNGs over time. It is important to notice that Bates and Morrison[4]'s results are shown from 16 hours before the measurement set point, so the comparison should be done from time equal Zero. Our calculated initial densities using GERG-2004 EOS are also in good

accordance with their measurements and both graphs have almost the same shape. Densities started to approach each other smoothly in Phase 1 (from 0 to 36 hours) and became faster with more slope in Phase 2 (from 36 to 56 hours). In our results, the lower layer density started to decrease from the initial value of 462.8 kg/m^3 to 461.6 kg/m^3 at the end of Phase 1 (36 hrs) and from 461.6 kg/m^3 to the final value of 460.1 kg/m^3 at the end of Phase 2 (56 hrs), while the reported lower layer density by Bates and Morrison at the end of Phase 1 was a little bit bigger than ours. For example, at t = 36 hours their lower layer density is 462 kg/m^3 (~0.8% bigger than ours); however, at the end of Phase 2 at 56 hours they were almost the same equal to 460.2 kg/m^3.

The initial upper layer density in our simulation, was 456.9 kg/m^3 and stayed almost constant through Phase 1 936 hours) very similar to Bates and Morrison's, and stayed constant half way through the Phase 2 (48 hours), then increased to the final value of 460.1 kg/m^3 at the time of rollover. While Bates and Morrison's upper layer density, started to increase almost immediately after Phase 1. This discrepancy between our results and Bates and Morrison's is mainly because of our assumptions on the critical data such as the compositions and heat leaks from the outside environment, due to lack of actual information on Nantes' rollover incident.
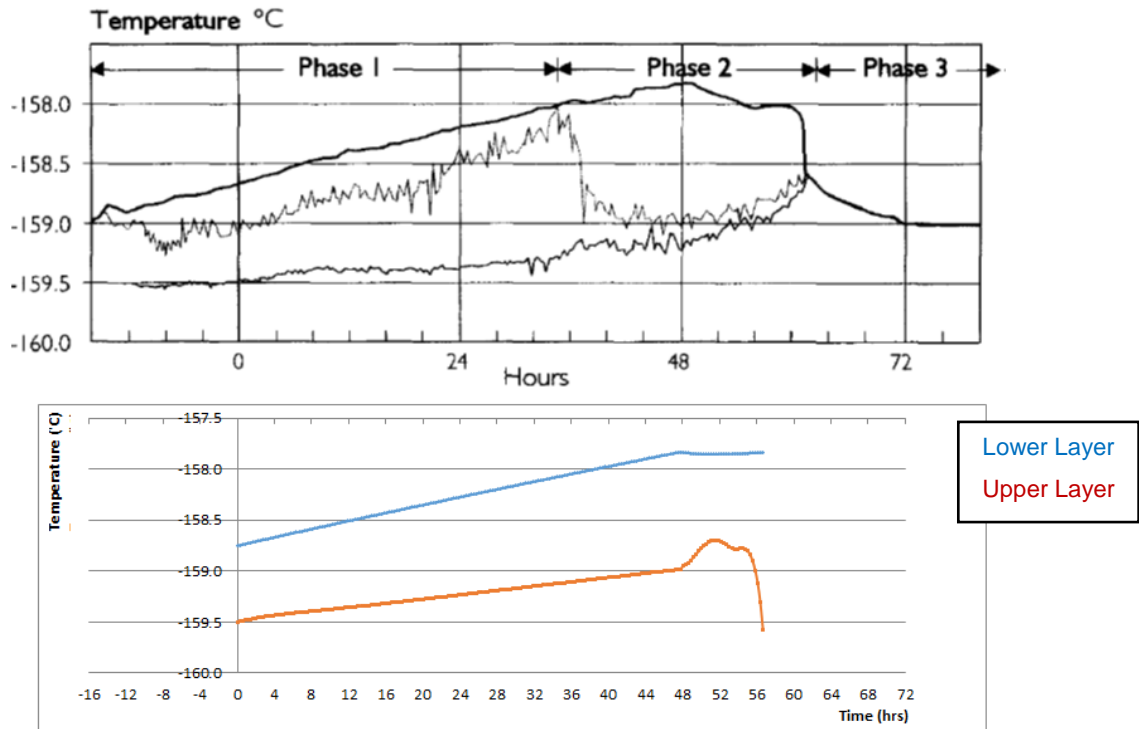
Figure 5.16: Simulation results for the evolution of temperatures of the lower and upper liquid layers in the Nantes rollover incident. The top Figure is Bates and Morrison[4]'s results and the bottom Figure is this research results.

Figure 5.16, shows the evolution of temperatures versus time of the Nantes rollover incident. Our results for the lower layer temperature is very similar to Bates and Morrison[4]'s, started from -158.8°C and increased to -158°C at the end of Phase 1 same as Bates and Morrison[4]'s. It continued to raise in Phase 2 to -157.8°C and then decreased. From hereafter, there is a slight difference between the slope of decreasing between our results and Bates and Morrison[4]'s, as their temperature decreased faster and ours stayed almost constant up to the rollover time.

The upper layer temperature, started from -159.5°C and increased in both ours and Bates and Morrison[4]'s results; to around -159.2°C at the end of Phase 1; however, the slope of increasing of the upper layer temperature in the Bates and Morrison[4]'s results in Phase 2 is slower than us. Just a few hours before the rollover, our results diverged and started to decrease while Bates and Morrison[4]'s upper layer temperature continued to increase. The discrepancy

between our simulated results and Bates and Morrison[4]'s measurements is because of the fact that in our lumped parameter model, as the final BOG starts, the upper layer temperature drops as a result of evaporation.
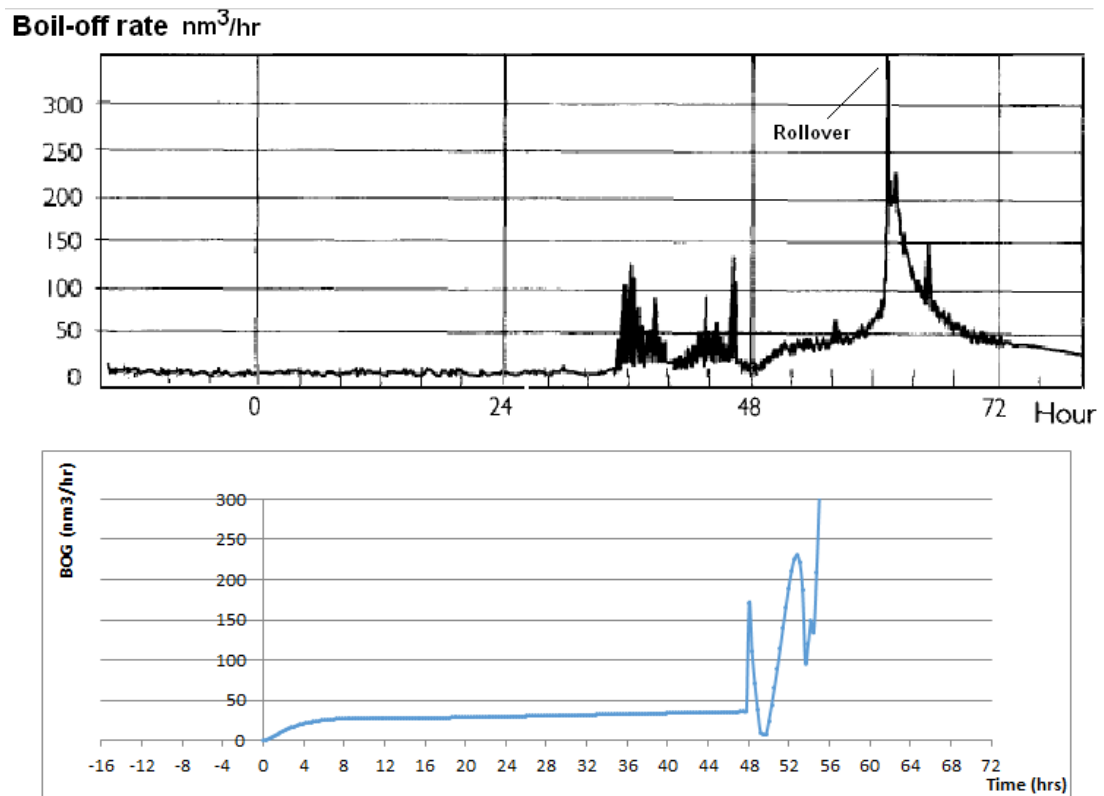
Figure 5.17: Simulation results for the evolution of BOG in the Nantes rollover incident. The top Figure is Bates and Morrison[4]'s results and the bottom Figure is this research results.

Figure 5.17, shows the evolution of BOG versus time in the mentioned rollover incident. Bates and Morrison[4]'s results showed two BOG peaks at around 36 to 42 hours before the major BOG peak at the time of rollover. Although our results followed the same shape as Bates and Morrison[4]'s results, but our peaks happened at 46 to 52 hours before the rollover final peak at 56 hours. The two pre-rollover BOG peaks in our results were higher than Bates and Morrison[4]'s results but the final BOG was lower than theirs (300 vs 400 nm^3/hr, 25% less). The reason for this discrepancy is the assumptions on initial data such as the compositions and environment heat leaks, due to lack of actual information.
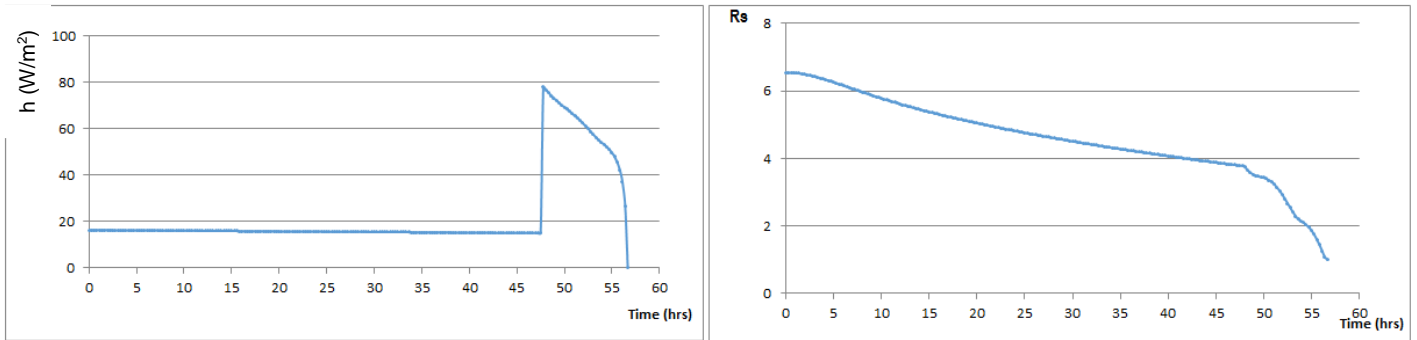
Figure 5.18: Simulation results for the evolution of heat transfer coefficients (left) in Nantes rollover incident and the evolution of stability ratio (right).

Figure 5.18 above (left graph), shows the evolution of the heat transfer coefficient "h" initially started from 16.3 W/m^2K, as the lower heat transfer coefficient was selected by the program ($R_s > R_c = 3.8$) in Phase 1. It continued to decrease slowly as the heat and mass transfer regime were slow in nature (natural convection), until the start of the Phase 2. From this point as the penetrative convection was started (simulated by the Reynolds analogy), the heat transfer coefficient increased to a higher value as well as the mass transfer until the occurrence of the rollover.

The right graph presents the evolution of R_s versus time. The stability ratio R_s, started from the initial value of 6.5 and as the density and temperature differences between the layers got smaller, R_s decreased too, until the rollover time that $R_s = 1$ as $\Delta\rho = 0$. R_s being bigger than R_c implies that both Chilton-Colburn and Reynolds analogies were applicable in the simulation.

151

5.3.4. Sensitivity analysis on the Nantes rollover incident simulation parameters

Table 5.4 presents some of the several simulation cases done as a sensitivity analysis to test the effect of the selection of the critical values on the time to rollover and the BOG. In this table, h1 is the heat transfer coefficient in Phase 1, which is a portion of the heat transfer coefficient in Phase 1 (same order of magnitude as the portion of mass transfers in Phase 1 and 2), and h2 is the Phase 2 heat transfer coefficient. A fine tuning was done through several tests to adjust this proportion. The same approach has been taken to test the effect of the selection of the external heat leak on the time to rollover and BOG, as the external heat leak was not available in the original Bates and Morrison[4]'s work and was calculated by us with some assumptions.

Test no.	h 1 proportion Coefficient	h 1 (W/m²)	h 2 proportion Coefficient	h 2 (W/m²)	External heat flux (W/m²)	Time to rollover (Hrs)	Remarks
0	0.10	12.1	0.77 equal to Heestand's	81.46	15	41.38	Only one peak of BOG before the rollover, Time to rollover is too short.
1	0.10	12.1	0.77 equal to Heestand's	81.12	16	45.83	Only one peak of BOG before the rollover, Time to rollover is too short.
2	0.12	14.52	0.77 equal to Heestand's	80.73	15	52.77	Two peaks of BOG before the rollover. Time to rollover is getting close to Bates & Morrison.
3	0.135	16.33	0.77 equal to Heestand's	79.97	15	59.16	Two peaks of BOG before the rollover. The amount of BOG in those peaks is bigger than reported by Bates & Morrison. Time to rollover is bigger than Bates & Morrison
4	0.11	13.31	1.0 Full Globe and Dropkin.	112.68	15	47.5	Two peaks of BOG, first one similar to Bates & Morrison, second one larger than Bates & Morrison. Time to rollover is shorter than reported.
5	0.12	14.52	1.0 Full Globe and Dropkin.	112.14	15	51.11	Two peaks of BOG before rollover. First peak amount is close to what reported by Bates & Morrison, the second peak is much larger. Time to rollover is still a little short.
6	0.135	16.33	1.0 Full Globe and Dropkin.	111.07	15	57.22	Two peaks of BOG before rollover. First peak amount is close to what reported by Bates & Morrison, the second peak is much larger. Time to rollover is longer than Bates & Morrison.

Table 5.4: Comparison between different selected simulation parameters in the Nantes rollover models

The sensitivity analysis showed that the system was not too sensitive to the selection of the external heat leaks of 15 or 16 W/m^2; however, the model was very sensitive to the ratio of h1 to h2. Although the order of magnitude of the ratio of the mass transfer coefficient obtained from the Reynolds analogy to the Chilton-Colburn analogy is about 0.1, but the ratio of the heat transfer coefficients which corresponds to the best result is about 0.135.

5.3.5. Partington rollover incident, (Case 1: 528.8 hrs, 22 days; Case 2: 34.9 hrs, 1.45 days)

As described in the previous chapters, the Partington rollover incident reported by Baker and Creed[18] lacks some vital data required for an accurate simulation. For example, in the industrial process of storage and transport of LNG, it is common to reliquefy a portion of the vapour with a BOG recovery compressor and return it to the tank. This will control the operating temperature as the recycling LNG will cool down the bulk LNG, as well as minimize the BOG generation. This recycling will become more important in long-term LNG storage to minimize the product loss. However, it seems that this important part of the data is missing in the Baker and Creed's report. Without knowing the exact amount of reliquefied gas that returned to the tank, which directly affect the temperature and the density of the LNGs, it is impossible to accurately simulate the Partington rollover incident and achieve the 68 days reported. This deficiency plus other deficiencies mentioned in Section 2.1 such as the initial LNGs' temperatures and the questionable value of the reported external heat leaks; make the Partington simulation very hard. Using the combination of Chilton-Colburn and Reynolds analogy and improved EOS can only improve the previous simulation of Deshpande et al.[25] by 22 days versus 18 hours; however, detailed information is needed for a successful simulation.

Considering all above-mentioned uncertainties, we decided to divide the simulations into two major categories of simulations:

1. Assumed the temperature difference between LNG layers to be $\Delta T = 2$ K (same as Deshpande et al.[25]), which resulted in a longer time to rollover if the layers' temperatures considered low enough (around 106 K), as it results in higher values of initial R_s. We believed that Deshpande et al.[25] tested different ΔT and chose the one which resulted in longest time to rollover in their results (18 hours); however, because of their uniform heat and mass transfer regime, they could not get more than 18 hours.

2. Assumed the temperature difference between LNG layers to be other than 2 K, such as 4.2 K, which resulted in shorter time to rollover. A 4.2 K initial temperature difference has been selected as it gave the longest time to rollover among all the cases that have been tested in this category.

All of these simulations predicted a longer time to rollover than reported by Deshpande et al.[25]. This improvement was mainly because of using of more advanced EOS (GERG-2004) and applying the hypothesis proposed in this research of using two heat transfer regimes and a combination of Reynolds and Chilton-Colburn analogy in our model to simulate the heat and mass transfers.

These simulation cases and sensitivity analyses on the critical parameters of rollover have been presented later in Section 5.4.6. One simulation case from each category mentioned above has been selected and demonstrated in this section.

Case 1 (Row 5 in Table 5.4):

For the first category ($\Delta T = 2$ K), the longest time to rollover achieved in our simulation model (22 days) is selected and described through Figures 5.18, 5.19, 5.20,5.21 and 5.22.
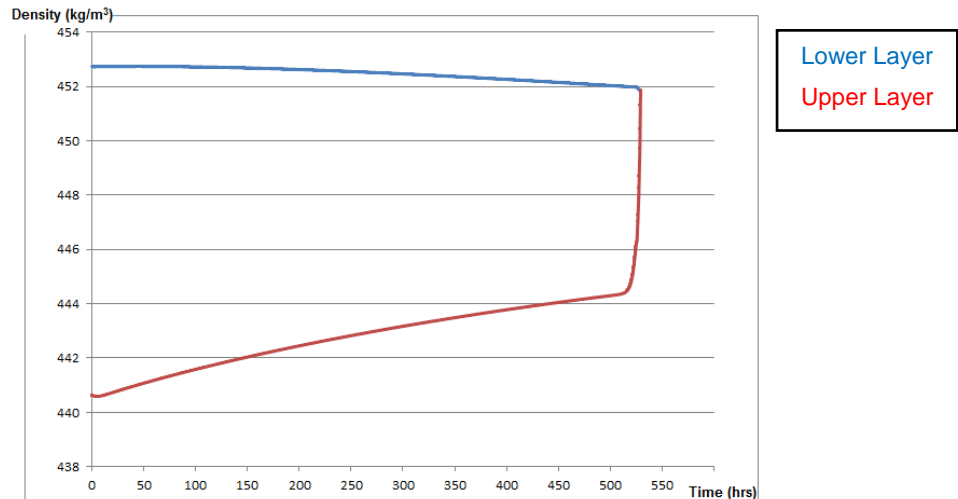
Figure 5.19: Case 1, simulation results for the evolution of mass densities of the lower and upper liquid layers in the Partington rollover incident.

Figure 5.19 shows the simulation results for the evolution of the mass densities of the lower and upper liquid layers in the Partington rollover incident. The lower layer density initially started at 452.5 kg/m^3 and smoothly decreased to the final value of 451.86 kg/m^3 at the end of Phase 2. The upper layer density started at 440.6 kg/m^3 at t = 0, and increased with a positive slope constantly until the end of Phase 1 at t = 525 hours (21.8 days); however, after change of the heat and mass transfer regime in Phase 2, the slope of increasing the upper layer density became much higher and reached to the final density of 451.86 kg/m^3 in few hours followed by the rollover (22 days predicted).
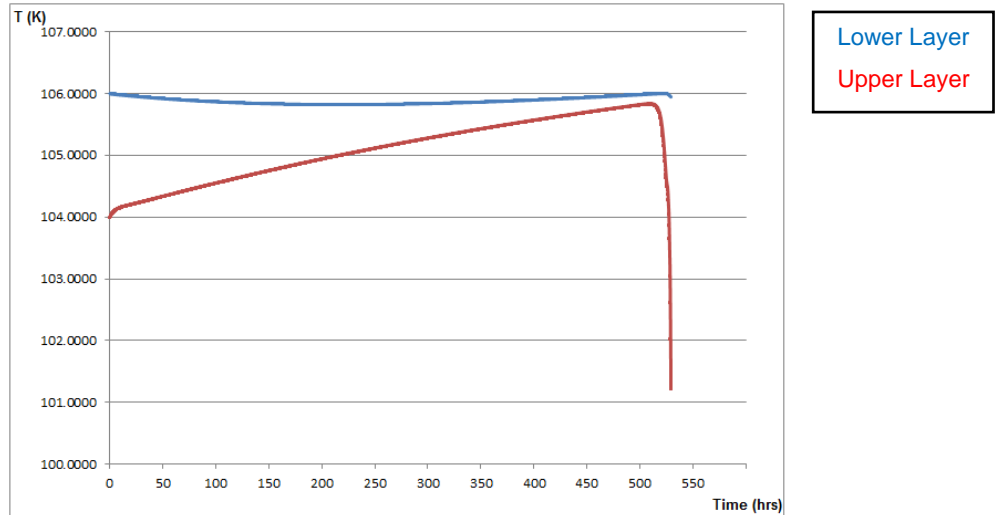
Figure 5.20: Case 1, simulation results for the evolution of temperatures of the lower and upper liquid layers in the Partington rollover incident.

Figure 5.20 shows our simulation results for the evolution of LNG layers' temperatures versus time. As mentioned before, we assumed the initial temperature difference to be 2 K. The lower layer initial temperature was 106 K, decreased slowly over time to 105.8 K until half way through the rollover process, and started to increase back to 106 K around rollover time. This increase is because of decreasing of the heat transfer coefficient until Phase 2.

The upper layer temperature initially started at 104 K and increasing almost linearly during the long Phase 1 (~525 hours, 21.8 days) to the maximum of 105.8 K at t = 509 hours and decreased after that to 104.57 K at the end of Phase 1 (at 525 hours) as the top layer started to evaporate, and continued to decrease very fast, due to large evaporation caused by increasing boil off, to the final temperature of 101.2 K at the time of rollover (528.8 hours).
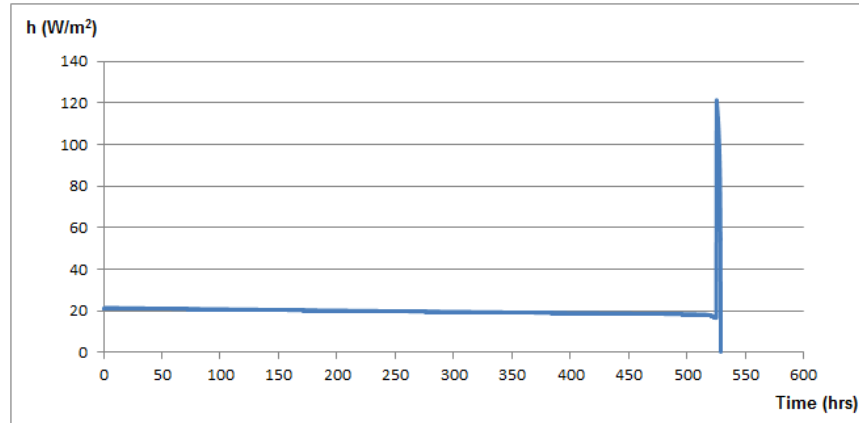
Figure 5.21: Case 1, simulation results for the evolution of the heat transfer coefficients in the Partington rollover incident.

Figure 5.21 shows the simulation results for the evolution of heat transfer coefficients over time. We used the same ratio of h1/h2 = 0.135 in this case as the best ratio to give the longest time to rollover. The Phase 1 heat transfer coefficient initially started from 21.2 W/m^{2}K, which decreased slowly through the Phase 1, as a result of slight layers' densities difference decrease, to 16.4 W/m^{2}K at the end of Phase 1, then increased rapidly to Phase 2 heat transfer coefficient, 121.1 W/m^{2}K and quickly reached to zero after a few hours (due to rapid penetrative convection in Phase 2) at the time of rollover.
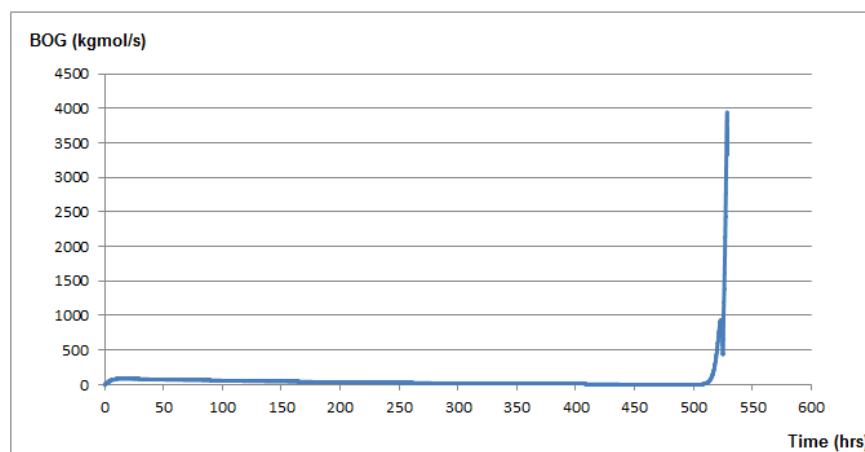
Figure 5.22: Case 1, simulation results for the evolution of the BOG in the Partington rollover incident.

157

Figure 5.22 shows the simulation results for the evolution of BOG over time. During most of the Phase 1, there was a minimum change in BOG, started from almost 0 kgmol/s until close to the end of Phase 1 the maximum value of at the end of Phase 1, which increased to its first peak, close to 938.5 kgmol/s at around 523 hours and down to 439.2 at 525 hours at the end of Phase1. At the start of the Phase 2, BOG reached to its final peak of ~4000 kgmol/s, with a sharp raise at the time of rollover.
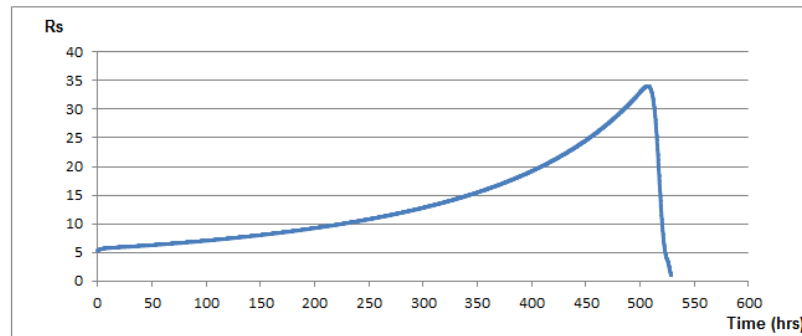
Figure 5.23: Case 1, simulation results for the evolution of the stability ratio in the Partington rollover incident. Results showed the system became more stable during Phase 1, due to the low initial temperature difference between layers.

Figure 5.23 shows the simulation results for the evolution of stability ratio versus time. The initial stability ratio was 5.32, being bigger than the critical stability ratio of 3.8, implied that the program modelled the system in Phase 1. R_s increased with time as the layers' temperature differences got smaller as shown in Figure 5.20, until it reached to a maximum value of 34.8 at around 507 hours, which corresponded to the lowest temperature difference between the layers; then started to decrease as the lower layer temperature diverged and layers' temperature difference got bigger. The slight divergence of the lower layer's temperature is because of decreasing the heat transfer coefficient during the Phase 1, which slowly accumulated more energy (heat) in the lower layer over time towards the end of Phase 1. At t = 525 hours, it reached to 3.8, which was the end of Phase 1 and it continued to decrease to 1 at the end of Phase 2 and rollover time (528.8 hours).

These results suggested that the reason for the long duration of the Partington rollover incident was the initial low temperature difference between layers and the low driving force, which initially made the system more stable until early Phase 2.

Case 2 (Row 3 in Table 5.4):

For the second category ($\Delta T \neq 2$ K), a case with $\Delta T = 4.2$ K, is selected for the comparison and have been described in Figures 5.23, 5.24, 5.25, 5.26 and 5.27 below. As the initial R_s is smaller than R_c, there is only one phase to rollover.
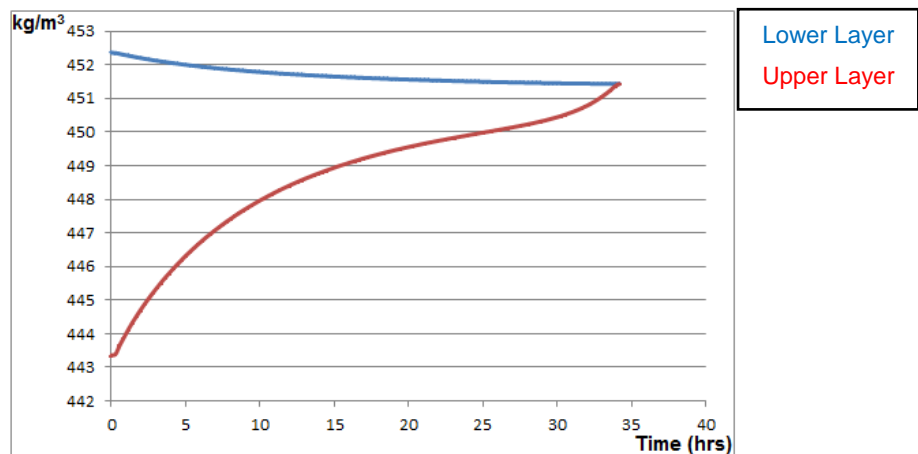

Figure 5.24: Case 2, simulation results for the evolution of mass densities of the lower and upper liquid layers in the Partington rollover incident.

Figure 5.24 shows the simulation results for the evolution of the mass densities of the lower and upper liquid layers in the Partington rollover incident case 2. There is a slight difference between layers' densities in case 1 and here as their initial temperatures are different. The lower layer density initially started at 452.4 kg/m^3 and smoothly decreased to the final value of 451.5 kg/m^3 at the end of Phase 2. The upper layer density started at 443.4 kg/m^3 at t = 0 and increased to the final density of 451.5 kg/m^3 at the time of rollover (34.9 hours). Although this case time to rollover, is smaller than case 1, but it is longer than predicted by Deshpande *et al.*[25] (18 vs 34.9 hours), because of lower initial

temperatures and more accurate modelling of the thermodynamics in our simulation.
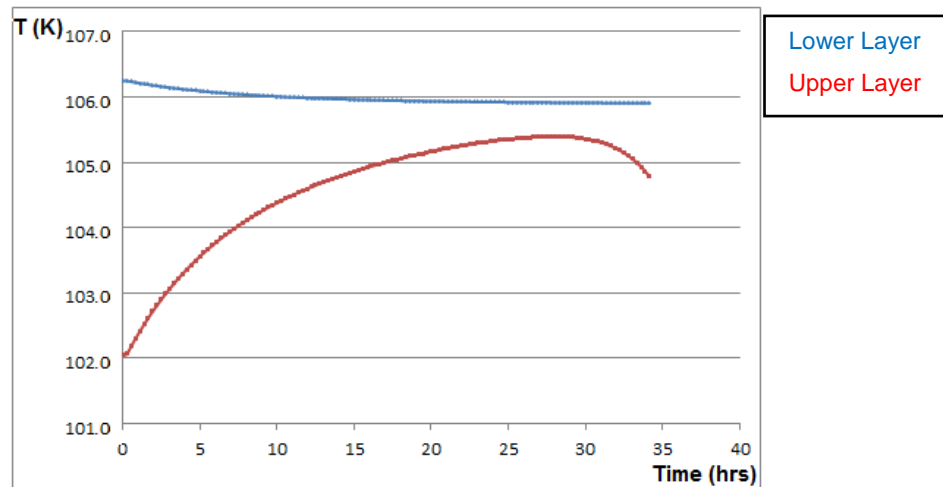

Figure 5.25: Case 2, simulation results for the evolution of temperatures of the lower and upper liquid layers in the Partington rollover incident.

Figure 5.25 shows our simulation results for the evolution of LNG layers' temperatures versus time in case 2 simulation of the Partington rollover incident. As mentioned before, we assumed the initial temperature difference to be around 4.2 K. The lower layer initial temperature was 106.2 K, decreasing slowly over time to 105.9 K at rollover time. The upper layer's temperature initially started at 102 K and increased to the maximum of 105.4 K at around t = 25 ~ 28 hours and decreased after that to 104.8 K at the end of the rollover process. The temperature decrease after 28 hours is due to evaporation caused by boil off close to rollover time.
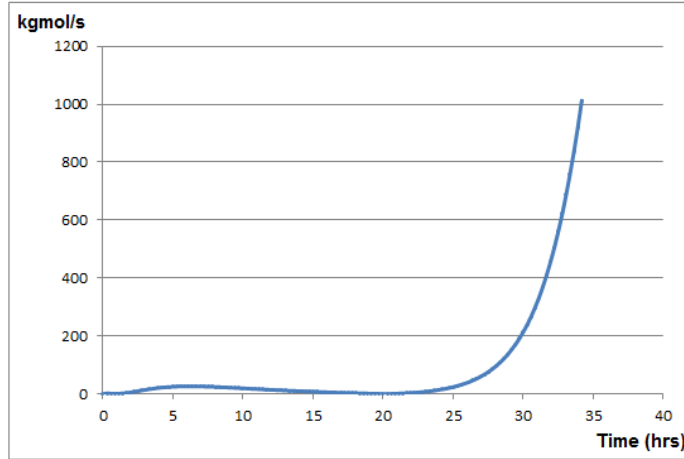
Figure 5.26: Case 2, simulation results for the evolution of the BOG in the Partington rollover incident.

Figure 5.26 shows the simulation results for the evolution of BOG over time. During most of the pre-rollover time, there was a minimum change in BOG, started from 0 kgmol/s until close to the rollover time. At t = ~25 hours, the BOG amount started to increase until it reached to its final value of about 1080 kgmol/s at the time of rollover. This increase in the BOG, corresponded to the time that the upper layer's temperature diverged (decreased) due to the evaporation.
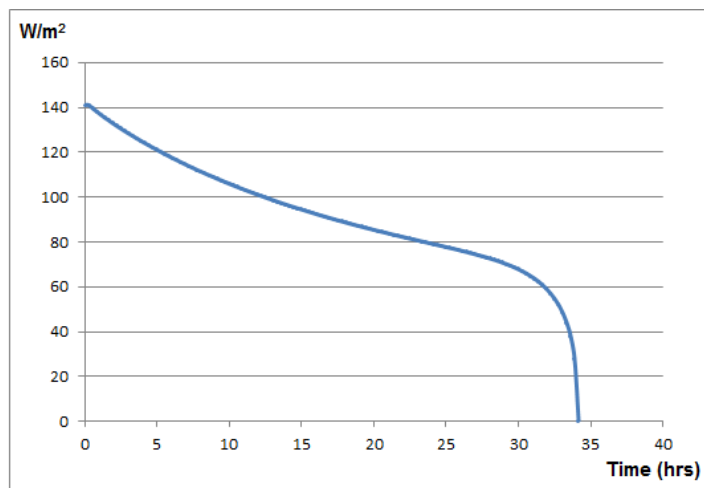
**Figure 5.27:** simulation results for the evolution of the heat transfer coefficients in the Partington rollover incident.

Figure 5.27 shows the simulation results for the evolution of the heat transfer coefficients over time in the second case of simulation of the Partington rollover incident. The heat transfer coefficient initially started from 141.2 W/m^2K, which decreased slowly to 65 W/m^2K at around t = 32 hours, then decreased more rapidly to zero as the density difference between layers become smaller closer to the time of rollover. As there was only a single phase in this process, only one heat transfer coefficient was used by our program to simulate the rollover.
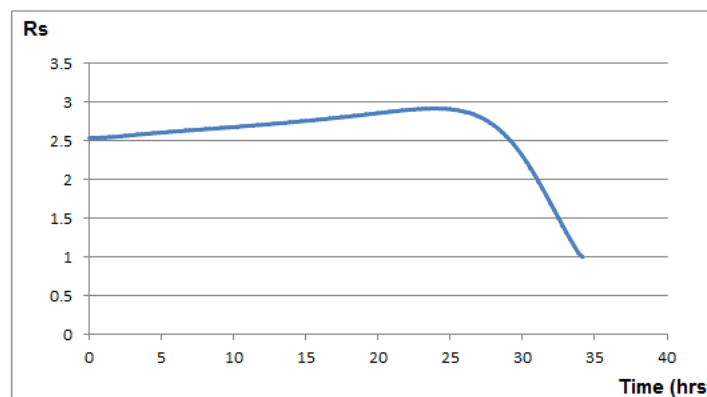

Figure 5.28: Case 2, simulation results for the evolution of the stability ratio in the Partington rollover incident.

Figure 5.28 shows the simulation results for the evolution of stability ratio versus time in case 2 simulation of the Partington rollover incident. The initial stability ratio was 2.5, being smaller than the critical stability ratio of 3.8, implied that the program modelled the system as a single phase. R_s increased with time as the layers' temperature differences got smaller as shown in Figure 5.25, until it reached to a maximum value of 2.95 at around 25 hours, which corresponded to the lowest temperature difference between the layers; then started to decrease as the lower layer temperature diverged and layers' temperature difference got bigger. At t = 34.9 hours, it reached to the final value of 1, which was the rollover time.

5.3.6. Sensitivity analysis on the Partington rollover incident simulation parameters:

Heestand *et al.*[24] performed their simulation by assuming that the vapour absorbs 5% of the heat transferred through it; however, they did not identify why they chose this figure. In this section, a sensitivity analysis was performed on the different percentage of heat absorption by the vapour, the ratio of h_1/h_2 and the initial LNG temperatures ($\Delta T = 2$ K or $\neq 2$ K) to check the sensitivity of the critical parameters of the simulation, to the time to the rollover, in the Partington rollover incident shown in Table 5.5. Cases 3 and 5 have been detailed in the previous section.

Test no.	h 1 Coef	h 1 (W/m2)	h 2 Coef	h 2 (W/m2)	%q Heat flux from the outside stays in the vapour phase	External heat flux Coefficient	Initial T Lower (K)	Initial T Upper (K)	ΔT (K)	Time to rollover (Days)	Remarks
1	NA	h1 =h2	1	121.31	95%	Equal to Baker and Creed	106.25	102.05	4.2	Less than 1	Only one heat transfer regime (h1 = h2) heat transfer coefficient is equal to Globe & Dropkin.
2	NA	h1 =h2	1	121.31	95%	Modified to give 4 W/m2	106.25	102.05	4.2	1.45	Only one heat transfer regime (h1 = h2) heat transfer coefficient is equal to Globe & Dropkin.
3	NA	h1 =h2	1	121.31	100%	Modified to give 4 W/m2	106.25	102.05	4.2	1.45	Only one heat transfer regime (h1 = h2) heat transfer coefficient is equal to Globe & Dropkin.
4	0.135	21.16	1	121.12	95%	Modified to give 4 W/m2	106.0	104.0	2	22.03	Two heat transfer regime; external heat leak is modified to 4 W/m^2
5	0.135	21.16	1	121.12	100%	Modified to give 4 W/m2	106.0	104.0	2	22.03	Two heat transfer regime; external heat leak is modified to 4 W/m^2
6	0.135	21.12	1	120.85	95%	Modified to give 4 W/m2	105.75	103.75	2	22.01	Two heat transfer regime; external heat leak is modified to 4 W/m^2
7	NA	h1 =h2	1	120.41	95%	Equal to Baker and Creed	114	112	2	Rollover did not occur	Original Deshpande conditions, only external heat leak is modified.
8	0.135	22.36	1	120.41	95%	Equal to Baker and Creed	114	112	2	Rollover did not occur	Deshpande *et al.* case
9	0.135	22.36	1	120.41	100%	Modified to give 4 W/m2	114	112	2	7.12	Initial temperatures equal to Deshpande Two heat transfer regime; external heat leak is modified to 4 W/m^2 Changing heat transferred % from vapour to liquid does not affect anything.

Table 5.5: 9 selected cases studied for sensitivity analysis of the Partington rollover incident in this research.

Cases 1, 2, 4, 6,7 and 8 were the simulations with 0.95% of the external heat absorption by the vapour, while cases 3, 5 and 9 were the similar cases with 100% of the external heat absorption by the vapour, for the comparison. Moreover, case 1 simulation used the total external heat leaks equal to what Baker and Creed[18] mentioned with initial temperatures of 106.25 K and 102.05 K. As described before, the value of external heat leaks reported by Baker and Creed[18] is questionable because the predicted time to rollover using this value was less than 1 day, while the reported time is 68 days. The second case was similar to case 1, with the external heat leaks modified to more realistic value (an average value between Nantes and La Spezia), which resulted in a longer time to rollover. Case 4 was case 3's external heat leaks absorbed by vapour modified from 90% to 100%. The three first cases have the initial temperature difference of 4.2 K, while the rest of the simulation cases have the initial temperature difference of 2 K. It is important to note that cases 7 and 8 are equal to what Deshpande et al. [25] assumed only different in selecting single phase or 2 phase transport regime; however, based on GERG-2004 calculation, with upper layer temperature being 112 K the system is unstable and started to boil off immediately (rollover never occurred).

Comparison between the results of the row 2/3, row 4/5 and row 8/9; showed that the system is not sensitive to the selection 95% or 100%. It seems that the value of 95%, was a tailor-made value chose by Heestand *et al.*[24] for their simulation to get the closest result for the La Spezia incident as for the Partington scenarios, it has no effect on the time to rollover. However, this selected value must be verified with the real-time data obtained from a LNG tank to be used in the later simulations. However, the system is very sensitive to the values selected for the external heat leaks, the initial temperatures and the initial temperature difference.

The key points and results obtained from our Partington simulations and its sensitivity analysis can be summarised as follows:

1. Estimation of the external heat flux values is very important. As the rollover process is very sensitive to this value.

2. The variety of the results obtained in the above simulation cases showed the importance of the parameter tested and how the system is sensitive to them, and the inadequacy of the values provided in the open literature for an accurate simulation.

3. Last but not the least, the importance of the selection of the initial LNG temperatures and the initial temperature differences, which results in the value of the initial R_s. As if the initial R_s, is sufficiently large then the rollover happens in two phases with longer duration.

5.3.7. Auto-stratification rollover in LNG storage tanks

In this section, several sensitivity analyses have been done to investigate the effect of additional nitrogen than what is currently used in industry (1%), on the critical parameters of rollover, including time to rollover and BOG. This matter is crucial to LNG industry as the purification of LNG from nitrogen is a very complex process and expensive. Auto-stratification rollover or self-induced rollover has been referred to by several LNG rollover researchers such as Baker and Creed[18] and Acton *et al.*[32]. They have reported that in a homogenous LNG tank, similar to those in peak shaving LNG storage facilities, with nitrogen content above 1% (mole), the risk of self-induced rollover, or as it called auto-stratification rollover is increased.

The auto-stratification mechanism can be described as similar to what Acton *et al.*[32] defined: As the lower portion of a homogenous LNG, rich in nitrogen stored in a tank, gets warmer through the heat leaks from the bottom and walls, its density decreases and moves to the surface and upon reaching the top it flashes and loses more nitrogen than other components. This will make the portion of liquid on the top less dense as it accumulates, and acts like a thin blanket on the top of the bulk liquid. This also prevents the bulk liquid from weathering as it gets warmer (flash), due to imposed static pressure, as well as the bulk liquid getting warmer due to external heat leaks. This what called "mini-

stratifications" can lead to a rollover, which could be repeated over time. Figure 5.29 shows a schematic of the stages of a hypothetical auto-stratification rollover.
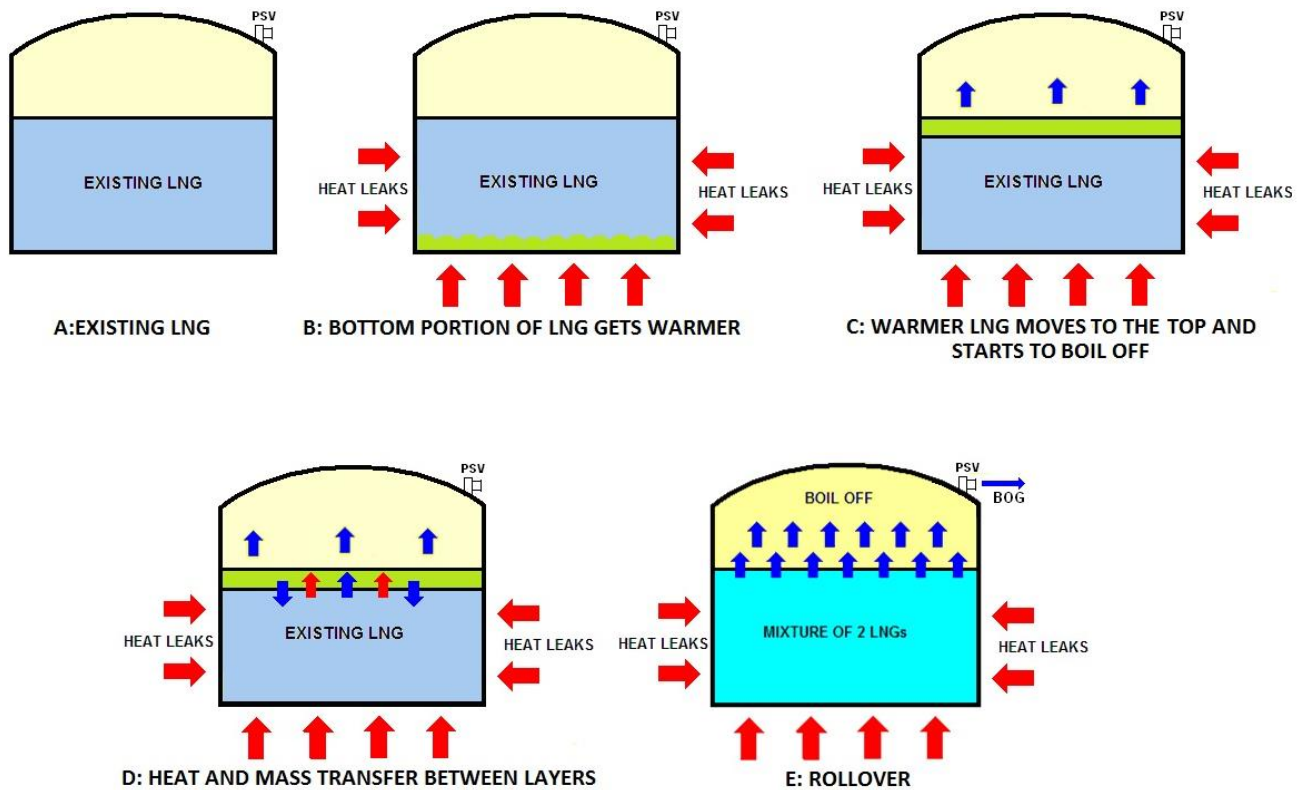
Figure 5.29: A schematic of the stages of auto-stratification rollover event.

In lack of any actual data or reference for an auto-stratification rollover incident, a hypothetical LNG composition, similar to the composition of an international LNG producer, such as Malaysia, Bintulu LNG (refer to Table 1.1), has been selected for the simulation shown in Table 5.6. For the same reason of unavailability of any actual information, a tank similar to the La Spezia LNG tank as described by Sarsten[6] has been considered and summarized in Table 5.7. Another assumption has been made that the top layer height is 10% ($\approx$1.8 m) of the total liquid height as it has been described as a thin layer by Baker and Creed[18] and Acton et al.[32]; however, 20% of the total height ($\approx$2.8 m) has also been simulated.

Composition	Bottom (mol%)	Upper (mol%)
C1	0.9100	0.9100
C2	0.0400	0.0400
C3	0.0400	0.0400
C4	0.0000	0.0000
N2	0.01 (In balance with C1)	0.01 (In balance with C1)
Temperature (K)	105	105
Pressure (kPaa)	118	110
Height (m)	17	1.8
Time to rollover (hr)	8.6 to 8.9 refer to Table 5.8	

Table 5.6: Hypothetical LNG composition (similar to Bintulu) selected for auto-stratification rollover simulation

	Bottom	Top	Vapour
Temperature (K)	105.0	105.0	105.0
Layer depth (m)	16.8	2.8	2.8
Tank diameter (m)	49.08		
Heat leaks (W)	58470	1071.57	34090

Table 5.7: Assumed LNG tank data used for auto-stratification

As all of those mentioned auto-stratification rollover cases (nitrogen varies from 1%, 2% and 2.5%, in balance with methane concentration; refer to Table 5.8) have very similar behaviour and the same path to rollover, only one sample for auto-stratification rollover has been graphically displayed in this section through Figures 5.29, 5.30, 5.31,5.32 and 5.23 (case 4b in Table 5.8). The compositions and temperatures of both layers are equal; however, due to slight extra static pressure on the bottom layer, the layers' densities are slightly different.

168
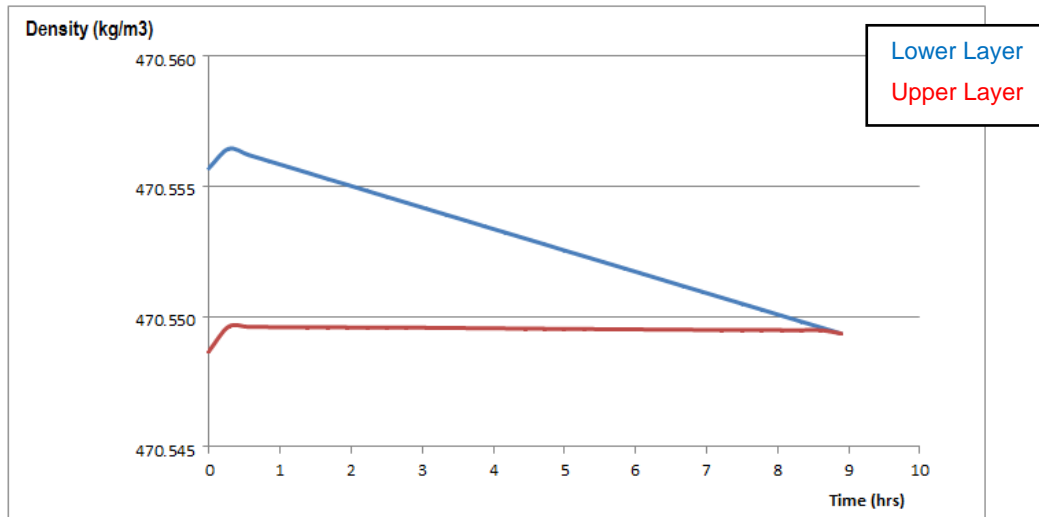
Figure 5.30: Simulation results for the evolution of mass densities of the lower and upper liquid layers in the auto-stratification rollover incident.

Figure 5.30 shows the simulation results for the evolution of the mass densities of the lower and upper liquid layers in a hypothetical auto-stratification rollover incident (Case 4b in Table 5.8). It is important to note that the density and temperature differences in an auto-stratification rollover incident are very small as the upper layer and lower layer are initially the same and due to a slight change in the temperature, they form separate strata.

The lower layer density initially started at 470.556 kg/m^3 and increased slightly to 470.558 kg/m^3 in the first 20 minutes, as it got warmer then decreased linearly to the final value of 470.549 kg/m^3 at the end rollover at t = 8.9 hours as the heat and mass transfer started. The upper layer density initially started at 470.547 kg/m^3 at t = 0 and increased to 470.549 kg/m^3 and at continued with the same value almost linearly until the time of rollover.
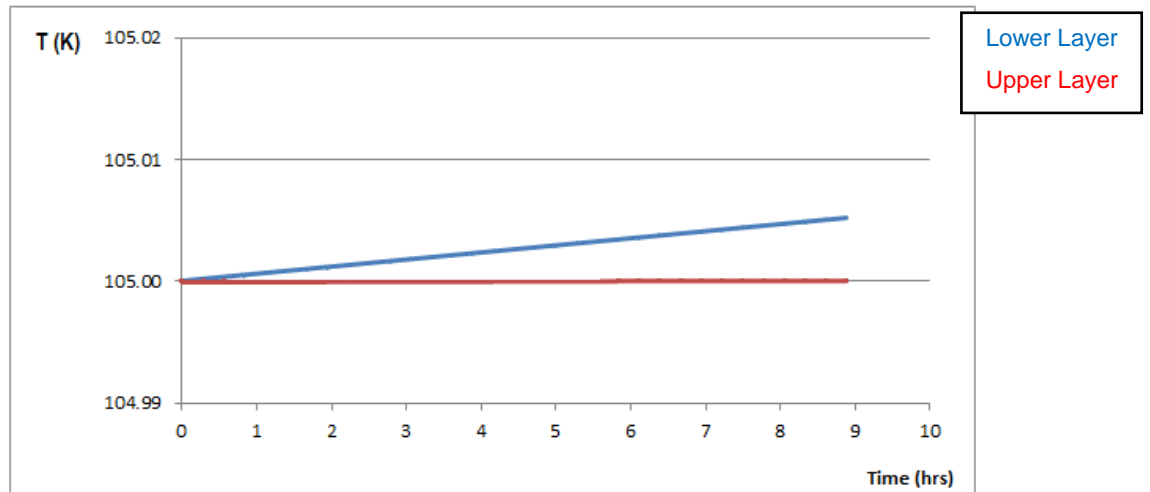
Figure 5.31: Simulation results for the evolution of temperatures of the lower and upper liquid layers in the auto-stratification rollover incident.

Figure 5.31 shows our simulation results for the evolution of LNG layers' temperatures versus time in the selected hypothetical auto-stratification rollover incident. As mentioned before, the initial temperature difference was zero as there was initially a uniform single layer LNG before the auto-stratification started. Opposite to the normal two-layered LNG rollover events, Layers' temperatures are initially equal and start to diverge as time goes by, because lower layer gets warmer much faster than the upper layer with the same composition in the short time of the auto-stratification rollover. The reason is that the bottom layer, is in contact with both tank's metal bottom plate and a big portion of the wall, compare to the top layer that is only in contact with a small portion of the wall and the bottom layer (vapour layer heat transfer is negligible). Hence, the bottom layer gets warmer faster as more heat traps in it, while the top layer losses a part of the energy as it boils off.

Here, the lower layer's initial temperature was 105 K, stayed almost the same during the rollover process. The upper layer's temperature also initially started at 105 K; however, increased to the maximum of 105.005 K at t = 8.9 hours at the end of the rollover process.
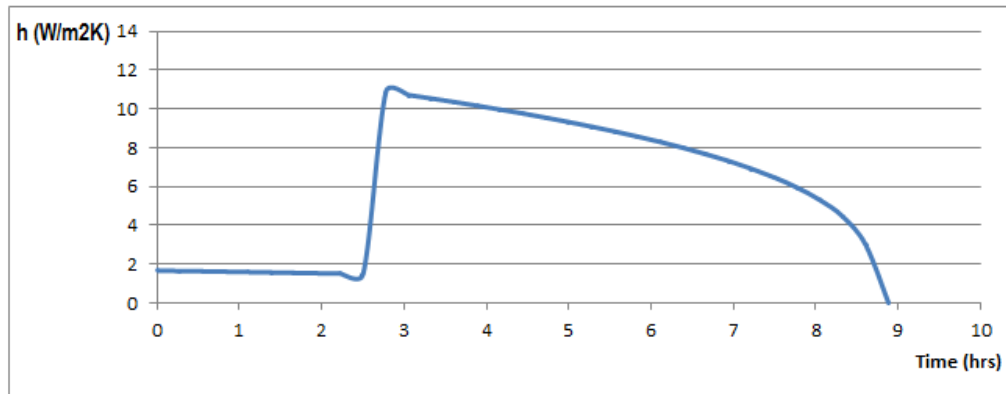
Figure 5.32: Simulation results for the evolution of the heat transfer coefficients in the auto-stratification rollover incident.

Figure 5.32 shows the simulation results for the evolution of the heat transfer coefficients over time in the selected hypothetical auto-stratification rollover incident. As the initial R_s is bigger than R_c, then we had two heat and mass transfer regimes and two phases of rollover. We also used the same ratio of h1/h2 ≈ 0.135 in this case as the best ratio to give the longest time to rollover in the previous cases. The Phase 1 heat transfer coefficient initially started from 1.8 W/m^{2}K (as the layers were almost the same), and decreased very slowly through the Phase 1, as a result of slight layers' densities differences. It was decreased to 1.5 W/m^{2}K at the end of Phase 1 (t = 2.3 hours), then increased rapidly to the Phase 2 heat transfer coefficient, 11.1 W/m^{2}K and decreased to zero after a few hours at the time of rollover t = 8.9 hours. The reason that the heat transfer coefficients in the hypothetical auto-stratification rollover event being relatively small is that as the layers are initially uniform, then the density difference over time is also very small, which results in a low Nusselt number and heat transfer coefficient.
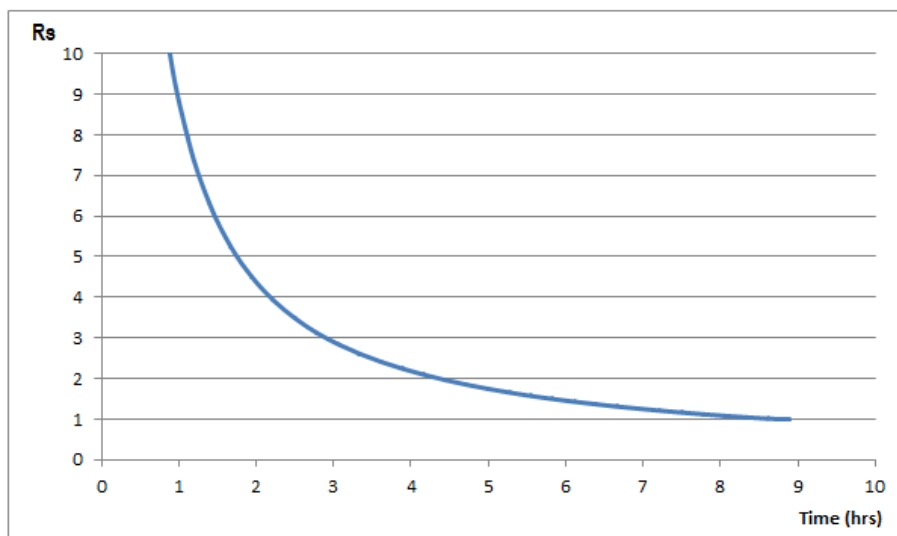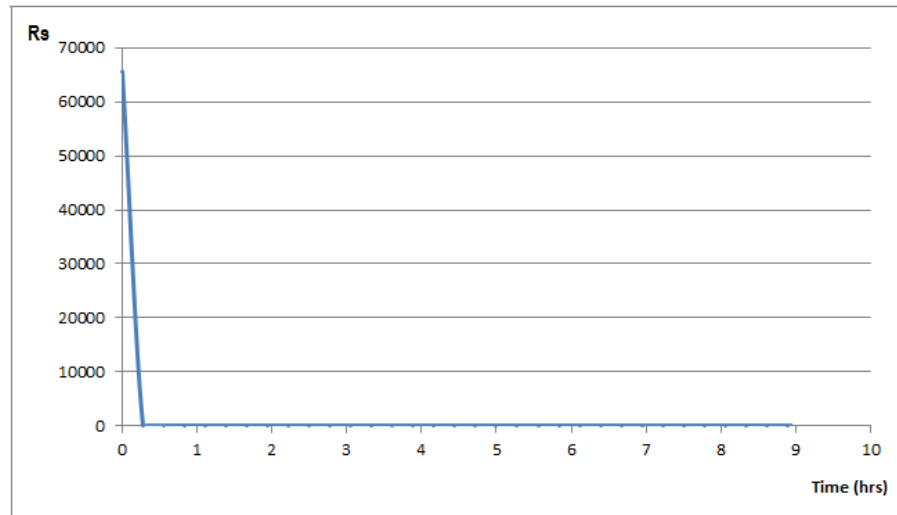
Figure 5.33: Simulation results for the evolution of the Rs in the auto-stratification rollover incident. Top Figure's Y axis maximum unit is 70,000 and the bottom Figure's Y axis maximum unit rescaled to 10.

Figure 5.33 shows the simulation results for the evolution of stability ratio versus time in the selected hypothetical auto-stratification rollover incident. The top Figure's Y axis maximum unit is 70,000 and the bottom Figure is the same plot with the Y axis maximum unit being rescaled to 10. The initial stability ratio theoretically was infinity as the $\Delta T = 0$ in the R_s equation (the denominator in Eq. 2-1). However, to be physically meaningful, the MATLAB program rounded it to a large value of 65000 as the initial R_s. R_s being bigger than the critical stability ratio of 3.8, implied that the program modelled the system in two

172

phases. Not long afterwards, this large initial R_s started to decrease quickly as there was a slight change in the layers' physical property and reached to around 8 in the first hour. Then decreased to the final value of 1 with time as the system reached to rollover. The Phase 1 evolved to Phase 2 at around 2.3 hours, corresponding to the change in the heat transfer coefficient rate, shown previously in Figure 5.32.
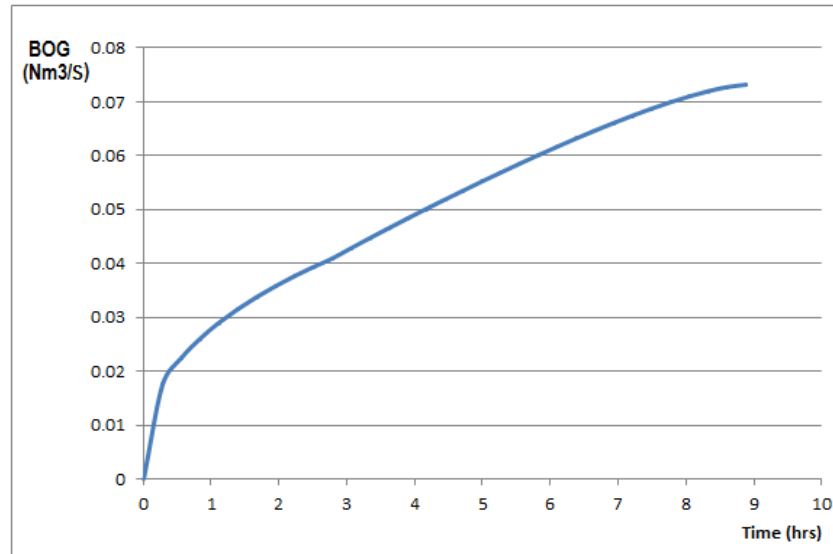
Figure 5.34: Simulation results for the evolution of the BOG in the auto-stratification rollover incident.

Figure 5.34 shows the Simulation results for the evolution of BOG over time. The BOG plot in an auto-stratification rollover incident is very different to a normal two-layered rollover incident. Although the amount of BOG is relatively small (due to slight temperature/composition difference between the layers, which continues during the rollover process); however, it increases more rapidly with time than the normal LNG rollover, which has a minimum initial value and a BOG peak at the end of the rollover.

In Figure 5.34, the BOG started initially at 0, increased sharply to 0.02 kgmol/s in the first 20 minutes, and then increased slower to the final value of 0.073 kgmol/s at the time of rollover.

5.3.8. Sensitivity analysis on hypothetical auto-stratification rollover event parameters

To investigate the effect of nitrogen content on the potential of rollover, in an auto-stratified LNG tank, we have assumed several hypothetical LNG cases in a tank at 110 kPaa for the upper layer and 8 kPa static pressure above that for the bottom layer. The main components, which had the most effects on the mixture's density and thermodynamic properties were mainly methane, ethane and nitrogen. However, to test the effect of different nitrogen concentrations, we changed the nitrogen contents from 1%, 2% and 2.5% (molar) in the bulk LNG as shown in Table 5.8. Nitrogen concentration more than 2.5% made the LNG system unstable as it started to boil off immediately.

There is no accurate indication for the top layer's height in the limited descriptions of the auto-stratification rollover incidents and it has been only described as "*a thin layer*" by Baker and Creed[18] and Acton *et al.*[32]. Hence, we tested the effect of the top layer's height being 10% ($\approx$1.8 m) of the total liquid height or 20% of the total height ($\approx$2.8 m) and checked its effect on the rollover process. The upper layer's height less than 10% was assumed to be not considered as a separate layer compared to the total bulk LNG's height; for example, in our case, 5% of the total height was 60 cm versus 17.8 meters of the bulk LNG (~30 times smaller). Same analogy is valid for upper layer's heights being more than 20%, which is not a thin layer anymore and will be considered as a normal conventional LNG rollover case.

Case 1a	Composition	Bottom	Upper	Case 1b	Composition	Bottom	Upper
	C1	0.9100	0.9100		C1	0.9100	0.9100
	C2	0.0400	0.0400		C2	0.0400	0.0400
	C3	0.0400	0.0400		C3	0.0400	0.0400
	C4	0.0000	0.0000		C4	0.0000	0.0000
	N2	0.0100	0.0100		N2	0.0100	0.0100
	Temperature (K)	105	105		Temperature (K)	105	105
	Pressure (kPaa)	118	110		Pressure (kPaa)	118	110
	Height (m)	17	1.8		Height (m)	16	2.8
	Time to rollover (hr)	8.6			Time to rollover (hr)	8.6	
Case 2a	Composition	Bottom	Upper	Case 2b	Composition	Bottom	Upper
	C1	0.9050	0.9050		C1	0.9050	0.9050
	C2	0.0400	0.0400		C2	0.0400	0.0400
	C3	0.0400	0.0400		C3	0.0400	0.0400
	C4	0.0000	0.0000		C4	0.0000	0.0000
	N2	0.0150	0.0150		N2	0.0150	0.0150
	Temperature (K)	105	105		Temperature (K)	105	105
	Pressure (kPaa)	118	110		Pressure (kPaa)	118	110
	Height (m)	17	1.8		Height (m)	16	2.8
	Time to rollover (hr)	8.6			Time to rollover (hr)	8.9	
Case 3a	Composition	Bottom	Upper	Case 3b	Composition	Bottom	Upper
	C1	0.9000	0.9000		C1	0.9000	0.9000
	C2	0.0400	0.0400		C2	0.0400	0.0400
	C3	0.0400	0.0400		C3	0.0400	0.0400
	C4	0.0000	0.0000		C4	0.0000	0.0000
	N2	0.0200	0.0200		N2	0.0200	0.0200
	Temperature (K)	105	105		Temperature (K)	105	105
	Pressure (kPaa)	118	110		Pressure (kPaa)	118	110
	Height (m)	17	1.8		Height (m)	16	2.8
	Time to rollover (hr)	8.9			Time to rollover (hr)	8.9	

Table 5.8. Table continues on the next page.

Case 4a	Composition	Bottom	Upper	Case 4b	Composition	Bottom	Upper
	C1	0.8950	0.8950		C1	0.8950	0.8950
	C2	0.0400	0.0400		C2	0.0400	0.0400
	C3	0.0400	0.0400		C3	0.0400	0.0400
	C4	0.0000	0.0000		C4	0.0000	0.0000
	N2	0.0250	0.0250		N2	0.0250	0.0250
	Temperature (K)	105	105		Temperature (K)	105	105
	Pressure (kPaa)	118	110		Pressure (kPaa)	118	110
	Height (m)	17	1.8		Height (m)	16	2.8
	Time to rollover (hr)	8.9			Time to rollover (hr)	8.9	

Table 5.8: Assumed hypothetical auto-stratified LNGs compositions (mole frac) with different N_2 content and top layer's height.

As all of those mentioned auto-stratification rollover cases have very similar behaviour and the same path to rollover, with time varied from 8.6 to 8.9 hours. Moreover, the results of the LNG cases with 1% or higher percentage of nitrogen up to 2.5% shows that the addition of nitrogen does not directly increase the potential of rollover; however, more nitrogen content makes the LNG harder to store at the preferred temperature. It means that changing the nitrogen content from 1% to 2.5% does not have a substantial effect on the physical and transport properties and that does not change the LNG path to rollover. However, the initial temperatures less than 105 is not a favourable temperature of storing LNG in the industry. The preferred storage temperature of LNG as described in Chapter 1, is normally around -163± 2 °C (110 K ± 2 K).

Therefore, the reason that the industry keeps the nitrogen level around 1%, is not directly related to rollover. It is the requirement of having a liquid phase, without too much flashing at the preferred economic temperature of around -163± 2 °C; hence, the nitrogen content of more than 1% increases the operating cost and waste of the product through flashing and venting. It could be a valid assumption that the cost of purifying LNG to have less than 1% nitrogen, is much less than the cost of excessively cooling down the storage tank operating temperature only to have a liquid LNG with 2.5% nitrogen, which after some time, may still evolve rollover.

To optimize the level of nitrogen, amounts of nitrogen lower than 1% were also tested. The selected cases were LNGs with 0.8%, 0.5%and 0.2% nitrogen. The important points observed in the second analysis was that with less amount of nitrogen, the initial temperature (operating) can rise to higher temperatures (~111 K), which is much more economical to store LNG.

Secondly, it seems that purification of LNG less than 1% is not worth it as the LNGs with lower than 1% N_2 has a shorter time to rollover than 1% nitrogen. Therefore, 1% nitrogen in LNG is just the optimum level that makes the operation most economical at the preferred industrial operating temperature of about 111 K.

However, it is important to mention that if the initial temperature of LNG is decreased to a lower temperate such as 108K or lower, LNG with lower than 1% nitrogen have longer times to rollover (less risk) than those above 1%, as well as less average BOG and post rollover BOG generation (loss of product). It is worth to mention that by increasing the operating pressure of the LNG tank to higher than atmospheric pressure, operating temperature could be increased to more economical temperatures; however, an optimum pressure, which does not change the design parameters and the material characteristics of the tank, should be selected. This optimization needs accurate technical and commercial data and requires a separate study, hence is not included as an objective of this research.

In this Chapter, both methods have been carefully tested and due to larger number of limitations of CFD modelling, especially in modelling the thermodynamics of the LNG system in Phase 2, CFD approach was only used for simulating the Phase 1, to detect the natural convection and heat transfer dominant stage of the rollover to verify Bates and Morrison's suggestion, then used the lumped parameter method to simulate both phases.

For lumped parameter simulation, in this study, a new approach for calculating the mass transfer coefficient from the heat transfer coefficient has been

developed based on a new hypothesis. The new hypothesis presented in this research is based on Cho *et al.*[39] and Bates and Morrison[4]'s works, which suggested that rollover happens in two stages (Phase 1 and 2) and the rate of the heat transfer is about 30 times bigger than the mass transfer in Phase 1, and in Phase 2, the mass transfer becomes dominant until the rollover occurs. The new hypothesis suggested that the use of lower heat transfer rate and lower mass transfer rate such as resulted by the Chilton-Colburn analogy for phase 1 and use of higher heat transfer regime and higher mass transfer rate such as the Reynolds analogy for phase 2, will improve the transport properties and hence the rollover simulation. This hypothesis was verified through several simulations shown in this chapter.

Chapter 6
Safety and risk assessment of LNG rollover incidents

As previously described, LNG is highly purified natural gas, rich in methane but in liquid form. It is stored in a cryogenic condition with temperature circa -160 °C and atmospheric pressure in double containment tanks. Similar to all other hydrocarbon fuels, the storage and transportation of LNG is also hazardous and has the potential of major risks.

Although, in the past 45 years of LNG international operations, there was no major event or incident causing public injuries or property damage and millions of tonnes of LNG have been transported and consumed, without any serious public exposure [58]; however, due to the increasing demand for LNG in global market and the risks associated with it, the need for applying accurate risk assessments and risk management methods becomes increasingly important.

In this chapter, a brief description of some of the main techniques for qualitative risk assessment has been given. Then these techniques have been used to identify the Hazards arising from a rollover event and investigate their consequence severity and recommended safeguards to mitigate those consequences.

Some of the nationally and internationally standards used in LNG industry are as follows[58]:

- NOHCS. National standard for control of major hazard facilities
- AS 2885. Pipelines: gas and liquid petroleum
- AS/NZS ISO 31000. Risk management, principals and guidelines
- AS 3961. The storage and handling of liquefied natural gas.
- EN 1160 and EN 1473 (BS) Installation and equipment for liquefied natural gas.

Although one of the major hazards of storing and transporting LNG is a rollover, unfortunately, due to the unavailability of a rigorous model in the open literature, which can accurately describe this phenomenon, the risk of rollover and its consequences are often under or overestimated in LNG industry. This causes poor assumptions and deficiencies to be inculcated in both LNG operating procedures and design standards such those mentioned above.

For example, one of the well-established and widely used set of standards in LNG industry is the British Standards (BS)[59]. The British Standards are the standards produced by the "BSI Group", which is a part of the National Standards Body (NSB) of the UK. Only from the late 2000's onward, there are some limited references to rollover added to the related BS standards for LNG such as BS EN 1160 and 1473 and prior to that there was no reference to the rollover event.

Unfortunately, there is no model proposed for calculation of BOG, density, temperature evolution path and the time to rollover. Some of the main references to safe handling and storage of LNG in BS standards are as follows:

- British Standard[59]: BS EN 1160, Installations and equipment for liquefied natural gas - General characteristics of liquefied natural gas, Section 5.7.1.
- British Standard[59]: BS EN 1473, Installation and equipment for liquefied natural gas - design of onshore installations, Section 6 and Annex B.

In the BS EN 1160, it is recommended to recirculate the LNG to avoid any stratification. However, recirculating a large volume of the stored LNG enough to break the stratification will generate more surface movement and therefore, more boil off, which is not desirable. Furthermore, recirculation of LNG consumes a huge amount of energy for pumping and keeping the recirculation line cold at the cryogenic conditions.

In the BS EN 1473, it is recommended to consider a maximum BOG flow rate of 100 times the normal BOG rate during the rollover. Unfortunately, the justification for choosing the factor of 100 is not clear or supported by any evidence.

Our simulation research results described in Chapter 5 showed that each LNG rollover case should be studied and modelled individually, based on its composition, number of moles, pressure, temperature, the amount of BOG generated and other critical parameters of rollover and it is highly dependent on the initial condition and the nature of LNG. This confirms the unavailability of an accurate model of rollover, forced the industry to use vague assumptions (such as the vague recommendation of using the value of 100 times bigger than the normal BOG) and generalised recommendations (such as circulate the LNGs, which also generates even more BOG) to avoid any LNG rollover incident. This also confirms the importance of applying a model that can simulate different LNG rollover cases, such as our proposed model in this research.

To highlight the importance of LNG rollover risk in the industry, we first conducted a qualitative risk assessment for a hypothetical LNG rollover, (either a conventional two-layered LNG or a homogenous auto-stratified LNG rollover), to investigate and rank the risk specific to the rollover phenomenon. The risk ranking calculation in Section 6.3, showed that rollover is ranked as "Extreme". This supports our initial argument that the risk associated with rollover must not be underestimated by industry. Later, by using two highly recognised risk assessment and management techniques of "Layer of Protection Analysis" (LOPA)[62] and "Hazard Identification" (HAZID)[62], we investigate the hazards and risks of a hypothetical rollover event in more details and study the common safeguarding available to detect and avoid the rollover and finally give our recommendations for better protection towards LNG rollover.

6.1. Risk assessment of a hypothetical LNG rollover

Process risk assessments can be done either qualitatively or quantitatively. Qualitative risk assessments provide initial ways of ranking risks with preliminary data as their input, while, quantitative risk assessments provide more accurate risk rankings, but need detailed data as the input. In this section, a qualitative risk assessment approach has been selected for LNG rollover, because:

- Firstly, the LNG rollover incident is considered to be a general incident (not specific to any technology or plant).
- Secondly, only preliminary and basic information is available in the literature.

To do a detailed assessment and quantify the risk of LNG rollover incident, further detailed design information is needed, which is not available for this research.

The first step in a qualitative risk assessment is to identify the major possible hazards of LNG rollover. Then by defining their likelihood and consequence severities, the risks related to those hazards will be ranked.

What is a hazard?

A hazard is a situation that has the potential to harm the health and safety of people or to damage plant and equipment. The situation could involve an activity, chemical, or equipment used. Hazard management is a continuous process that can be used to improve the health and safety of all workplaces[60]. Hazard analysis is the identification of hazards and estimating the extent, magnitude and likelihood of any harmful events.

What is risk?

Risk is the probability (or likelihood) of occurrence of a hazardous event that could cause a specific level of harm to people, property and environment over a specified period of time (consequence). In general, risk can be formulated as:

$$\text{Risk = (likelihood) x (consequence severity)}$$

The risk could be one of the following categories:

- Occupational risks including safety and risks of the employees.
- Plant and property loss.
- Environmental risk (including public and heritage).
- Liability risks, public, product, failure to service.
- Business interruption risks.
- Project risks, design, contract, delivery.
- Not limited to above.

In this study, only the technical elements of occupational risk and safety, plant and property loss and environmental risk of rollover will be assessed. Other mentioned categories of risks such as liabilities, business and projects risks need more data in order to be assessed and are very dependent on the country and location of the project as well as the organizations involved hence will not be considered in this study.

The widely used risk-ranking matrix for industrial purposes is shown in Table 6.1[61,62]. The axes of this table are likelihood (frequency) of an event (hazard) and consequence severity of that hazard.

Likelihood or Frequency	Consequence Severity				
	Low	Minor	Moderate	Major	Critical
Almost Certain	High	High	Extreme	Extreme	Extreme
Likely	Moderate	High	High	Extreme	Extreme
Possible	Low	Moderate	High	Extreme	Extreme
Unlikely	Low	Low	Moderate	High	Extreme
Rare	Low	Low	Moderate	High	High

Table 6.1: Standard risk ranking matrix [61, 61].

To define the extent of each dimension of the risk, reference data such as presented in the Tables 6.2 and 6.3 on the next page is required. After identifying the level of each dimension, the risk will be ranked as the product of likelihood and consequence severity or simply by using Table 6.1 above.

Likelihood	Description	Frequency Scores
Almost Certain	Event expected to occur in most circumstances	Does Occur Definite history of occurrence Frequency between once and ten times a year
Likely	Event will probably occur in most circumstances.	Possible history of occurrence Probably occur once per decade and history of near miss Frequency between 1 every 10 years and 1 per year
Possible	Event should occur at some time.	May happen once in plant lifetime Possible history of near miss Frequency between 1 every 100 years and 1 every 10 years
Unlikely	Event could occur at some time.	Low likelihood of occurrence Frequency between 1 every 1000 years and 1 every 100 years
Rare	Event may occur, but only under exceptional circumstances.	Very Low likelihood of occurrence Frequency between 1 every 10,000 years and 1 every 1000 years

Table 6.2: Likelihood (frequency) ranking of an event[61].

	Low	Minor	Moderate	Major	Critical
Injury	Minor injury. Low level short-term subjective inconvenience or symptoms. Cuts, bruises, no measurable physical effects. No medical treatment	Significant injury. Objective but reversible disability/impairment and/or medical treatment injuries requiring hospitalisation. Major burns, broken bones, severe bruises, cuts.	Serious Injury. Moderate irreversible or impairment (<30%) to one or more persons. Serious burns to large parts of the body, serious internal and skull injuries. Gassings requiring hospitalisation.	Single fatality and/or severe irreversible disability or impairment (>30%) to one or more persons	Multiple fatalities, as a result of short or long term health effects, or significant irreversible human health effects to >50 people
Environmental effects	Minor Pollution. No lasting effect. Low-level impacts on the biological or physical environment. Limited damage to the minimum area of low significance. Not EPA notifiable. Relatively easy to clean up.	Significant Pollution Minor effects on the biological or physical environment. Minor short-medium term damage to small area of limited significance. EPA notifiable. Some clean-up costs.	Serious Pollution. Moderate effects on biological or physical environment but not affecting ecosystem function. Moderate short-medium term widespread impacts (e.g. Oil spill impacting shoreline).	Major Environmental Release. Serious environmental effects with some impairment of ecosystem function Relatively widespread medium-long term impacts.	Extreme Environmental Event. Very serious environmental effects with impairment of ecosystem function. Long-term, widespread effects on significant environment (e.g. Unique habitat, National Park).

Table 6.3: Consequence severity ranking of an event[61].

6.2. Hazards arising from LNG rollover

As described before, LNG rollover is sudden mixing of stratified LNG layers, which releases a large amount of vapour (BOG) in a very short period of time. The major hazards and risks related to the rollover incident are:

- Damaging the equipment (tank, exchangers, piping, accessories, …), due to over pressurization, which can lead to liquid leaks that are under tank static pressure and in severe cold temperature (around -160°C), these could cause further hazards and risks such as explosion, fire, asphyxiation and freeze burns.
- Damaging the relief network, especially if the rollover happens in a refinery, where most of the relieving valves use a common flare and flare header.
- Loss of containments, which has both financial and technical impacts
- Environmental pollution, as described above.

These hazards will be further assessed in the following section.

6.3. Qualitative risk assessment of LNG rollover, Hazard Identification (HAZID)

The hazard identification (HAZID) technique is a systematic and structured process that defines all the possible hazards, which are identified during each phase of project lifecycle so they can be assessed and safely managed[63].

In order to perform the HAZID, all above mentioned hazards and risks are tabulated in a HAZID worksheet, as shown in Table 6.5, which has been developed specifically to assess LNG rollover. Using a sample of industrial HAZID guidewords (Appendix 2), each hazard likelihood and consequence severity is defined in order to rank the risk. Finally, evaluate the existing safeguarding, whether being satisfactory towards the risks and then recommendations (if any) to be added to the risk assessment table.

The key findings of the Hazard identification analysis are summarized in HAZID table (Table 6.5) are as follows:

- LNG as a hazardous material being flammable and cryogenic (Dangerous goods, class 2.1, flammable gas), Australian Standards; AS 1216-2006, Class labels for dangerous goods[64].
- Referent as a hazardous material being flammable and cryogenic (Dangerous goods, class 2.1, flammable gas)

These hazardous materials have the potential to cause injury or damage to people, properties and environment[64].

LNG Being categorised as Dangerous Goods class 2.1 (Flammable and combustible liquids/gases) as per AS 1216-2006[64], and has been studied against the following hazardous characteristics:

a) Flammability, (the potential to burn or explode when ignited).

b) Instability, (the potential to undergo a spontaneous reaction, e.g. decomposition, polymerization, which could be violent.)

c) Reactivity, (the potential to react with other chemicals, water or fire extinguishing media.)

d) Toxicity, (the immediate, delayed or long-term health effects on humans or animals, through inhalation, skin absorption or ingestion).

e) Environmental impact, including Ecotoxicity, (the effect on the environment, in particular to aquatic life.)

f) Corrosively (the potential corrosive chemical action on other materials, in particular, packaging and living tissues, including skin.)

Note: Further information may be obtained from the product labels, MSDS and the suppliers. (Refer to Appendix 3)

The major hazards of storing LNG are items (a) and (e) above, which both can be a consequence of a rollover event. For example, a tank damage (rupture) due to over pressure caused by a severe rollover, will lead to hydrocarbon

leakage, which both in liquid or vapour form has the potential risks of fire, explosion and environmental impacts. To rank these risks, using the Table 6.2, the likelihood of a rollover incident happening is "Possible". It has happened at least twice previously in La Spezia-Italy and Partington-UK and it may happen once in a plant lifetime, with the frequency of one every 10 to 100 years (Table 6.2).

For example, the consequence severity of a rollover incident lead to an overpressure (Row 1 of Table 6.5) is "Critical" as it can easily be propagated into multiple fatalities, especially if it would be followed by an explosion or fire (Table 6.3). The authorities in the La Spezia rollover incident of 1971, for the same reason stated above, were forced to evacuate the people from the region to avoid any possible fatalities due to the gas release[6].

The product of "Possible" on the likelihood column and "Critical" on the consequence severity row in Table 21, has been reproduced below in Table 6.4. This Table shows that any rollover incident is an "Extreme" risk. This risk is not only for the people directly involved with the LNG facility but also on the environment and the LNG plant.

Likelihood or Frequency	Consequence Severity				
	Low	Minor	Moderate	Major	Critical
Almost Certain	High	High	Extreme	Extreme	Ex...me
Likely	Moderate	High	High	Extreme	Ex...me
Possible					Extreme
Unlikely	Low	Low	Moderate	High	Extreme
Rare	Low	Low	Moderate	High	High

Table 6.4: LNG rollover risk ranking matrix

HAZARD ID	HAZARD CATEGORY (GUIDEWORD)	HAZARD DESCRIPTION / HAZARDOUS EVENT	HAZARD CONSEQUENCES	PREVENTION / DETECTION / BARRIERS (Existing)	RISK ASSESSMENT			RECOMMENDATIONS	ACTION (By)
					LIKELIHOOD	CONSEQUENCE SEVERITY	RISK RANKING		
1	**Process Upsets:** Pressure deviations, Over pressure due to excessive BOG generation caused by rollover	• LNG liquid leakage • LNG vapour leakage	• Fire and Explosion • Personnel injury • Loss of containment • Damaging the equipment (tank) • Environmental pollutions	• Using of double haul storage tanks. • Instruments for detection and relief of the excessive BOG • Constant monitoring of the temperature and density of LNG at different levels • Bounded area (dike walls) • Firefighting and safety equipment	Possible	Critical	Extreme	See Section 6.5 and Chapter 7 of this thesis	Process and safety design team
2	**Leakage or uncontrolled release:** Leak in pipe or tank due to rollover	• LNG liquid leakage • LNG vapour leakage • Spills	• Fire • Personnel injury • Loss of containment • Environmental pollutions	• Same as number 1	Unlikely due to hydro tests before commissioning	Major	High	Follow the commissioning /operation procedures and personnel training	Process, operators and safety design team
3	**Natural Events:** Such as flood, storm, bushfire, etc. (NOT directly related to rollover; however, if natural events	• LNG liquid leakage • LNG vapour leakage	• Same as number 1	• Choice of safe site location • Good Structural Design	Possible	Minor	Moderate	Follow the recommended practises for emergency response	Process, operators and safety design team

189

	damage the control or monitoring system it could lead to rollover)			• Utilizing required design standards • Safety in design					
4	**Environmental Impact:** Flaring/venting during emergency condition such as rollover	• LNG liquid leakage • LNG vapour leakage	• Same as number 1	• Same as number 1	Possible	Critical	Extreme	See Section 6.5 and Chapter 7 of this thesis	Process and safety design team
5	**Road and transport:** Any small scale rollover in road tankers or ocean carrier, which may lead to excessive BOG generation and transport interruption	• LNG liquid leakage • LNG vapour leakage • Spills	• Same as number 1	• High national and international transport and road safety standards • Continuous inspection and monitoring	Unlikely	Moderate	Moderate	Follow the operation procedures and personnel training	safety design team

Table 6.5: HAZID worksheet for LNG rollover in an onshore above ground tank.

NOTE: This table has been filtered for only the Hazards related or arising out of the rollover incidents. Hence, other Hazards identified during the construction, transportation and the operations other than rollover-related have not been listed here.

6.4. Qualitative risk assessment of LNG rollover, layer of protection analysis (LOPA)

Layer of protection analysis (LOPA)[62] is a semi-qualitative risk analysis method, which is usually applied following a qualitative hazard identification tool such as HAZID and is a powerful analytical risk assessment tool for assessing the adequacy of protection layers used to mitigate process risk[65]. Figure 6.1 shows a schematic of LOPA risk assessment technique.
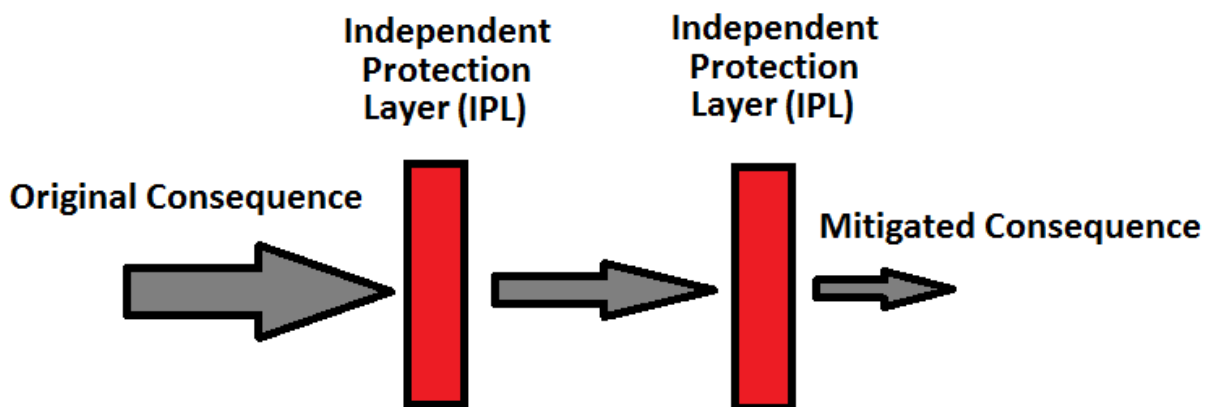
Figure 6.1: Schematic of LOPA approach.

LOPA analysis starts with evaluation of an undesired situation, such as environmental, health, safety event, with business, or economic impact, then evaluate the system safeguards capabilities against the consequences to remove or mitigate them to have less impact. These events and consequences are called scenarios and each independent safeguard is called independent protection layer (IPL). LOPA focuses on one scenario at a time.

Each identified safeguard is evaluated for two key characteristics:
- Is the safeguard effective in preventing the scenario from reaching the consequence?
- Is the safeguard independent of the initiating event and the other IPLs[65]?

In a modern LNG terminal facility, LNG storage safety can be ensured using multiple layers of protection created by four major elements[66]:

1. Primary containment (primary wall) of the LNG storage tank, using appropriate materials suitable for storing for LNG in cryogenic conditions.
2. Secondary containment (secondary wall), which can hold any leaks or spills in case of primary containment, fails.
3. Safeguard systems (Instrument and controls plus the safety devices such as PSVs and detectors)
4. Applying safe distance from nearby equipment, plants, communities and other public areas.

The multiple layers of protection mentioned above, are proven to be effective for both the safety of the workers dealing with LNG and the safety of the communities that surround LNG facilities[66]. However, these minimum requirements of safety are not optimal without having an accurate model to forecast the amount of BOG generated before and during the rollover.

6.5. Recommendations on the existing safeguarding in the modern LNG tanks

Most modern LNG tanks have four layers of protections, as mentioned above, due to improvements in technology, tighter regulations and applying higher standards. Furthermore, all tanks are equipped with instruments that monitor the process variables such as pressure, temperature and density so they can relieve excess pressure if required. However, it is still needed to predict the evolution of these process variables over time and consider the amount of BOG that may be generated during the rollover incidents. This can only be done with understanding the phenomenon of rollover and having a realistic rollover model that can quickly calculate the possibility of a rollover incident.

In practice, a simulation program tool such as presented in this study can predict the time to rollover and other critical parameters such as the amount of BOG generated, which is directly related to the risk of rollover. This prediction enables the terminal operators, to manage their existing LNG inventories and safely unload any new LNG cargoes into the tanks with existing LNG residues.

Operators can simply run such simulation programs (if incorporated in their tank farm control system) with the new LNG cargo condition (P, T and composition) and the existing residue LNG condition in the tank as the inputs and predict the time to the possible rollover and amount of BOG generated. The tank with the longest time to possible rollover and minimum BOG generated during rollover will be the safest option.

Figure 6.2 below, shows a suggested schematic of a hypothetical LNG tank farm configuration, with half-full tank A and B, waiting to receive arriving LNG cargo. Using the above-mentioned procedure and a rollover simulation program such as the one developed in this research, enable operators to choose the safest tank for unloading.
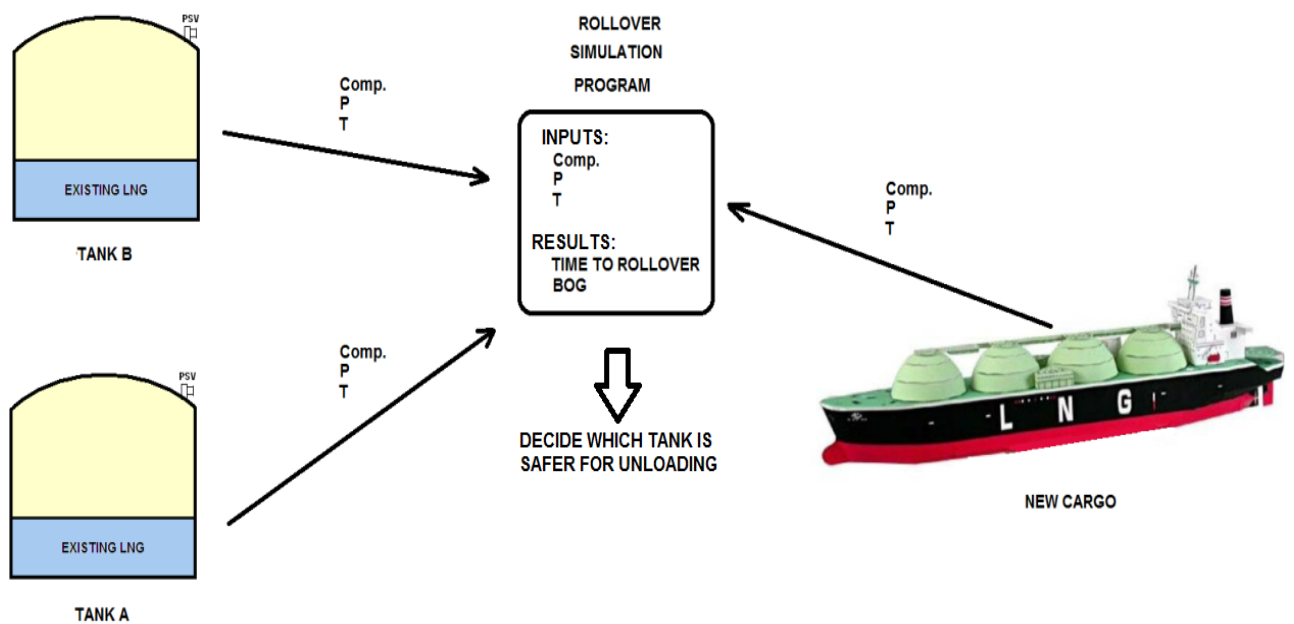
Figure 6.2: LNG Proposed operation configuration for LNG unloading facility.

In summary, the hydrocarbon industry approach to LNG rollover risk is currently not considered as critical as it should be. As demonstrated in previous sections of this chapter, a qualitative risk assessment and the HAZID showed that LNG rollover was categorised as "extreme". Although new features of the modern LNG tanks provide the minimum requirements for safety and protection, they are not sufficient and optimal against a rollover incident without understanding the consequences of a rollover event. Therefore, incorporating a novel simulation model such as presented in this research, with the "tank farm management system" (software), is highly recommended to ensure safer operation of any LNG tanks in refineries and terminals.

Chapter 7

Conclusions and recommendations

7.1. Conclusions

Since the first recorded LNG rollover incident of La Spezia-Italy in 1972, which was reported by Sarsten[6], many groups have attempted to simulate LNG rollover incidents: Chatterjee *et al.*[16], Germeles[17], Heestand *et al.*[24] and recently Deshpande *et al.*[25]. All of these researchers used the analogies between heat and mass transfer that are diffusive in nature. Chatterjee *et al.* [16] and Germeles[17] utilized Turner's model for saline solutions to estimate their mass transfer coefficient from the estimated heat transfer coefficient. Germeles[17] attempted to modify Turner's observations to account for the different physical properties of LNG. The simulations of Chatterjee *et al.*[16] and Germeles[17] both predicted much longer times to rollover than were reported. Heestand *et al.*[24] concluded that this was because the ratio of (diffusive) heat to mass transfer was too small and, dispensing with Turner's model, obtained a simulated rollover time consistent with the reports by utilising the Reynolds analogy. However, to do so Heestand *et al.*[24] were forced to use a correlation for the heat transfer coefficient that was inconsistent with the empirical relationships reported by Globe and Dropkin[29] and McAdams[28].

In this work, a model for LNG rollover has been developed and used to simulate the La Spezia and the Partington rollover incidents. This model has also been used to simulate several hypothetical auto-stratification rollover cases. Similar to Heestand *et al.*[24], the new model was based on energy and material balance relationships between two liquid LNG layers, a vapour phase in equilibrium with the film and assumed diffusive heat and mass transfer regimes. However, the new model used the concept suggested by Bates and Morrison of having 2 phases or transport regimes during a rollover event and improved the previous models by using the Chilton-Colburn analogy for Phase 1 of the rollover and the Reynolds analogy for Phase 2 of rollover. Furthermore, our model used a

more accurate, multi-parameter equation of state to calculate the thermodynamic properties of the LNG and the vapour. In addition, the transport properties of the LNG and vapour phase were evaluated throughout the simulation as a function of temperature, pressure and composition using recommended transport property correlations[51]. These recommended correlations gave values for the transport properties up to 45% larger than used by Heestand *et al.*[24]. In the new model, a rigorous approach was taken to calculate the vapour phase properties and to the criterion for establishing when rollover occurred.

The results of Heestand *et al.*[24] for the La Spezia incident was successfully reproduced in this research, using the new approach, to verify the accuracy of the model. Those results along with the Nantes data, then was used to estimate the heat transfer coefficients in both phases. Finally, an advanced model was developed to simulate the Nantes and Partington incidents plus several auto-stratification rollover cases. The new model was also used to conduct a sensitivity analysis to show the important role played by the boil-off rate and that varying parameters in the model that affected the boil-off rate had a significant effect on the predicted rollover time. Alternatively, by changing the initial temperature difference between the bottom and upper liquid layers in the Partington incident the predicted rollover time increased significantly. These results qualitatively showed that initial temperature difference has a major effect on the system stability and driving force towards evolving rollover. These sensitivity studies demonstrate that the data from the La Spezia, Nantes and the Partington incidents can only be used to a limited extent for the purpose of fundamental studies of LNG rollover[11].

The model was used to investigate the rate of auto-stratification in an LNG tanker and its effect on the system's hydrostatic stability. Initially, the value of R_s should be high enough to place the system in Phase 1 and so the current model could simulate the evolution of R_s as auto-stratification occurs and if R_s were seen to approach $R_c \approx 3.8$ then this would indicate the strong potential for the auto-stratification to lead to a rollover event. Thus, the current model was

also used to investigate the rate of decrease in R_s as a function of initial N_2 content in the LNG.

Another sensitivity analysis was also conducted on the level of nitrogen in industrial LNG, to investigate if the current standard of maximum 1% nitrogen is too conservative or whether it could be increased to around 2.5%. The results showed that, although the nitrogen content above 1% did not directly have an effect on rollover occurrence, it is not efficient nor cost effective on operating costs of storing LNG, as it requires lower storage temperatures and more BOG handling.

7.2. Recommendations for future work

In principle, the current model could be used to investigate a practical problem for the LNG shipping and storage industry: N_2 content specifications for avoiding auto-stratification. Currently, the specifications for N_2 content in LNG are conservative to avoid auto-stratification and possible rollover events during long storage periods. Consequently, the expensive "double-handling" of N_2 can often occur in the liquefaction – re-gasification cycle. For example, cryogenic distillation is sometimes used in the liquefaction process to meet the conservative auto-stratification N_2 specification. Then upon re-gasification N_2 ballast is added to meet the heating value and/or Wobbe index[23] specifications of the customer's gas pipeline distribution network.

Future research into LNG rollover can be classified into either simulation or experiment. In terms of the model developed here, the most important simulation task would be to incorporate a description of penetrative convection to describe Phase 2. However, the structure of the new simulation would not be significantly different from that represented here with Reynolds analogy, with the physical properties still being updated and calculated at user-defined time intervals.

Bates and Morrison[4] proposed models for both Phase 1 and Phase 2. Upon closer inspection of their model for Phase 1, several deficiencies were found. They acknowledged that their model for Phase 2 was somewhat simplistic but they argued it captured the essential physics of penetrative convection. It requires that the speeds of the migrating interfaces be calculated or physically measured, which in principle could be done using empirical correlations in the literature[4] or direct measurement in the lab. It might also be possible to identify alternative, improved correlations or models for penetrative convection elsewhere and this should be determined in any future research by a thorough review of the broader literature on fluid dynamics and convection.

The current model included the calculation of the stability ratio and used this parameter to switch from the slower heat and mass transfer regime describing Phase 1 to the extremely different regime that was required for Phase 2. The current model used diffusive transport regimes of Chilton-Colburn analogy for Phase 1 and Reynolds analogy for Phase 2 of rollover.

Other areas of possible improvement for future LNG rollover simulations include:

1. Using a correlation for the heat transfer coefficient that is known to be more accurate for LNG than those of McAdams[28] or Globe and Dropkin[29]. This might be possible in the first instance with a thorough review of the relevant LNG specific heat transfer literature combining with direct lab measurements.

2. Using a more physical basis to estimate the fraction of heat entering the top of the tank that is absorbed by the vapour phase. Heestand *et al.*[24] commented that the 95% value used in their simulation was somewhat arbitrary and it has been shown in this work that the simulation results are not sensitive to its value when we used 100% as we assumed vapour is in equilibrium with the film and at the same temperature. To verify this, real-time operational data is required.

3. Developing better models for the transport properties of LNG. This is of course, a non-trivial problem that many workers have contributed to. In order to develop these models, new experimental data measured at the challenging cryogenic conditions of LNG are required as are improved theoretical descriptions of their dependence on pressure, temperature and composition.

4. Incorporating the operational data of any existing vapour recovery compressors and recirculation systems for long-term LNG storage in future models.

Finally, direct measurements of LNG rollover in a controlled system would, of course, provide the most benefits to models of this process, which is of both fundamental and applied interest. To be of maximum use the data generated would need to include the initial compositions of various LNG strata and the evolution of temperature and density as a function of depth with the tank. Ideally, compositions of the evolving strata would also be measured but the complexity of acquiring reliably representative samples might prevent this.

Data on the boil-off rate would be critical and sufficient instrumentation should be deployed to adequately characterise the evolution of the vapour phase. Just as important as information about the tank and the heat flux into it from the environment as a function position. The costs and difficulties of such measurements are of course high but given the scale of the LNG industry and the possible efficiencies in engineering practice that could be gained; the potential benefits of such measurements probably justify the cost.

Appendix 1: Mass (mole) fluxes in different methods:

Turner:

$$F_{Salinity} = k_{Salin} A \Delta S$$

$$\frac{kgSolute}{s} = k_{Salin} m^2 \frac{kgSolute}{kgSolution}$$

or

$$F_{Mass} = k_{Mass} A \Delta X_{MassFraction}$$

$$\frac{kgSolute}{s} = k_{Mass} m^2 \frac{kgSolute}{kgTotal}$$

$$k_{Mass} = k_{Salinity}$$

Heestand *et al.*:

$$F_{Molar} = k_{mole} A \Delta X_{MoleFraction}$$

$$\frac{moleSolute}{s} = k_{mole} m^2 \frac{moleSolute}{moleTotal}$$

$$k_{Mass} = MW_{Solute} k_{mole}$$

This Work:

$$F_{Concentraion} = k_{Conc} A \Delta X_{Conc}$$

$$\frac{moleSolute}{s} = k_{mole} m^2 \frac{moleSolute}{MassSolvent}$$

$$k_{Conc} = \frac{1}{MW_{Solvent} X_{Solvent}} k_{mole}$$

$$k_{Mass} = MW_{Solute} MW_{Solvent} X_{Solvent} k_{Conc}$$

Appendix 2: HAZID guidewords sample:

Natural Disasters	Equipment / Instrumentation Malfunction	Loss of Containment /Fire / Explosion
High winds / Hurricane / Tornado	Pump failure	Leakage from Piping/flange
Extreme wave / Extreme current	Pump seal failure	Leakage from process area
Extreme heat	Safety systems	Drains / Vents
High humidity	Communication	Explosive hazards
Lightning	Common cause failures	Energy release
Earthquake / Tsunami		
External Effects	**Process Upsets**	**Environmental Impact**
Dropped object	Pressure deviations	Flaring/venting during normal operations
Reduced visibility	Temperature deviations	Flaring/venting during emergency
Sabotage/terrorism	Flow deviations	Hydrocarbon / Chemical leak
Structural failure	Level deviations	Waste water treatment
Fatigue/cracking	Improper mixing	Oily water treatment / disposal
	Corrosion/erosion	
	Start-up/shutdown	
Human Factors	**Composition Problems**	**Utility Failures**
Occupational accidents	Contamination	Blackout / Power Failure
Improper/inadequate training	Moisture (H2O)	Cooling water
Weather monitoring	H2S Concentrations	Instrument air
Shipping / traffic monitoring	CO2	Inert gas / Nitrogen
Material handling	**Inspection / Maintenance**	Firewater
	Confined space	HVAC system
Emergency Operations	Machinery/instrument accessibility	
Escape / rescue	Equipment Mechanical /Electrical isolation	
Release from vent		

Appendix 3: LNG Material Safety Data Sheet (MSDS):

THE LINDE GROUP
Linde

Liquefied Natural Gas
Material Safety Data Sheet

1. PRODUCT AND COMPANY IDENTIFICATION

Product Name	**Liquefied Natural Gas**
UN-Number	**UN1972**
Recommended Use	Industrial use.
Synonyms	LNG
Supplier Address*	Linde Gas North America LLC - Linde Merchant Production Inc. - Linde LLC 575 Mountain Ave. Murray Hill, NJ 07974 Phone: 908-464-8100 www.lindeus.com
	Linde Gas Puerto Rico, Inc. Las Palmas Village Road No. 869, Street No. 7 Catano, Puerto Rico 00962 Phone: 787-641-7445 www.pr.lindegas.com
	Linde Canada Limited 5860 Chedworth Way Mississauga, Ontario L5R 0A2 Phone: 905-501-1700 www.lindecanada.com
	* May include subsidiaries or affiliate companies/divisions.
	For additional product information contact your local customer service.
Chemical Emergency Phone Number	Chemtrec: 1-800-424-9300 for US/ 703-527-3887 outside US

2. HAZARDS IDENTIFICATION

DANGER!

Emergency Overview

Extremely flammable
Extremely cold liquid and gas under pressure.
May cause skin, eye, and respiratory tract irritation
Asphyxiant at high concentrations
May cause central nervous system depression
Contents under pressure
Keep at temperatures below 52°C / 125°F

Appearance Colorless.	**Physical State** Cryogenic Liquid.	**Odor** Petroleum like

OSHA Regulatory Status	This material is considered hazardous by the OSHA Hazard Communication Standard (29 CFR 1910.1200).

Potential Health Effects

Principle Routes of Exposure	Inhalation.
Acute Toxicity	
Inhalation	May cause central nervous system depression with nausea, headache, dizziness, vomiting, and incoordination. Simple asphyxiant. May cause suffocation by displacing the oxygen in the air. Exposure to oxygen-deficient atmosphere (<19.5%) may cause dizziness, drowsiness, nausea, vomiting, excess salivation, diminished mental alertness, loss of consciousness and death. Exposure to atmospheres containing 8-10% or less oxygen will bring about unconsciousness without warning and so quickly that the individuals cannot help or protect themselves. Lack of sufficient oxygen may cause serious injury or death.
Eyes	Contact with product may cause frostbite.
Skin	May cause frostbite.
Skin Absorption Hazard	No known hazard in contact with skin.
Ingestion	Not an expected route of exposure.
Chronic Effects	None known.
Aggravated Medical Conditions	Respiratory disorders.
Environmental Hazard	See Section 12 for additional Ecological Information.

3. COMPOSITION/INFORMATION ON INGREDIENTS

Chemical Name	CAS-No	Volume %	Chemical Formula
Methane	74-82-8	62-93	CH_4
Nitrogen	7727-37-9	1-9	N_2
Propane	74-98-6	1-7	C_3H_8
Ethane	74-84-0	3-11	C_2H_6
N-Butane	106-97-8	1-3	C_4H_{10}
Isobutane	75-28-5	1-3	C_4H_{10}
Helium	7440-59-7	<2	He
Isopentane	78-78-4	<1	C_5H_{12}
Pentane	109-66-0	<1	C_5H_{12}
Carbon dioxide	124-38-9	<1	CO_2

4. FIRST AID MEASURES

Eye Contact	In the case of contact with eyes, rinse immediately with plenty of water and seek medical advice. If frostbite is suspected, flush eyes with cool water for 15 minutes and obtain immediate medical attention.
Skin Contact	Wash off immediately with plenty of water. If skin irritation persists, call a physician. For dermal contact or suspected frostbite, remove contaminated clothing and flush affected areas with lukewarm water. DO NOT USE HOT WATER. A physican should see the patient promptly if contact with the product has resulted in blistering of the dermal surface or in deep tissue freezing.

203

Inhalation	PROMPT MEDICAL ATTENTION IS MANDATORY IN ALL CASES OF INHALATION OVEREXPOSURE. RESCUE PERSONNEL SHOULD BE EQUIPPED WITH SELF-CONTAINED BREATHING APPARATUS. Conscious inhalation victims should be assisted to an uncontaminated area and inhale fresh air. If breathing is difficult, administer oxygen. Unconscious persons should be moved to an uncontaminated area and, as necessary, given artificial resuscitation and supplemental oxygen. Treatment should be symptomatic and supportive.
Ingestion	None under normal use. Get medical attention if symptoms occur.
Notes to Physician	Treat symptomatically.

5. FIRE-FIGHTING MEASURES

Flammable Properties	Extremely flammable.
Suitable Extinguishing Media	Dry chemical or CO_2. Water spray or fog. DO NOT EXTINGUISH A LEAKING GAS FIRE UNLESS LEAK CAN BE STOPPED.
Hazardous Combustion Products	Carbon monoxide. Carbon dioxide (CO_2).
Explosion Data	
Sensitivity to Mechanical Impact	None
Sensitivity to Static Discharge	Yes.
Specific Hazards Arising from the Chemical	May form explosive mixtures with air. Continue to cool fire exposed cylinders until flames are extinguished. Cylinders may rupture under extreme heat. Damaged cylinders should be handled only by specialists. Vapors from liquefied gas are initially heavier than air and spread along ground. Vapors may travel to source of ignition and flash back.
Protective Equipment and Precautions for Firefighters	If possible, stop the flow of gas. Do not extinguish the fire until supply is shut off as otherwise an explosive-ignition may occur. If the fire is extinguished and the flow of gas continues, use increased ventilation to prevent build-up of explosive atmosphere. Ventilation fans must be explosion proof. Use non-sparking tools to close container valves.
	Use water spray to cool surrounding containers. Be cautious of a Boiling Liquid Evaporating Vapor Explosion, BLEVE, if flame is impinging on surrounding containers.
	As in any fire, wear self-contained breathing apparatus pressure-demand, MSHA/NIOSH (approved or equivalent) and full protective gear.

6. ACCIDENTAL RELEASE MEASURES

Personal Precautions	ELIMINATE all ignition sources (no smoking, flares, sparks or flames in immediate area). All equipment used when handling the product must be grounded. Do not touch or walk through spilled material. Stop leak if you can do it without risk. Wear self-contained breathing apparatus when entering area unless atmosphere is proved to be safe. Monitor oxygen level.
Environmental Precautions	Use water spray to reduce vapors or divert vapor cloud drift. Avoid allowing water runoff to contact spilled material. Prevent spreading of vapors through sewers, ventilation systems and confined areas.
Methods for Containment	Stop the flow of gas or remove cylinder to outdoor location if this can be done without risk. If leak is in container or container valve, contact the appropriate emergency telephone number in Section 1 or call your closest Linde location.
Methods for Cleaning Up	Return cylinder to Linde or an authorized distributor.

204

7. HANDLING AND STORAGE

Handling

Ground and bond all lines and equipment associated with product system. All equipment should be non-sparking and explosion proof. Remove all sources of ignition. Use only in ventilated areas. "NO SMOKING" signs should be posted in storage and use areas.

Never attempt to lift a cylinder by its valve protection cap. Protect cylinders from physical damage; do not drag, roll, slide or drop. When moving cylinders, even for short distance, use a cart designed to transport cylinders. Use equipment rated for cylinder pressure. Use backflow preventive device in piping.

Use an adjustable strap wrench to remove over-tight or rusted caps. Never insert an object (e.g. wrench, screwdriver, pry bar,etc.) into valve cap openings. Doing so may damage valve, causing leak to occur. If user experiences any difficulty operating cylinder valve discontinue use and contact supplier.

Never put cylinders into trunks of cars or unventilated areas of passenger vehicles. Never attempt to refill a compressed gas cylinder without the owner's written consent. Never strike an arc on a compressed gas cylinder or make a cylinder a part of an electrical circuit.

For additional recommendations, consult Compressed Gas Association Pamphlets P-1, P-14, and Safety Bulletin SB-2.

Storage

Outside or detached storage is preferred. Protect from physical damage. Cylinders should be stored upright with valve protection cap in place and firmly secured to prevent falling. Store in cool, dry, well-ventilated area of non-combustible construction away from heavily trafficked areas and emergency exits. Keep at temperatures below 52°C / 125°F. Full and empty cylinders should be segregrated. Use a "first in-first out" inventory system to prevent full cylinders from being stored for excessive periods of time. Always store and handle compressed gas cylinders in accordance with Compressed Gas Association, pamphlet CGA-P1, Safe Handling of Compressed Gases in Containers.

8. EXPOSURE CONTROLS / PERSONAL PROTECTION

Exposure Guidelines

Chemical Name	ACGIH TLV	OSHA PEL	NIOSH IDLH
Isopentane 78-78-4	TWA: 600 ppm		
Carbon dioxide 124-38-9	STEL = 30000 ppm TWA: 5000 ppm	TWA: 5000 ppm TWA: 9000 mg/m³ (vacated) TWA: 10000 ppm (vacated) TWA: 18000 mg/m³ (vacated) STEL: 30000 ppm (vacated) STEL: 54000 mg/m³	IDLH: 40000 ppm TWA: 5000 ppm TWA: 9000 mg/m³ STEL: 30000 ppm STEL: 54000 mg/m³
N-Butane 106-97-8	TWA: 1000 ppm	(vacated) TWA: 800 ppm (vacated) TWA: 1900 mg/m³	TWA: 800 ppm TWA: 1900 mg/m³
Pentane 109-66-0	TWA: 600 ppm	TWA: 1000 ppm TWA: 2950 mg/m³ (vacated) TWA: 600 ppm (vacated) TWA: 1800 mg/m³ (vacated) STEL: 750 ppm (vacated) STEL: 2250 mg/m³	IDLH: 1500 ppm Ceiling: 610 ppm 15 min Ceiling: 1800 mg/m³ 15 min TWA: 120 ppm TWA: 350 mg/m³
Methane 74-82-8	TWA: 1000 ppm		
Ethane 74-84-0	TWA: 1000 ppm		
Propane 74-98-6	TWA: 1000 ppm	TWA: 1000 ppm TWA: 1800 mg/m³	IDLH: 2100 ppm TWA: 1000 ppm TWA: 1800 mg/m³
Isobutane 75-28-5	TWA: 1000 ppm	N/A	N/A

Immediately Dangerous to Life or Health.

Other Exposure Guidelines	Vacated limits revoked by the Court of Appeals decision in AFL-CIO v. OSHA, 965 F.2d 962 (11th Cir., 1992).
Engineering Measures	Showers. Eyewash stations. Explosion proof ventilation systems.
Ventilation	Use ventilation adequate to keep exposures below recommended exposure limits.

Personal Protective Equipment

Eye/Face Protection	Wear protective eyewear (safety glasses).
Skin and Body Protection	Work gloves and safety shoes are recommended when handling cylinders. Wear cold insulating gloves when handling liquid. Cotton or Nomex® clothing is recommended to prevent static build-up.

Respiratory Protection

General Use	If exposure limits are exceeded or irritation is experienced, NIOSH/MSHA approved respiratory protection should be worn. Positive-pressure supplied air respirators may be required for high airborne contaminant concentrations. Respiratory protection must be provided in accordance with current local regulations.
Emergency Use	Use positive pressure airline respirator with escape cylinder or self contained breathing apparatus for oxygen-deficient atmospheres (<19.5%).
Hygiene Measures	Wear suitable gloves and eye/face protection.

206

9. PHYSICAL AND CHEMICAL PROPERTIES

Product Information

Appearance	Colorless.	Odor	Petroleum like.
Odor Threshold	No information available	Physical State	Cryogenic Liquid
Flash Point	-306°F / -188°C	Flashpoint Method	Closed cup
Autoignition Temperature	580°C / 1076°F	Flammability Limits in Air	
		Upper	15%
		Lower	5%

The following information is for the NON-INERT components of this mixture:

Chemical Name	Boiling Point	Melting Point	Molecular Weight	Evaporation Rate	Water Solubility	Vapor Pressure	Vapor Density (Air=1)	Gas Density Kg/m³@20°C
Isopentane	28 °C	-160 °C	72.14	-	No information available		2.5	3.212 @15°
Carbon dioxide	56 °C	-56 °C	44.00	-	0.145 g/ml @ 25°C	838 psig (5778 kPa) @ 21.1°C	1.522	1.839
Pentane	36°C	<-50 °C	72.14		No information available	1100 hPa @ 38 °C	2.5	3.228 @15°
N-Butane	-0.5 °C	-138.3 °C	58.12	-	No information available	2200 hPa @ 20 °C	2.11	2.52 @15°
Methane	-162 °C	-182.5 °C	16.04	-	No information available	46700 hPa @ -82.5 °C	0.56	0.668 @15°
Ethane	-88.7°C	-183 - -20 °C	30.06	-	No information available	600 - 39000 hPa @ 20 °C	1.05	1.282 @15°
Propane	-42.1°C	-183 - -20 °C	44.09	-	No information available	600 - 39000 hPa @ 20 °C	1.55	1.99 @15°
Isobutane	-11.7 °C	-255 °C	58.12	-	No information available	2100 hPa @ 20 °C	2.06	2.51 @15°

The following information is for the INERT components that may be part of this mixture:

Chemical Name	Boiling Point	Melting Point	Molecular Weight	Evaporation Rate	Water Solubility	Vapor Pressure	Vapor Density (Air=1)	Gas Density Kg/m³@20°C
Helium	-268.94 °C	-272.0 °C	4.00	-	0.0089 (vol/vol @ 20°C and 1 atm)	Above critical temperature	0.138	0.166
Nitrogen	-196 °C	-210 °C	28.01	-	0.023 (vol/vol @ 20°C and 1 atm)	Above critical temperature	0.97	1.165

10. STABILITY AND REACTIVITY

Stability	Stable.
Incompatible Products	Oxidizing agents.
Conditions to Avoid	Heat, flames and sparks.
Hazardous Decomposition Products	Carbon monoxide (CO). Carbon dioxide (CO_2).
Hazardous Polymerization	Hazardous polymerization does not occur.

11. TOXICOLOGICAL INFORMATION

Acute Toxicity

Product Information

LD50 Oral:	No information available.
LD50 Dermal:	No information available.
LC50 Inhalation:	No information available.
Repeated Dose Toxicity	No information available.
Component Information	No information available.

Chemical Name	LD50 Oral	LD50 Dermal	LC50 Inhalation
Propane		-	= 658 mg/L (Rat) 4 h
Ethane			= 658 mg/L (Rat) 4 h
N-Butane			658 mg/L (Rat) 4 h
Isobutane			= 658 mg/L (Rat) 4 h
Isopentane			= 280000 mg/m³ (Rat) 4 h
Pentane	> 2000 mg/kg (Rat)	= 3000 mg/kg (Rabbit)	= 364 g/m³ (Rat) 4 h
Carbon dioxide			470000 ppm (Rat)

Chronic Toxicity

Chronic Toxicity	None known.
Carcinogenicity	Contains no ingredient listed as a carcinogen.
Irritation	No information available.
Sensitization	No information available.
Reproductive Toxicity	No information available.
Developmental Toxicity	Oxygen deficiency during pregnancy has produced developmental abnormalities in humans and experimental animals.
Synergistic Materials	None known.
Target Organ Effects	None known.

12. ECOLOGICAL INFORMATION

Ecotoxicity

Will not bioconcentrate.

Ozone depletion potential; ODP; (R-11 = 1): Does not contain ozone depleting chemical (40 CFR Part 82).

Chemical Name	Toxicity to Algae	Toxicity to Fish	Toxicity to Microorganisms	Daphnia Magna (Water Flea)
Isopentane				EC50 48 h: = 2.3 mg/L (Daphnia magna)

Chemical Name	Toxicity to Algae	Toxicity to Fish	Toxicity to Microorganisms	Daphnia Magna (Water Flea)
Pentane		LC50 96 h: = 11.59 mg/L (Pimephales promelas) LC50 96 h: = 9.87 mg/L (Oncorhynchus mykiss) LC50 96 h: = 9.99 mg/L (Lepomis macrochirus)		EC50 48 h: = 9.74 mg/L (Daphnia magna)

Chemical Name	Log Pow
Isopentane	3.3
N-Butane	2.89
Pentane	3.39
Ethane	2.8
Propane	2.3
Isobutane	2.88

13. DISPOSAL CONSIDERATIONS

Waste Disposal Methods

Do not attempt to dispose of residual waste or unused quantities. Return in the shipping container PROPERLY LABELED WITH ANY VALVE OUTLET PLUGS OR CAPS SECURED AND VALVE PROTECTION CAP IN PLACE to Linde for proper disposal. This material, as supplied, is a hazardous waste according to federal regulations (40 CFR 261).

14. TRANSPORT INFORMATION

DOT

Proper shipping name	Methane, refrigerated liquid
Hazard Class	2.1
Subsidiary Class	None
UN-Number	UN1972
Description	UN1972,Methane, refrigerated liquid,2.1
Emergency Response Guide Number	115

TDG

Proper Shipping Name	Methane, refrigerated liquid
Hazard Class	2.1
UN-Number	UN1972
Description	UN1972,METHANE, REFRIGERATED LIQUID,2.1

MEX

Proper Shipping Name	Methane, refrigerated liquid
Hazard Class	2.1
UN-Number	UN1972
Description	UN1972 Methane, refrigerated liquid,2.1

IATA

UN-Number	UN1972
Proper Shipping Name	Natural gas, refrigerated liquid
Hazard Class	2.1
ERG Code	10L

209

Description	UN1972,Natural gas, refrigerated liquid,2.1
Maximum Quantity for Passenger	Forbidden
Maximum Quantity for Cargo Only	Forbidden
Limited Quantity	Forbidden

IMDG/IMO

Proper Shipping Name	Methane, refrigerated liquid
Hazard Class	2.1
UN-Number	UN1972
EmS No.	F-D, S-U
Description	UN1972, Methane, refrigerated liquid,2.1, FP -188C

ADR

Proper Shipping Name	Methane, refrigerated liquid
Hazard Class	2.1
UN-Number	UN1972
Classification Code	3F
Description	UN1972 Methane, refrigerated liquid,2.1,

15. REGULATORY INFORMATION

International Inventories

TSCA	Complies
DSL	Complies
EINECS/ELINCS	Complies

Legend

TSCA - United States Toxic Substances Control Act Section 8(b) Inventory
DSL/NDSL - Canadian Domestic Substances List/Non-Domestic Substances List
EINECS/ELINCS - European Inventory of Existing Commercial Chemical Substances/EU List of Notified Chemical Substances

U.S. Federal Regulations

SARA 313
Section 313 of Title III of the Superfund Amendments and Reauthorization Act of 1986 (SARA). This product does not contain any chemicals which are subject to the reporting requirements of the Act and Title 40 of the Code of Federal Regulations, Part 372.

SARA 311/312 Hazard Categories

Acute Health Hazard	Yes
Chronic Health Hazard	No
Fire Hazard	Yes
Sudden Release of Pressure Hazard	Yes
Reactive Hazard	No

Clean Water Act
This product does not contain any substances regulated as pollutants pursuant to the Clean Water Act (40 CFR 122.21 and 40 CFR 122.42).

Risk and Process Safety Management Programs
This material, as supplied, contains one or more regulated substances with specified thresholds under 40 CFR Part 68 or regulated as a highly hazardous chemical pursuant to the 29 CFR Part 1910.110 with specified thresholds:

210

Chemical Name	U.S. - CAA (Clean Air Act) - Accidental Release Prevention - Toxic Substances	U.S. - CAA (Clean Air Act) - Accidental Release Prevention - Flammable Substances	U.S. - OSHA - Process Safety Management - Highly Hazardous Chemicals
Isopentane		10000 lbs	
N-Butane		10000 lbs	
Pentane		10000 lbs	
Methane		10000 lbs	
Ethane		10000 lbs	
Propane		10000 lbs	
Isobutane		10000 lbs	

Clean Air Act, Section 112 Hazardous Air Pollutants (HAPs) (see 40 CFR 61)
This product does not contain any substances regulated as hazardous air pollutants (HAPS) under Section 112 of the Clean Air Act Amendments of 1990.

CERCLA/SARA
This material, as supplied, does not contain any substances regulated as hazardous substances under the Comprehensive Environmental Response Compensation and Liability Act (CERCLA) (40 CFR 302) or the Superfund Amendments and Reauthorization Act (SARA) (40 CFR 355). There may be specific reporting requirements at the local, regional, or state level pertaining to releases of this material.

U.S. State Regulations

California Proposition 65
This product does not contain any Proposition 65 chemicals.

U.S. State Right-to-Know Regulations

Chemical Name	Massachusetts	New Jersey	Pennsylvania	Illinois	Rhode Island
Helium	X	X	X	-	X
Isopentane	X	X	X		
Carbon dioxide	X	X	X	-	X
N-Butane	X	X	X		X
Pentane	X	X	X		X
Methane	X	X	X		X
Ethane	X	X	X		X
Propane	X	X	X		X
Isobutane	X	X	X		
Nitrogen	X	X	X	-	X

International Regulations

Chemical Name	Carcinogen Status	Exposure Limits
Carbon dioxide	-	Mexico: TWA= 5000 ppm Mexico: TWA= 9000 mg/m³ Mexico: STEL= 15000 ppm Mexico: STEL= 27000 mg/m³
N-Butane		Mexico: TWA 800 ppm Mexico: TWA 1900 mg/m³
Pentane		Mexico: TWA 600 ppm Mexico: TWA 1800 mg/m³ Mexico: STEL 760 ppm Mexico: STEL 2250 mg/m³

Canada

211

This product has been classified in accordance with the hazard criteria of the Controlled Products Regulations (CPR) and the MSDS contains all the information required by the CPR.

WHMIS Hazard Class
A Compressed gases
B1 Flammable gas

16. OTHER INFORMATION

Prepared By	Product Stewardship 23 British American Blvd. Latham, NY 12110 1-800-572-6501
Issuing Date	22-Sep-2011
Revision Date	
Revision Number	0
Revision Note	Initial Release.

NFPA	Health Hazard 3	Flammability 4	Stability 0	Physical and Chemical Hazards -
HMIS	Health Hazard 3	Flammability 4	Physical Hazard 2	Personal Protection -

Note: Ratings were assigned in accordance with Compressed Gas Association (CGA) guidelines as published in CGA Pamphlet P-19-2009, CGA Recommended Hazard Ratings for Compressed Gases, 3rd Edition.

General Disclaimer
For terms and conditions, including limitation of liability, please refer to the purchase agreement in effect between Linde LLC, Linde Merchant Production, Inc. or Linde Gas North America LLC (or any of their affiliates and subsidiaries) and the purchaser.

DISCLAIMER OF EXPRESSED AND IMPLIED WARRANTIES
Although reasonable care has been taken in the preparation of this document, we extend no warranties and make no representations as to the accuracy or completeness of the information contained herein, and assume no responsibility regarding the suitability of this information for the user's intended purposes or for the consequences of its use. Each individual should make a determination as to the suitability of the information for their particular purpose(s).

End of Safety Data Sheet

Appendix 4: Chronology of papers in open literature related to LNG rollover

No.	Year	Title	Authors	Summary	Remarks
1	1965	THE COUPLED TURBULENT TRANSPORTS OF SALT AND HEAT ACROSS A SHARP DENSITY INTERFACE	J. S. Turner	When a layer of cold fresh water is resting on top of the hot salty water with a sharp interface between them, the system as a whole may be unstable, even though the differences of density $\beta\Delta S$ due to salinity are far greater than those due to temperature $\alpha\Delta T$. Convective motions are produced in both layers by the transfer of heat and at the same time, salt is transported across the interface. Measurements are presented here of the rates of transport in such a two-layer system in which the temperature difference is maintained by heating continuously from below.	Introduced relation between α, β and heat and mass flux in saline solutions. Flux ratio and stability.

				Both the heat transfer and the ratio of the rates of turbulent transport of salt and heat have been found to depend systematically on the density ratio $\beta\Delta S / \alpha\Delta T$, at least over the small range of heat fluxes used in these experiments. This is in agreement with the result of a simple dimensional analysis and suggests that the form of the functions should have a wider application. The measurements also indicate that over a wide range of density differences the potential energy change of the top layer due to the lifting of salt is a constant fraction of that released by the transfer of heat.	
2	1971	Cut LNG storage costs	H. T. Hashemi H. R. Wesson	The rate of evaporation of LNG in a storage tank is essentially controlled by the amount of supersaturation pressure of the bulk of the stored LNG and the surface area of the vapor-liquid interface. The relationship between the rate of evaporation and supersaturation pressure, ΔP_s is	Suggested an equation, to calculate BOG flowrate

				$m_{LNG} = 0.0082\ \Delta P^{4/3}$, (lbs./hr. sq. ft.) where, ΔP. is a function of the average rate of change of the saturation temperature of the liquid with pressure, dP / dTs (19.34 inches of water/°F for LNG at 14.7 psia) and the total temperature difference between the bulk of the liquid and the surface.	
3	1972	LNG STRATIFICATION AND ROLLOVER	J.A. Sarsten	Detail operational data and report on La Spezia LNG Rollover incident occurred in 1971	The first reported industrial LNG rollover available in open literature
4	1972	THE EFFECT OF STRATIFICATION ON BOIL-OFF RATES IN LNG TANKS	N. Chatterjee J. M. Geist	First simulation of La Spezia incident (Lumped method)	1: Use of Turner Thermohaline model for saline solution for LNG 2: First criteria for rollover, equalization of temperature 3: Considered "n" layered LNG
5	1975	A model for LNG tank Rollover	A. E. Germeles	Second simulation of La Spezia incident (Lumped method)	1: Use of Turner Thermohaline model for saline solution for LNG 2: Better criteria for rollover, equalization of density

					3: Considered "n" layered LNG
6	1983	A Predictive model FOR Rollover IN STRATIFIED LNG TANKS	J. Heestand C. W. Shipman J. W. Meader	Third simulation of La Spezia incident (Lumped method)	1: Reject Turner Thermohaline model for saline solution for LNG 2: Used Reynolds analogy to calculate mass transfer coefficient. 3: Criteria for rollover, equalization of density 4: used Hashemi- Wesson BOG
7	1986	C3- MR PROCESSES FOR BASELOAD LIQUEFIED NATURAL GAS	C. L. Newton G. E. Kinard Y. N. Liu	The combination of technology advance, energy conservation incentives and the typical remote location of LNG plants has led to the development of a range of process variations and equipment arrangements. This paper reviews the evolution of the propane precooled mixed refrigerant (C3-MR) process starting with the Brunei plant. Over this period of time, the process variations for the C3-MR have expanded to meet the needs of the changing plant situations which include plant location, economic criteria, etc. More recently, the C3-MR has been adapted for future needs	Referred to Chatterjee's paper about optimum level of N_2 in LNG (less %1and Auto- stratification)

				through a range of cycle variations which can be integrated with the feed and site conditions for the currently proposed base load facilities. The factors which influence the selection and integration of the associated equipment such as compression, power generation, heat rejection, separation, etc. will be reviewed.	
8	1986	FULLY AUTOMATED CONTROL SYSTEM FOR LNG RECEIVING TERMINALS	Y. SHIRASAKI M. TAKAHASHI	To operate an LNG receiving terminal smoothly and safely, it is essential to adopt a highly reliable control system. During ship unloading operations and normal operation, the pressure of LNG tanks must be kept constant by starting/stopping the BOG compressors. The delivery pressure of the vaporized natural gas must also be kept constant by corresponding to the vastly changing send out rate of the gas. This is done by: 1) starting/stopping the LNG pumps and sea water pumps; and 2) starting/stopping and load controlling of the	Monitoring Density, temperature and the pressure of the tank to adjust BOG compressors (importance of BOG on rollover, which is ignored in Bates and Morrison model)

				vaporizers (open-rack type vaporizers, combustion type vaporizers and power generation plants using cryogenic energy). When Demand gas is very low, all vaporizers must be stopped and send out rare must be controlled according to the boil off gas (BOG) rate under gap-pressure control of the tanks. An advanced control system using a microprocessor-based distributed control system with supervisory computers performs all of these operations fully and automatically, thereby minimizing manpower requirements at LNG receiving terminals. The system is designed and developed to be reliable, flexible, expandable and economical from an operational and maintenance standpoint. Such fully automatic control systems have been successfully used at several LNG receiving terminals in Japan.	

| 9 | 1986 | ROLLOVER IN LNG STORAGE – AN INDUSTRIAL VIEW | A. ACTON R. C. VAN MEERBEKE | A study group set up by the International LNG Importers Group (GIIGNL) has recently completed a study of available data on rollover. Rollovers are a result of stratification from filling a tank with different density liquids which remain unmixed or of auto stratification due to the preferential loss of nitrogen. Evaporation from the heavy bottom layer is suppressed by the head of the light top layer until the layers approach each other in density by heat and mass transfer and mix. Stratification can be prevented by mixing different density liquids using jet nozzles, recirculation, distributed fill systems and alternate top and bottom filling. Auto stratification is prevented by ensuring that the nitrogen content of the stored LNG is sufficiently low. Instrumentation to monitor temperature and density profiles and boil off can be used to | 1: Surface layer exist 2: Surface layer is slightly cooler than bulk liquid (should be upper layer) 3: Surface layer is at saturation T with vapor at P_{VAP} 4: bulk liquid (upper layer) is at the temperature defined by Hashemi - Wesson Eq. 5: Referred to several Rollover incidents (41) not available in open literature, gathered by GIIGNL Study Group directly from operations. 6: Highlighted the importance of vapor evolution (BOG) 6: Produced (repeated) previous graphs for rollover |

				detect any stratification and allow the preventive action to be taken before the rollover can occur. Our conclusion that most rollovers produce manageable increases in the boil off rate should enhance the acceptability of LNG storage.	
10	1993	Numerical modelling and flow visualization of mixing of stratified layers and rollover in LNG	J. Q. Shi C. Beduz R.G. Scurlock	A numerical model has been developed to study the mixing of two initially stratified layers, which are subjected to a uniform lateral heat flux. An important distinction is made between the free surface and the liquid/liquid interface with regard to the different flow characteristics of the two layers. In the upper layer where the warm liquid is cooled at the evaporating surface, the convective circulation is featured by a strong downward core flow; in contrast, the fluid flow in the lower layer is mainly confined to the wall boundary and is much weaker. Flow visualization experiments show that mixing of	1: Used distributed parameter method for modeling. 2: Free convective fluid flows modeled in rectangular tanks 3: Modeled as two-dimensional system (per unit of length) 4: Heterogeneous flow system involving two incompressible miscible Liquids 5: The governing differential equations are the Navier-Stokes equations, the continuity equation and the transport equations for

				two stratified layers generally involves two stages in sequence: migration of the interface and rapid mixing between the remaining liquids. The interface movement is due to entrainment mixing at the interface. When the two layers approach density equalization, the interface becomes increasingly unstable and the core flow in the upper layer is able to break into the lower layer. The base to side heat flux ratio appears to be a major factor in determining the mode and intensity of the subsequent mixing at a rollover incident.	thermal energy and the solute concentration. 6: Simplify the model by using the vorticity (rotation) stream function method rather than a primitive variables approach. They eliminate the pressure terms in the Navier-Stokes equations and introducing the vorticity and stream function, the number of independent variables is reduced by one. Limitations: What about vapor phase? Are these results valid for hydrocarbon (volatile) liquids? Effect of BOG on rollover?
11	1997	Modelling the behavior of stratified liquid	S. Bates D.S. Morrison	The evolution of stratified liquid natural gas (LNG), from its formation to its breakdown, is considered. Experimental observations have shown this evolution to consist of two principal	1: Introduced phase 1 and phase 2 concept for rollover.

				phases: a quiescent, stable phase 1 where the interface between the two layers is stationary; and an unstable phase 2 characterized by a migrating interface and culminating in a rollover. Mathematical models of the two phases are proposed and considered separately. For phase 1 a parametric solution is derived; the corresponding numerical solution of phase 2 equations is given and shown to compare well with experimental data.	2: Referred to Turner stability diagram. 3: used penetrative convection for determining phase 2 mass transfer.
		natural gas in storage tanks: a study of the rollover phenomenon			
12	2002	Mixing Phenomena through the Heat and Salt Transports Across a Density Interface in a Stratified Two-layer System	E. Cho H. Kim	They have investigated the mixing phenomena in a stratified two-layer fluid system where a layer of fresh water is initially put on top of salt water. When this stabilized system by a salt gradient is heated from below, it becomes unstable by an onset of convection in the lower layer due to the thermal buoyancy effect. Thereafter the heat and salt are ready to diffuse into the upper layer through the adjacent diffusive interface.	

| | | | | To examine quantitatively the merging process of the two layers as the destabilizing temperature gradient gets more dominant, we have measured many profiles of temperature and salinity in both layers by using accurate microscale measurement probes. Each run of the experiment, with several different initial concentration of salt, is followed until there appears a sudden overturning into a perfect mixing state. The order of thermal Rayleigh number has been kept as the order of 10^7 around which we have observed uniform temperature and salt profiles in the upper layer without any, external mixing force. Since the employed measuring probes show good reproducibility" and very fast response time to the variations of the temperature and salt concentration, the mixing phenomena with the double-diffusive convection has been pursued easily. | |

13	2003	MODEL PREDICTIONS FOR EFFICIENCY OPERATION OF THE LNG STORAGE TANK	C. S. Park S. K. Hong S. J. Kim	Calculation of BOG using Hashemi-Wesson and for physical properties using SRK VLE, with some operational data on BOG of LNG tanks.	
14	2004	Heat Transfer in Turbulent Rayleigh–Benard Convection below the Ultimate Regime	PE. Roche B. Castaing B. Chabaud B. Hébral	A Rayleigh–Benard cell has been designed to explore the Prandtl (Pr) dependence of turbulent convection in the cross-over range $0.7 < Pr < 21$ and for the full range of soft and hard turbulences, up to Rayleigh number Ra ≈ 10^{11}. The set-up benefits from the favorable characteristics of cryogenic helium-4 in fluid mechanics, in situ fluid property measurements and special care on thermometry and calorimetric instrumentation. The cell is cylindrical with diameter/height=0.5. The effective heat transfer Nu (Ra, Pr) has been measured with unprecedented accuracy for cryogenic turbulent convection experiments in this range of Rayleigh numbers. Spin-off of this study	Not directly related to LNG rollover; however, has reviewed the effect of Pr and Ra in turbulent systems

				includes improved fits of helium thermodynamics and viscosity properties. Three main results were found. First, the Nu(Ra) dependence exhibits a bimodality of the flow with 4–7% difference in Nu for a given Ra and Pr. Second, a systematic study of the side-wall influence reveals a measurable effect on the heat transfer. Third, the Nu (Pr) dependence is very small or null: the absolute value of the average logarithmic slope $(d \ln Nu/d \ln Pr)_{Ra}$ is smaller than 0.03 in our range of Pr, which allows discriminating between experiments with contradictory results.	
15	2006	Modelling and Simulation of Rollover IN LNG STORAGE TANKS	A. Bashiri L. Fatehnejad	This paper gives none adequate theoretical framework for rollover analysis and presents quantitative computer results for the simulation of the La Spezia Rollover incident. Therewith some recommendations have been proposed in order to minimize the risk of	Limitations: 1: No model has been shown in the paper 2: Repeated Heestand result using SRK VLE to calculate physical properties

				rollover incident in refrigerated LNG storage tank.	
16	2006	LNG Rollover: CONVERTING A Safety PROBLEM to Tank Loading OPERATIONAL Asset	Y. Wang B. Cormier H.H. West	LNG rollover predictive models are widely used tools in conjunction with internal tank travelling temperature and density instrumentation to predict and update the behavior of LNG stratification. Several proprietary and commercial rollover software models are identified and the potential use of Computational Fluid Dynamics (CFD) models for the non-circular tanks proposed for off-shore applications is described in this paper.	Recommendation of CFD modeling over conventional lumped parameter methods.
17	2007	Rollover instability due to double diffusion in a stably stratified cylindrical tank	W. B. Zimmerman J. M. Rees	Double diffusion of a viscous fluid is simulated for heat leakage driven by buoyant convection under cryogenic storage conditions in a cylindrical tank with laminar flow. If the tank is stably stratified, There is a potential instability due to the inability of the fluid in the lower layer to release heat to the top vapor space, whereas the upper liquid layer can exchange heat and	1: Further discussion on Rayleigh number 2: Introduced a distributed model based on Shi paper.

| | | | | mass through sensible heat transfer and evaporation with the vapor space. Eventually, the lower layer becomes less dense due to thermal expansion and is no longer constrained in the stratification. The rapid rise and overturning of the fluid is termed rollover and can be accompanied by a potentially explosive release of vapor. | |
| | | | | In this paper, hydrodynamics and heat and mass transport are used to study the stability characteristics of rollover. The transient state is used as a base state for a linear stability analysis which shows the transition from a "corner eddy" mode spinning down to spinning up is the driver for the rollover instability. Four different vapor-liquid interfacial boundary conditions are tested, with similar results for the time to rollover. Surprisingly, the longtime pre-rollover state is dominated in the laminar flow regime by heat conduction and diffusion, as the expected | |

				double roll structure is suppressed and advection plays a small role in the majority of the pre-rollover period. Scalings are suggested for controlling dimensionless groups on this pre-rollover basis that can be used as a guideline to determine the regime of double diffusion, as well as the severity of the eventual rollover event. An energy analysis demonstrates the switch from practically advection free to free convection regimes.	
18	2008	CFD Simulation on LNG Storage Tank to Improve Safety and Reduce Cost	K. KOYAMA	When a storage tank containing LNG (Liquefied Natural Gas) is further filled with different-density LNG, stratification may occur. It occasionally results in rollover accompanied by a sudden release of large amounts of BOG (Boil-off Gas), which causes a rapid tank-pressure rise and sometimes damage to the tank. In this paper, we study on tank filling procedures with different-density LNG by using CFD (Computational Fluid Dynamics)	Used CFD model to simulate LNG tank filling procedures with different density LNGs

				simulation, in order to improve safety and reduce LNG storage costs. The calculated results of a developed numerical model agree well with the measured data. A case study on the filling of a small tank indicates that the initial density difference, the initial LNG depth and the filling rate affect the final density difference that is the density difference at the end of the filling that will directly be related to stratification.	
19	2010	Synthesis of Unloading Operation Procedure for a Mixed Operation of Above-Ground and In-Ground Liquefied Natural Gas Storage Tanks Using Dynamic Simulation	C. J. Lee Y. Lim C. Park S. Lee C. Han	Because of increased liquefied natural gas (LNG) demand, the operation of LNG receiving terminals having both above ground and in-ground LNG storage tanks will soon be required. In such cases, there exists a pressure head difference between the two types of tanks. As such, during the depressurization step of LNG unloading, vapor can be generated at the top of the unloading pipeline of the above-ground tank due to pressure head.	Unloading Operation Procedure for LNG and BOG generation during unloading.

				The vapour produced in a branch pipeline of the above-ground tank can thereby cause congestion during depressurization, resulting in a pressure difference across the unloading valve. This can, in turn, cause excessive boil-off gas inflow into the storage tank. In this paper, we suggest a reliable unloading operation procedure for a mixed operation of aboveground and in-ground storage tanks using dynamic simulation.	
20	2010	Calculation models for prediction of Liquefied Natural Gas (LNG) ageing during ship transportation	M. Miana R.D. Hoyo V. Rodrigalvarez J. R. Valdés R. Llorens	A group of European gas transportation companies within the European Gas Research Group launched in 2007 the 'MOLAS' Project to provide a software program for the analysis of the Liquefied Natural Gas (LNG) ageing process during ship transportation. This program contains two different modeling approaches: a physical algorithm and an 'intelligent' model. Both models are fed with the same input data, which is composed of the ship characteristics	Models for predicting LNG ageing during shipping referred to Bates and Morrison model for LNG rollover

| | | | | (BOR and capacity), voyage duration, LNG composition, temperature, pressure and volume occupied by liquid phase at the port of origin, together with pressure at the port of destination. The results obtained are the LNG composition, temperature and liquid volume at the port of destination. Furthermore, the physical model obtains the evolution over time of such variables en route as it is based on unsteady mass balances over the system, while the i-model applies neural networks to obtain regression coefficients from historical data composed only of origin and destination measurements. This paper describes both models and validates them from previously published models and experimental data measured in ENAGAS LNG regasification plants. | |

Appendix 5:

Copyright permissions, which have been granted from the following Journals/associations:

1. AIChE Journal
2. ASME
3. BG Group
4. IChemE
5. IGC
6. Linde
7. Pipeline and Gas Journal
8. Science Direct - Elsevier
9. Springer
10. The University of Western Australia (UWA)

AIChE Journal:

(8/01/2016)

AIChE Journal; *120 Wall Street, FL 23 New York, NY 10005-4020*

Dear **Mr. Steve Smith, Publications Director**

Email: steps@aiche.org

It is my understanding that you/your organisation are the copyright holder for the following material:

1. Arjomandnia P., M. O. Tade, V. Pareek, E. F. May; Analysis of available data from liquefied natural gas rollover incidents to determine critical stability ratios, AIChE Journal, Jan 2014 Vol. 60, No. 1
2. Heestand, J. and C. W. Shipman, "A Predictive Model for Rollover in Stratified LNG Tanks", AIChE Journal, Vol. 29, No.2, Page 199, March 1983.
3. Wang Y., B. Cormier, H.H. West, LNG Rollover Safety to Tank Loading Asset, AIChE Spring Conference, April 2006.

I would like to reproduce an extract of this work in a doctoral thesis which I am currently undertaking at Curtin University in Perth, Western Australia. The subject of my research is **LNG rollover simulation**. I am carrying out this research in my own right and have no association with any commercial organisation or sponsor.

The specific material / extract that I would like to use for the purposes of the thesis is **photos, graphs and abstract text.**

Once completed, the thesis will be made available in online form via Curtin University's Institutional Repository espace@Curtin (http://espace.library.curtin.edu.au). The material will be provided strictly for educational purposes and on a non-commercial basis.

I would be most grateful for your consent to the copying and communication of the work as proposed. If you are willing to grant this consent, please complete and sign the attached approval slip and return it to me at the address shown. Full acknowledgement of the ownership of the copyright and the source of the material will be provided with the material.

If you are not the copyright owner of the material in question, I would be grateful for any information you can provide as to who is likely to hold the copyright.

I look forward to hearing from you and thank you in advance for your consideration of my request.

Yours sincerely

Pooya Arjomandnia

PhD Candidate Curtin University

PERMISSION TO USE COPYRIGHT MATERIAL AS SPECIFIED BELOW:

1. Arjomandnia P., M. O. Tade, V. Pareek, E. F. May; Analysis of available data from liquefied natural gas rollover incidents to determine critical stability ratios, AIChE Journal, Jan 2014 Vol. 60, No. 1
2. Heestand, J. and C. W. Shipman, "A Predictive Model for Rollover in Stratified LNG Tanks", AIChE Journal, Vol. 29, No.2, Page 199, March 1983.
3. Wang Y., B. Cormier, H.H. West, LNG Rollover Safety to Tank Loading Asset, AIChE Spring Conference, April 2006.

I hereby give permission for **Pooya Arjomandnia** to include the abovementioned material(s) in his/her higher degree thesis for Curtin University, and to communicate this material via the espace@Curtin institutional repository. This permission is granted on a non-exclusive basis and for an indefinite period.

I confirm that I am the copyright owner of the specified material.

Signed: *[signature]*

Name: Stephen R. Smith

Position: Director, Publications

Date: Jan. 8, 2016

Please return signed form to:

Pooya Arjomandnia, PhD Candidate,

School of Chemical Engineering, Curtin University WA Australia

ASME Journal:

Dear Prof. Arjomandnia:

It is our pleasure to grant you permission to use ASME paper "Natural Convection Heat Transfer in Liquid Confined by Two Horizontal Plates and Heated from Below," by S. Globe and D. Dropkin, J. Heat Transfer, 81, 1959,, cited in your letter for inclusion in a doctoral thesis to be published by Curtin University.

Permission is granted for the specific use as stated herein and does not permit further use of the materials without proper authorization. Proper attribution must be made to the author(s) of the materials. As is customary, we request that you ensure full acknowledgment of this material, the author(s), source and ASME as original publisher. Acknowledgment must be retained on all pages printed and distributed.

Many thanks for your interest in ASME publications.

Sincerely,

Beth Darchi
Publishing Administrator
ASME
2 Park Avenue, 6th Floor
New York, NY 10016-5990

Tel 1.212.591.7700

darchib@asme.org

BG Group:

Hi Pooya

Yes, this email can be used as a record for permission to reuse the materials.

Regards
Janice

Good morning Janice

Is this one acceptable?

Regards
Pooya

Sent from my iPhone

On 19 Feb 2016, at 3:55 PM, Blomley, Kim <Kim.Blomley@bg-group.com> wrote:

Approved

Best
Kim

Hi Again Kim,

I've talked to our librarian and she told me if you re-approve this email with the following text, I can use it in my thesis.
If possible, please kindly reply this email with your approval.
Sorry for any inconvenience and many thanks in advance.

Kind Regards
Pooya

(19/02/2016)
BG Group plc
100 Thames Valley Park Drive, Reading, Berkshire, RG6 1PT, United Kingdom

Dear **Sir,**
Email: box.info@bg-group.com

It is my understanding that you/your organisation are the copyright holder for the following material:

- **Global LNG Market Outlook 2014-2015, Forecast: Growing Supply and Increasing Market Volatility**

  Available at:

http://www.bg-group.com/~/tiles/?tiletype=infographic&id=593#opentile

I would like to reproduce an extract of this work in a doctoral thesis which I am currently undertaking at Curtin University in Perth, Western Australia. The subject of my research is **LNG rollover simulation**. I am carrying out this research in my own right and have no association with any commercial organisation or sponsor.

The specific material / extract that I would like to use for the purposes of the thesis are **photos, graphs and abstract text.**

Once completed, the thesis will be made available in online form via Curtin University's Institutional Repository espace@Curtin (http://espace.library.curtin.edu.au). The material will be provided strictly for educational purposes and on a non-commercial basis.

I would be most grateful for your consent to the copying and communication of the work as proposed. If you are willing to grant this consent, please complete and sign the attached approval slip and return it to me at the address shown. Full acknowledgement of the ownership of the copyright and the source of the material will be provided with the material.

If you are not the copyright owner of the material in question, I would be grateful for any information you can provide as to who is likely to hold the copyright.

I look forward to hearing from you and thank you in advance for your consideration of my request.

Yours sincerely
Pooya Arjomandnia
PhD Candidate Curtin University

PERMISSION TO USE COPYRIGHT MATERIAL AS SPECIFIED BELOW:
- **Global LNG Market Outlook 2014-2015, Forecast: Growing Supply and Increasing Market Volatility**

Available at:
http://www.bg-group.com/~/tiles/?tiletype=infographic&id=593#opentile

I hereby give permission for **Pooya Arjomandnia** to include the above mentioned material(s) in his/her higher degree thesis for Curtin University, and to communicate this material via the

espace@Curtin institutional repository. This permission is granted on a non-exclusive basis and for an indefinite period.
I confirm that I am the copyright owner of the specified material.

Signed:
Name:
Position:
Date:

Please return signed form to:
Pooya Arjomandnia, PhD Candidate,
School of Chemical Engineering, Curtin University WA Australia

---

From: Blomley, Kim <Kim.Blomley@bg-group.com>
Sent: Thursday, 11 February 2016 4:52 PM
To: Pooya Arjomandnia; Bates, Toby (Fircroft); Johnston, Lachlan
Subject: Re: [External] URGENT - Permission request to use material in PhD thesis

Dear Pooya

Fine by BG.

Best
Kim

IChemE:

Dear **Sir,**

Email: customerservices@icheme.org

It is my understanding that you/your organisation are the copyright holder for the following material:

- **Baker N., Creed M., Stratification and rollover in liquefied natural gas storage tanks. Trans IChemE. 1996, 74 (Part B), Page:25–30**

I would like to reproduce an extract of this work in a doctoral thesis which I am currently undertaking at Curtin University in Perth, Western Australia. The subject of my research is **LNG rollover simulation**. I am carrying out this research in my own right and have no association with any commercial organisation or sponsor.

The specific material / extract that I would like to use for the purposes of the thesis is **photos, graphs and abstract text.**

Once completed, the thesis will be made available in online form via Curtin University's Institutional Repository espace@Curtin (http://espace.library.curtin.edu.au). The material will be provided strictly for educational purposes and on a non-commercial basis.

I would be most grateful for your consent to the copying and communication of the work as proposed. If you are willing to grant this consent, please complete and sign the attached approval slip and return it to me at the address shown. Full acknowledgement of the ownership of the copyright and the source of the material will be provided with the material.

If you are not the copyright owner of the material in question, I would be grateful for any information you can provide as to who is likely to hold the copyright.

I look forward to hearing from you and thank you in advance for your consideration of my request.

Yours sincerely

Pooya Arjomandnia

PhD Candidate Curtin University

PERMISSION TO USE COPYRIGHT MATERIAL AS SPECIFIED BELOW:

- Baker N., Creed M., Stratification and rollover in liquefied natural gas storage tanks. Trans IChemE. 1996, 74 (Part B), Page:25–30

I hereby give permission for **Pooya Arjomandnia** to include the abovementioned material(s) in his/her higher degree thesis for Curtin University, and to communicate this material via the espace@Curtin institutional repository. This permission is granted on a non-exclusive basis and for an indefinite period.

I confirm that 'The Institution of Chemical Engineers' are the copyright owner of the specified material.

Signed: *Catherine Cliffe*

Name: Catherine Cliffe

Position: Managing Editor

Date: 14/1/16

Please return signed form to:

Pooya Arjomandnia, PhD Candidate,

School of Chemical Engineering, Curtin University WA Australia

RE: Request for permission - IChemE

Catherine Cliffe <CCliffe@icheme.org>

Thu 14/01/2016 9:11 PM

To: Pooya Arjomandnia <pooya.arjomandnia@curtin.edu.au>;

📎 1 attachment (16 KB)

HDR_Students_Permission_Request IChemE (2).docx;

Dear Pooya,

I have now been able to locate the original article and am happy to grant permission for you to use the material specified in the intended way. Please just make sure the original source is fully cited and the copyright holder, The Institution of Chemical Engineers, acknowledged.

Best wishes,

Catherine

Catherine Cliffe
Managing editor
Institution of Chemical Engineers (IChemE)
+44 (0)1788 534441
+44 (0)7785 618518
[ccliffe@icheme.org]ccliffe@icheme.org
www.icheme.org
Kuala Lumpur | London | Melbourne | Rugby | Singapore | Wellington

Submit to IChemE's journals online via www.icheme.org/journals

---

From: Pooya Arjomandnia [mailto:pooya.arjomandnia@curtin.edu.au]
Sent: 14 January 2016 04:27
To: Catherine Cliffe
Subject: Fw: Request for permission – IChemE

Hi again Catherine,

Any feedback on the progress of my permission request?
I appreciate if you would kindly sign ans send back the attached form.

Kind regards
Pooya

From: Pooya Arjomandnia
Sent: Tuesday, 12 January 2016 8:12 AM
To: Catherine Cliffe
Subject: Re: Request for permission - IChemE

Dear Catherine,

Thank you very much for your reply.
The material I need is :
Baker N., Creed M., Stratification and rollover in liquefied natural gas storage tanks. Trans IChemE. 1996, 74 (Part B), Page:25–30

I want to use some of its data for my new simulation and reference to some of its tables and graphs for my PhD thesis. I will reference to the original paper in my thesis properly as well.
I appreciate if you grand me the permission and sign and send me back the attached form please.
Many thanks in advance.

Regards
Pooya

241

International Gas Conference (IGC):

(18/01/2016)

IGU, Office of the Secretary General, c/o Statoil, PO Box 3
1330 Fornebu, Norway

Dear **Sir**,

Email: secrigu@statoil.com

It is my understanding that you/your organisation are the copyright holder for the following material:

- **Development of the World's largest above ground full containment LNG storage tank**, Yang Y. M., J. H. Kim, H. S. Seo, K. Lee, I. Yoon, 23rd World Gas Conference, Amsterdam 2006.

I would like to reproduce an extract of this work in a doctoral thesis which I am currently undertaking at Curtin University in Perth, Western Australia. The subject of my research is **LNG rollover simulation**. I am carrying out this research in my own right and have no association with any commercial organisation or sponsor.

The specific material / extract that I would like to use for the purposes of the thesis is **photos, graphs and abstract text.**

Once completed, the thesis will be made available in online form via Curtin University's Institutional Repository espace@Curtin (http://espace.library.curtin.edu.au). The material will be provided strictly for educational purposes and on a non-commercial basis.

I would be most grateful for your consent to the copying and communication of the work as proposed. If you are willing to grant this consent, please complete and sign the attached approval slip and return it to me at the address shown. Full acknowledgement of the ownership of the copyright and the source of the material will be provided with the material.

If you are not the copyright owner of the material in question, I would be grateful for any information you can provide as to who is likely to hold the copyright.

I look forward to hearing from you and thank you in advance for your consideration of my request.

Yours sincerely

Pooya Arjomandnia

PhD Candidate Curtin University

PERMISSION TO USE COPYRIGHT MATERIAL AS SPECIFIED BELOW:

- Development of the World's largest above ground full containment LNG storage tank, Yang Y. M., J. H. Kim, H. S. Seo, K. Lee, I. Yoon, 23rd World Gas Conference, Amsterdam 2006.

I hereby give permission for **Pooya Arjomandnia** to include the abovementioned material(s) in his/her higher degree thesis for Curtin University, and to communicate this material via the espace@Curtin institutional repository. This permission is granted on a non-exclusive basis and for an indefinite period. The user should describe the source with proper citation and referring.

I hereby clarify the IGU Standard Copyright policy, and give permission of the usage for the above mentioned material; "This publication is produced under the auspices of INTERNATIONAL GAS UNION (IGU) by the Author(s) mentioned. The Author(s) and IGU enjoy joint copyright to this publication. This publication may not be reproduced in whole or in part without the written permission of the above mentioned holders of the copyright. However, irrespective of the above, established journals and periodicals shall be permitted to reproduce this publication or part of it, in abbreviated or edited form, provided that credit is given to the Author(s) and IGU."

Signed: *Taeksang Kwon*

Name: Taeksang Kwon

Position: Advisor, IGU

Date: 26 January 2016/ OSLO , NORWAY

Please return signed form to:

Pooya Arjomandnia, PhD Candidate,

School of Chemical Engineering, Curtin University WA Australia

Linde:

Fw: Permission to use Linde MSDS in my doctoral thesis

Pooya Arjomandnia

Mon 11/01/2016 9:55 AM

To: Pooya Arjomandnia <arjomandnia@yahoo.com>;

From: keith.martin@linde.com <keith.martin@linde.com> on behalf of sales.lg.us@linde.com <sales.lg.us@linde.com>
Sent: Monday, 4 January 2016 9:40 PM
To: Pooya Arjomandnia
Subject: Re: Permission to use Linde MSDS in my doctoral thesis

You have our permission

From:	Pooya Arjomandnia <pooya.arjomandnia@curtin.edu.au>
To:	"sales.lg.us@linde.com" <sales.lg.us@linde.com>
Date:	01/04/2016 01:16 AM
Subject:	Permission to use Linde MSDS in my doctoral thesis

Hi,

My name is Pooya Arjomandnia. I have done my research on LNG subject and I need your permission to use Linde MSDS in my doctoral thesis.

http://lindelng.com/pdf/LindeLNG_msds_un1972.pdf

Liquefied Natural Gas - lindelng.com

lindelng.com

1. PRODUCT AND COMPANY IDENTIFICATION Product Name Liquefied Natural Gas UN-Number UN1972 Recommended Use Industrial use. Synonyms LNG Supplier Address* Linde Gas ...

Please kindly reply back if I can copy your MSDS as a part of my thesis appendix, with referencing to your website.

Kind regards
Pooya Arjomandnia

Pipeline and Gas Journal:

(8/01/2016)

Pipeline and Gas journal, 1160 Dairy Ashford Rd., Suite 610, Houston, TX 77079
281-558-6930

Dear **Mr. Oliver Klinger**

Email: oklinger@oildom.com

     rtubb@oildom.com

It is my understanding that you/your organisation are the copyright holder for the following material:

1. Sarsten, J.S., "LNG Stratification and Rollover", Pipeline and Gas Journal, 199, Page: 37-42, 1972
2. Chatterjee, N. and J. M. Geist, "The Effects of Stratification on Boil-off Rate in LNG Tanks", Pipeline and Gas Journal, Vol. 99, Page 40, 1972.

I would like to reproduce an extract of this work in a doctoral thesis which I am currently undertaking at Curtin University in Perth, Western Australia. The subject of my research is **LNG rollover simulation**. I am carrying out this research in my own right and have no association with any commercial organisation or sponsor.

The specific material / extract that I would like to use for the purposes of the thesis is **photos, graphs and abstract text.**

Once completed, the thesis will be made available in online form via Curtin University's Institutional Repository espace@Curtin (http://espace.library.curtin.edu.au). The material will be provided strictly for educational purposes and on a non-commercial basis.

I would be most grateful for your consent to the copying and communication of the work as proposed. If you are willing to grant this consent, please complete and sign the attached approval slip and return it to me at the address shown. Full acknowledgement of the ownership of the copyright and the source of the material will be provided with the material.

If you are not the copyright owner of the material in question, I would be grateful for any information you can provide as to who is likely to hold the copyright.

I look forward to hearing from you and thank you in advance for your consideration of my request.

Yours sincerely

Pooya Arjomandnia

PhD Candidate Curtin University

PERMISSION TO USE COPYRIGHT MATERIAL AS SPECIFIED BELOW:

1. Sarsten, J.S., "LNG Stratification and Rollover", Pipeline and Gas Journal, 199, Page: 37-42, 1972
2. Chatterjee, N. and J. M. Geist, "The Effects of Stratification on Boil-off Rate in LNG Tanks", Pipeline and Gas Journal, Vol. 99, Page 40, 1972.

I hereby give permission for **Pooya Arjomandnia** to include the abovementioned material(s) in his/her higher degree thesis for Curtin University, and to communicate this material via the espace@Curtin institutional repository. This permission is granted on a non-exclusive basis and for an indefinite period.

I confirm that I am the copyright owner of the specified material.

Signed:

Name: *Cleve Hogarth*

Position: *Managing Publisher*

Date: *Jan 8, 2016*

Please return signed form to:

Pooya Arjomandnia, PhD Candidate,

School of Chemical Engineering, Curtin University WA Australia

Science Direct - Elsevier:

ELSEVIER LICENSE
TERMS AND CONDITIONS

Jan 12, 2016

This is a License Agreement between Pooya Arjomandnia ("You") and Elsevier ("Elsevier") provided by Copyright Clearance Center ("CCC"). The license consists of your order details, the terms and conditions provided by Elsevier, and the payment terms and conditions.

All payments must be made in full to CCC. For payment instructions, please see information listed at the bottom of this form.

Supplier	Elsevier Limited The Boulevard,Langford Lane Kidlington,Oxford,OX5 1GB,UK
Registered Company Number	1982084
Customer name	Pooya Arjomandnia
Customer address	School of Chemical Engineering
	Bentley, WA 6102
License number	3786840725804
License date	Jan 12, 2016
Licensed content publisher	Elsevier
Licensed content publication	International Journal of Heat and Mass Transfer
Licensed content title	The coupled turbulent transports of salt and and heat across a sharp density interface
Licensed content author	J.S. Turner
Licensed content date	May 1965
Licensed content volume number	8
Licensed content issue number	5
Number of pages	9
Start Page	759
End Page	767
Type of Use	reuse in a thesis/dissertation
Intended publisher of new work	other
Portion	full article
Format	both print and electronic
Are you the author of this Elsevier article?	No
Will you be translating?	No
Title of your thesis/dissertation	Simulation of LNG rollover
Expected completion date	Jul 2016
Estimated size (number of pages)	180

Elsevier VAT number	GB 494 6272 12
Permissions price	0.00 USD
VAT/Local Sales Tax	0.00 USD / 0.00 GBP
Total	0.00 USD

Terms and Conditions

INTRODUCTION

1. The publisher for this copyrighted material is Elsevier. By clicking "accept" in connection with completing this licensing transaction, you agree that the following terms and conditions apply to this transaction (along with the Billing and Payment terms and conditions established by Copyright Clearance Center, Inc. ("CCC"), at the time that you opened your Rightslink account and that are available at any time at http://myaccount.copyright.com).

GENERAL TERMS

2. Elsevier hereby grants you permission to reproduce the aforementioned material subject to the terms and conditions indicated.

3. Acknowledgement: If any part of the material to be used (for example, figures) has appeared in our publication with credit or acknowledgement to another source, permission must also be sought from that source. If such permission is not obtained then that material may not be included in your publication/copies. Suitable acknowledgement to the source must be made, either as a footnote or in a reference list at the end of your publication, as follows:

"Reprinted from Publication title, Vol /edition number, Author(s), Title of article / title of chapter, Pages No., Copyright (Year), with permission from Elsevier [OR APPLICABLE SOCIETY COPYRIGHT OWNER]." Also Lancet special credit - "Reprinted from The Lancet, Vol. number, Author(s), Title of article, Pages No., Copyright (Year), with permission from Elsevier."

4. Reproduction of this material is confined to the purpose and/or media for which permission is hereby given.

5. Altering/Modifying Material: Not Permitted. However figures and illustrations may be altered/adapted minimally to serve your work. Any other abbreviations, additions, deletions and/or any other alterations shall be made only with prior written authorization of Elsevier Ltd. (Please contact Elsevier at permissions@elsevier.com)

6. If the permission fee for the requested use of our material is waived in this instance, please be advised that your future requests for Elsevier materials may attract a fee.

7. Reservation of Rights: Publisher reserves all rights not specifically granted in the combination of (i) the license details provided by you and accepted in the course of this licensing transaction, (ii) these terms and conditions and (iii) CCC's Billing and Payment terms and conditions.

8. License Contingent Upon Payment: While you may exercise the rights licensed immediately upon issuance of the license at the end of the licensing process for the transaction, provided that you have disclosed complete and accurate details of your proposed use, no license is finally effective unless and until full payment is received from you (either by publisher or by CCC) as provided in CCC's Billing and Payment terms and conditions. If full payment is not received on a timely basis, then any license preliminarily granted shall be deemed automatically revoked and shall be void as if never granted. Further, in the event that you breach any of these terms and conditions or any of CCC's Billing and Payment terms and conditions, the license is automatically revoked and shall be void as if never granted. Use of materials as described in a revoked license, as well as any use of the materials beyond the scope of an unrevoked license, may constitute copyright infringement and publisher reserves the right to take any and all action to protect its copyright in the materials.

9. Warranties: Publisher makes no representations or warranties with respect to the licensed

248

material.

10. Indemnity: You hereby indemnify and agree to hold harmless publisher and CCC, and their respective officers, directors, employees and agents, from and against any and all claims arising out of your use of the licensed material other than as specifically authorized pursuant to this license.

11. No Transfer of License: This license is personal to you and may not be sublicensed, assigned, or transferred by you to any other person without publisher's written permission.

12. No Amendment Except in Writing: This license may not be amended except in a writing signed by both parties (or, in the case of publisher, by CCC on publisher's behalf).

13. Objection to Contrary Terms: Publisher hereby objects to any terms contained in any purchase order, acknowledgment, check endorsement or other writing prepared by you, which terms are inconsistent with these terms and conditions or CCC's Billing and Payment terms and conditions. These terms and conditions, together with CCC's Billing and Payment terms and conditions (which are incorporated herein), comprise the entire agreement between you and publisher (and CCC) concerning this licensing transaction. In the event of any conflict between your obligations established by these terms and conditions and those established by CCC's Billing and Payment terms and conditions, these terms and conditions shall control.

14. Revocation: Elsevier or Copyright Clearance Center may deny the permissions described in this License at their sole discretion, for any reason or no reason, with a full refund payable to you. Notice of such denial will be made using the contact information provided by you. Failure to receive such notice will not alter or invalidate the denial. In no event will Elsevier or Copyright Clearance Center be responsible or liable for any costs, expenses or damage incurred by you as a result of a denial of your permission request, other than a refund of the amount(s) paid by you to Elsevier and/or Copyright Clearance Center for denied permissions.

LIMITED LICENSE

The following terms and conditions apply only to specific license types:

15. **Translation**: This permission is granted for non-exclusive world **English** rights only unless your license was granted for translation rights. If you licensed translation rights you may only translate this content into the languages you requested. A professional translator must perform all translations and reproduce the content word for word preserving the integrity of the article.

16. **Posting licensed content on any Website**: The following terms and conditions apply as follows: Licensing material from an Elsevier journal: All content posted to the web site must maintain the copyright information line on the bottom of each image; A hyper-text must be included to the Homepage of the journal from which you are licensing at http://www.sciencedirect.com/science/journal/xxxxx or the Elsevier homepage for books at http://www.elsevier.com; Central Storage: This license does not include permission for a scanned version of the material to be stored in a central repository such as that provided by Heron/XanEdu.

Licensing material from an Elsevier book: A hyper-text link must be included to the Elsevier homepage at http://www.elsevier.com . All content posted to the web site must maintain the copyright information line on the bottom of each image.

Posting licensed content on Electronic reserve: In addition to the above the following clauses are applicable: The web site must be password-protected and made available only to bona fide students registered on a relevant course. This permission is granted for 1 year only. You may obtain a new license for future website posting.

17. **For journal authors:** the following clauses are applicable in addition to the above:
Preprints:
A preprint is an author's own write-up of research results and analysis, it has not been peer-reviewed, nor has it had any other value added to it by a publisher (such as formatting, copyright, technical enhancement etc.).

249

Authors can share their preprints anywhere at any time. Preprints should not be added to or enhanced in any way in order to appear more like, or to substitute for, the final versions of articles however authors can update their preprints on arXiv or RePEc with their Accepted Author Manuscript (see below).

If accepted for publication, we encourage authors to link from the preprint to their formal publication via its DOI. Millions of researchers have access to the formal publications on ScienceDirect, and so links will help users to find, access, cite and use the best available version. Please note that Cell Press, The Lancet and some society-owned have different preprint policies. Information on these policies is available on the journal homepage.

Accepted Author Manuscripts: An accepted author manuscript is the manuscript of an article that has been accepted for publication and which typically includes author-incorporated changes suggested during submission, peer review and editor-author communications.

Authors can share their accepted author manuscript:

- immediately
  - via their non-commercial person homepage or blog
  - by updating a preprint in arXiv or RePEc with the accepted manuscript
  - via their research institute or institutional repository for internal institutional uses or as part of an invitation-only research collaboration work-group
  - directly by providing copies to their students or to research collaborators for their personal use
  - for private scholarly sharing as part of an invitation-only work group on commercial sites with which Elsevier has an agreement
- after the embargo period
  - via non-commercial hosting platforms such as their institutional repository
  - via commercial sites with which Elsevier has an agreement

In all cases accepted manuscripts should:

- link to the formal publication via its DOI
- bear a CC-BY-NC-ND license - this is easy to do
- if aggregated with other manuscripts, for example in a repository or other site, be shared in alignment with our hosting policy not be added to or enhanced in any way to appear more like, or to substitute for, the published journal article.

Published journal article (JPA): A published journal article (PJA) is the definitive final record of published research that appears or will appear in the journal and embodies all value-adding publishing activities including peer review co-ordination, copy-editing, formatting, (if relevant) pagination and online enrichment.

Policies for sharing publishing journal articles differ for subscription and gold open access articles:

Subscription Articles: If you are an author, please share a link to your article rather than the full-text. Millions of researchers have access to the formal publications on ScienceDirect, and so links will help your users to find, access, cite, and use the best available version. Theses and dissertations which contain embedded PJAs as part of the formal submission can be posted publicly by the awarding institution with DOI links back to the formal publications on ScienceDirect.

If you are affiliated with a library that subscribes to ScienceDirect you have additional private sharing rights for others' research accessed under that agreement. This includes use for classroom teaching and internal training at the institution (including use in course packs and courseware programs), and inclusion of the article for grant funding purposes.

Gold Open Access Articles: May be shared according to the author-selected end-user license and should contain a CrossMark logo, the end user license, and a DOI link to the

formal publication on ScienceDirect.

Please refer to Elsevier's posting policy for further information.

18. **For book authors** the following clauses are applicable in addition to the above: Authors are permitted to place a brief summary of their work online only. You are not allowed to download and post the published electronic version of your chapter, nor may you scan the printed edition to create an electronic version. **Posting to a repository:** Authors are permitted to post a summary of their chapter only in their institution's repository.

19. **Thesis/Dissertation**: If your license is for use in a thesis/dissertation your thesis may be submitted to your institution in either print or electronic form. Should your thesis be published commercially, please reapply for permission. These requirements include permission for the Library and Archives of Canada to supply single copies, on demand, of the complete thesis and include permission for Proquest/UMI to supply single copies, on demand, of the complete thesis. Should your thesis be published commercially, please reapply for permission. Theses and dissertations which contain embedded PJAs as part of the formal submission can be posted publicly by the awarding institution with DOI links back to the formal publications on ScienceDirect.

Elsevier Open Access Terms and Conditions

You can publish open access with Elsevier in hundreds of open access journals or in nearly 2000 established subscription journals that support open access publishing. Permitted third party re-use of these open access articles is defined by the author's choice of Creative Commons user license. See our open access license policy for more information.

Terms & Conditions applicable to all Open Access articles published with Elsevier:

Any reuse of the article must not represent the author as endorsing the adaptation of the article nor should the article be modified in such a way as to damage the author's honour or reputation. If any changes have been made, such changes must be clearly indicated.

The author(s) must be appropriately credited and we ask that you include the end user license and a DOI link to the formal publication on ScienceDirect.

If any part of the material to be used (for example, figures) has appeared in our publication with credit or acknowledgement to another source it is the responsibility of the user to ensure their reuse complies with the terms and conditions determined by the rights holder.

Additional Terms & Conditions applicable to each Creative Commons user license:

CC BY: The CC-BY license allows users to copy, to create extracts, abstracts and new works from the Article, to alter and revise the Article and to make commercial use of the Article (including reuse and/or resale of the Article by commercial entities), provided the user gives appropriate credit (with a link to the formal publication through the relevant DOI), provides a link to the license, indicates if changes were made and the licensor is not represented as endorsing the use made of the work. The full details of the license are available at http://creativecommons.org/licenses/by/4.0.

CC BY NC SA: The CC BY-NC-SA license allows users to copy, to create extracts, abstracts and new works from the Article, to alter and revise the Article, provided this is not done for commercial purposes, and that the user gives appropriate credit (with a link to the formal publication through the relevant DOI), provides a link to the license, indicates if changes were made and the licensor is not represented as endorsing the use made of the work. Further, any new works must be made available on the same conditions. The full details of the license are available at http://creativecommons.org/licenses/by-nc-sa/4.0.

CC BY NC ND: The CC BY-NC-ND license allows users to copy and distribute the Article, provided this is not done for commercial purposes and further does not permit distribution of the Article if it is changed or edited in any way, and provided the user gives appropriate credit (with a link to the formal publication through the relevant DOI), provides a link to the license, and that the licensor is not represented as endorsing the use made of the work. The full details of the license are available at http://creativecommons.org/licenses/by-nc-nd/4.0.

Any commercial reuse of Open Access articles published with a CC BY NC SA or CC BY NC ND license requires permission from Elsevier and will be subject to a fee.

Commercial reuse includes:

- Associating advertising with the full text of the Article
- Charging fees for document delivery or access
- Article aggregation
- Systematic distribution via e-mail lists or share buttons

Posting or linking by commercial companies for use by customers of those companies.

20. Other Conditions:

v1.8

Questions? customercare@copyright.com or +1-855-239-3415 (toll free in the US) or +1-978-646-2777.

252

ELSEVIER LICENSE
TERMS AND CONDITIONS

Jan 12, 2016

This is a License Agreement between Pooya Arjomandnia ("You") and Elsevier ("Elsevier") provided by Copyright Clearance Center ("CCC"). The license consists of your order details, the terms and conditions provided by Elsevier, and the payment terms and conditions.

All payments must be made in full to CCC. For payment instructions, please see information listed at the bottom of this form.

Supplier	Elsevier Limited The Boulevard,Langford Lane Kidlington,Oxford,OX5 1GB,UK
Registered Company Number	1982084
Customer name	Pooya Arjomandnia
Customer address	School of Chemical Engineering
	Bentley, WA 6102
License number	3786840309771
License date	Jan 12, 2016
Licensed content publisher	Elsevier
Licensed content publication	Cryogenics
Licensed content title	Numerical modelling and flow visualization of mixing of stratified layers and rollover in LNG
Licensed content author	J.Q. Shi,C. Beduz,R.G. Scurlock
Licensed content date	December 1993
Licensed content volume number	33
Licensed content issue number	12
Number of pages	9
Start Page	1116
End Page	1124
Type of Use	reuse in a thesis/dissertation
Intended publisher of new work	other
Portion	full article
Format	both print and electronic
Are you the author of this Elsevier article?	No
Will you be translating?	No
Title of your thesis/dissertation	Simulation of LNG rollover
Expected completion date	Jul 2016
Estimated size (number of pages)	180

253

ELSEVIER LICENSE
TERMS AND CONDITIONS

Jan 12, 2016

This is a License Agreement between Pooya Arjomandnia ("You") and Elsevier ("Elsevier") provided by Copyright Clearance Center ("CCC"). The license consists of your order details, the terms and conditions provided by Elsevier, and the payment terms and conditions.

All payments must be made in full to CCC. For payment instructions, please see information listed at the bottom of this form.

Supplier	Elsevier Limited The Boulevard,Langford Lane Kidlington,Oxford,OX5 1GB,UK
Registered Company Number	1982084
Customer name	Pooya Arjomandnia
Customer address	School of Chemical Engineering
	Bentley, WA 6102
License number	3786840145524
License date	Jan 12, 2016
Licensed content publisher	Elsevier
Licensed content publication	Chemical Engineering Research and Design
Licensed content title	Application of inverse methods based algorithms to Liquefied Natural Gas (LNG) storage management
Licensed content author	M.W. Lukaszewski,W.B.J. Zimmerman,M.T. Tennant,M.B. Webster
Licensed content date	March 2013
Licensed content volume number	91
Licensed content issue number	3
Number of pages	7
Start Page	457
End Page	463
Type of Use	reuse in a thesis/dissertation
Intended publisher of new work	other
Portion	full article
Format	both print and electronic
Are you the author of this Elsevier article?	No
Will you be translating?	No
Title of your thesis/dissertation	Simulation of LNG rollover
Expected completion date	Jul 2016
Estimated size (number of pages)	180

254

ELSEVIER LICENSE
TERMS AND CONDITIONS

Jan 12, 2016

This is a License Agreement between Pooya Arjomandnia ("You") and Elsevier ("Elsevier") provided by Copyright Clearance Center ("CCC"). The license consists of your order details, the terms and conditions provided by Elsevier, and the payment terms and conditions.

All payments must be made in full to CCC. For payment instructions, please see information listed at the bottom of this form.

Supplier	Elsevier Limited The Boulevard,Langford Lane Kidlington,Oxford,OX5 1GB,UK
Registered Company Number	1982084
Customer name	Pooya Arjomandnia
Customer address	School of Chemical Engineering
	Bentley, WA 6102
License number	3786840546967
License date	Jan 12, 2016
Licensed content publisher	Elsevier
Licensed content publication	Chemical Engineering Journal
Licensed content title	Optimization methods for the real-time inverse problem posed by modelling of liquefied natural gas storage
Licensed content author	Kiran B. Deshpande,William B. Zimmerman,Malcolm T. Tennant,Marcus B. Webster,Michal W. Lukaszewski
Licensed content date	15 May 2011
Licensed content volume number	170
Licensed content issue number	1
Number of pages	9
Start Page	44
End Page	52
Type of Use	reuse in a thesis/dissertation
Intended publisher of new work	other
Portion	full article
Format	both print and electronic
Are you the author of this Elsevier article?	No
Will you be translating?	No
Title of your thesis/dissertation	Simulation of LNG rollover
Expected completion date	Jul 2016
Estimated size (number of	180

255

ELSEVIER LICENSE
TERMS AND CONDITIONS

Jan 12, 2016

This is a License Agreement between Pooya Arjomandnia ("You") and Elsevier ("Elsevier") provided by Copyright Clearance Center ("CCC"). The license consists of your order details, the terms and conditions provided by Elsevier, and the payment terms and conditions.

All payments must be made in full to CCC. For payment instructions, please see information listed at the bottom of this form.

Supplier	Elsevier Limited The Boulevard,Langford Lane Kidlington,Oxford,OX5 1GB,UK
Registered Company Number	1982084
Customer name	Pooya Arjomandnia
Customer address	School of Chemical Engineering Bentley, WA 6102
License number	3786840432863
License date	Jan 12, 2016
Licensed content publisher	Elsevier
Licensed content publication	International Journal of Heat and Mass Transfer
Licensed content title	Modelling the behaviour of stratified liquid natural gas in storage tanks: a study of the rollover phenomenon
Licensed content author	S. Bates,D.S. Morrison
Licensed content date	May 1997
Licensed content volume number	40
Licensed content issue number	8
Number of pages	10
Start Page	1875
End Page	1884
Type of Use	reuse in a thesis/dissertation
Intended publisher of new work	other
Portion	full article
Format	both print and electronic
Are you the author of this Elsevier article?	No
Will you be translating?	No
Title of your thesis/dissertation	Simulation of LNG rollover
Expected completion date	Jul 2016
Estimated size (number of pages)	180

256

Springer:

Material to be used: Figure 2 and 4

Your project
Requestor: Pooya Arjomandnia
                 pooya.arjomandnia@curtin.edu.au
University: Curtin University
Purpose: Dissertation/Thesis

With reference to your request to reuse material in which **Springer** controls the copyright, our permission is granted free of charge under the following conditions:

Springer material
- represents original material which does not carry references to other sources (if material in question refers with a credit to another source, authorization from that source is required as well);
- requires full credit (Springer book/journal title, chapter/article title, volume, year of publication, page, name(s) of author(s), original copyright notice) to the publication in which the material was originally published by adding: "With permission of Springer";
- figures, illustrations, and tables may be altered minimally to serve your work. Any other abbreviations, additions, deletions and/or any other alterations shall be made only with prior written authorization of the author;
- Springer does not supply original artwork or content.

This permission
- is non-exclusive;
- is valid for one-time use only for the purpose of defending your thesis limited to university-use only and with a maximum of 100 extra copies in paper. If the thesis is going to be published, permission needs to be reobtained.
- includes use in an electronic form, provided it is an author-created version of the thesis on his/her own website and his/her university's repository, including UMI (according to the definition on the Sherpa website: http://www.sherpa.ac.uk/romeo/);
- is subject to courtesy information to the author (address is given in the publication);
- is personal to you and may not be sublicensed, assigned, or transferred by you to any other person without Springer's written permission;
- is only valid if no personal rights, trademarks, or competitive products are infringed.

This license is valid only when the conditions noted above are met.

Permission free of charge does not prejudice any rights we might have to charge for reproduction of our copyrighted material in the future.

Springer

PERMISSION LETTER

Rights and Permissions
Springer
Tiergartenstr. 17
69121 Heidelberg
Germany

Springer

PERMISSION LETTER

January 11, 2016

Springer reference

Systems Modeling and Simulation
pp 39-43
CFD Simulation on LNG Storage Tank to Improve Safety and Reduce Cost
Kazuo Koyama
© Springer 2007
DOI 10.1007/978-4-431-49022-7_8
Print ISBN 978-4-431-49021-0
Online ISBN 978-4-431-49022-7

Material to be used: Excerpts pp. 1, 2, 3 and 5

Advances in Cryogenic Engineering
Volume 21 of the series Advances in Cryogenic Engineering pp 326-336
A Model for LNG Tank Rollover
A. E. Germeles
© *Springer Science+Business Media New York 1960*
DOI 10.1007/978-1-4757-0208-8_42
Print ISBN 978-1-4757-0210-1
Online ISBN 978-1-4757-0208-8

Material to be used: Excerpts pp. 326-335

Your project

Requestor:	Pooya Arjomandnia
	pooya.arjomandnia@curtin.edu.au
University:	Curtin University
Purpose:	Dissertation/Thesis

With reference to your request to reuse material in which Springer controls the copyright, our permission is granted free of charge under the following conditions:

Springer material

- represents original material which does not carry references to other sources (if material in question refers with a credit to another source, authorization from that source is required as well);
- requires full credit (Springer book/journal title, chapter/article title, volume, year of publication, page, name(s) of author(s), original copyright notice) to the publication in which the material was originally published by adding: "With permission of Springer";
- may not be altered in any manner. Abbreviations, additions, deletions and/or any other alterations shall be made only with prior written authorization of the author;
- Springer does not supply original artwork or content.

This permission

- is non-exclusive;
- is valid for one-time use only for the purpose of defending your thesis and with a maximum of 100 extra copies in paper. If the thesis is going to be published, permission needs to be reobtained.
- includes use in an electronic form, provided it is an author-created version of the thesis on his/her own website and his/her university's repository, including UMI (according to the definition on the Sherpa website: http://www.sherpa.ac.uk/romeo/);

Springer

PERMISSION LETTER

- is subject to courtesy information to the co-author or corresponding author;
- is personal to you and may not be sublicensed, assigned, or transferred by you to any other person without Springer's written permission;
- is only valid if no personal rights, trademarks, or competitive products are infringed.

This license is valid only when the conditions noted above are met.

Permission free of charge does not prejudice any rights we might have to charge for reproduction of our copyrighted material in the future.

Rights and Permissions
Springer
Tiergartenstr. 17
69121 Heidelberg
Germany

UWA (Master thesis):

Re: Permission to reproduce an extract in a doctoral thesis

Pooya Arjomandnia

Thu 14/01/2016 12:32 PM

To: Repository - LIB <repository-lib@uwa.edu.au>;

Hi dear Kate,

Thanks for your reply.

Regards
Pooya

___

From: Repository - LIB <repository-lib@uwa.edu.au>
Sent: Wednesday, 13 January 2016 1:27 PM
To: Pooya Arjomandnia
Cc: Repository - LIB
Subject: RE: Permission to reproduce an extract in a doctoral thesis

Hi again Pooya,
Just to clarify you do <u>not</u> need to seek our permission to produce parts of your thesis.

Regards,
Kate

Kate Croker
Associate Manager (eResearch Support)
Workdays: Tuesday, Wednesday, Thursday
University Library • M209, Perth WA 6009 Australia
T +61 8 6488 4705 • **E** kate.croker@uwa.edu.au

___

From: Kate Croker
Sent: Wednesday, 13 January 2016 1:08 PM
To: pooya.arjomandnia@curtin.edu.au
Cc: Repository – LIB
Subject: FW: Permission to reproduce an extract in a doctoral thesis

Hi Pooya,

Apologies for my delay in replying to you.
I contacted our legal services and they advised that you do not need to seek our permission to reproduce sections of your Masters thesis as you are the copyright owner under UWA rules.
Please feel free to pass on my details to the Curtin officer requiring my signature if they would like to discuss this further.

Regards,
Kate
Kate Croker
Associate Manager (eResearch Support)
Workdays: Tuesday, Wednesday, Thursday
University Library • M209, Perth WA 6009 Australia
T +61 8 6488 4705 • **E** kate.croker@uwa.edu.au

___

From: Repository – LIB
Sent: Monday, 11 January 2016 8:03 AM
To: Kate Croker

261

Subject: FW: Permission to reproduce an extract in a doctoral thesis

---

From: Pooya Arjomandnia [mailto:pooya.arjomandnia@curtin.edu.au]
Sent: Friday, 8 January 2016 11:42 AM
To: Kate Croker; Repository – LIB
Subject: Re: Permission to reproduce an extract in a doctoral thesis

Hi again Kate,

Happy new year.
Curtin university library asked me to get a signature on the attached form.
Could you please kindly sign it for me (Page 2)?

Kindest regards
Pooya Arjomandnia

From: Kate Croker <kate.croker@uwa.edu.au>
Sent: Thursday, 24 September 2015 12:59 PM
To: Repository - LIB; Pooya Arjomandnia
Subject: RE: Permission to reproduce an extract in a doctoral thesis

Dear Pooya,

Thanks for contacting us about your thesis.
As the author of this thesis you are still the copyright holder and therefore do not need our permission to reproduce it in your PhD.
Just remember to acknowledge that you are reusing this work by citing it within your thesis.

If you had it published as a journal article or book/book chatper then you would need to contact the publisher for permission.

If you have any queries about this please let me know.

Regards,
Kate

Kate Croker
Associate Manager (eResearch Support)
Workdays: Tuesday, Wednesday, Thursday
University Library • M209, Perth WA 6009 Australia
T +61 8 6488 4705 • E kate.croker@uwa.edu.au

THE UNIVERSITY OF
WESTERN
AUSTRALIA

From: Pooya Arjomandnia [mailto:pooya.arjomandnia@curtin.edu.au]
Sent: Thursday, 24 September 2015 10:21 AM
To: Repository – LIB
Cc: Pooya Arjomandnia
Subject: Permission to reproduce an extract in a doctoral thesis

Hi,

My name is Pooya Arjomandnia. I was UWA postgrad student and did my master of engineering during 2007 – 2010. I am a PhD student at Curtin University at the moment. As my current research is continuation of my master's research, I would like to grant UWA's Permission to reproduce an extract of my master thesis in my doctoral thesis. I will reference to the previous work properly and will follow UWA's Theses and research publications copyright instruction.

My master thesis is available at:
http://research-repository.uwa.edu.au/en/publications/simulation-of-rollover-in-stratified-lng-storage-tanks(29fb0277-a778-49c0-9eb1-1fb51911006a).html
(Simulation of rollover in stratified LNG storage tanks)

If the permission is granted, Please kindly fill the second page of the attached from and return it to this email.
Thanks in advance.

Kind regards
Pooya Arjomandnia

References:

[1] Lemmon, E. W., M. L. Huberand M. O. McLinden, NIST Reference Fluid Thermodynamic and Transport Properties Database, NIST 23, (REFPROP), v8.0. 2007, National Institute of Standards and Technology: Gaithersburg, MD.

[2] http://au.mathworks.com

[3] Kunz O., Klimeck R., Wagner W., Jaeschke M., The GERG-2004 Wide-Range Equation of State for Natural Gases and Other Mixtures, VDI Verlag GmbH

[4] Bates, S., Morrison, D.S., Modelling the behaviour of stratified liquid natural gas in storage tank a study of the rollover phenomenon, Int journal of heat transfer, Vol. 40, No. 8, Page 1875-1884, 1997

[5] Turner, J. S., The Coupled Turbulent Transports of Salt and Heat across a Sharp Density Interface, International Journal of Heat Mass Transfer, 1965, vol.8, 759-767.

[6] Sarsten, J. S., "LNG Stratification and Rollover", Pipeline and Gas Journal, 199, Page: 37-42, 1972

[7] Arjomandnia P., M. O. Tade, V. Pareek, E. F. May; Analysis of available data from liquefied natural gas rollover incidents to determine critical stability ratios, AIChE Journal, Jan 2014 Vol. 60, No. 1

[8] Australian Government, The Department of Industry website:
http://www.industry.gov.au/resource/UpstreamPetroleum/AustralianLiquefied
NaturalGas/Pages/default.aspx

[9] Global LNG Market Outlook, BG Group, Singapore, 11th March 2015:
http://www.bg-group.com/~/tiles/?tiletype=news&id=771

[10] Mokhatab S., University of Wyoming & Michael J. Economides, University of Houston, World Oil Magazine, Feb 2006.

[11] Arjomandnia Pooya, Simulation of rollover in stratified LNG storage tanks, University of Western Australia, Perth 2010:
http://repository.uwa.edu.au/dtl_publish/Theses/47/13183.htm"

[12] Rojey A., C. Jaffret, Natural gas production, processing, transport, Technip edition, IFP publications,

[13] Yang Y. M., J. H. Kim, H. S. Seo, K. Lee, I. Yoon, "Development of the World's largest above ground full containment LNG storage tank", 23rd World Gas Conference, Amsterdam 2006.

[14] http://en.wikipedia.org/wiki/LNG_carrier

[15] Rice A., Rollover in volcanic crater lakes: a possible cause for Lake Nyos type disasters, Journal of Volcanology and Geothermal Research, Page 233–239, 2000.

[16] Chatterjee, N. and J. M. Geist, "The Effects of Stratification on Boil-off Rate in LNG Tanks", Pipeline and Gas Journal, Vol. 99, Page 40, 1972.

[17] Germeles, A. E., "A model for LNG tank Rollover", Advanced in Cryogenic Engineering, 21, 326, Plenum Press, 1975.

[18] Baker N., Creed M., Stratification and rollover in liquefied natural gas storage tanks. Trans IChemE. 1996, 74 (Part B), Page:25–30.

[19] Newton, C. L., Kinard, G. E, Liu Y. N., C3- MR Processes for Baseload Liquefied Natural Gas, Eight International conference on LNG, LA, California, June 15-19, 1986.

[20] Wang Y., B. Cormier, H.H. West, LNG Rollover Safety to Tank Loading Asset, AIChE Spring Conference, April 2006.

[21] Miana M., R. D. Hoyo, V. Rodrigalvarez, J. R. Valdes, R. Llorens, Calculation models for prediction of Liquefied Natural Gas (LNG) ageing during ship transportation, Applied Energy Vol. 87, 2010, Pages 1687–1700

[22] Rufford. T. E, S. Smart, G. C. Y. Watson, B.F. Graham, J. Boxall, J.C. Dinizda Costa, E. F. May, The removal of CO2 and N2 from natural gas: A review of conventional and emerging process technologies, Journal of Petroleum Science and Engineering, 94–95 2012, page 123–154

[23] The Wobbe Index and Natural Gas Interchangeability, Emerson Process Management, 2007-07-30,
http://www.documentation.emersonprocess.com/groups/public/documents/ap plication_notes tech._briefs/d301334x012.pdf

[24] Heestand, J. and C. W. Shipman, "A Predictive Model for Rollover in Stratified LNG Tanks", AIChE Journal, Vol. 29, No.2, Page 199, March 1983.

[24] Arjomandnia P., M. O. Tade, V. Pareek, E. F. May; Analysis of available data from liquefied natural gas rollover incidents to determine critical stability ratios, AIChE Journal, Jan 2014 Vol. 60, No. 1

[25] Deshpande Kiran B., William B. Zimmerman, Malcolm T. Tennant, Marcus B. Webster, Michal W. Lukaszewski, "Optimization methods for the real–time inverse problem posed by modelling of liquefied natural gas storage", Chemical Engineering Journal Vol. 170, 2011, pages 44–52.

[26] Temam, R., Navier-Stokes equations: theory and numerical analysis, Studies in Mathematics and its Applications, 1977, North Holland publishing company, Amsterdam Nederland.

[27] Introduction to CFD Methodology, Lecture 2, ANSYS, Inc., 2010
 http://imechanica.org/files/fluent_13.0_lecture02-intro-to-cfd.pdf

[28] McAdams W. H., Heat transmission, 3rd ed., Chapter 7, 1954, McGraw Hill Book Co., New York

[29] Globe S., D. Dropkin, Natural convection heat transfer in liquids confined by two horizontal plates and heated from below, Trans. ASME journal heat trans. C81, 24 (1959)

[30] Soave, G., Equilibrium Constants from a Modified Redlich-Kwong Equation of State. Chem. Eng. Sci. 1972, 27, 1197-1203.

[31] http://www.nist.gov

[32] Acton A., R. C. Van Meerbeke, Rollover in LNG Storage – An Industrial View, Eight International conference on LNG, LA, California, June 15-19, 1986.

[33] Lukaszewski M. W., W. B. J. Zimmerman, M. T. Tennant, M. B. Webster, "Application of inverse methods based algorithms to Liquefied Natural Gas (LNG) storage management", chemical engineering research and design 91, Elsevier, 2013 Pages 457–463

[34] Radko, T., Double-Diffusive Convection, Chapter 1, 2013, Cambridge University Press. ISBN: 9780521880749

[35] http://en.wikipedia.org/wiki/Double_diffusive_convection

[36] Turner, J. S., Double Diffusive Phenomena, Annual Review of Fluid Mechanics, Vol. 6: 37-54 (Volume publication date January 1974)

[37] Pickard G. L., S. Pond, Introductory Dynamical Oceanography, Chapter 5, Second Edition, 1983, Butterworth–Heinemann

[38] www.oceanworld.tamu.edu/resources/ocng_textbook/chapter06/chapter06_01.htm

[39] Cho, E., Kim, H., Mixing Phenomena through the Heat and Salt Transports Across a Density Interface in a Stratified Two-layer System, Korean J. Chem. Eng., 19(1), 11-16 (2002)

[40] Hashemi, H. T., Wesson, H.R., Cut LNG Storage Cost, Hydrocarbon Processing, Page 117, August 1971.

[41] Shi J. Q., C. Beduz, R.G. Scurlock, Numerical modelling and flow visualization of mixing of stratified layers and rollover in LNG, Cryogenics Vol 33, No 12, 1993.

[42] Bashiri A., L. Fatehnejad, Modelling and Simulation of Rollover in LNG Storage Tanks, Sazeh, World Gas Conference, Netherlands, 2006

[43] Peng, D., Robinson, D. B. A New Two-Constant Equation of State, Ind. Eng. Chem. Fundam. 1976, 15(1), 59-64.

[44] Hosoo Kim, Myung-Wook Shin, En Sup Yoon, Optimization of Operating Procedure of LNG Storage Facilities Using Rigorous BOR Model, 17th World Congress, The International Federation of Automatic Control, Seoul, Korea, July 6-11, 2008

[45] Kazuo Koyama, Kaigan, Minato ku, CFD Simulation on LNG Storage Tank to Improve Safety and Reduce Cost, Tokyo Gas Co. Ltd., Asia Simulation Conference, 2007

[46] ANSYS FLUENT software:

http://www.ansys.com/Products/Simulation+Technology/Fluid+Dynamics/Fluid+Dynamics+Products/ANSYS+Fluent

[47] Zimmerman William B., Julia M. Rees, Rollover instability due to double diffusion in a stably stratified cylindrical tank, PHYSICS OF FLUIDS, (published online), 2007

[48] Tosun I., Modelling in Transport Phenomena a Conceptual Approach, 2002 Elsevier Science B. V., Chapters 3 to 5

[49] Perry's Chemical Engineers' Handbook, 7th edition, Heat and Mass Transfer, Diffusivity estimation – Liquids, Page 5-50

[50] Span, R.; Wagner, W., Lemmon, E.W.; Jacobsen, R. T. Multi-parameter Equations of State – Recent Trends and Future Challenges, Fluid Phase Equilibria 2001, 183-184, 1-20.

[51] Ely J. F., H. J. M. Hanley, Prediction of transport properties, Industrial and Engineering Chemistry Fundamentals, 1981, 20 (4), page 323-332.

[52] http://imechanica.org/files/fluent_13.0_lecture10-transient.pdf

[53] Doering C. R., J. D. Gibbon, Applied Analysis of the Navier-Stokes Equations, Cambridge University Press, 28Apr.,1995, Page 18-21

[54] http://iom.invensys.com/AP/Pages/SimSci_ProcessEngSuite_PROII.aspx

[55] AspenTech website:

http://www.aspentech.com/products/aspen-hysys.aspx

[56] Getling A. V., Rayleigh-Bénard Convection: Structures and Dynamics, World Scientific, 1998

[57] http://www.detect-easure.com/pdfs/whessoe/LNGApplicationSummary.pdf

[58] Environmental Impact Assessment, Arrow LNG Plant, Coffey Environment 7033-7-Ch29-v3-29-1, 2007

https://www.arrowenergy.com.au/__data/assets/pdf_file/0015/2634/Chapter20 0720-20Impact20Assessment20Method.pdf

[59] http://www.bsigroup.com/en-GB/about-bsi

[60] Safe Work Australia, South Australia government:

http://www.safework.sa.gov.au/contentPages/EducationAndTraining/HazardM anagement/DealingWithHazards/dealDefinition.htm

[61] Cameron, I. T., Raman, R., Process Systems Risk Management, Academic Press; 1 edition, 2005, Page 88-89

[62] Standards Australia/Standards New Zealand Standard Committee, AS/NZS ISO 31000:2009, Risk Management-Principles and Guidelines, November 2009.

[63] Work Safe Australia, Victoria-Australia:

Hazard identification at a major hazard facility, section 2.4: Selecting the hazard identification technique.

http://www.worksafe.vic.gov.au/__data/assets/pdf_file/0005/8573/50712_WS_ 9_Hazard_ID_3HR.pdf

[64] Australian Standards: AS 1216-2006 Class labels for dangerous goods.

[65] Dowell A. M., D. C. Hendersho, Simplified Risk Analysis–Layer of Protection Analysis (LOPA), t, Paper 281a, AIChE 2002 National Meeting, Indianapolis, November 3-8, 2002

[66] Foss, M., Introduction to LNG: An overview on Liquefied Natural Gas (LNG), its properties, 2007, Organization of the LNG industry and safety considerations. Available from:

http://www.beg.utexas.edu/energyecon/lng/documents/CEE_INTRODUCTIO N_TO_LNG_FINAL.pdf [22 June 2010]